#### **Application of Plasma Phenomena**



#### Po-Yu Chang

Institute of Space and Plasma Sciences, National Cheng Kung University

Lecture 7

2025 fall semester

Thursday 9:00-12:00

#### **Materials:**

https://capst.ncku.edu.tw/PGS/index.php/teaching/

#### **Online courses:**

https://nckucc.webex.com/nckucc/j.php?MTID=m50e2008a7e216ef32c42db2 d027415ec

## AC electrical discharges deliver energy to the plasma without contact between electrodes and the plasma



- DC electrical discharge a true current in the form of a flow of ions or electrons to the electrodes.
- AC electrical discharge the power supply interacts with the plasma by displacement current.
  - Inductive radio frequency (RF) electrical discharges
  - Capacitive RF electrical discharges
  - Microwave electrical discharges
  - Dielectric-barrier discharges (DBDs)
- Other mechanism
  - Laser produced plasma
  - Pulsed-power generated plasma

#### Advantage of using microwave electrical discharges



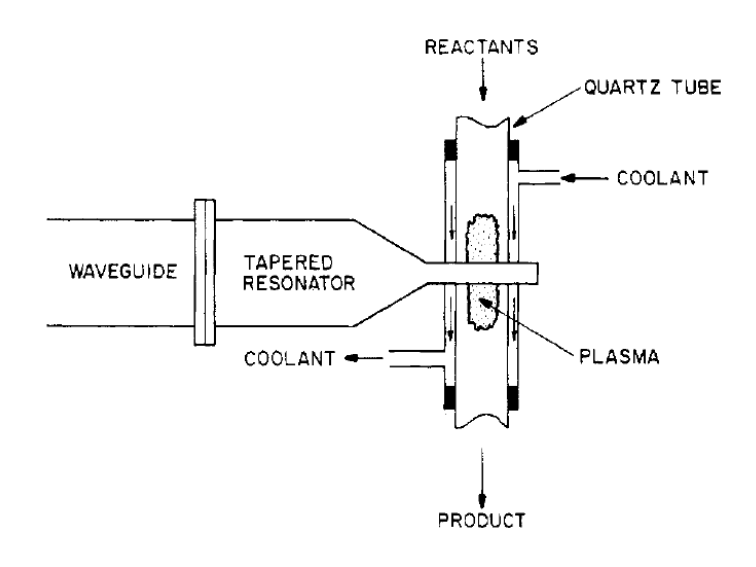
- The wavelength of the microwave is in centimeters range. In contract, the wavelength is 22 m for RF frequency f = 13.6 MHz.
- The electron number density can approach the critical number density. (7x10<sup>16</sup> m<sup>-3</sup>) at a frequency of 2.45 GHz.
- The plasma in microwave discharges is quasi-optical to microwave.
- Microwave-generated plasmas have a higher electron kinetic temperature (5 ~ 15 eV) than DC or low frequency RF-generated plasmas (1 or 2 eV).
- Capable of providing a higher fraction of ionization.
- Do not have a high voltage sheath.
- No internal electrodes.

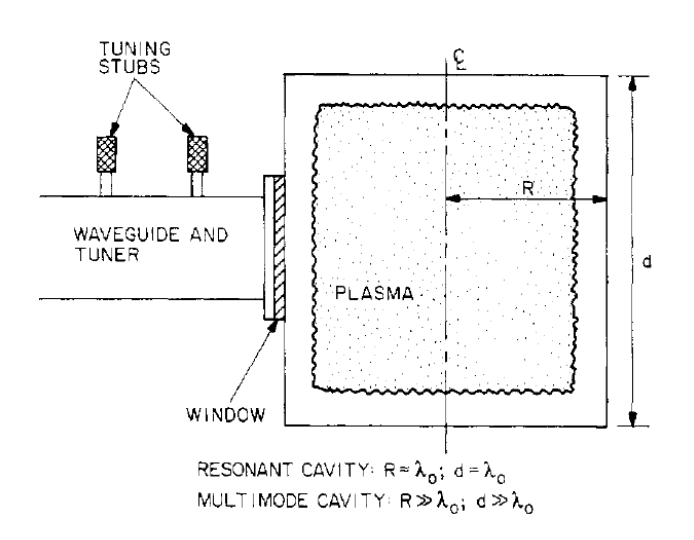
### Microwave plasma reactor configurations



Waveguide coupled reactor

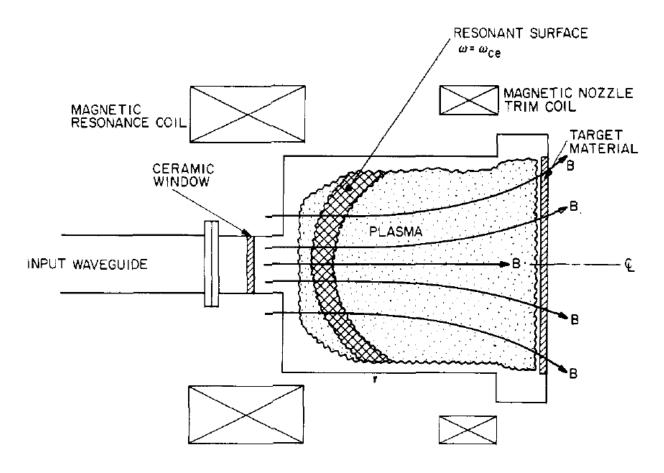
Resonant or multimode cavity –
if the impedance matching is
good, more energy can be fed
into the cavity.





## Strong absorption occurs when the frequency matches the electron cyclotron frequency

Electron cyclotron resonance (ECR) plasma reactor



### Electron cyclotron frequency depends on magnetic field only

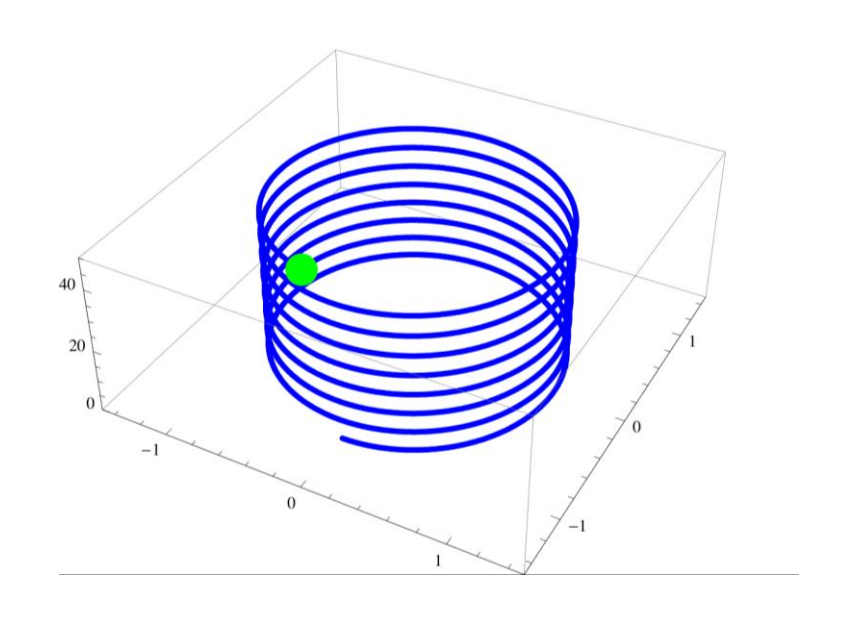


$$m_e \frac{d \overrightarrow{v}}{dt} = -\frac{e}{c} \overrightarrow{v} \times \overrightarrow{B}$$

• Assuming  $\overrightarrow{B} = B\widehat{z}$  and the electron oscillates in x-y plane

$$m_e v_x = -\frac{e}{c} B v_y$$
 $m_e v_z = 0$ 
 $m_e v_y = \frac{e}{c} B v_x$ 

$$\ddot{v}_{x} = -\frac{eB}{m_{e}c}\dot{v}_{y} = -\left(\frac{eB}{m_{e}c}\right)^{2}v_{x}$$
$$\ddot{v}_{y} = -\frac{eB}{m_{e}c}\dot{v}_{x} = -\left(\frac{eB}{m_{e}c}\right)^{2}v_{y}$$



Therefore

$$\omega_{\mathrm{ce}} = \frac{eB}{m_e c}$$

### Electrons keep getting accelerated when a electric field rotates in electron's gyrofrequency



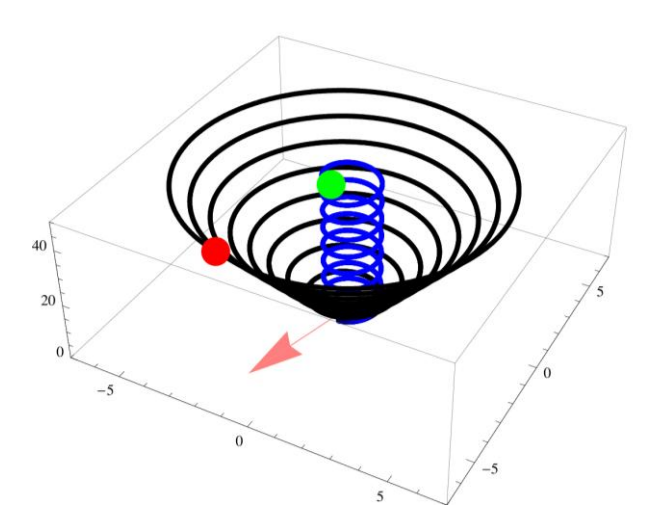
$$m_e \frac{d \vec{v}}{dt} = -\frac{e}{c} \vec{v} \times \vec{B} - e \vec{E} \qquad \vec{B} = B_0 \hat{z} \qquad \vec{E} = E_0 [\hat{x} \cos(\omega t) + \hat{y} \sin(\omega t)]$$

$$m_e \dot{v}_x = -\frac{e}{c}Bv_y + E_0\cos(\omega t)$$
  $m_e \dot{v}_y = \frac{e}{c}Bv_x + E_0\sin(\omega t)$   $m_e \dot{v}_z = 0$ 

$$\ddot{v}_x = -\frac{eB}{m_e c}\dot{v}_y - \frac{E_0}{m_e}\omega\sin(\omega t) = -\omega_{ce}^2 v_x - \frac{E_0}{m_e}(\omega_{ce} + \omega)\sin(\omega t)$$

$$\ddot{v}_y = -\frac{eB}{m_e c}\dot{v}_x + \frac{E_0}{m_e}\omega\cos(\omega t) = -\omega_{ce}^2 v_y + \frac{E_0}{m_e}(\omega_{ce} + \omega)\cos(\omega t)$$

$$\omega_{\mathrm{ce}} = \frac{eB}{m_e c}$$

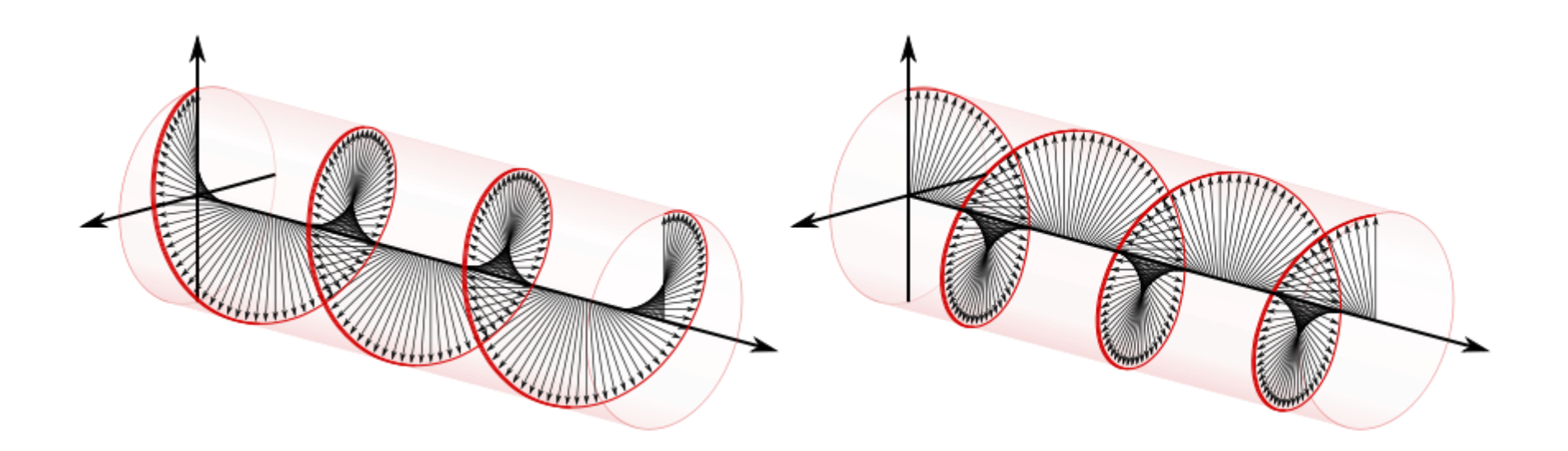


## Electric field in a circular polarized electromagnetic wave keeps rotating as the wave propagates



Right-handed polarization

Left-handed polarization

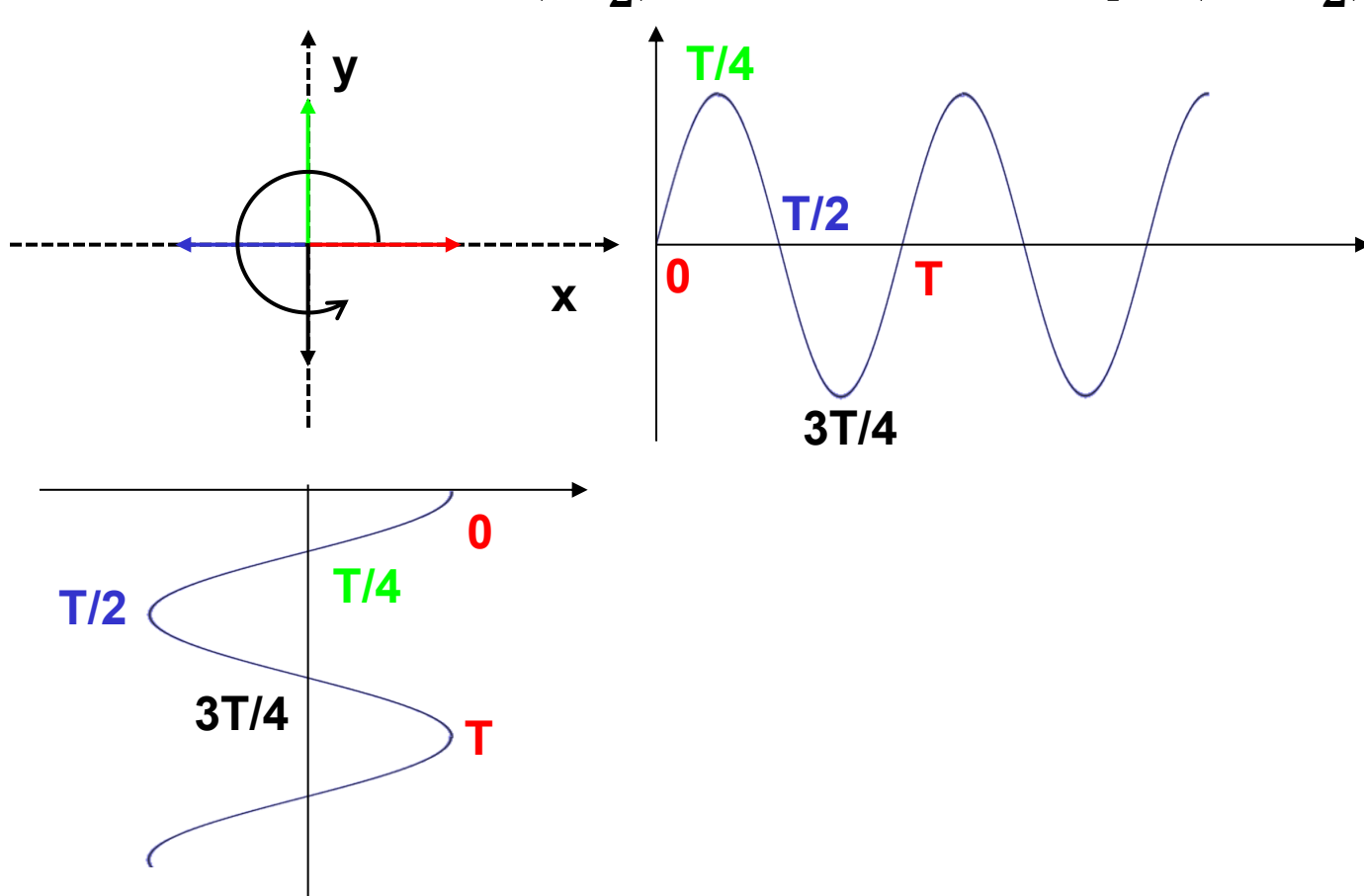


#### Electric field rotates in a circular polarization



$$E_{\rm x} = E_{\rm o} \exp(-i\omega t)$$

$$E_{y} = \pm iE_{x} = iE_{0}\exp(-i\omega t) = E_{0}\exp\left(\pm i\frac{\pi}{2}\right)\exp(-i\omega t) = E_{0}\exp\left[-i\left(\omega t \pm \frac{\pi}{2}\right)\right]$$

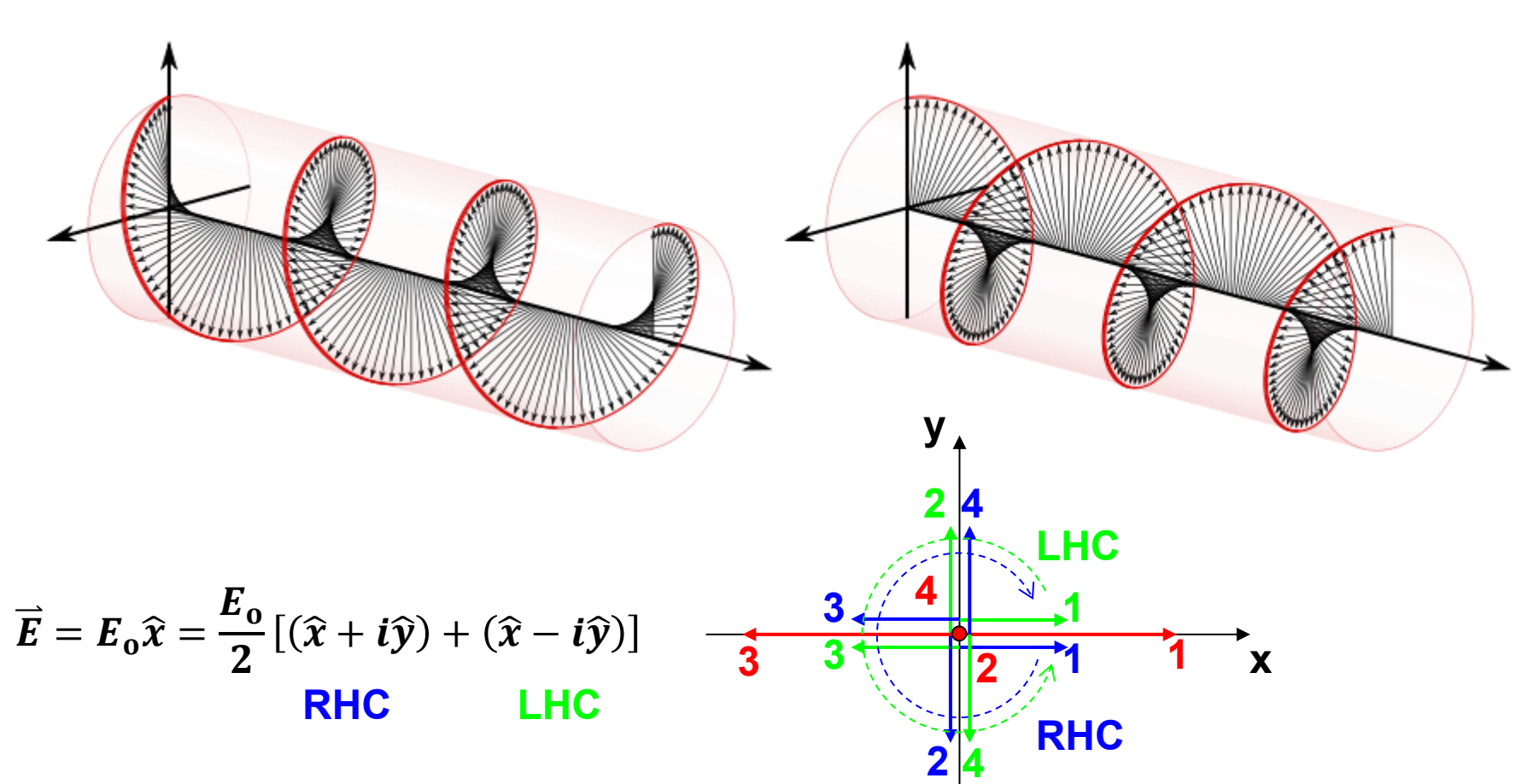


### A linear polarized wave can be decomposed by a lefthanded and a right-handed polarized wave



Right-handed polarization

Left-handed polarization



## Only right-handed polarization can resonance with electron's gyromotion



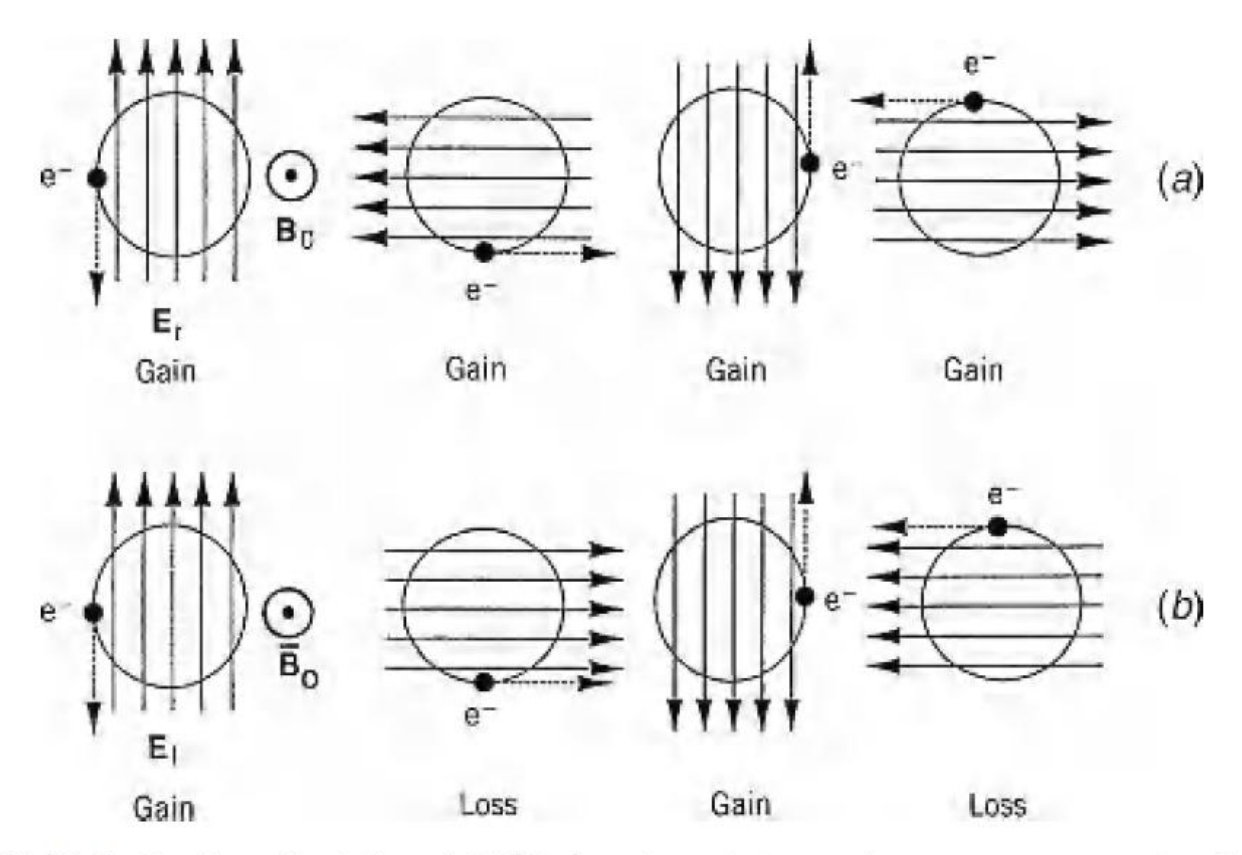
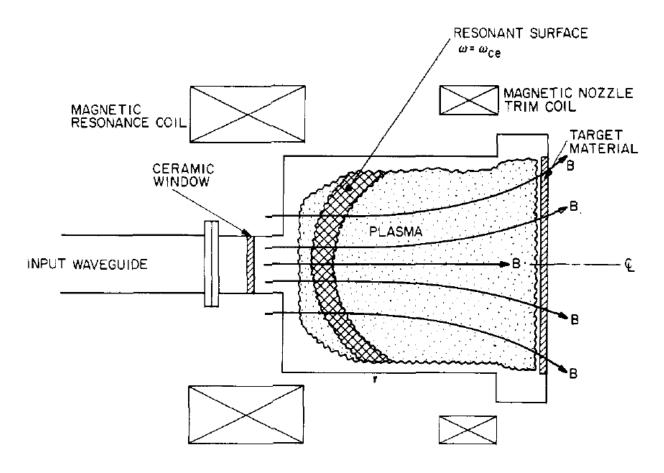


**FIGURE 13.5.** Basic principle of ECR heating: (a) continuous energy gain for right-hand polarization; (b) oscillating energy for left-hand polarization (after Lieberman and Gottscho, 1994).

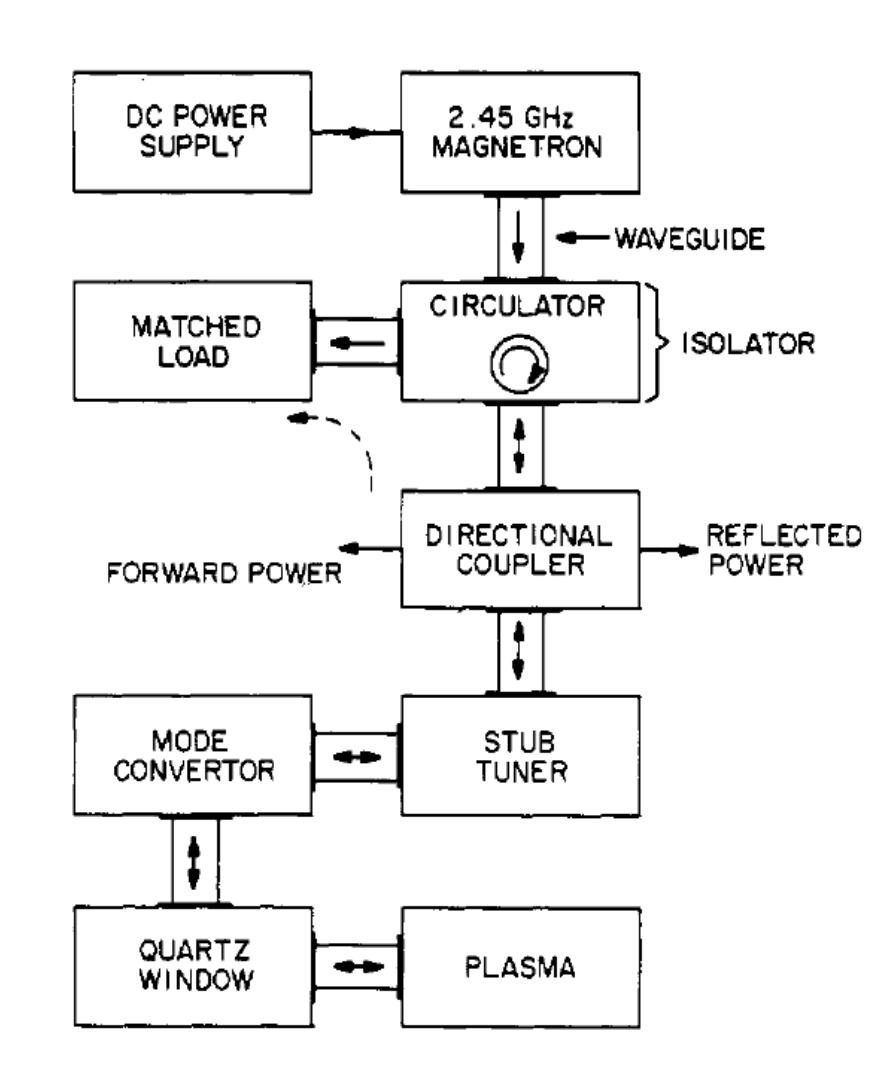
## Strong absorption occurs when the frequency matches the electron cyclotron frequency

Electron cyclotron resonance (ECR) plasma reactor



# Electron cyclotron resonance (ECR) microwave systems



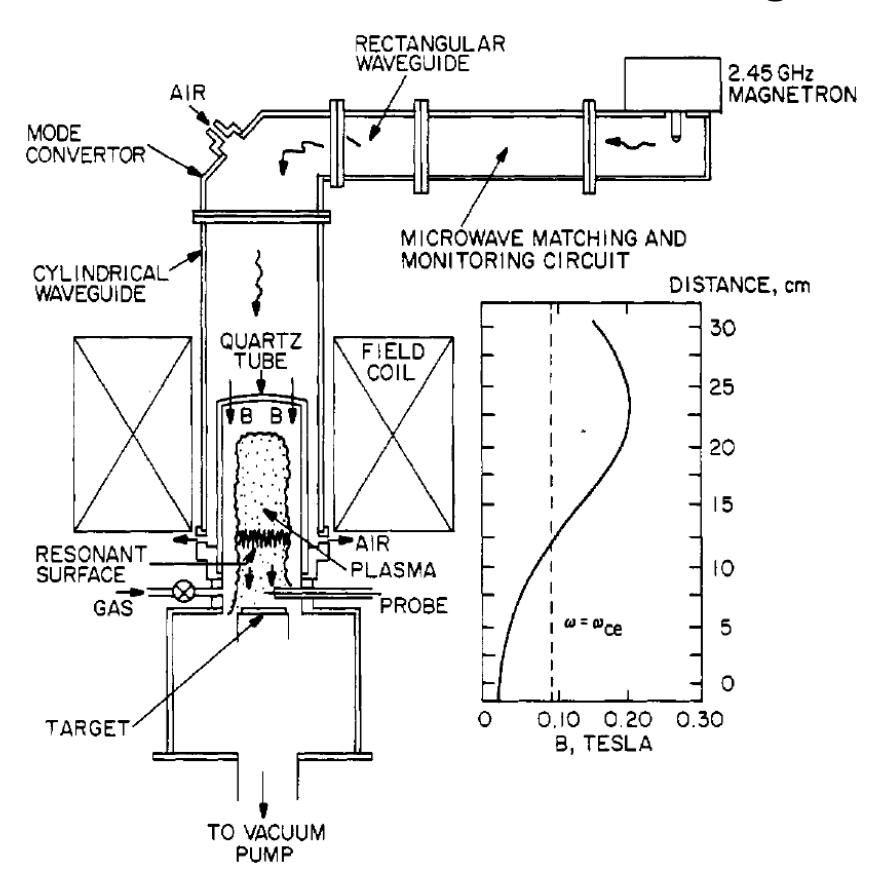


microwave systems

### Immersed ECR plasma source

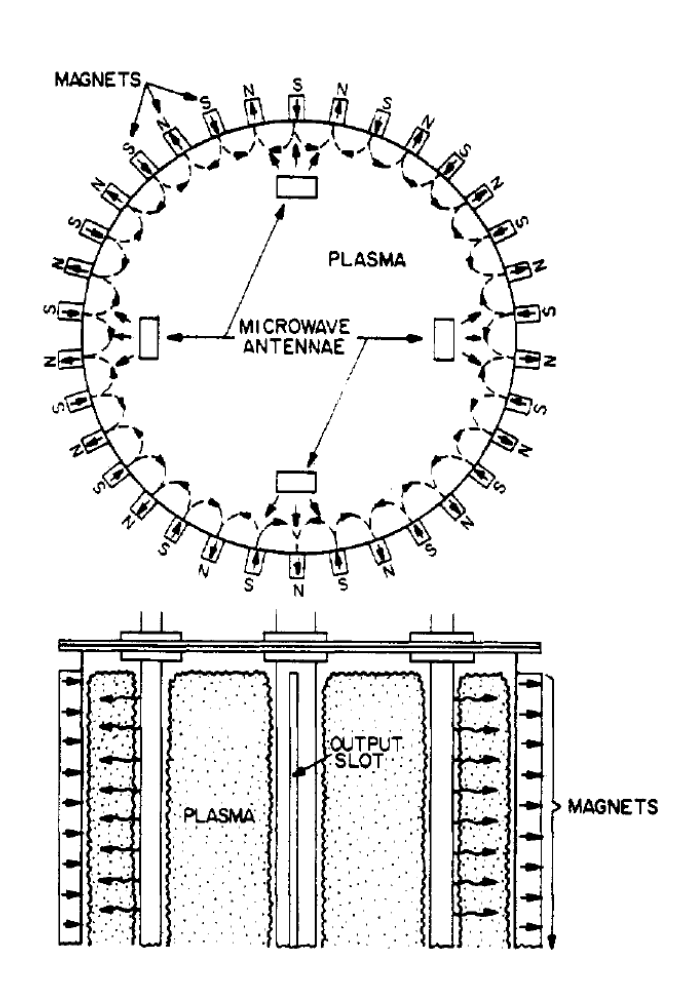


- High particle fluxes on targets for diamond or other thin film deposition
- The ions in the plasma flux can be used for etching.



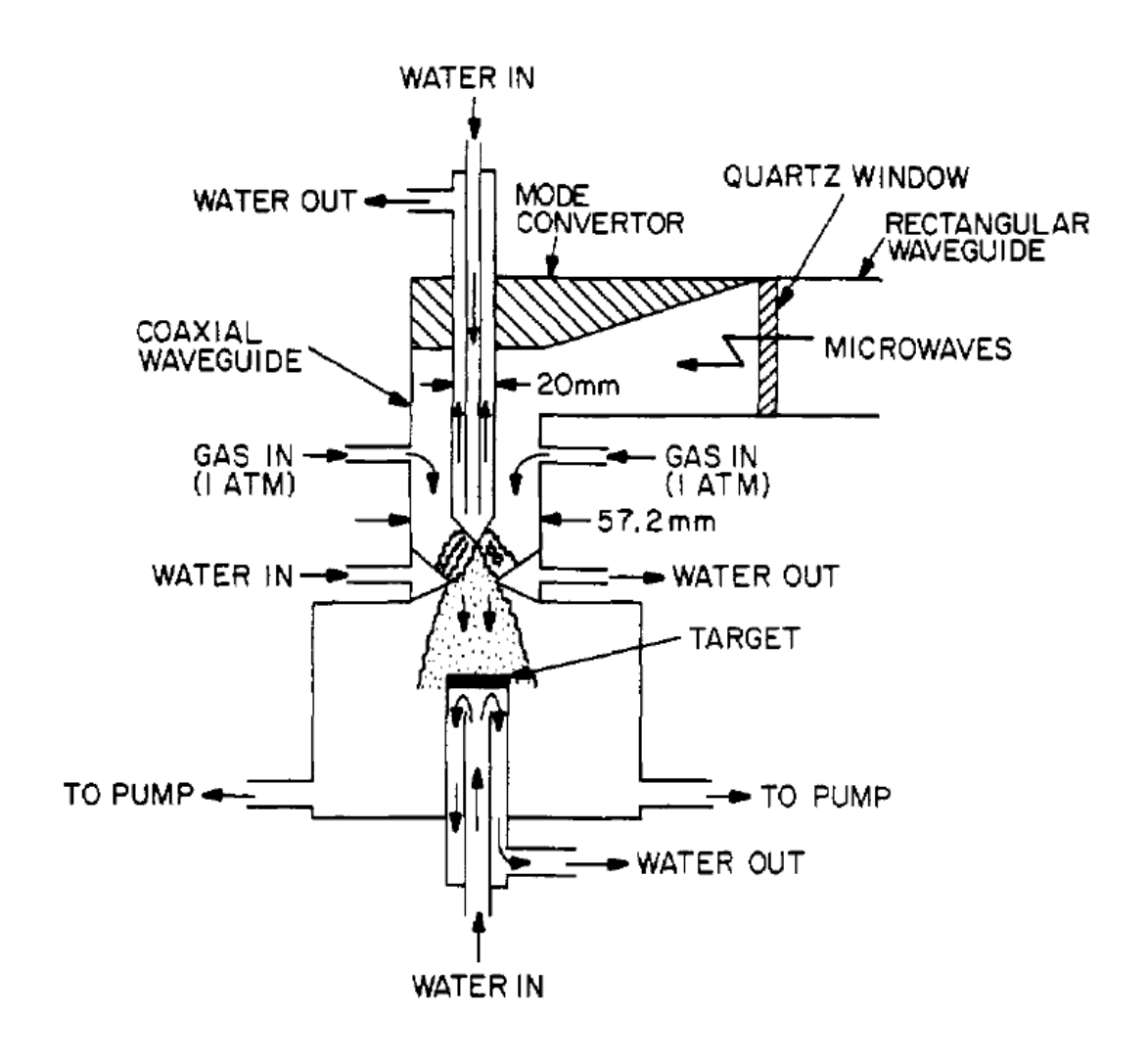
#### **Distributed ECR system**





- Function of the multipolar magnetic field at the tank boundary:
  - Provide a resonant surface for ECR absorption
  - Improve the confinement of the plasma

## Microwave plasma torch deposit a much faster rate than other types of plasma source for diamond film deposition



### Microwave-generated plasmas have the capability of filling very large volumes with moderately high density

#### Advantages

- Lower neutral gas pressure, i.e., longer ion and neutral mean free paths.
- Higher fraction ionize.
- Higher electron density.

#### Disadvantages

- Lower ion bombardment energies.
- Less control of the bombarding ion energy.
- Difficult in tuning up and achieving efficient coupling.
- Much more difficult and expensive to make uniform over a large area.
- More expensive.

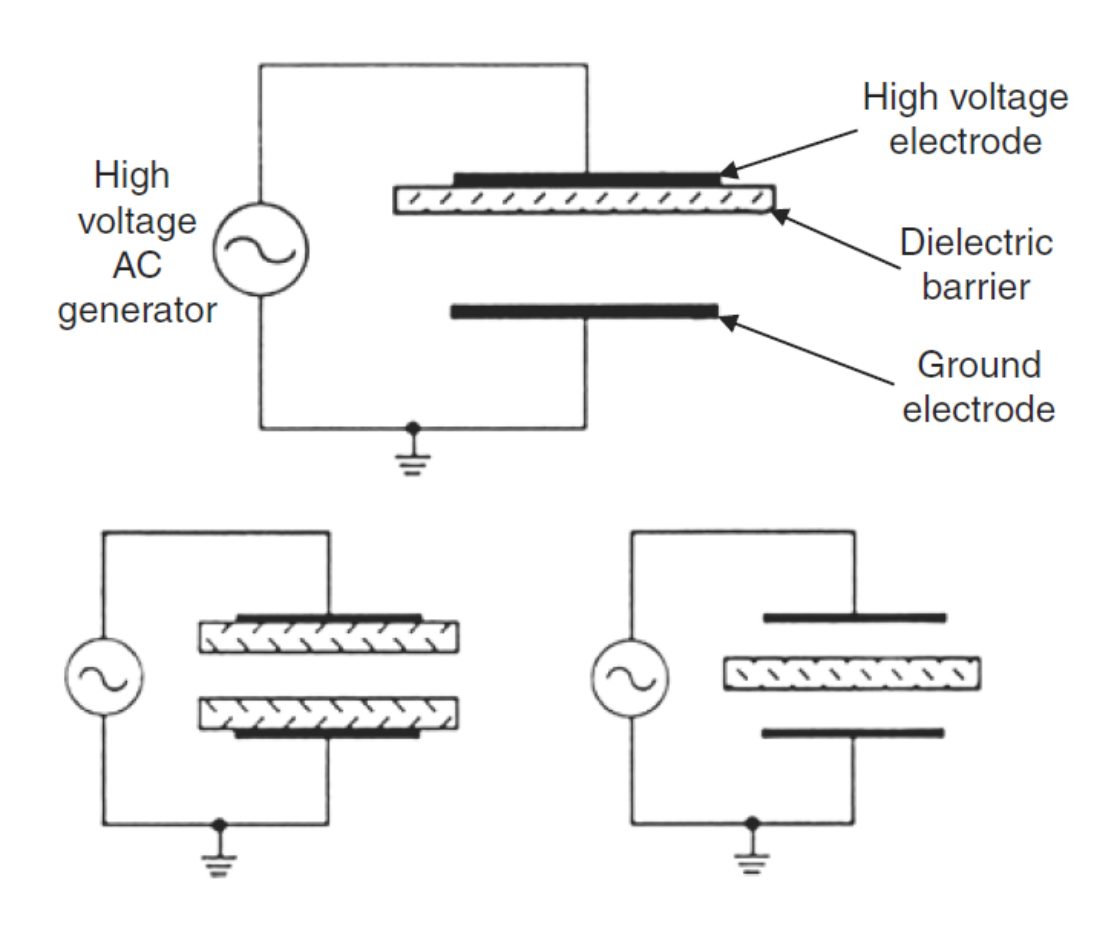
### AC electrical discharges deliver energy to the plasma without contact between electrodes and the plasma

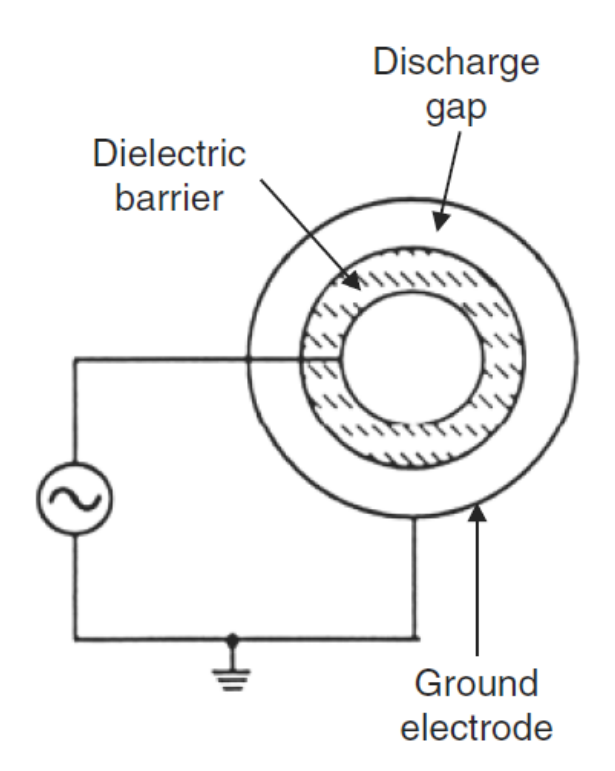


- DC electrical discharge a true current in the form of a flow of ions or electrons to the electrodes.
- AC electrical discharge the power supply interacts with the plasma by displacement current.
  - Inductive radio frequency (RF) electrical discharges
  - Capacitive RF electrical discharges
  - Microwave electrical discharges
  - Dielectric-barrier discharges (DBDs)
- Other mechanism
  - Laser produced plasma
  - Pulsed-power generated plasma

### **Dielectric-barrier discharges (DBDs)**

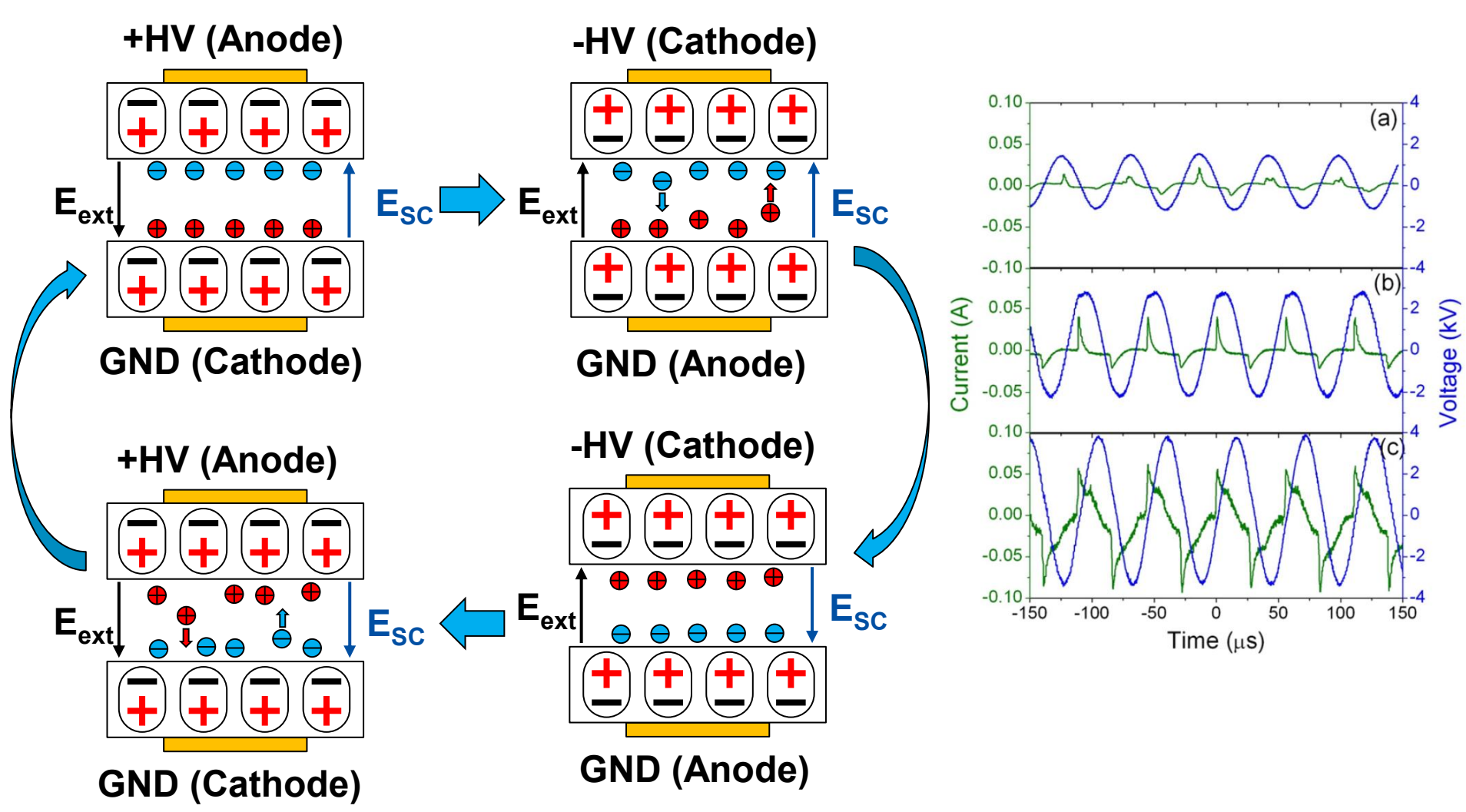






### Space charge effect enhance the electric field

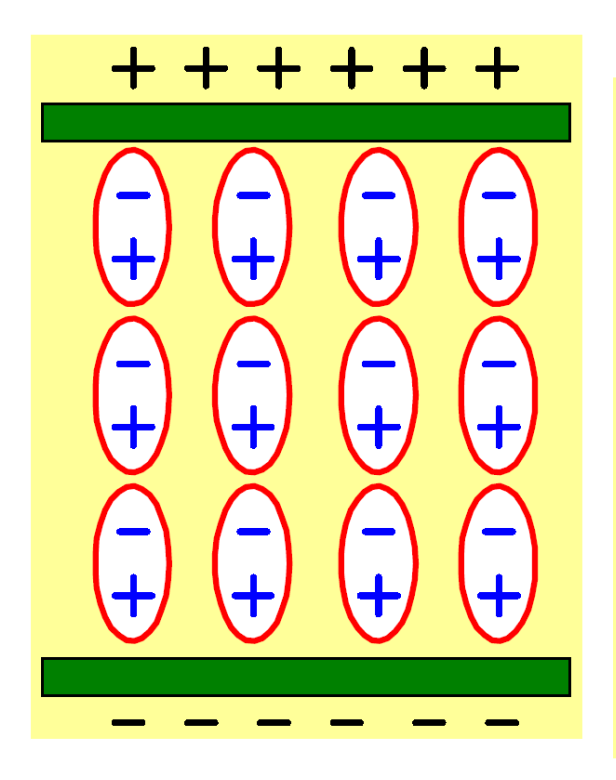


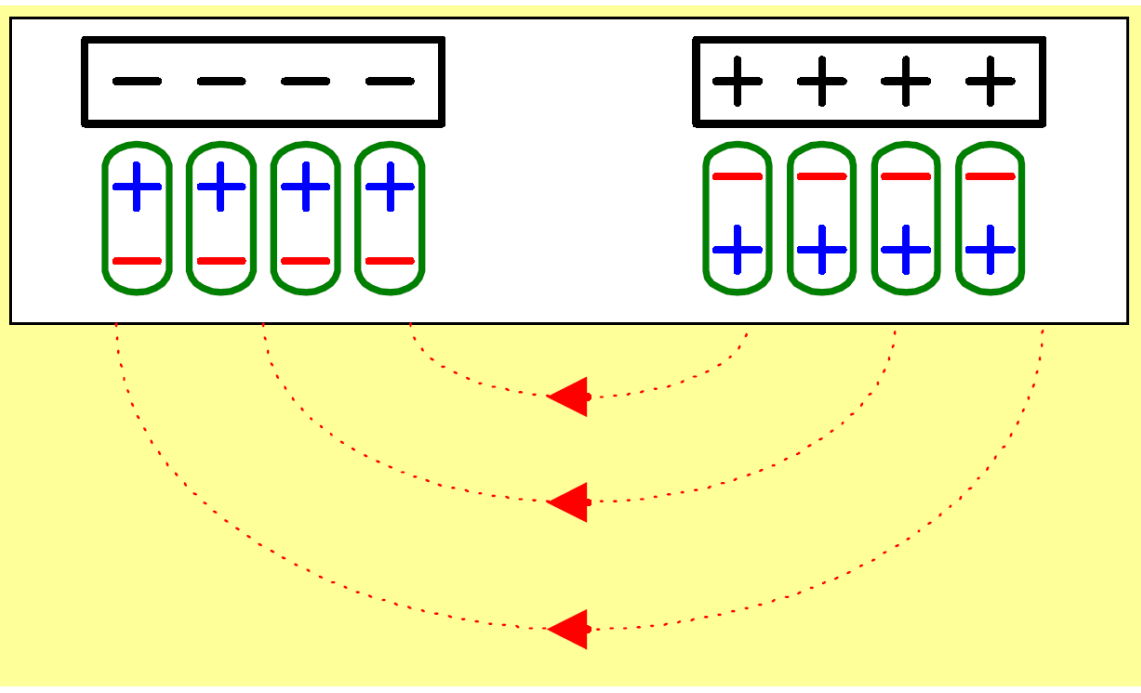


J. L. Walsh, et al., J. Phys. D: Appl. Phys., 43, 075201 (2010)

### The foundation of AC discharge in plasma display panel

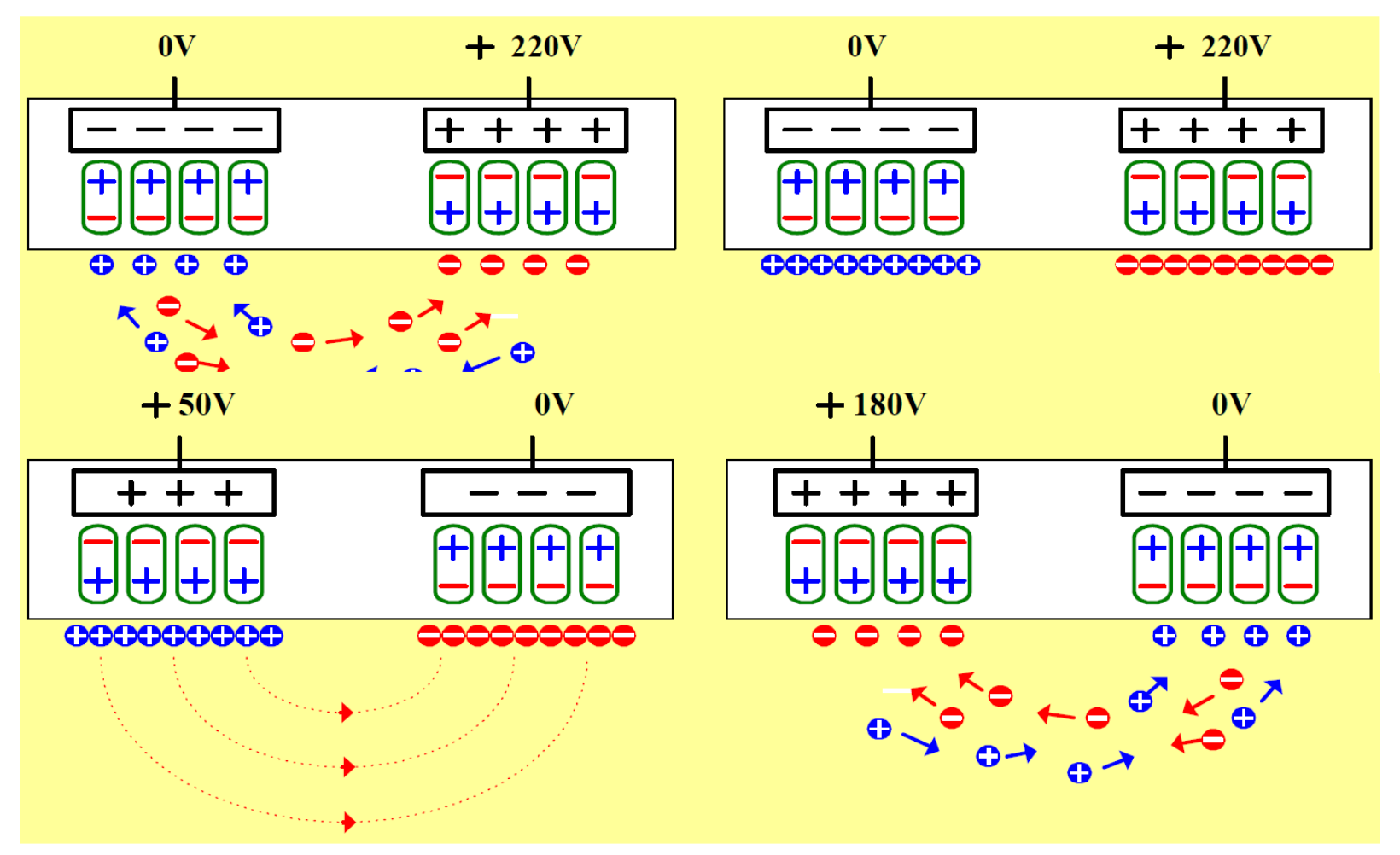






# The plasma can be sustained using ac discharged in plasma display panel

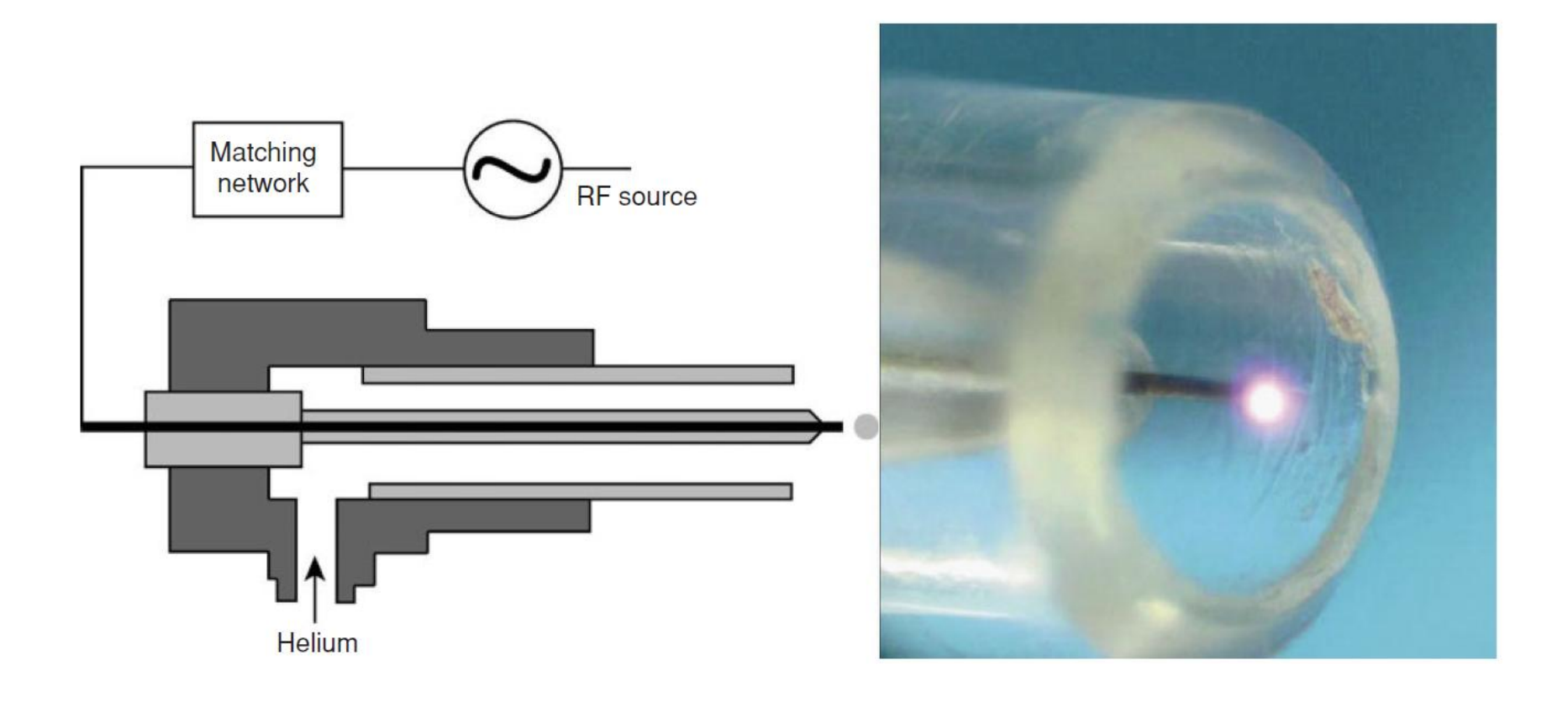




Wall discharge reduced the required discharge voltage

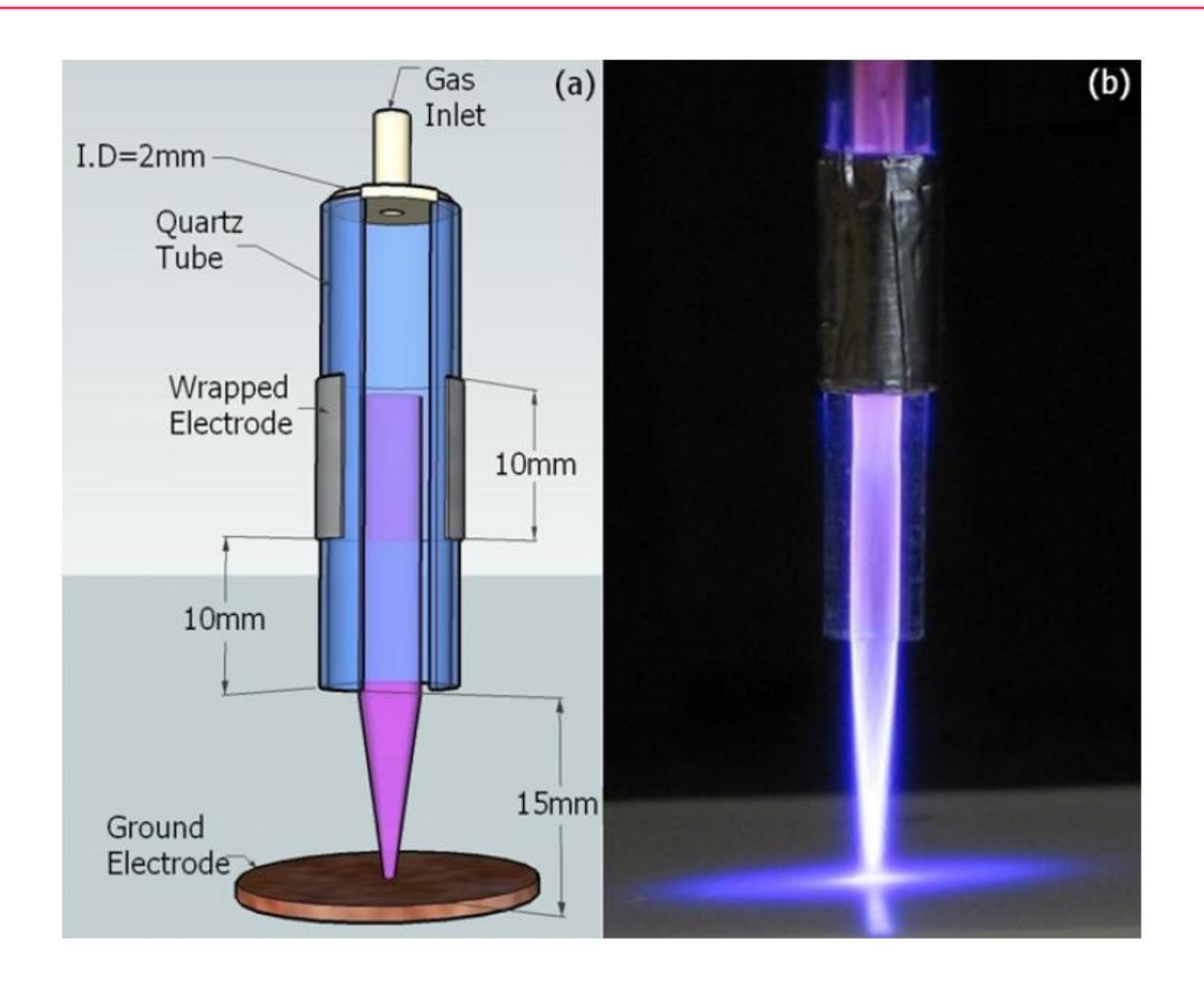
### Plasma-needle discharge





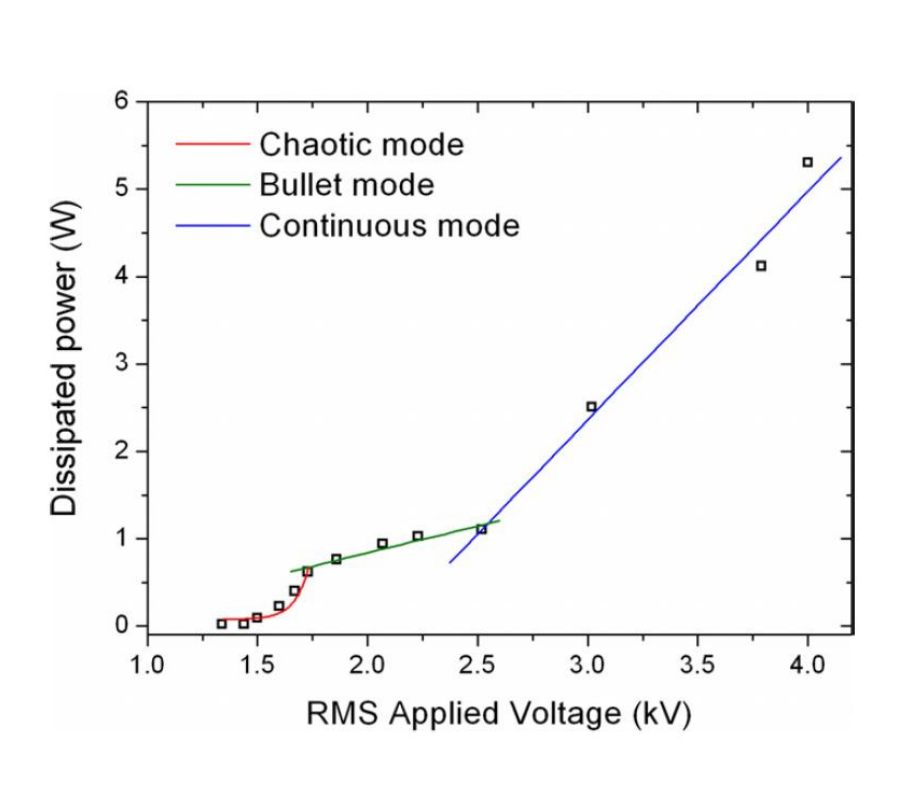
### Atmospheric-pressure cold helium microplasma jets

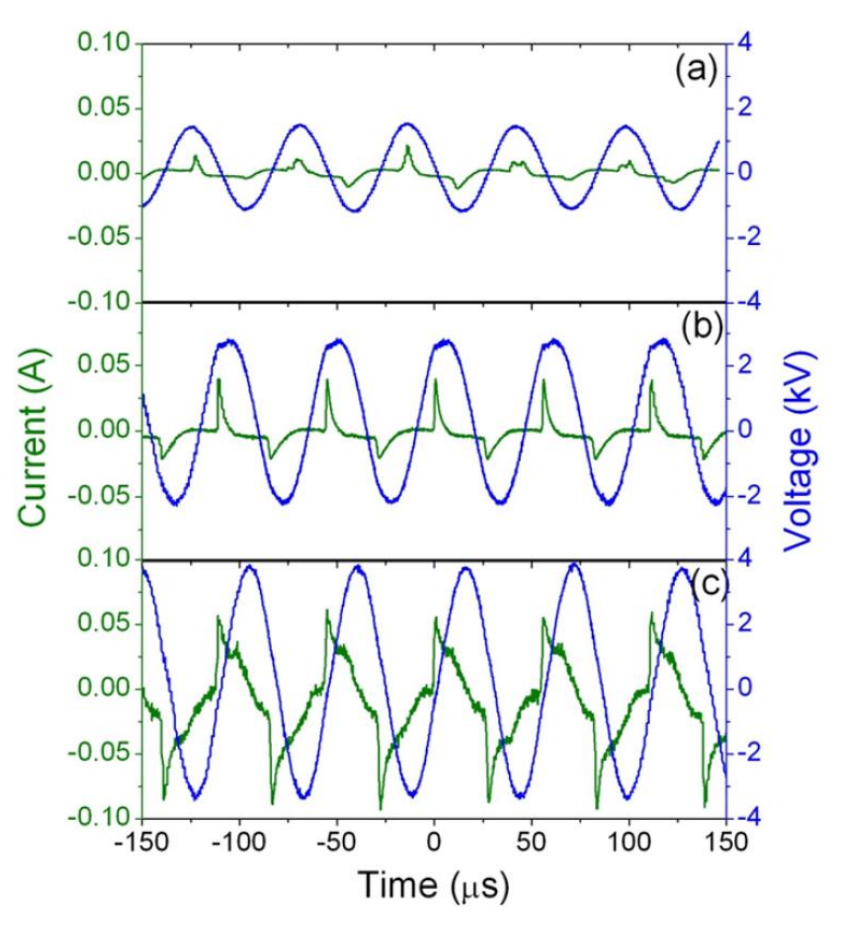




### There are three different modes: chaotic, bullet, and continuous mode



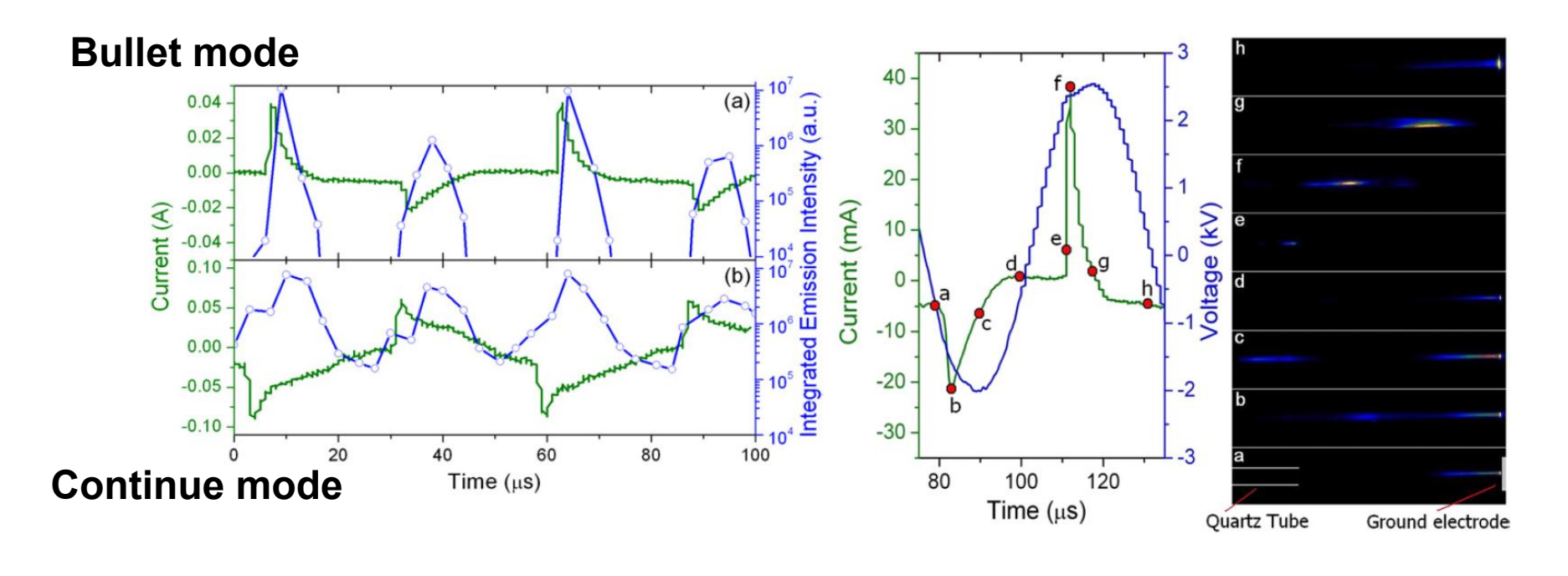




#### In bullet mode, the plasma jet comes out as a pulse



 wavelength-integrated optical emission signal (350–800 nm) Images of bullet mode



### AC electrical discharges deliver energy to the plasma without contact between electrodes and the plasma

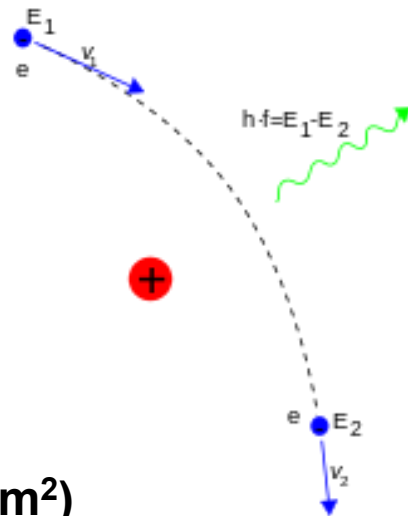


- DC electrical discharge a true current in the form of a flow of ions or electrons to the electrodes.
- AC electrical discharge the power supply interacts with the plasma by displacement current.
  - Inductive radio frequency (RF) electrical discharges
  - Capacitive RF electrical discharges
  - Microwave electrical discharges
  - Dielectric-barrier discharges (DBDs)
- Other mechanism
  - Laser produced plasma
  - Pulsed-power generated plasma

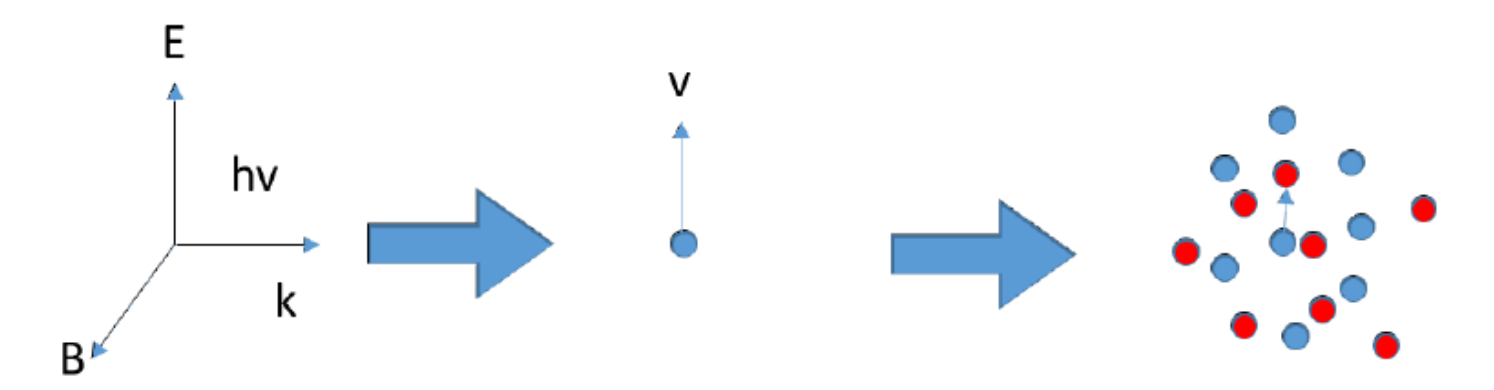
## Laser is absorbed in underdense plasma through collisional process called inverse bremsstrahlung



Bremsstrahlung



Inverse bremsstrahlung (For I < 10<sup>18</sup> w/cm<sup>2</sup>)



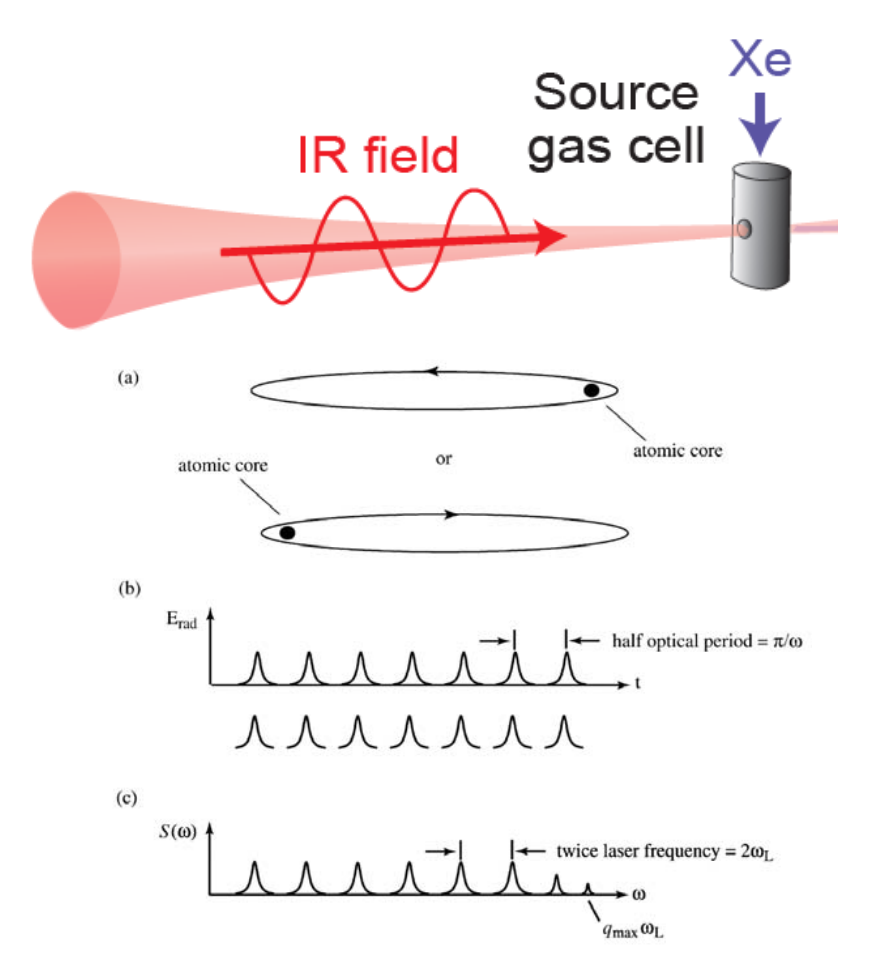
Electrons accelerated by electric fields

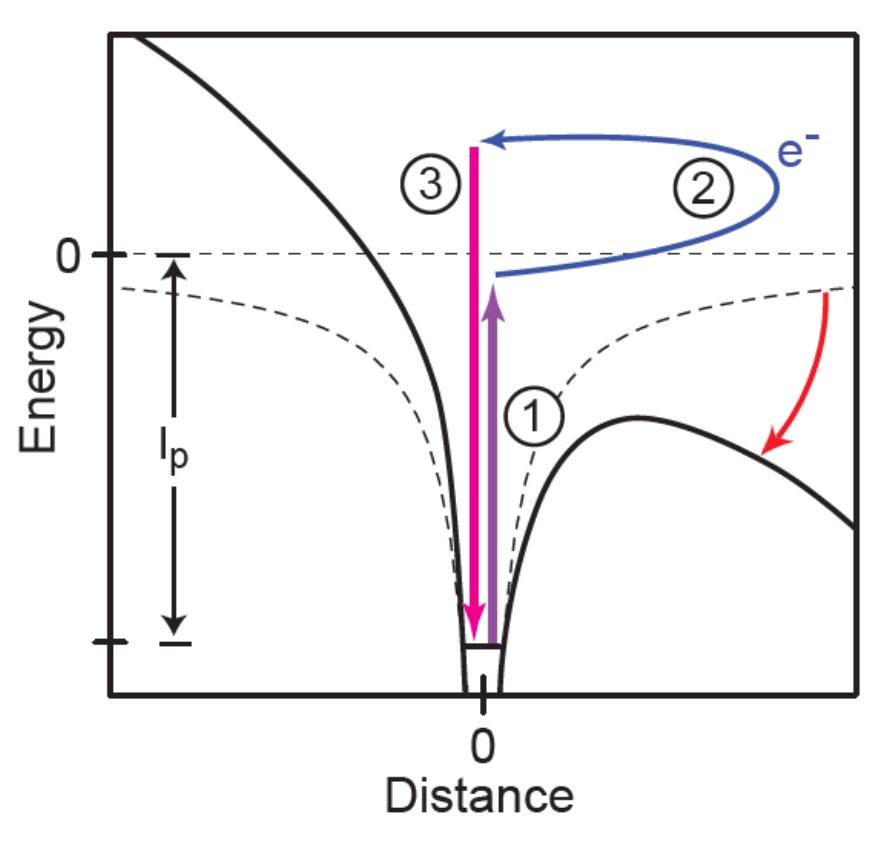
Electrons collide with other electrons / ions

## Electric field of a high-power laser can perturb the potential of a nuclear and thus ionize the atom directly

For I ~ 10<sup>14</sup> ~ 10<sup>16</sup> w/cm<sup>2</sup>

 $E_{\rm cutoff} \approx I_{\rm p} + 3.17 U_{\rm p}$   $I_{\rm p}$ : ionization potential  $U_{\rm p}$ : ponderomotive energy





M. Krüger, etc., Appl. Sci. 9, 378 (2019) Robert Boyd. Nonlinear optics.

## AC electrical discharges deliver energy to the plasma without contact between electrodes and the plasma



- DC electrical discharge a true current in the form of a flow of ions or electrons to the electrodes.
- AC electrical discharge the power supply interacts with the plasma by displacement current.
  - Inductive radio frequency (RF) electrical discharges
  - Capacitive RF electrical discharges
  - Microwave electrical discharges
  - Dielectric-barrier discharges (DBDs)
- Other mechanism
  - Laser produced plasma
  - Pulsed-power generated plasma it will be introduced later.

### **Diagnostics**



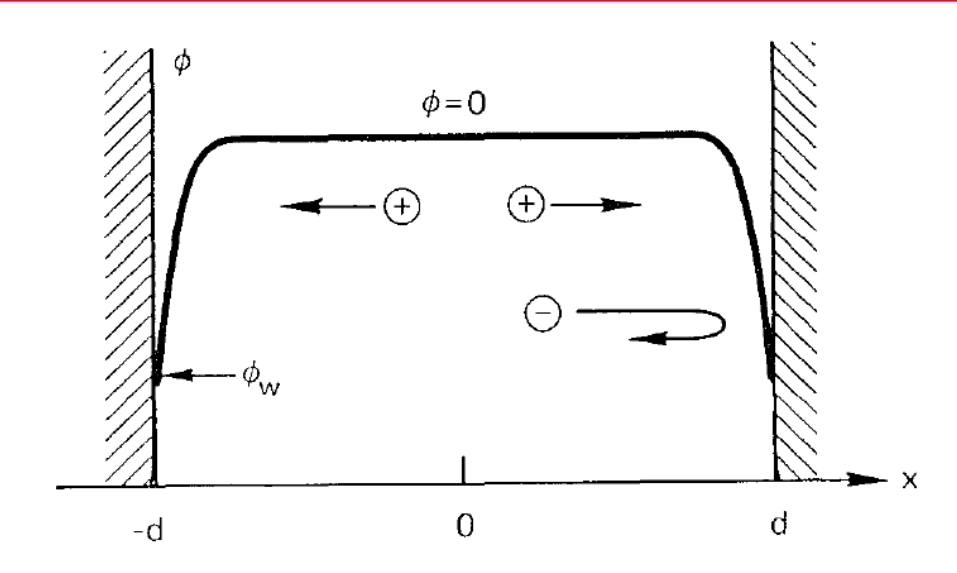
- Single/double Langmuir probe n<sub>e</sub>, T<sub>e</sub>
- Interferometer n<sub>e</sub>
- Schlieren dn<sub>e</sub>/dx
- Faraday rotator B
- Bdot probe B
- Charged particle B
- Spectroscopy T<sub>e</sub>, n<sub>e</sub>
- Thomson scattering T<sub>e</sub>, n<sub>e</sub>, T<sub>i</sub>, n<sub>i</sub>
- Faraday cup dn<sub>i</sub>/dt
- Retarding Potential Analyzer v<sub>i</sub>

- Intensified CCD 2D image
- Framing camera 2D image
- Streak camera 1D image
- VISAR shock velocity
- Neutron time of flight (NToF)
  - Neutron yield, T<sub>i</sub>
- Thomson parabola e/m
- Data analysis using Pulse Shaping
- Stimulated Brillouin scattering
  - Laser pulse compression



### All plasmas are separated from the walls surrounding them by a sheath

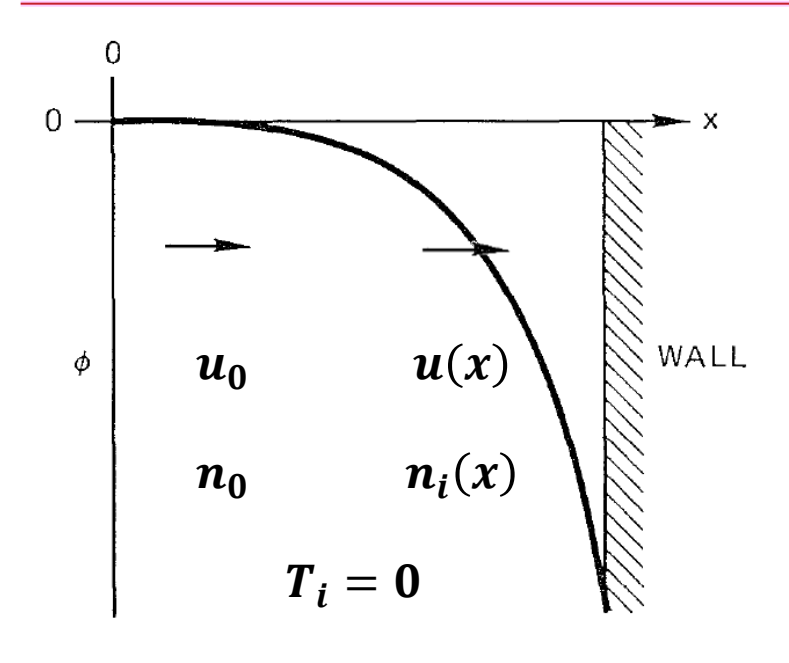




- When ions and electrons hit the wall, they recombine and are lost.
- Since electrons have much higher thermal velocities than ions, they are lost faster and leave the plasma with a net positive charge.
- Debye shielding will confine the potential variation to a layer of the order of several Debye lengths in thickness.
- A potential barrier is formed to confine electrons electrostatically.
- The flux of electrons is just equal to the flux of ions reaching the wall.

### The planar sheath equation





$$\frac{1}{2}mu^{2} = \frac{1}{2}mu_{0}^{2} - e\phi(x)$$

$$u = \left(u_{0}^{2} - \frac{2e\phi}{m}\right)^{1/2}$$

$$n_{0}u_{0} = n_{i}(x)u(x)$$

$$n_{i}(x) = n_{0}\left(1 - \frac{2e\phi}{mu_{0}^{2}}\right)^{-1/2}$$

• Boltzmann relation:

$$n_e(x) = n_0 \exp\left(\frac{e\phi}{KT_e}\right)$$

· Poisson's equation:

$$\epsilon_0 \frac{d^2 \phi}{dx^2} = e(n_e - n_i)$$

$$= e n_0 \left[ \exp\left(\frac{e \phi}{K T_e}\right) - \left(1 - \frac{2e \phi}{m u_0^2}\right)^{-1/2} \right]$$

$$\chi \equiv -\frac{e \phi}{K T_e}, \xi \equiv \frac{x}{\lambda_D}, M \equiv \frac{u_0}{(K T_e/m)^{1/2}}$$

$$\lambda_D = \left(\frac{K T_e}{4\pi n e^2}\right)^{1/2}$$

$$\chi'' = \left(1 + \frac{2\chi}{M^2}\right)^{-1/2} - e^{-\chi}$$

#### The Bohm sheath criterion



$$\chi'' = \left(1 + \frac{2\chi}{M^2}\right)^{-1/2} - e^{-\chi}$$

$$\chi'\chi''=\chi'\left(1+\frac{2\chi}{M^2}\right)^{-1/2}-\chi'e^{-\chi}$$

$$\frac{d}{d\xi} \left( \frac{\chi'^2}{2} \right) = \frac{d\chi}{d\xi} \left( 1 + \frac{2\chi}{M^2} \right)^{-1/2} - \frac{d\chi}{d\xi} e^{-\chi}$$

$$\chi_0=0$$
 ,  $\chi_0'=0$  , @  $\xi=0$ 

$$\int_{\chi_0/}^{\chi'} d\left(\frac{\chi'^2}{2}\right) = \int_0^{\chi} \left(1 + \frac{2\chi}{M^2}\right)^{-1/2} d\chi - \int_0^{\chi} e^{-\chi} d\chi$$

$$\frac{1}{2}(\chi'^2 - \chi_0'^2) = M^2 \left[ \left( 1 + \frac{2\chi}{M^2} \right)^{1/2} - 1 \right] + e^{-\chi} - 1$$

- Needs to be solved numerically
- The right-hand side must be positive for all  $\chi$  .

#### The Bohm sheath criterion - continued



$$\frac{1}{2}(\chi'^2 - \chi_0'^2) = M^2 \left[ \left( 1 + \frac{2\chi}{M^2} \right)^{1/2} - 1 \right] + e^{-\chi} - 1$$

• for 
$$|\chi| \ll 1$$
 
$$\left(1 + \frac{2\chi}{M^2}\right)^{1/2} - 1 = 1 + \frac{\chi}{M^2} - \frac{1}{2} \left(\frac{\chi}{M^2}\right)^2 + \dots - 1 \approx \frac{\chi}{M^2} - \frac{1}{2} \left(\frac{\chi}{M^2}\right)^2$$
$$e^{-\chi} - 1 = 1 - \chi + \frac{1}{2} \chi^2 + \dots - 1 \approx -\chi + \frac{1}{2} \chi^2$$
$$M^2 \left[ \left(1 + \frac{2\chi}{M^2}\right)^{1/2} - 1 \right] + e^{\chi} - 1 \approx M^2 \left[ \frac{\chi}{M^2} - \frac{1}{2} \left(\frac{\chi}{M^2}\right)^2 \right] - \chi + \frac{1}{2} \chi^2 = \frac{1}{2} \chi^2 \left( -\frac{1}{M^2} + 1 \right) > 0$$

$$M^2 > 1$$
 or  $mu_0^2 > KT_e$ 

- lons must enter the sheath region with a velocity greater than the acoustic velocity v<sub>s</sub>.
- There must be a finite electric field in the plasma.
- The scale of the sheath region is usually much smaller than the scale of the main plasma region in which the ions are accelerated.

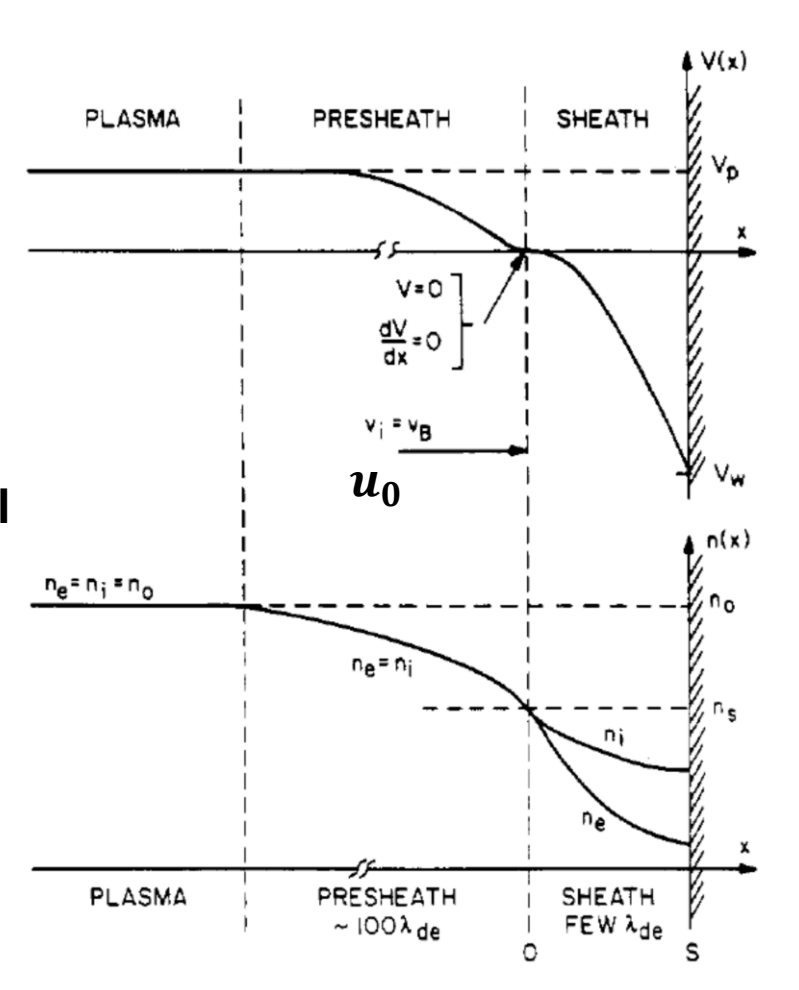
# The potential variation in a plasma-wall system can be divided into three parts

#### Sheath:

- ~Debye length, n<sub>e</sub> is appreciable.
- A dark layers where no electrons were present to excite atoms to emission.
- It has been measured by the electrostatic deflection of a thin electron beam shot parallel to a wall
- Presheath: ions are accelerated to the required velocity u<sub>0</sub> by a potential drop

$$|\phi| \geq \frac{1}{2} \frac{KT_e}{e} .$$

$$\frac{1}{2}m{u_0}^2 = |e\phi|, \ m{u_0}^2 > KT_e$$



#### **Electrostatic probes**



 The electron current can be neglected if the probe is sufficiently negative relative to the plasma to repel most electrons.

$$mu_0^2 > KT_e$$
  $J = enu$   $I = n_s eA \left(\frac{KT_e}{m}\right)^{1/2}$   $|\phi| \simeq \frac{1}{2} \frac{KT_e}{e}$   $n_s = n_0 \exp\left(\frac{e\phi}{KT_e}\right) = n_0 e^{-1/2} = 0.61 n_0$  Bohm current:  $I_B \simeq 0.5 n_0 eA \left(\frac{KT_e}{m}\right)^{1/2}$ 

The plasma density can be obtained once the temperature is known.

#### **Electrostatic probes**



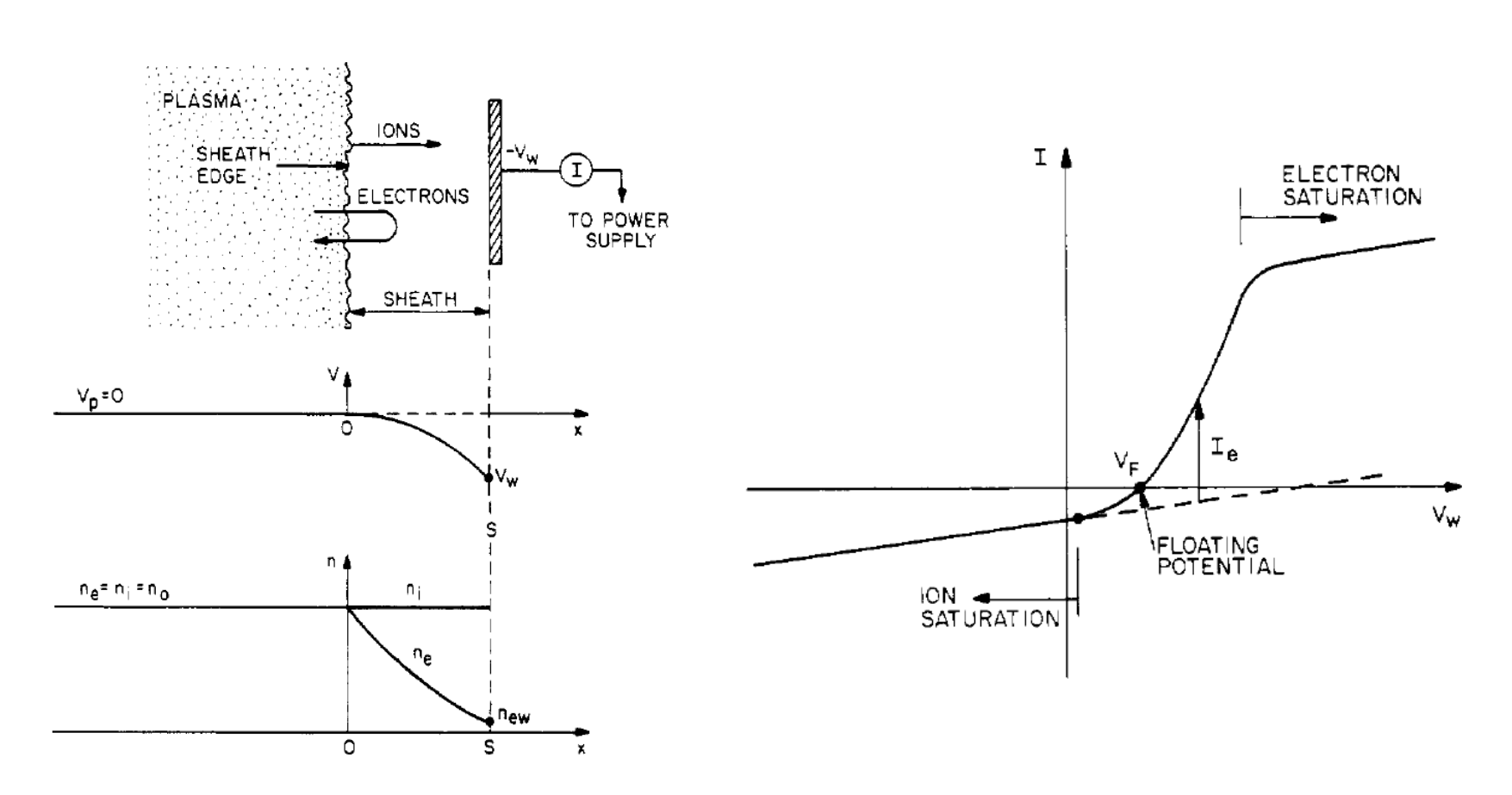
 The electron current can be neglected if the probe is sufficiently negative relative to the plasma to repel most electrons.

$$mu_0^2 > KT_e$$
  $J = enu$   $I = n_s eA \left(\frac{KT_e}{m}\right)^{1/2}$   $|\phi| \simeq \frac{1}{2} \frac{KT_e}{e}$   $n_s = n_0 \exp\left(\frac{e\phi}{KT_e}\right) = n_0 e^{-1/2} = 0.61 n_0$  Bohm current:  $I_B \simeq 0.5 n_0 eA \left(\frac{KT_e}{m}\right)^{1/2}$   $u_0$   $u_0$   $n_s$ 

The plasma density can be obtained once the temperature is known.

## A plasma sheaths is formed when plasma is contact to a surface





## Floating voltage is determined when ion flux is balanced by electron flux



Wall flux of ions:

$$\Gamma_i = \frac{1}{4} n_0 \bar{v}_i = n_0 \sqrt{\frac{8KT_i}{\pi m_i}}$$

Wall flux of electrons due to random motion:

$$n_{ew}=n_0 ext{exp}\left(rac{eoldsymbol{\Phi}_w}{KT_e}
ight)$$
 (Boltzman equation)  $\Gamma_e=rac{1}{4}n_{ew}ar{v}_e=n_0 ext{exp}\left(rac{eoldsymbol{\Phi}_w}{KT_e}
ight)\sqrt{rac{8KT_e}{\pi m_e}}$ 

Balance between electron and ion flux (current)

$$I = eA(\Gamma_i - \Gamma_e) = 0$$

$$\boldsymbol{\Phi}_{w} = -\frac{KT_{e}}{2e}\ln\left(\frac{m_{i}T_{e}}{m_{e}T_{i}}\right)$$

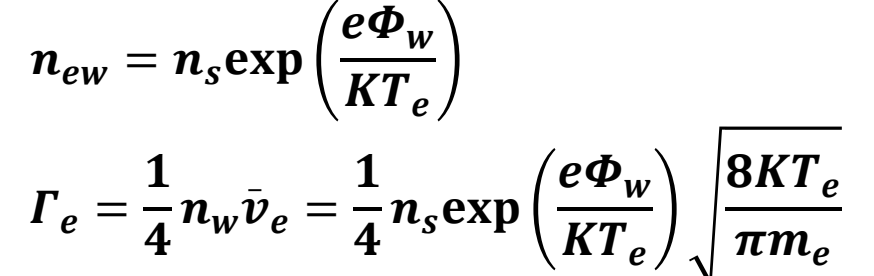
# Floating voltage can also be calculated using Bohm's velocity

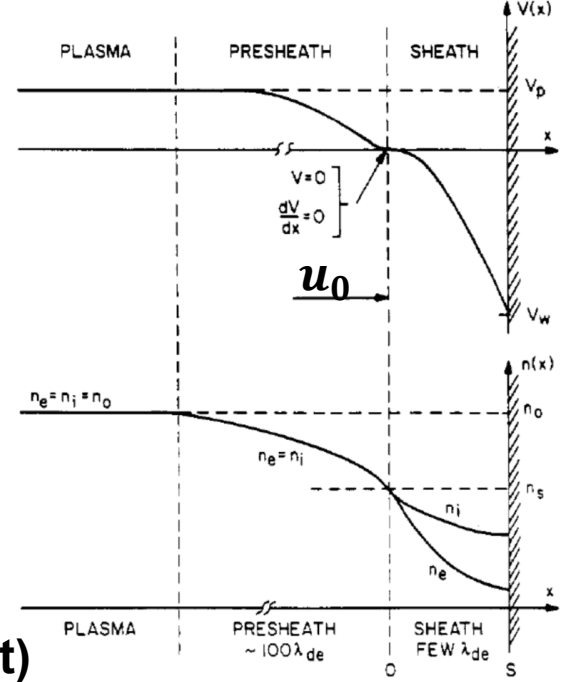


Wall flux of ions using Bohm's velocity:

$$u_0 = \sqrt{\frac{KT_e}{m_i}} \qquad \Gamma_i = n_s u_0$$

Wall flux of electrons due to random motion:





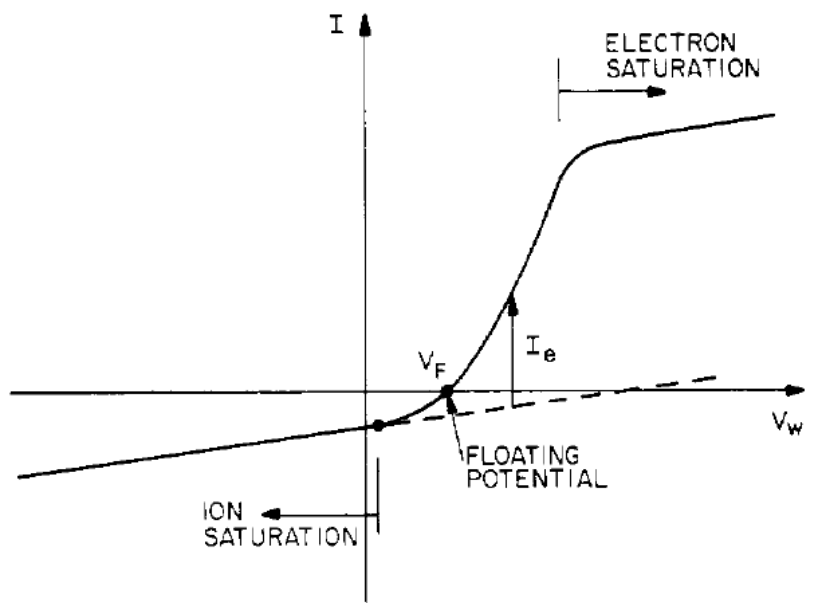
Balance between electron and ion flux (current)

$$I = eA(\Gamma_i - \Gamma_e) = 0$$

$$\Phi_{wB} = -\frac{KT_e}{2e} \ln \left( \frac{m_i}{2\pi m_e} \right) \quad \Longleftrightarrow \quad \Phi_w = -\frac{KT_e}{2e} \ln \left( \frac{m_i T_e}{m_e T_i} \right)$$

## Electron temperature can be determined by the slope of the I-V curve between ion and electron saturation





#### Ion saturation current:

$$I_{is} = AJ_{is} = eA\Gamma_{is}$$

$$= eA\frac{1}{4}n_i\bar{v}_i$$

$$= \frac{eAn_i}{4}\sqrt{\frac{8KT_i}{\pi m_i}}$$
 $n_i = \frac{4I_{is}}{eA}\sqrt{\frac{\pi m_i}{8KT_i}}$ 

$$n_i = \frac{4I_{is}}{eA} \sqrt{\frac{\pi m_i}{8KT_i}}$$

• Total current: 
$$I = I_{is} + I_e = I_{is} + \frac{1}{4} n_s \exp\left(\frac{eV}{KT_e}\right) \bar{v}_e eA$$
  $V \equiv \Phi$ 

Assuming:  $\frac{dI_{is}}{dV} \ll \frac{dI}{dV}$ 

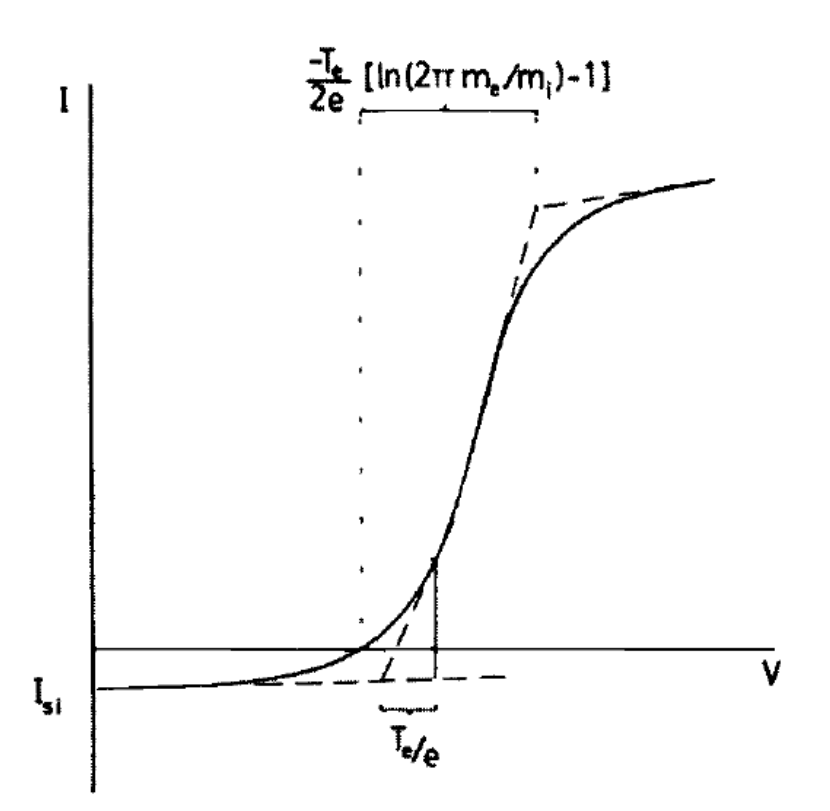
$$\frac{dI}{dV} = \frac{dI_{is}}{dV} + \frac{1}{4} \frac{e}{KT_e} n_s \exp\left(\frac{eV}{KT_e}\right) \bar{v}_e eA = \frac{dI_{is}}{dV} + \frac{e}{KT_e} I_e = \frac{dI_{is}}{dV} + \frac{e}{KT_e} (I - I_{is})$$

$$\approx \frac{e}{KT_e} (I - I_{is})$$

$$T_e = \frac{e(I - I_{is})}{dV/dV}$$

# Electron temperature can be obtained alternatively by finding the slope of I-V curve in Log-Linear plot





#### Electron saturation

$$V = V_p$$
  $I_{es} = \frac{1}{4} n_s \exp\left(\frac{eV_p}{KT_e}\right) \bar{v}_e eA$ 

$$\begin{split} I &= I_e + I_{\rm is} \approx I_{\rm es} = \frac{1}{4} n_s \exp\left(\frac{\rm eV}{KT_e}\right) \bar{v}_e \rm eA \\ &= \frac{1}{4} n_s \exp\left(\frac{\rm eV - eV_p + eV_p}{KT_e}\right) \bar{v}_e \rm eA \\ &= \frac{1}{4} n_s \exp\left(\frac{\rm eV_p}{KT_e}\right) \exp\left(e\frac{V - V_p}{KT_e}\right) \bar{v}_e \rm eA \\ &= I_{\rm es} \exp\left(e\frac{V - V_p}{KT_e}\right) \end{split}$$

$$T_e = \frac{e(V - V_p)}{K(\ln I_{es} - \ln I)}$$

## Plasma density can be obtained by finding the electron saturation current

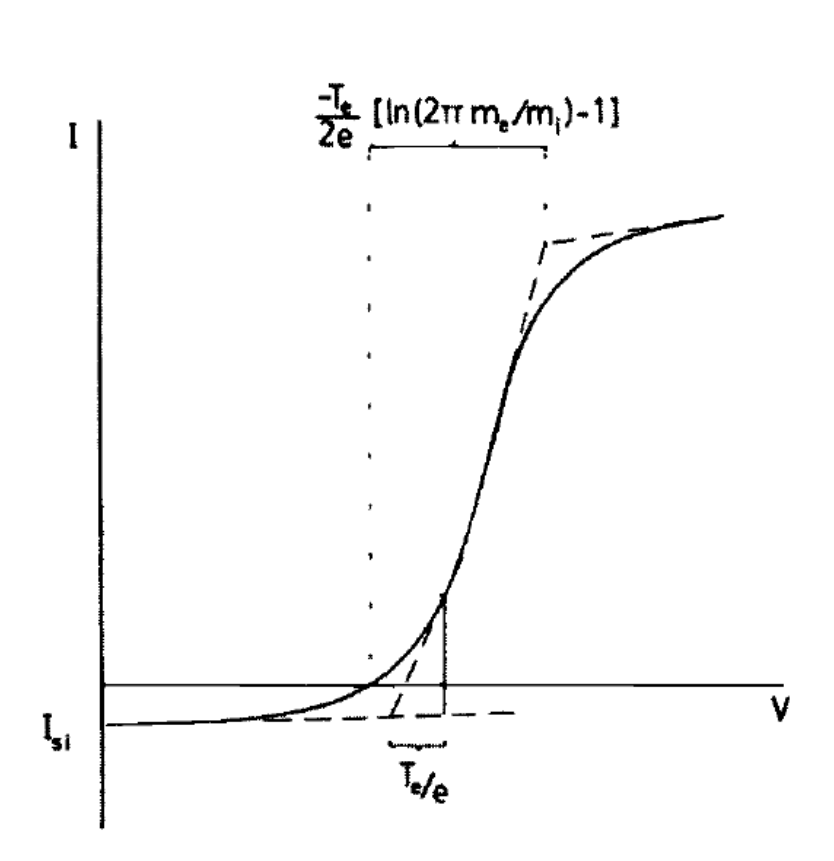




$$I_{\mathrm{es}} = \frac{1}{4} n_{s} \mathrm{exp} \left( \frac{\mathrm{eV}_{p}}{KT_{e}} \right) \bar{v}_{e} \mathrm{eA}$$

$$= \frac{1}{4} n_{0} \mathrm{eA} \sqrt{\frac{8KT_{e}}{\pi m_{e}}}$$

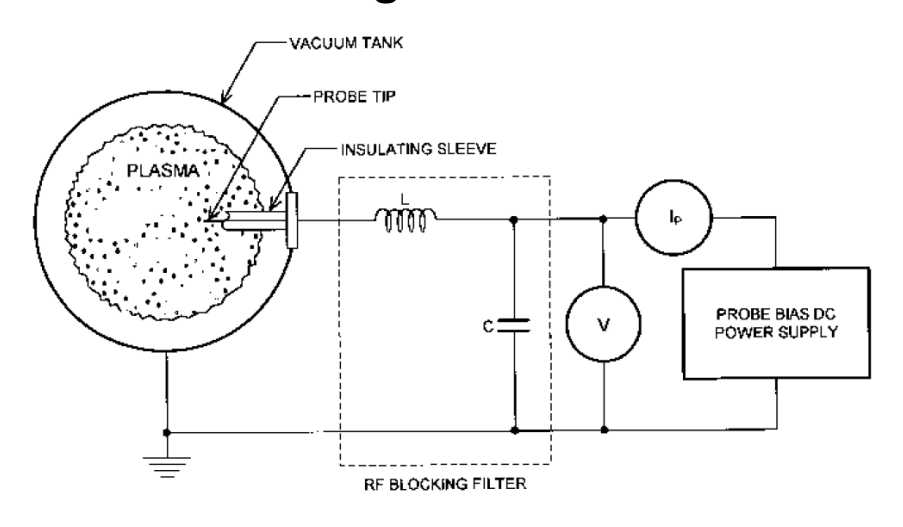
$$n_0 = \frac{4I_{\rm es}}{\rm eA} \sqrt{\frac{\pi m_e}{8KT_e}}$$

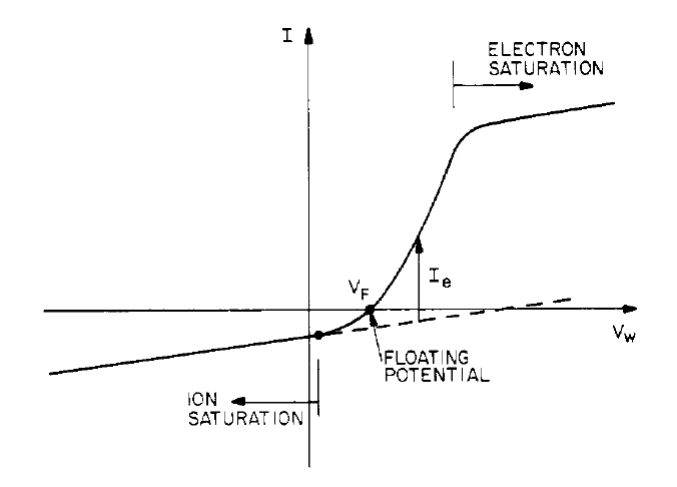


## Two Langmuir probes can be operated simultaneously

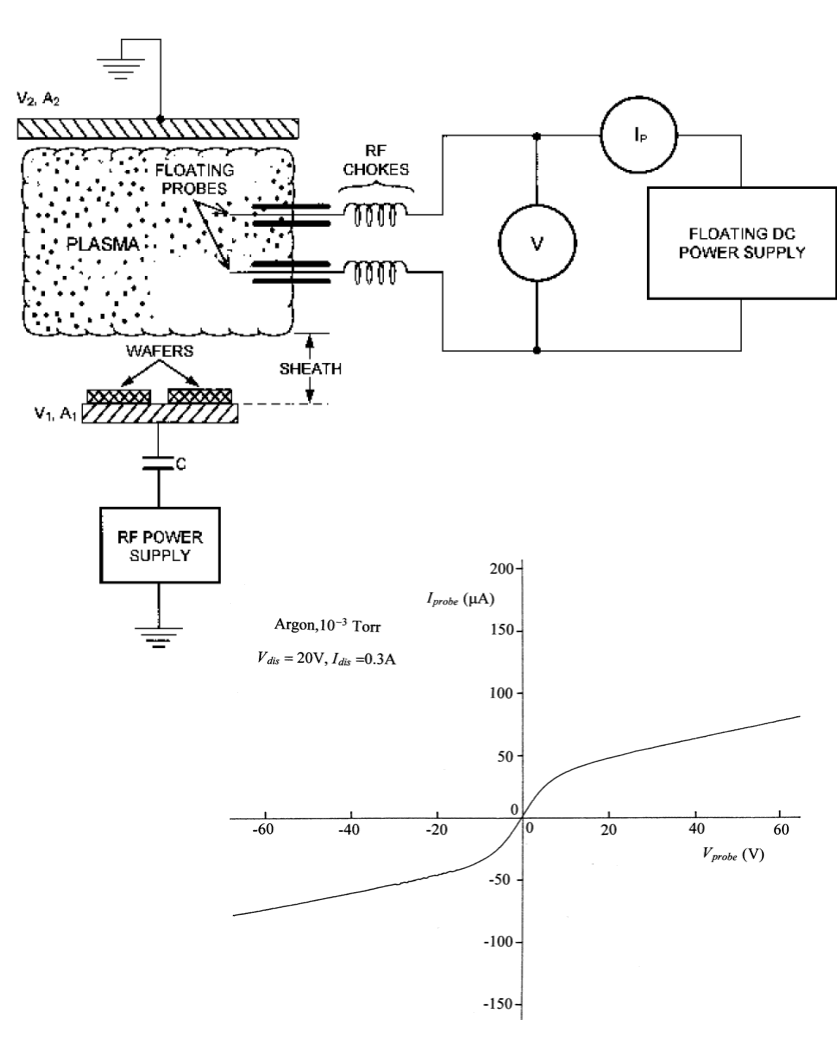


#### **Single Probe**



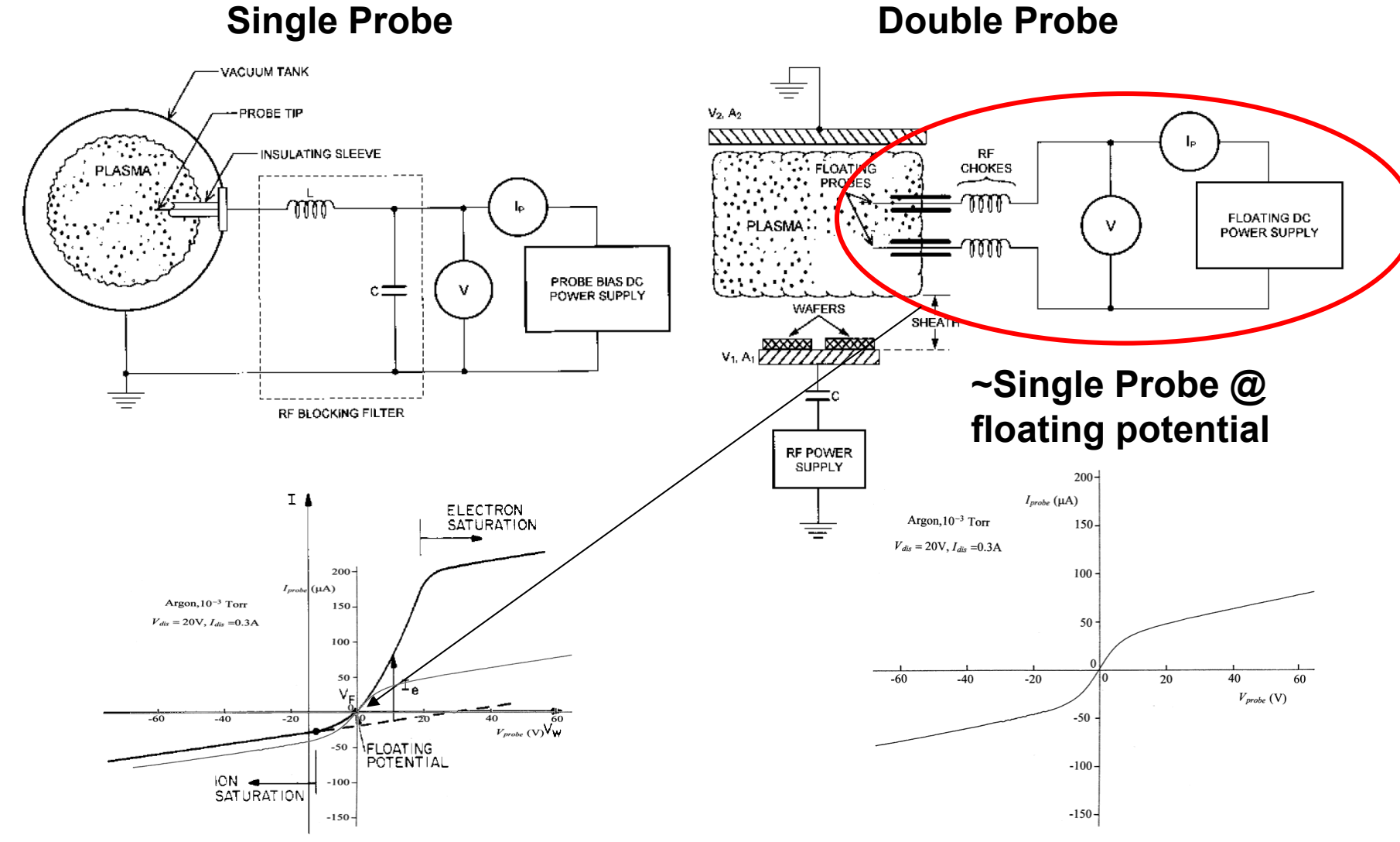


#### **Double Probe**



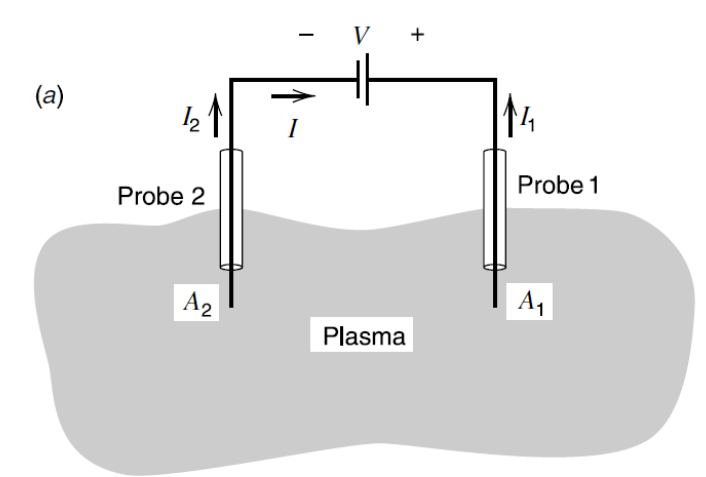
## Two Langmuir probes can be operated simultaneously





### Double Langmuir probe is not disturbed by the discharge





$$I \downarrow I_{2i} I_{$$

$$I = I_{1e} - I_{1i} = I_{2i} - I_{2e}$$

$$I_{1e} = A_1 \frac{\bar{v}_e e}{4} n_s \exp\left(\frac{eV_1}{KT_e}\right)$$

$$I_{2e} = A_2 \frac{\bar{v}_e e}{4} n_s \exp\left(\frac{eV_2}{KT_e}\right)$$

$$I_{1e} = I + I_{1i}$$
  $I_{2e} = I_{2i} - I$ 

$$\frac{I + I_{1i}}{I_{2i} - I} = \frac{A_1}{A_2} \exp\left(\frac{e(V_1 - V_2)}{KT_e}\right)$$

$$= \frac{A_1}{A_2} \exp\left(\frac{eV}{KT_e}\right)$$

$$I = I_i \tanh\left(\frac{eV}{2KT_e}\right)$$
  $\frac{dI}{dV}|_{v=0} = \frac{eI_i}{2KT_e}$ 

• The net current never exceeds the ion saturation current, minimizing the disturbance to the discharge.

# An electromagnetic wave is described using Maxwell's equation



$$\begin{cases}
\nabla \times \vec{E} &= -\frac{\partial \vec{B}}{\partial t} \\
\nabla \times \vec{B} &= \mu_0 \vec{j} + \epsilon_0 \mu_0 \frac{\partial \vec{E}}{\partial t}
\end{cases}$$

$$\nabla \times \left(\nabla \times \vec{E}\right) = -\frac{\partial}{\partial t} \left(\nabla \times \vec{B}\right) = -\frac{\partial}{\partial t} \left(\mu_0 \vec{j} + \epsilon_0 \mu_0 \frac{\partial \vec{E}}{\partial t}\right)$$

Conductivity:  $\vec{j} = \overleftarrow{\sigma} \cdot \vec{E}$ 

$$\nabla \times \left( \nabla \times \vec{E} \right) = -\frac{\partial}{\partial t} \left( \nabla \times \vec{E} \right) = -\frac{\partial}{\partial t} \left( \mu_0 \overleftrightarrow{\sigma} \cdot \vec{E} + \epsilon_0 \mu_0 \frac{\partial \vec{E}}{\partial t} \right)$$

Plane wave: 
$$\vec{E} = \vec{E} \exp \left[ i \left( \vec{k} \cdot \vec{x} - \omega t \right) \right]$$

$$i\vec{k} \times \left(i\vec{k} \times \vec{E}\right) = i\omega \left(\mu_0 \overleftrightarrow{\sigma} \cdot \vec{E} - i\omega\epsilon_0\mu_0\vec{E}\right)$$

## Dispersion relation is determined by the determinant of the matrix of coefficient



$$-\vec{k}\times\left(\vec{k}\times\vec{E}\right) \ = \ -\left[\left(\vec{k}\cdot\vec{E}\right)\vec{k}-\left(\vec{k}\cdot\vec{k}\right)\vec{E}\right] = -\left(\vec{k}\colon\vec{k}\right)\vec{E} + k^2\vec{E}$$

$$i\omega\left(\mu_0 \overleftrightarrow{\sigma} \cdot \vec{E} - i\omega\epsilon_0\mu_0\vec{E}\right) = i\omega\left(\mu_0 \overleftrightarrow{\sigma} \cdot \vec{E} - \frac{i\omega}{c^2}\vec{E}\right) = \frac{\omega^2}{c^2} \left[-\frac{c^2}{i\omega}\mu_0 \overleftrightarrow{\sigma} \cdot \vec{E} + \vec{E}\right]$$
$$= \frac{\omega^2}{c^2} \left(\overleftrightarrow{1} + \frac{i}{\omega\epsilon_0} \overleftrightarrow{\sigma}\right) \vec{E} \equiv \frac{\omega^2}{c^2} \overleftrightarrow{\varepsilon} \vec{E}$$

Dielectric tensor: 
$$\overleftarrow{\varepsilon} \equiv \overleftarrow{1} + \frac{i}{\omega \epsilon_0} \overleftarrow{\sigma}$$

$$i\vec{k} \times \left(i\vec{k} \times \vec{E}\right) = i\omega \left(\mu_0 \overleftrightarrow{\sigma} \cdot \vec{E} - i\omega\epsilon_0\mu_0\vec{E}\right)$$

$$\left(\vec{k} : \vec{k} - k^2 \overleftrightarrow{1} + \frac{\omega^2}{c^2} \overleftrightarrow{\varepsilon}\right) \vec{E} = 0$$

$$\det\left(\vec{k} : \vec{k} - k^2 \overleftrightarrow{1} + \frac{\omega^2}{c^2} \overleftrightarrow{\varepsilon}\right) = 0$$

#### Two mode can propagate in the plasma



$$\det\left(\vec{k} : \vec{k} - k^2 \overleftarrow{1} + \frac{\omega^2}{c^2} \overleftarrow{\varepsilon}\right) = 0$$

#### Assuming the wave propagates along the z direction and isotropic medium:

$$\vec{k} = k\hat{z}$$

$$\Leftrightarrow = \varepsilon \overleftrightarrow{1}$$

$$\begin{pmatrix} -k^2 + \frac{\omega^2}{c^2} \varepsilon & 0 & 0\\ 0 & -k^2 + \frac{\omega^2}{c^2} \varepsilon & 0\\ 0 & 0 & \frac{\omega^2}{c^2} \varepsilon \end{pmatrix} = 0$$

$$\left(-k^2 + \frac{\omega^2}{c^2}\varepsilon\right)^2 \frac{\omega^2}{c^2}\varepsilon = 0$$

$$\frac{\omega^2}{c^2}\varepsilon = 0$$

$$\left(-k^2 + \frac{\omega^2}{c^2}\varepsilon\right)^2 = 0$$

Longitudinal wave

**Transverse wave** 

### The reflective index is determined by the dielectric



Longitudinal wave:

$$\frac{\omega^2}{c^2}\varepsilon = 0$$

$$\begin{pmatrix} -k^2 + \frac{\omega^2}{c^2} \varepsilon & 0 & 0 \\ 0 & -k^2 + \frac{\omega^2}{c^2} \varepsilon & 0 \\ 0 & 0 & 0 \end{pmatrix} \begin{pmatrix} E_{\mathbf{x}} \\ E_{\mathbf{y}} \\ E_{\mathbf{z}} \end{pmatrix} = 0 = \begin{pmatrix} \left( -k^2 + \frac{\omega^2}{c^2} \varepsilon \right) E_{\mathbf{x}} \\ \left( -k^2 + \frac{\omega^2}{c^2} \varepsilon \right) E_{\mathbf{y}} \\ 0 \end{pmatrix}$$

$$E_{\mathbf{x}} = E_{\mathbf{v}} = 0$$

Transverse wave:

$$\left(-k^2 + \frac{\omega^2}{c^2}\varepsilon\right)^2 = 0$$

$$\begin{pmatrix} 0 & 0 & 0 \\ 0 & 0 & 0 \\ 0 & 0 & \frac{\omega^2}{c^2} \varepsilon \end{pmatrix} \begin{pmatrix} E_{\mathbf{x}} \\ E_{\mathbf{y}} \\ E_{\mathbf{z}} \end{pmatrix} = 0$$

$$E_{\mathbf{z}} = 0$$

Reflective index: 
$$n \equiv \frac{kc}{\omega} = \varepsilon^{1/2}$$

## Conductivity tensor can be determined from equation of motion for electron



$$m_{e} \frac{\partial \vec{v}}{\partial t} = -e \left( \vec{E} + \vec{v} \times \vec{B} \right) \qquad \vec{v} = \vec{v} \exp \left[ i \left( \vec{k} \cdot \vec{x} - \omega t \right) \right]$$

$$\begin{cases}
-i\omega m_{e} v_{x} &= -e E_{x} - e B_{0} v_{y} \\
-i\omega m_{e} v_{y} &= -e E_{y} + e B_{0} v_{x} \\
-i\omega m_{e} v_{z} &= -e E_{z}
\end{cases} \qquad \Omega \equiv \frac{e B_{0}}{m_{e}} \qquad \Sigma$$

$$\begin{cases}
v_{x} &= -\frac{ie}{\omega m_{e}} \frac{1}{1 - \Omega^{2} / \omega^{2}} \left( E_{x} - i \frac{\Omega}{\omega} E_{y} \right) & \vec{j} = -e n_{e} \vec{v}_{e} \equiv \vec{\sigma} \vec{E} \\
v_{y} &= -\frac{ie}{\omega m_{e}} \frac{1}{1 - \Omega^{2} / \omega^{2}} \left( i \frac{\Omega}{\omega} E_{x} + E_{y} \right) & \vec{j} = -e n_{e} \vec{v}_{e} \equiv \vec{\sigma} \vec{E} \\
v_{z} &= -\frac{ie}{\omega m_{e}} E_{z}
\end{cases}$$

$$\vec{\sigma} = -e n_{e} \left( \frac{-ie}{\omega m_{e}} \right) \frac{1}{1 - \Omega^{2} / \omega^{2}} \left( i \frac{1}{i \frac{\Omega}{\omega}} \frac{-i \frac{\Omega}{\omega}}{1} \frac{0}{0} \\
0 & 0 & 1 - \frac{\Omega^{2}}{\omega^{2}} \right)$$

$$= i \frac{n_{e} e^{2}}{\omega m_{e}} \frac{1}{1 - \Omega^{2} / \omega^{2}} \left( i \frac{\Omega}{\omega} \frac{1}{1} \frac{0}{0} \\
0 & 0 & 1 - \frac{\Omega^{2}}{\omega^{2}} \right)$$

#### Dielectric tensor is obtained from conductivity tensor



$$\frac{i}{\omega\epsilon_{0}} \stackrel{\longleftrightarrow}{\longleftrightarrow} = -\frac{n_{e}e^{2}}{\epsilon_{0}m_{e}} \frac{1}{\omega^{2}} \frac{1}{1 - \Omega^{2}/\omega^{2}} \begin{pmatrix} \frac{1}{i} & -i\frac{\Omega}{\omega} & 0\\ i\frac{\Omega}{\omega} & 1 & 0\\ 0 & 0 & 1 - \frac{\Omega^{2}}{\omega^{2}} \end{pmatrix}$$

$$= -\frac{\omega_{p}^{2}}{\omega^{2} - \Omega^{2}} \begin{pmatrix} \frac{1}{i} & -i\frac{\Omega}{\omega} & 0\\ i\frac{\Omega}{\omega} & 1 & 0\\ 0 & 0 & 1 - \frac{\Omega^{2}}{\omega^{2}} \end{pmatrix}$$

$$\omega_{p}^{2} = \frac{n_{e}e^{2}}{\epsilon_{0}m_{e}}$$

$$= \begin{pmatrix} -\frac{\omega_{p}^{2}}{\omega^{2} - \Omega^{2}} & i\frac{\Omega}{\omega} \frac{\omega_{p}^{2}}{\omega^{2} - \Omega^{2}} & 0\\ -i\frac{\Omega}{\omega} \frac{\omega_{p}^{2}}{\omega^{2} - \Omega^{2}} & -\frac{\omega_{p}^{2}}{\omega^{2} - \Omega^{2}} & 0\\ 0 & 0 & -\frac{\omega_{p}^{2}}{\omega^{2}} \end{pmatrix}$$

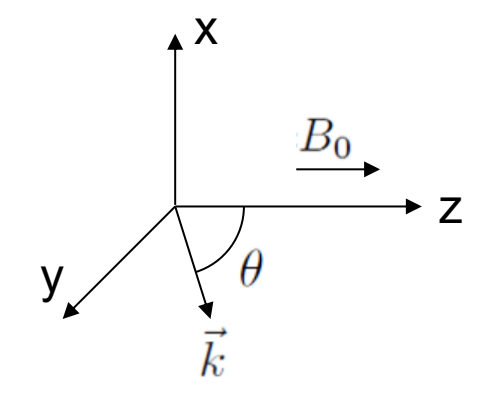
### Assuming the wave is on the yz plane



$$\text{let} \quad X \equiv \frac{\omega_{\mathrm{p}}^2}{\omega^2}$$

$$Y \equiv \frac{\Omega}{\omega}$$

$$\mathbf{let} \quad X \equiv \frac{\omega_{\mathrm{p}}^2}{\omega^2} \qquad Y \equiv \frac{\Omega}{\omega} \qquad \qquad \stackrel{\longleftrightarrow}{\varepsilon} \quad = \quad \left( \begin{array}{ccc} 1 - \frac{X}{1 - Y^2} & i \frac{XY}{1 - Y^2} & 0 \\ -i \frac{XY}{1 - Y^2} & 1 - \frac{X}{1 - Y^2} & 0 \\ 0 & 0 & 1 - X \end{array} \right)$$



$$\vec{k} = k \left( 0, \sin \theta, \cos \theta \right)$$

$$k_{\mathbf{i}} = 0 , k_{\mathbf{j}} = k \sin \theta , k_{\mathbf{k}} = k \cos \theta$$

$$\vec{k} \colon \vec{k} = \begin{pmatrix} 0 \\ k \sin \theta \\ k \cos \theta \end{pmatrix} \cdot \begin{pmatrix} 0 & k \sin \theta & k \cos \theta \end{pmatrix} = \begin{pmatrix} 0 & 0 & 0 \\ 0 & \sin^2 \theta & \sin \theta \cos \theta \\ 0 & \sin \theta \cos \theta & \cos^2 \theta \end{pmatrix}$$

$$n \equiv \frac{kc}{\omega} \qquad \qquad \frac{\omega^2}{c^2} \overleftrightarrow{\varepsilon} = \frac{k^2 \omega^2}{k^2 c^2} \overleftrightarrow{\varepsilon} = \frac{k^2}{n^2} \overleftrightarrow{\varepsilon}$$

$$\det\left(\vec{k} : \vec{k} - k^2 \overleftarrow{1} + \frac{\omega^2}{c^2} \overleftarrow{\varepsilon}\right) = 0$$

#### Reflective index



$$\begin{vmatrix} -k^2 + \frac{k^2}{n^2} \left( 1 - \frac{X}{1 - Y^2} \right) & i \frac{k^2}{n^2} \frac{XY}{1 - Y^2} & 0 \\ -i \frac{k^2}{n^2} \frac{XY}{1 - Y^2} & k^2 \sin^2 \theta - k^2 + \frac{k^2}{n^2} \left( 1 - \frac{X}{1 - Y^2} \right) & k^2 \sin \theta \cos \theta \\ 0 & k^2 \sin \theta \cos \theta & k^2 \cos^2 \theta - k^2 + \frac{k^2}{n^2} \left( 1 - X \right) \end{vmatrix} = 0$$

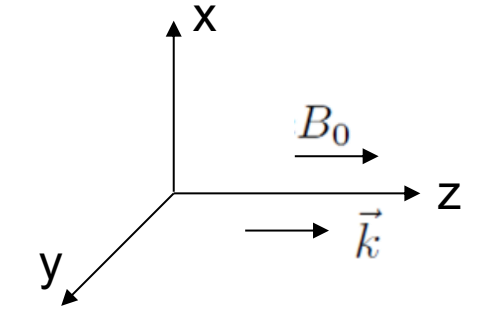
$$\begin{vmatrix} -n^2 + 1 - \frac{X}{1 - Y^2} & i\frac{XY}{1 - Y^2} & 0 \\ -i\frac{XY}{1 - Y^2} & -n^2\cos^2\theta + 1 - \frac{X}{1 - Y^2} & n^2\sin\theta\cos\theta \\ 0 & n^2\sin\theta\cos\theta & -n^2\sin^2\theta + 1 - X \end{vmatrix} = 0$$

$$n^{2} = 1 - \frac{X(1-X)}{1 - X - \frac{1}{2}Y^{2}\sin^{2}\theta \pm \left[\left(\frac{1}{2}Y^{2}\sin^{2}\theta\right)^{2} + (1-X)^{2}Y^{2}\cos^{2}\theta\right]^{1/2}}$$

## Wave is circular polarized propagating along the magnetic field



• Parallel to  $\mathbf{B_0}$   $(\theta = 0)$ 



$$n^2 = 1 - \frac{X (1 - X)}{1 - X \pm \left[ (1 - X)^2 Y^2 \right]^{1/2}} = 1 - \frac{X}{1 \pm Y} = 1 - \frac{\omega_{\rm p}^2 / \omega^2}{1 \pm \Omega / \omega} = 1 - \frac{\omega_{\rm p}^2}{\omega (\omega \pm \Omega)}$$

$$\begin{pmatrix} -n^2 + 1 - \frac{X}{1 - Y^2} & i\frac{XY}{1 - Y^2} & 0 \\ -i\frac{XY}{1 - Y^2} & -n^2\cos^2\theta + 1 - \frac{X}{1 - Y^2} & 0 \\ 0 & 0 & 1 - X \end{pmatrix} \begin{pmatrix} E_{\mathbf{x}} \\ E_{\mathbf{y}} \\ E_{\mathbf{z}} \end{pmatrix} = 0$$

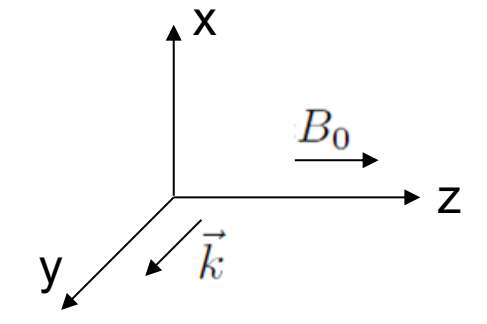
$$\left(-n^2 + 1 - \frac{X}{1 - Y^2}\right)E_{\mathbf{x}} + i\frac{XY}{1 - Y^2}E_{\mathbf{y}} = \frac{\mp XY}{1 - Y^2}E_{\mathbf{x}} + i\frac{XY}{1 - Y^2}E_{\mathbf{y}} = 0$$

 $\frac{E_{\mathrm{x}}}{E_{\mathrm{x}}} = \pm i$  Left hang circular (LHC) or right hang circular (RHC) polarized.

# Electric field is not necessary parallel to the propagating direction which is perpendicular to B<sub>0</sub>



• Perpendicular to  $B_0$   $\left(\theta = \frac{\pi}{2}\right)$ 



$$n^2 = 1 - \frac{X(1-X)}{1-X-\frac{1}{2}Y^2 \pm \frac{1}{2}Y^2} = 1 - X \text{ or } 1 - \frac{X(1-X)}{1-X-Y^2}$$

$$\begin{pmatrix} -n^2 + 1 - \frac{X}{1 - Y^2} & i\frac{XY}{1 - Y^2} & 0 \\ -i\frac{XY}{1 - Y^2} & 1 - \frac{X}{1 - Y^2} & 0 \\ 0 & 0 & -n^2 + 1 - X \end{pmatrix} \begin{pmatrix} E_{\mathbf{x}} \\ E_{\mathbf{y}} \\ E_{\mathbf{z}} \end{pmatrix} = 0$$

$$n^2=1-rac{\omega_{
m p}^2}{\omega^2}$$
  $E_{
m x}=E_{
m y}=0$  Ordinary wave (O-wave)

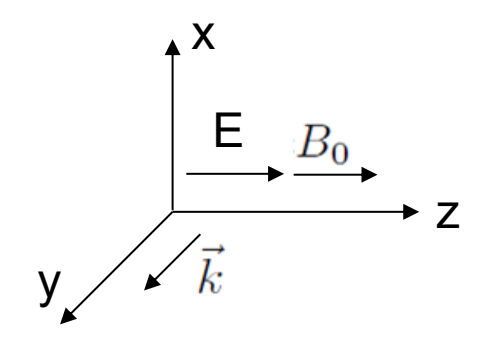
$$n^{2} = 1 - \frac{\omega_{\rm p}^{2} \left(1 - \omega_{\rm p}^{2} / \omega^{2}\right)}{\omega^{2} - \omega_{\rm p}^{2} - \Omega^{2}} \quad \frac{E_{\rm x}}{E_{\rm y}} = -i\omega \left(\frac{\omega^{2} - \omega_{\rm p}^{2} - \Omega^{2}}{\omega_{\rm p}^{2}\Omega}\right) \qquad E_{\rm z} = 0$$

**Extraordinary wave (E-wave)** 

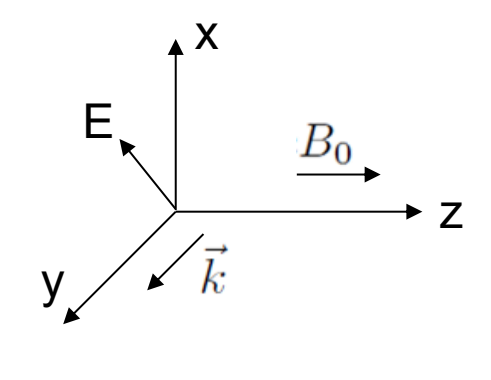
# The electric field of an extraordinary wave rotates elliptically

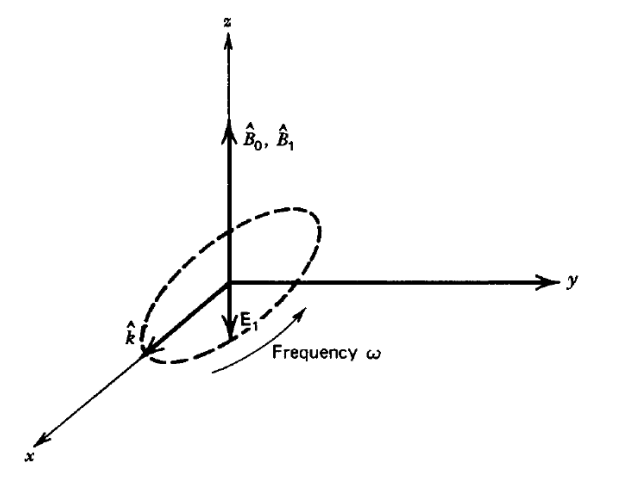


#### **Ordinary wave (O-wave)**



#### **Extraordinary wave (E-wave)**





## Electromagnetic wave can be used to measure the density or the magnetic field in the plasma



Nonmagnetized isotropic plasma (interferometer needed):

$$n^{2} = 1 - \frac{X(1 - X)}{1 - X - \frac{1}{2}Y^{2}\sin^{2}\theta \pm \left[\left(\frac{1}{2}Y^{2}\sin^{2}\theta\right)^{2} + (1 - X)^{2}Y^{2}\cos^{2}\theta\right]^{1/2}}$$

$$= 1 - X = 1 - \frac{\omega_{\mathrm{p}}^{2}}{\omega^{2}} = 1 - \frac{n_{\mathrm{e}}}{n_{\mathrm{cr}}} \qquad \left(\mathbf{Y} \equiv \frac{\mathbf{\Omega}}{\boldsymbol{\omega}} \equiv \mathbf{0}\right)$$

$$\mathbf{Note:} \qquad \omega_{\mathrm{p}}^{2} = \frac{n_{\mathrm{e}}e^{2}}{\epsilon_{0}m_{\mathrm{p}}} \qquad n_{\mathrm{cr}} = \frac{\epsilon_{0}m_{\mathrm{e}}\omega^{2}}{e^{2}}$$

Magnetized isotropic plasma (Polarization detected needed):

Parallel to B<sub>0</sub> 
$$n^2 = 1 - \frac{\omega_{\rm p}^2}{\omega \left(\omega \pm \Omega\right)} \qquad \qquad \frac{E_{\rm x}}{E_{\rm y}} = \pm i \qquad \Omega \equiv \frac{eB_0}{m_{\rm e}}$$

Faraday rotation: linear polarization rotation caused by the difference between the speed of LHC and RHC polarized wave.

## Electromagnetic wave can be used to measure the density or the magnetic field in the plasma



Nonmagnetized isotropic plasma (interferometer needed):

$$n^{2} = 1 - \frac{X(1 - X)}{1 - X - \frac{1}{2}Y^{2}\sin^{2}\theta \pm \left[\left(\frac{1}{2}Y^{2}\sin^{2}\theta\right)^{2} + (1 - X)^{2}Y^{2}\cos^{2}\theta\right]^{1/2}}$$

$$= 1 - X = 1 - \frac{\omega_{\mathrm{p}}^{2}}{\omega^{2}} = 1 - \frac{n_{\mathrm{e}}}{n_{\mathrm{cr}}} \qquad \left(\mathbf{Y} \equiv \frac{\mathbf{\Omega}}{\boldsymbol{\omega}} \equiv \mathbf{0}\right)$$

$$\mathbf{Note:} \qquad \omega_{\mathrm{p}}^{2} = \frac{n_{\mathrm{e}}e^{2}}{\epsilon_{0}m_{\mathrm{p}}} \qquad n_{\mathrm{cr}} = \frac{\epsilon_{0}m_{\mathrm{e}}\omega^{2}}{e^{2}}$$

Magnetized isotropic plasma (Polarization detected needed):

Parallel to 
$$B_0$$
 
$$n^2 = 1 - \frac{\omega_{\rm p}^2}{\omega \left(\omega \pm \Omega\right)} \qquad \qquad \frac{E_{\rm x}}{E_{\rm y}} = \pm i \qquad \Omega \equiv \frac{eB_0}{m_{\rm e}}$$

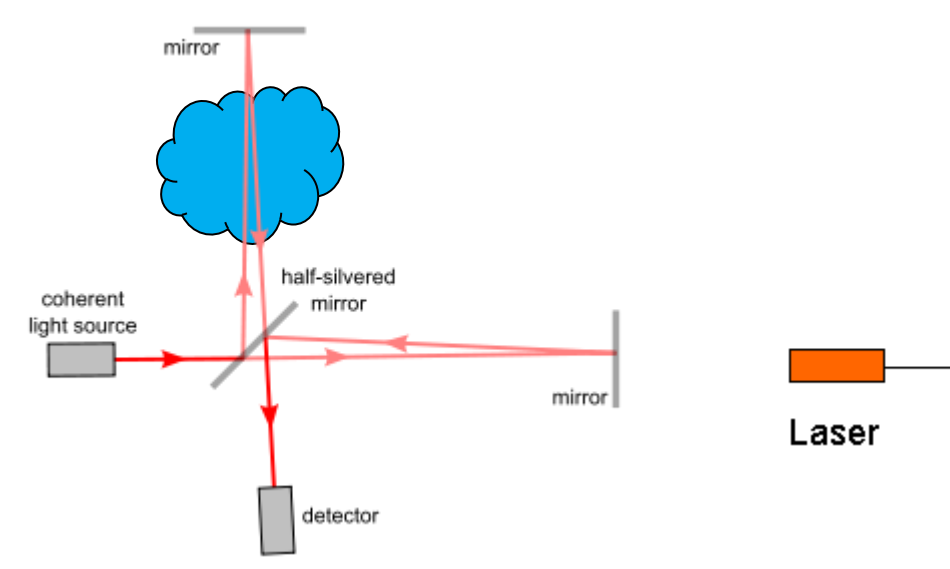
Faraday rotation: linear polarization rotation caused by the difference between the speed of LHC and RHC polarized wave.

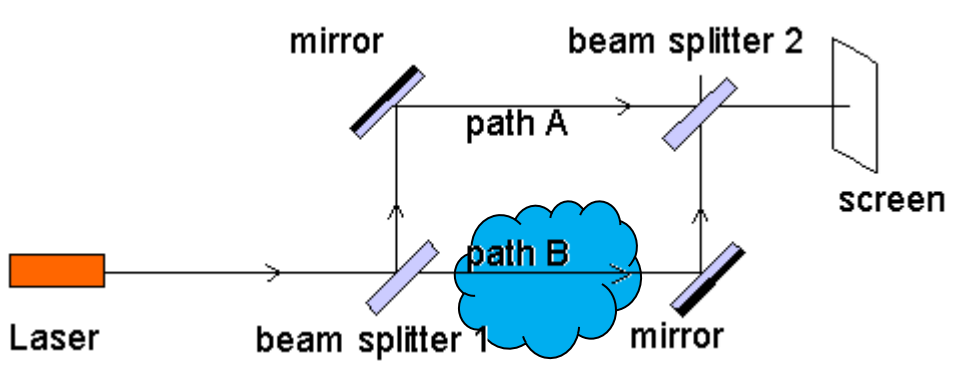
## There are two main style of interferometer



#### Michelson interferometer

#### Mach-zehnder interferometer



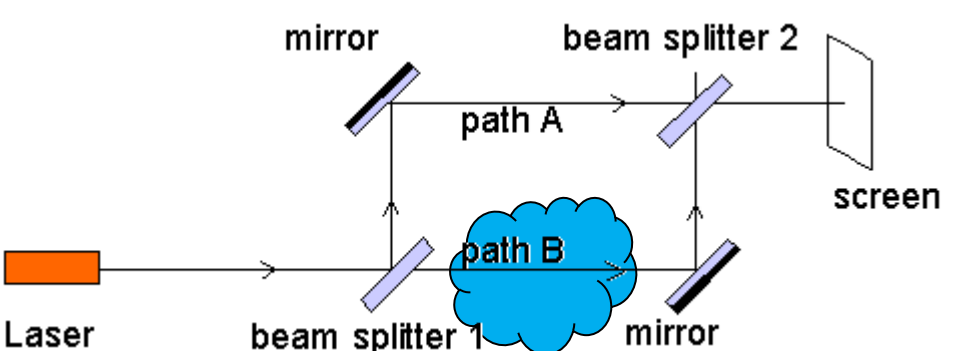


## Interference pattern are due to the phase difference between two different path



$$E_1 = E_1 \exp\left(-i\omega t\right)$$

$$E_2 = E_2 \exp\left(-i\omega t + i\phi\right)$$



$$E = E_1 + E_2 = [E_1 + E_2 \exp(i\phi)] \exp(-i\omega t)$$

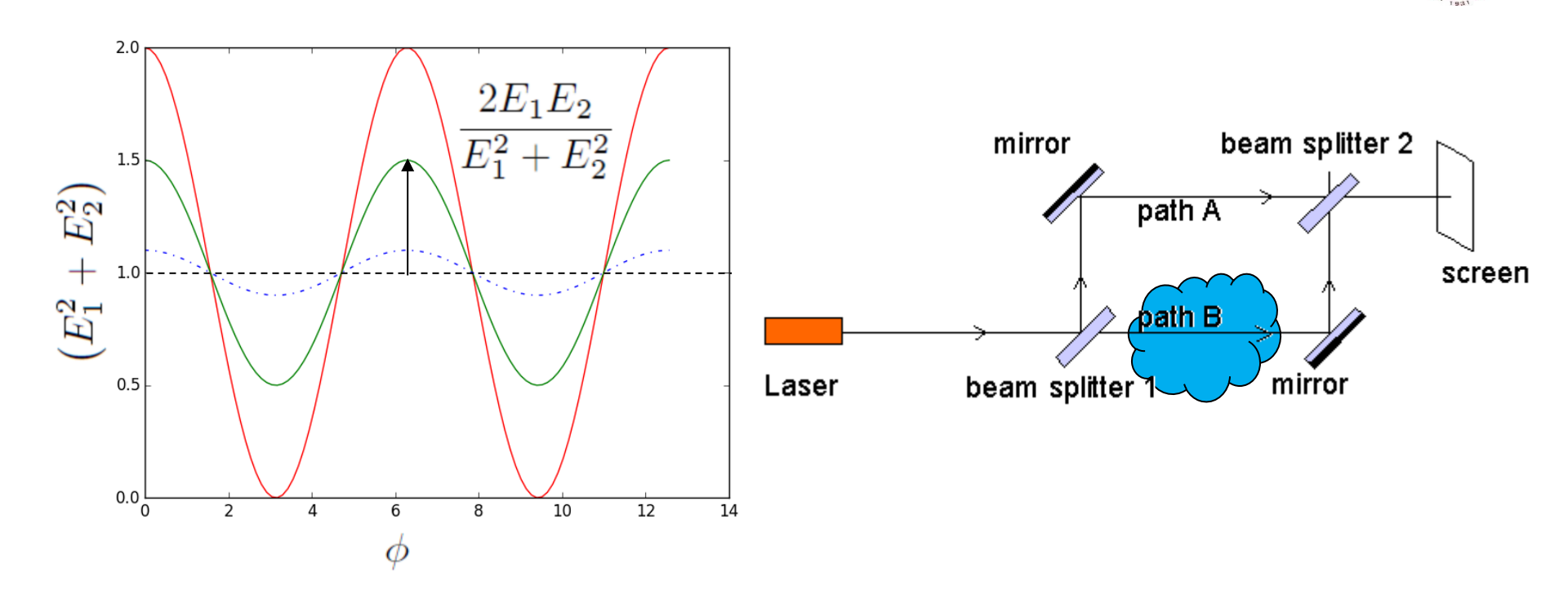
$$I = |E|^{2} = E^{*}E = [E_{1} + E_{2} \exp(-i\phi)] \exp(i\omega t) [E_{1} + E_{2} \exp(i\phi)] \exp(-i\omega t)$$

$$= E_{1}^{2} + E_{2}^{2} + E_{1}E_{2} \exp(i\phi) + E_{1}E_{2} \exp(-i\phi)$$

$$= E_{1}^{2} + E_{2}^{2} + 2E_{1}E_{2} \cos \phi$$

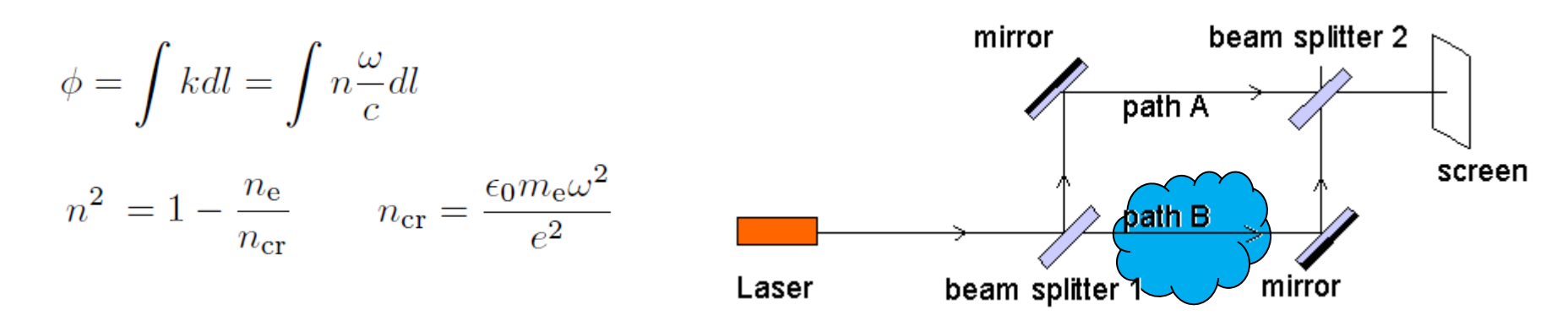
$$= (E_{1}^{2} + E_{2}^{2}) \left(1 + \frac{2E_{1}E_{2}}{E_{1}^{2} + E_{2}^{2}} \cos \phi\right)$$

## The intensity on screen depends on the phase different between two paths



$$I = \left(E_1^2 + E_2^2\right) \left(1 + \frac{2E_1 E_2}{E_1^2 + E_2^2} \cos \phi\right)$$

## The phase different depends on the line integral of the electron density along the path



$$\Delta \phi = \int (k_{\text{plasma}} - k_0) \, dl = \frac{\omega}{c} \int (n - 1) \, dl$$

$$= \frac{\omega}{c} \int \left( \sqrt{1 - \frac{n_e}{n_c}} - 1 \right) \, dl \approx \frac{\omega}{c} \int \left( 1 - \frac{1}{2} \frac{n_e}{n_c} - 1 \right) \, dl$$

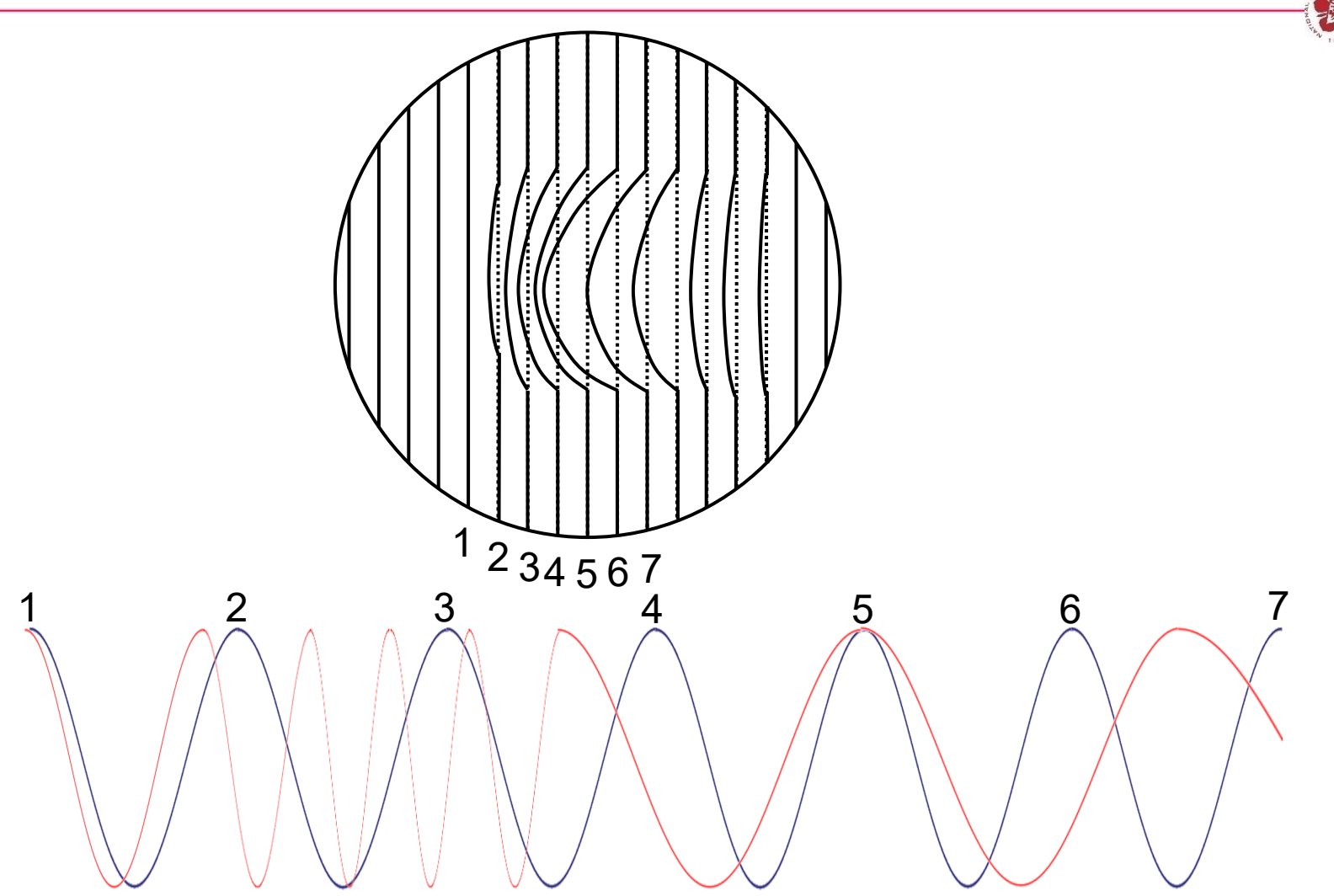
$$= -\frac{\omega}{2cn_c} \int n_e \, dl$$

Note that  $n_{
m e} << n_{
m cr}$  is assumed,

$$\sqrt{1 - \frac{n_{\rm e}}{n_{\rm cr}}} \approx 1 - \frac{1}{2} \frac{n_{\rm e}}{n_{\rm cr}}$$

# The phase is determined by comparing to the pattern without the phase shift





## Fourier transform can be used to retrieve the data from the interferometer image

$$I(x,y) = I_0(x,y) + m(x,y)\cos[2\pi\nu_0 x + \phi(x,y)] \qquad cos(x) = \frac{e^{ix} + e^{-ix}}{2}$$

$$= I_0(x,y) + \frac{1}{2}m(x,y)\left(e^{i[2\pi\nu_0 x + \phi(x,y)]} + e^{-i[2\pi\nu_0 x + \phi(x,y)]}\right)$$

$$= I_0(x,y) + \frac{1}{2}m(x,y)e^{i\phi(x,y)}e^{i2\pi\nu_0 x} + \frac{1}{2}m(x,y)e^{-i\phi(x,y)}e^{-i2\pi\nu_0 x}$$

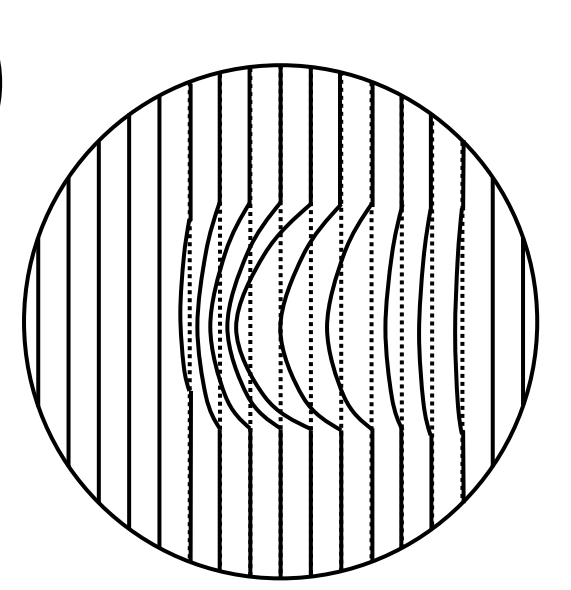
$$= I_0(x,y) + c(x,y)e^{i2\pi\nu_0 x} + c^*(x,y)e^{-i2\pi\nu_0 x}$$

$$c(x,y) \equiv \frac{1}{2}m(x,y)e^{i\phi(x,y)} \qquad \phi(x,y) = \tan^{-1}\left(\frac{\operatorname{Im}[c(x,y)]}{\operatorname{Re}[c(x,y)]}\right)$$

$$\widehat{g}(f_x, y) \equiv \text{FT}[g(x, y)]$$

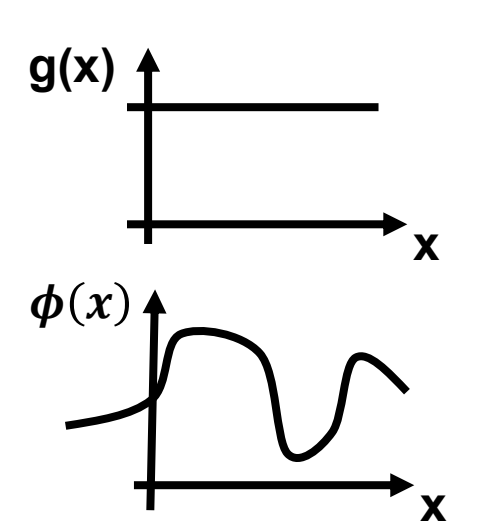
$$\widehat{g}(f_x - \nu_0, y) = \text{FT}[g(x, y)e^{i2\pi\nu_0 x}]$$

$$\hat{I}(f_x, y) = \hat{I}_0(f_x, y) + \hat{c}(f_x - \nu_0, y) + \hat{c}^*(f_x + \nu_0, y)$$

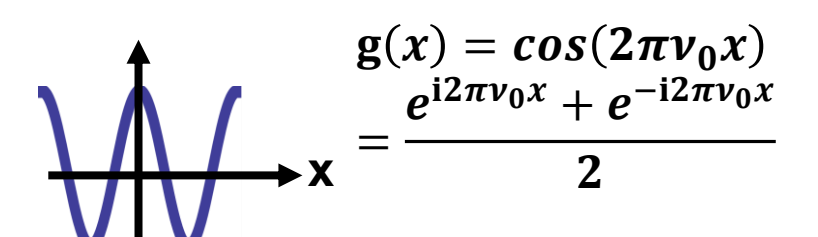


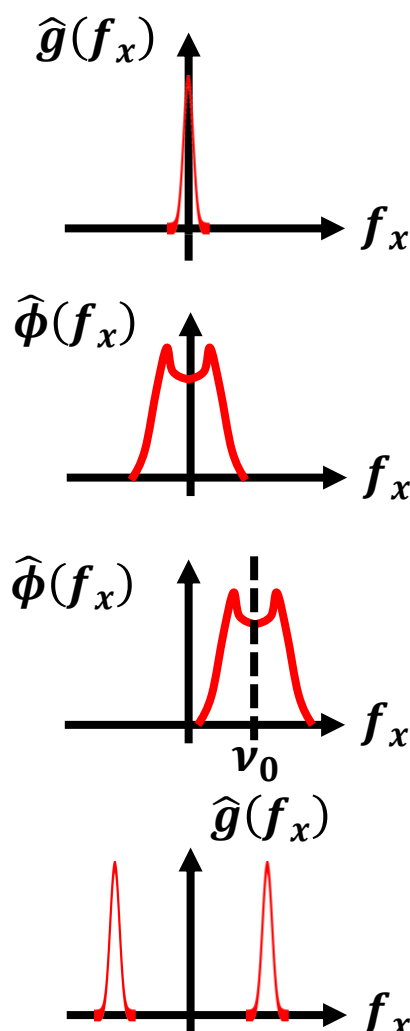
## **Basic knowledge of Fourier transform**

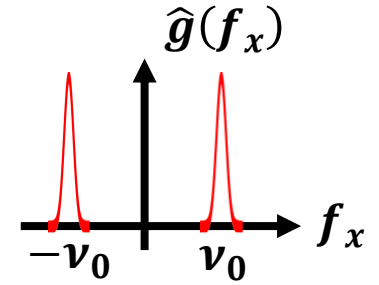




$$\mathbf{h}(x) = \boldsymbol{\phi}(x) \times e^{-\mathrm{i}2\pi\nu_0 x}$$







#### Procedure of retrieving data



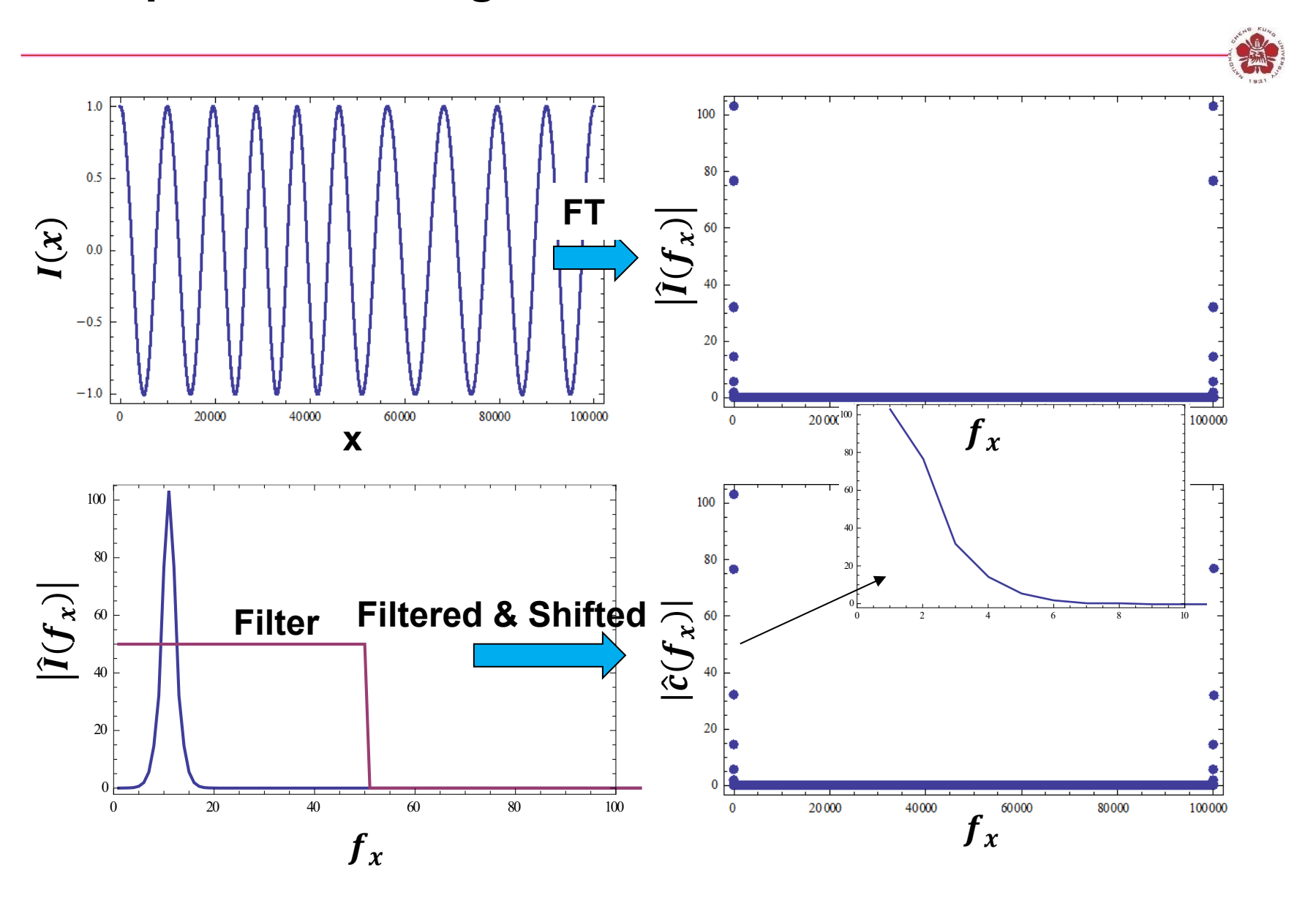
$$I(x) = I_{0}(x) + m(x)\cos[2\pi\nu_{0}x + \phi(x)]$$

$$\equiv \cos[2\pi\nu_{0}x + \phi(x)]$$

$$= c^{*}(x,y)e^{i2\pi\nu_{0}x} + c(x,y)e^{-i2\pi\nu_{0}x}$$

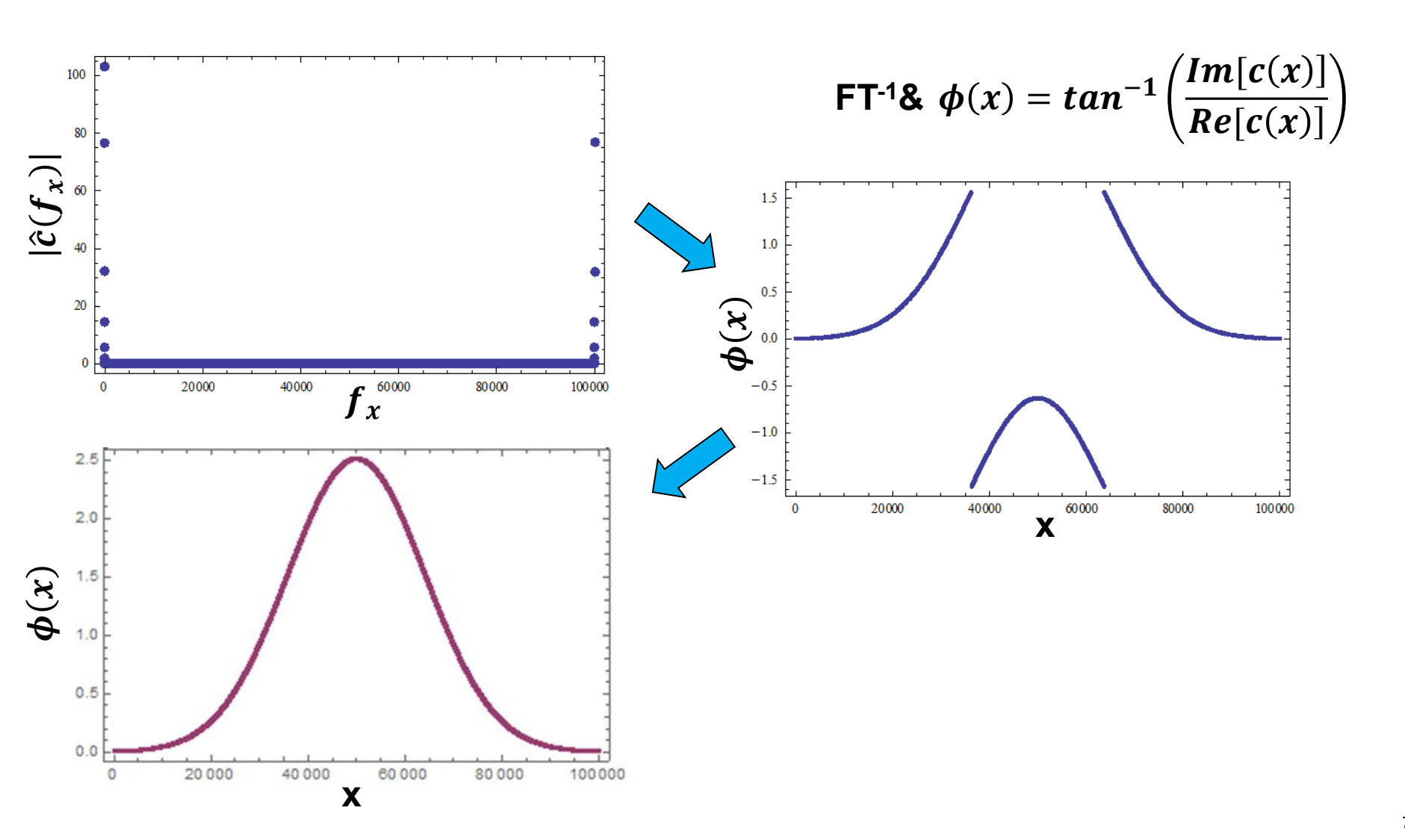
$$\hat{c}(f_{x})$$

## **Example of retrieving data from 1D interferometer**



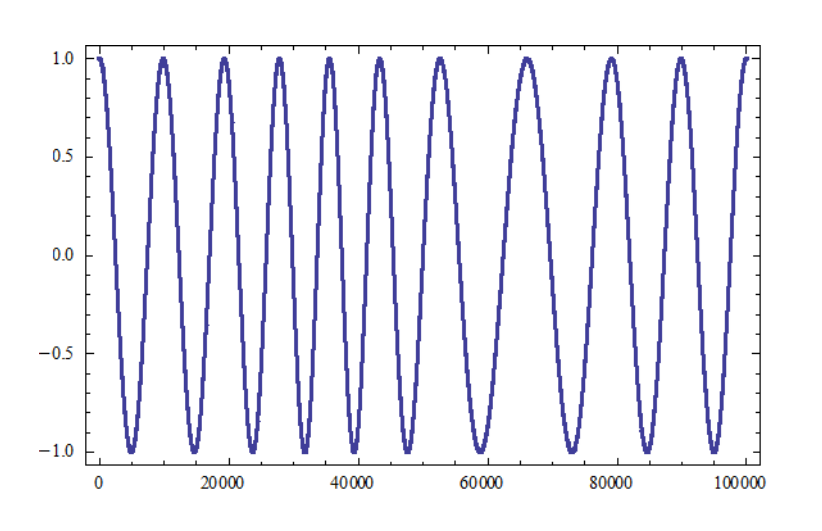
## The retrieved data need to be modified if the phase change is too much

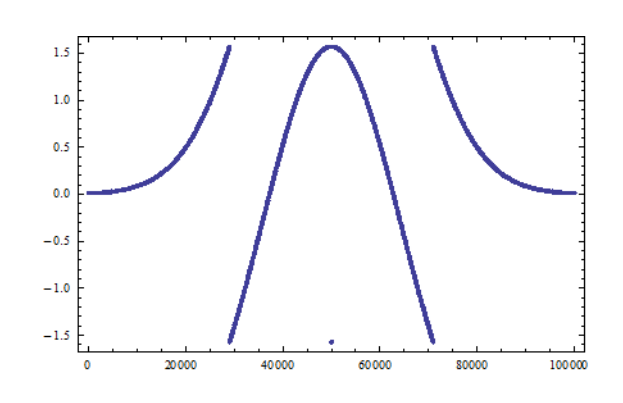


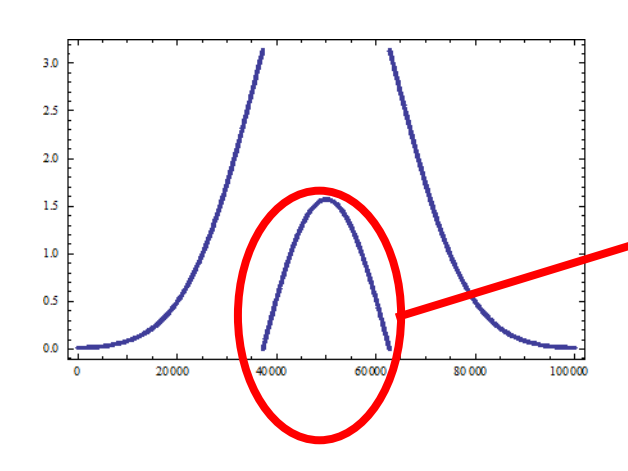


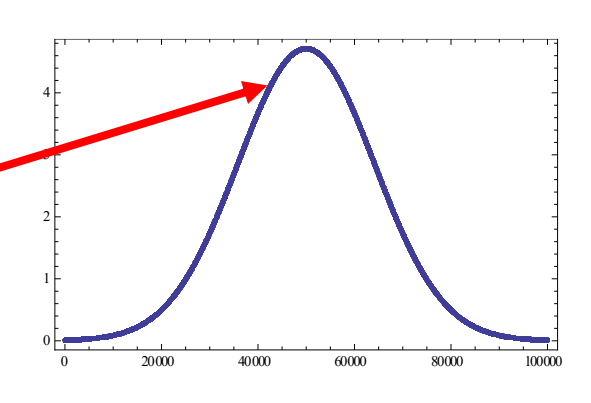
# The final phase difference needs to be determined manually since it may exceeds $2\pi$



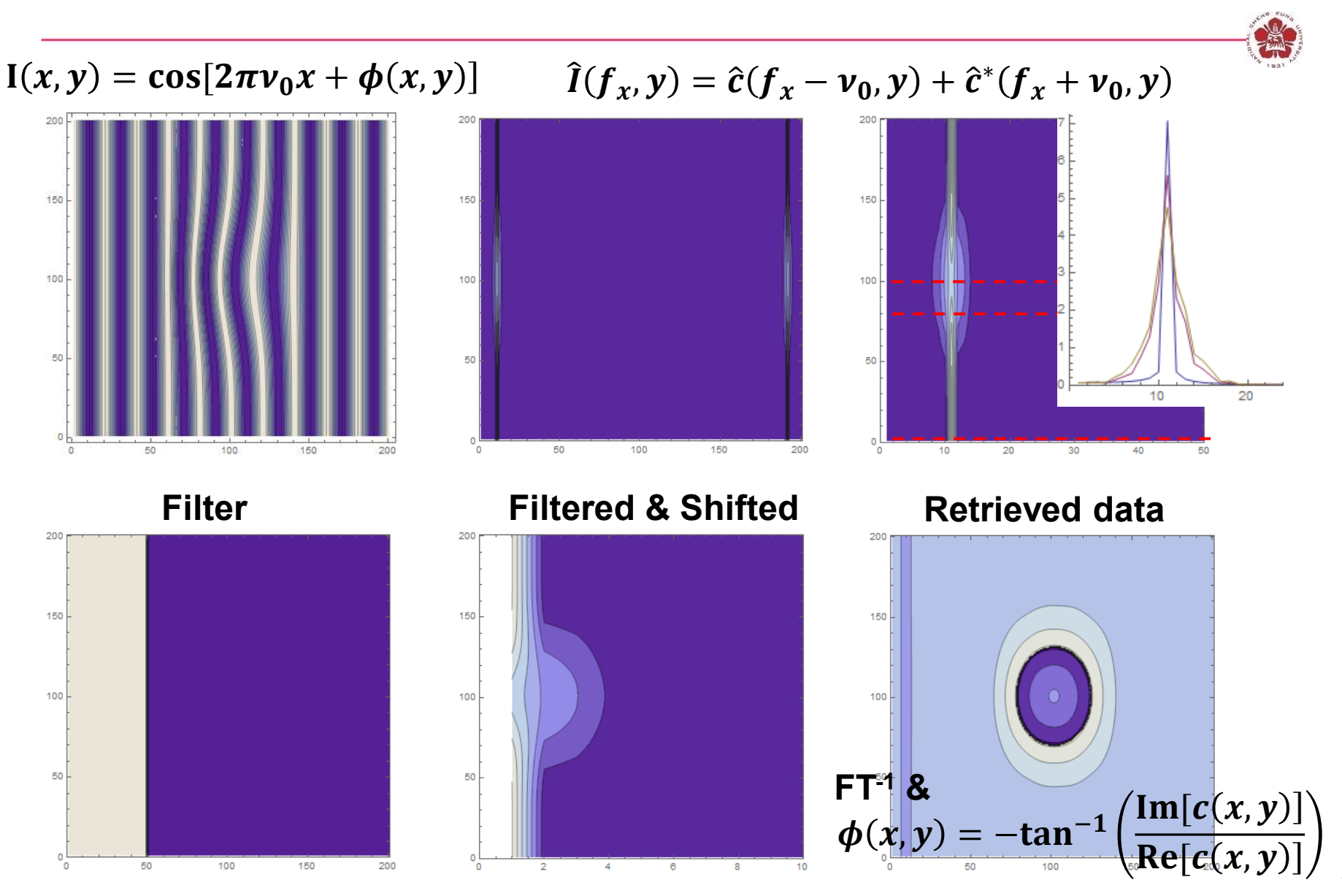






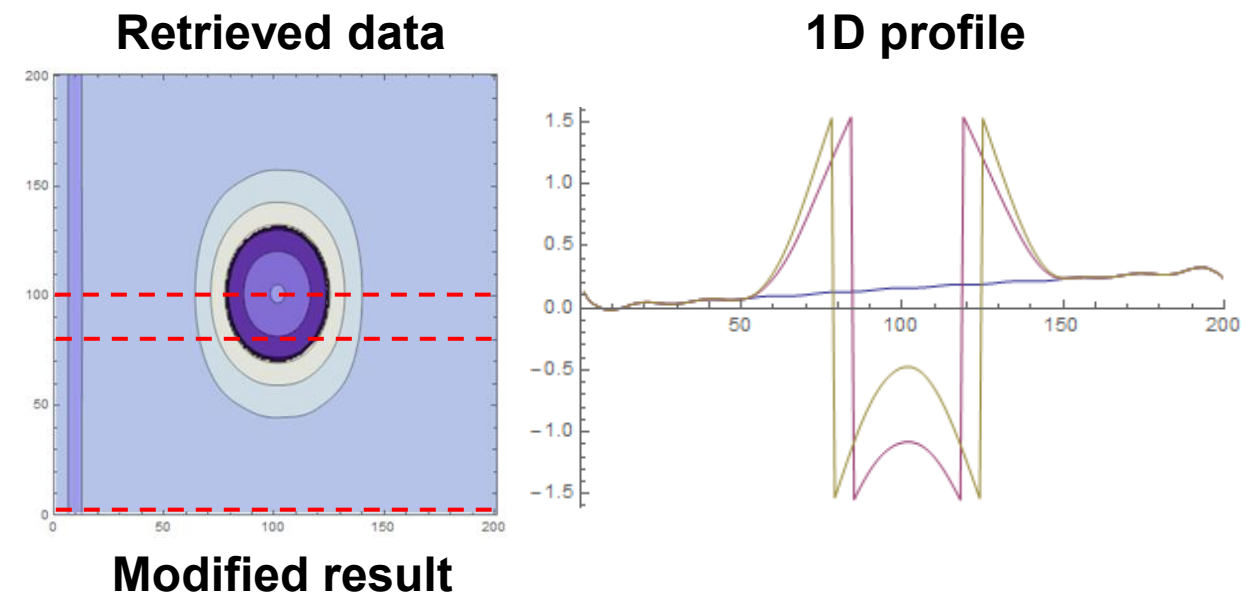


#### **Example of retrieving data from 2D interferometer**



### The retrieved data may need to be modified if the phase change is too large

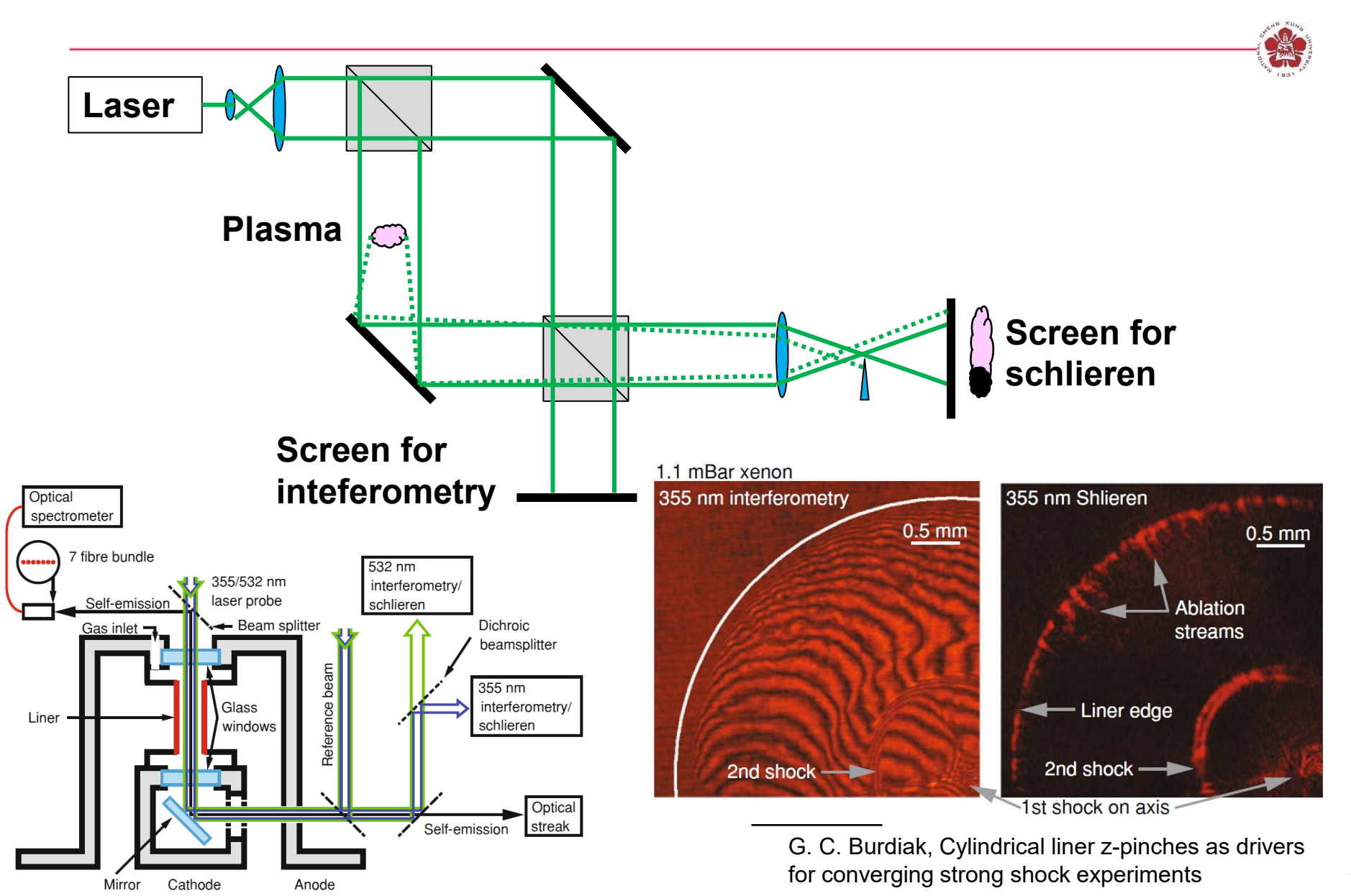




150

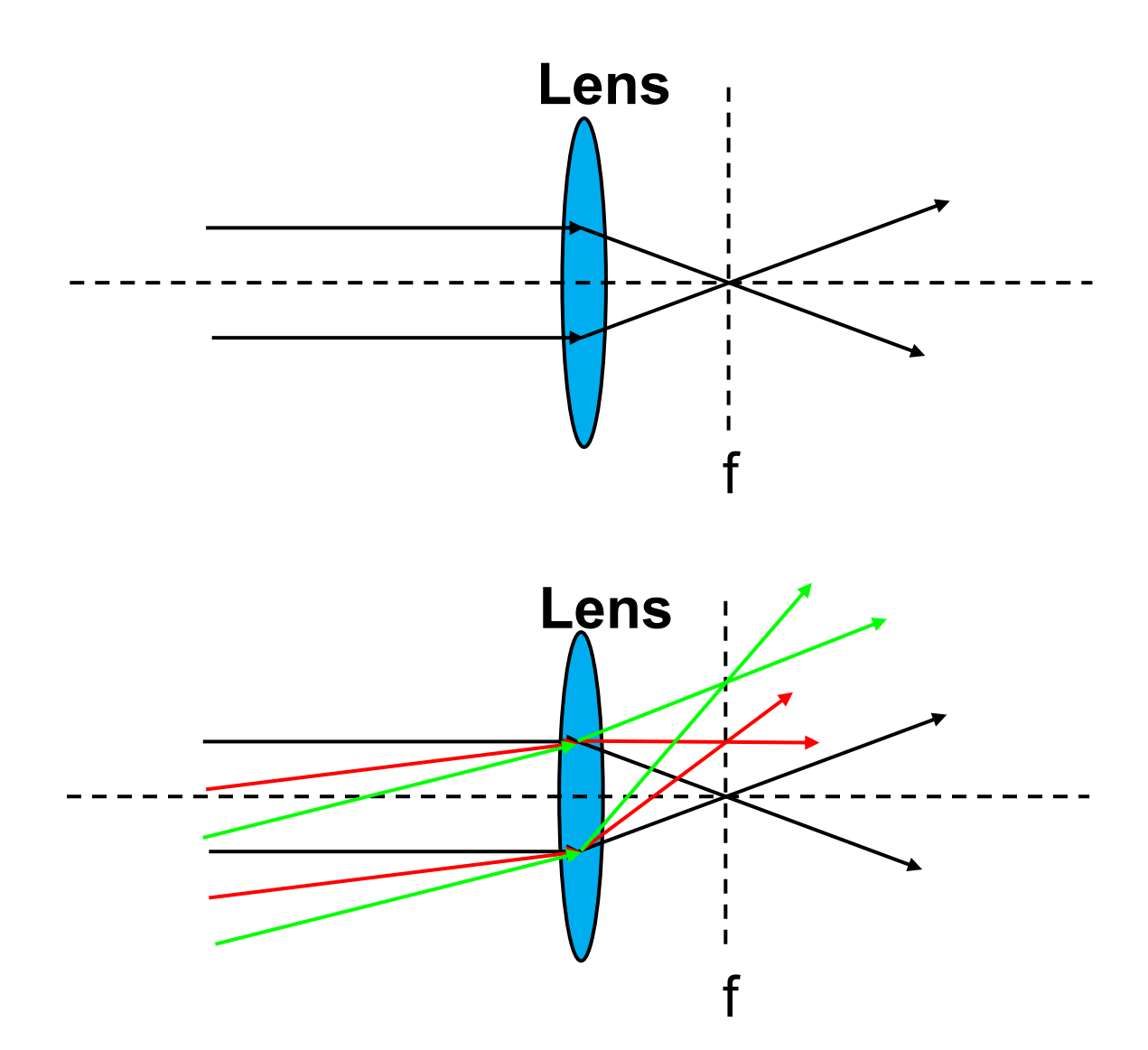
Noise came from low spatial resolution.

#### Schlieren imaging system can detect density gradient



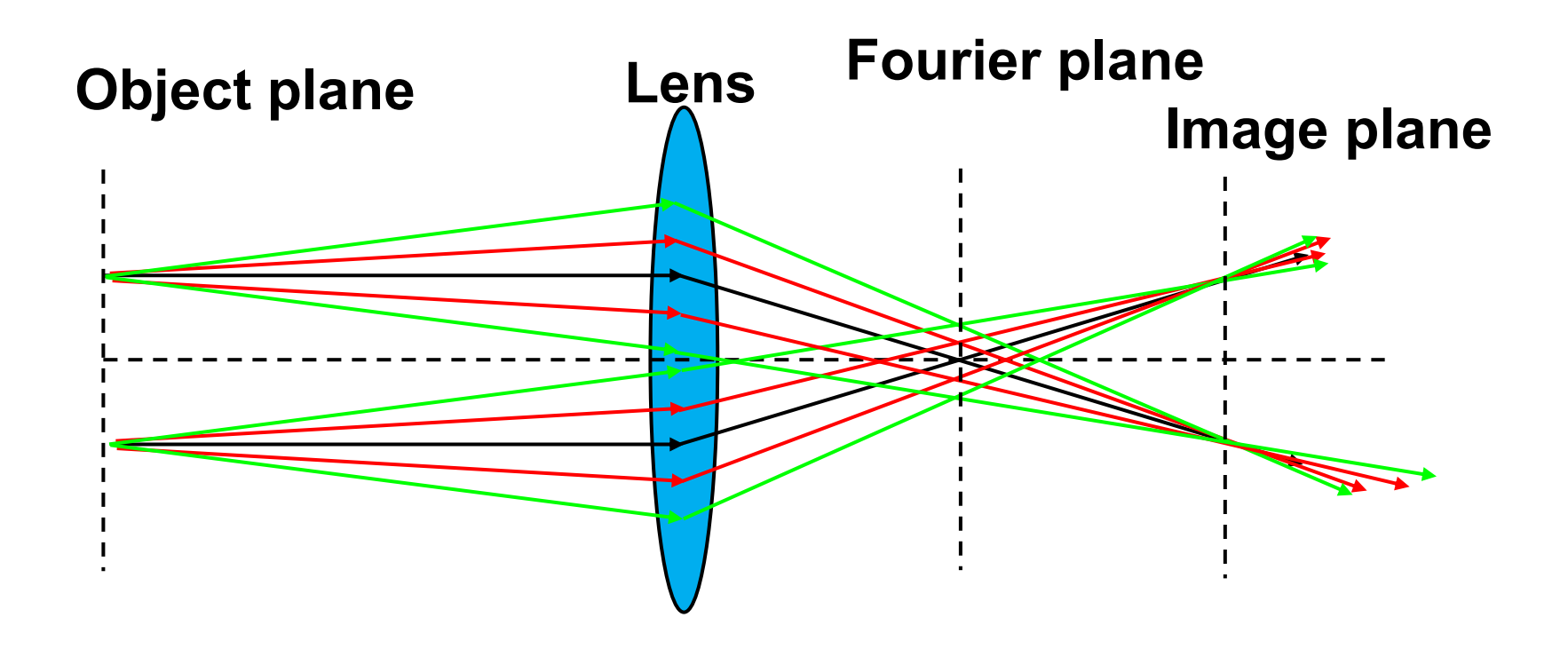
# Angular spectrum of plane waves can be used for diagnostic





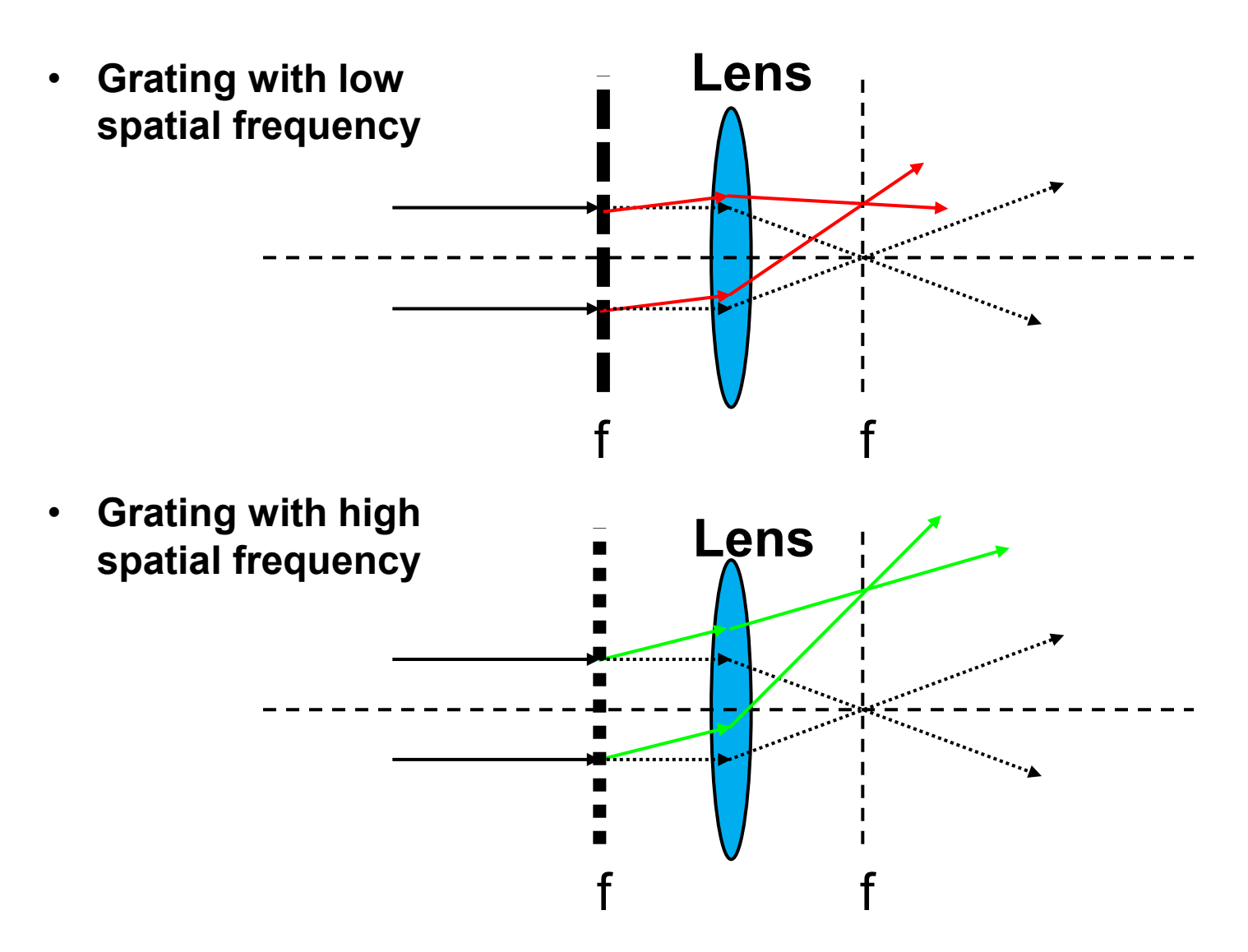
### Rays with different angles go through different focal points on the focal points





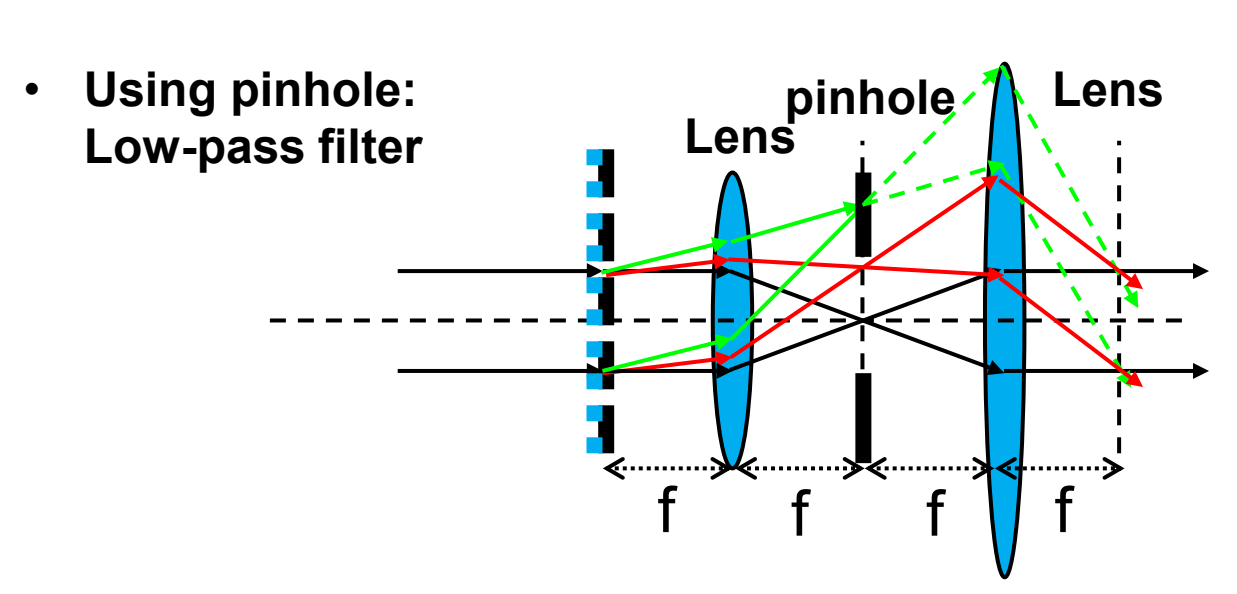
# Parallel beams are deflected to different angles with grating with different spatial frequencies

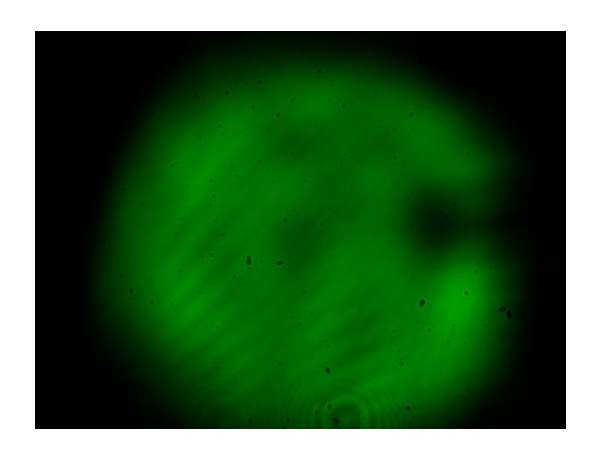




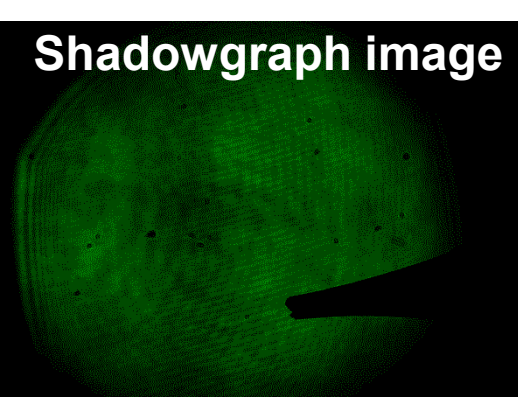
#### A pinhole or a dot acts like a low-pass / high-pass filter

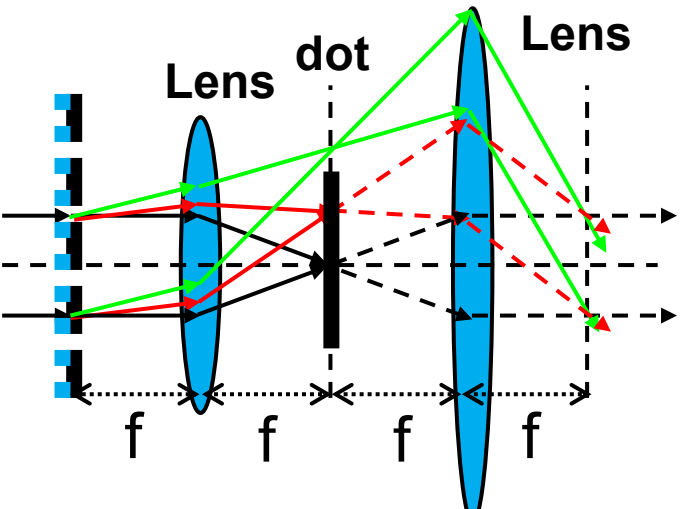


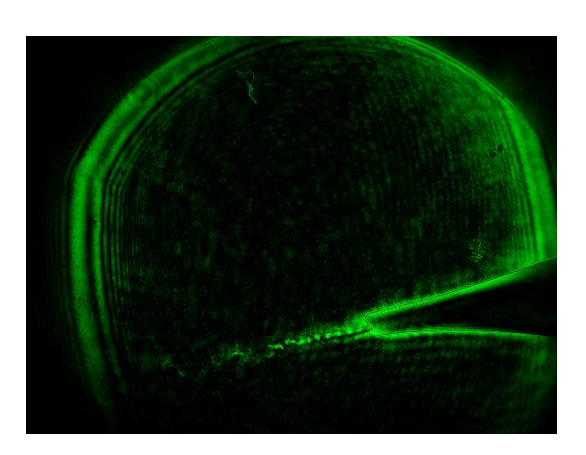




Using dot: High-pass filter



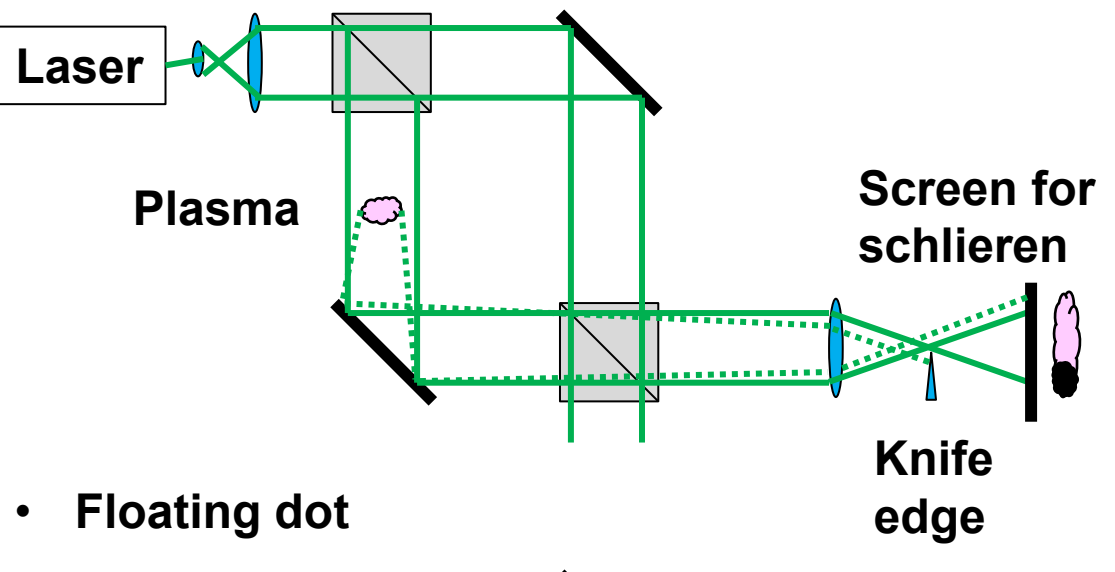


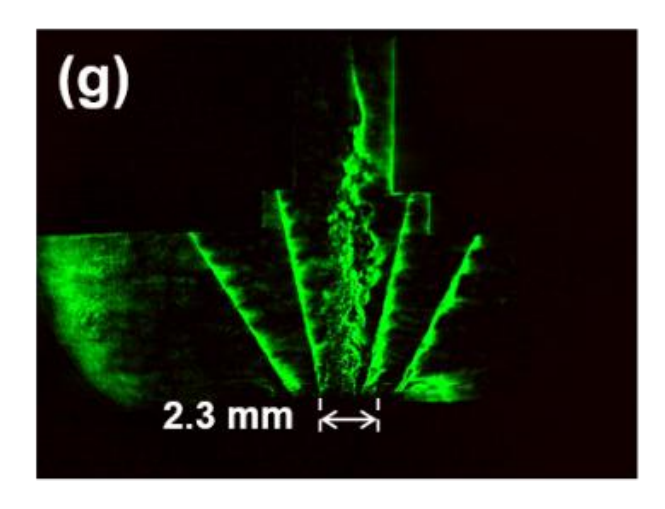


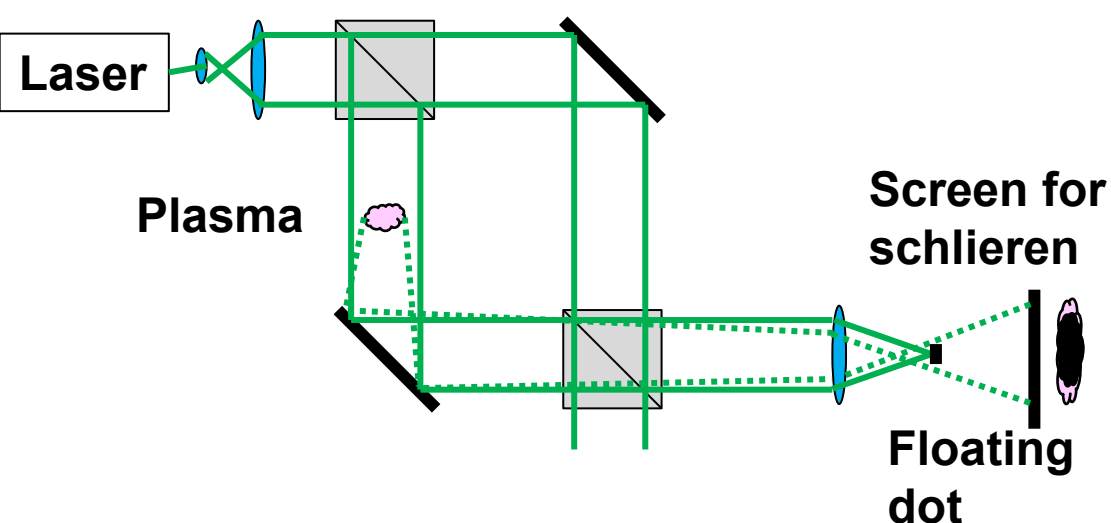
### A symmetric Schlieren image can be obtained if the knife edge is replaced by a "floating dot"

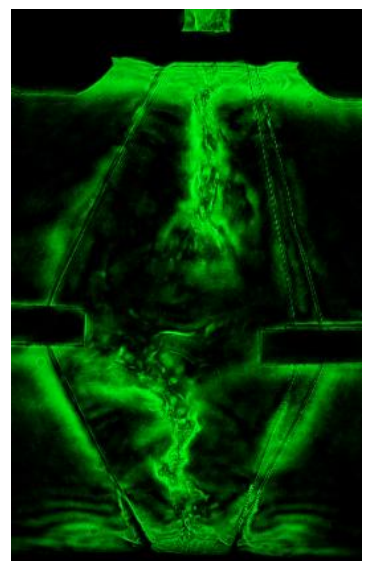






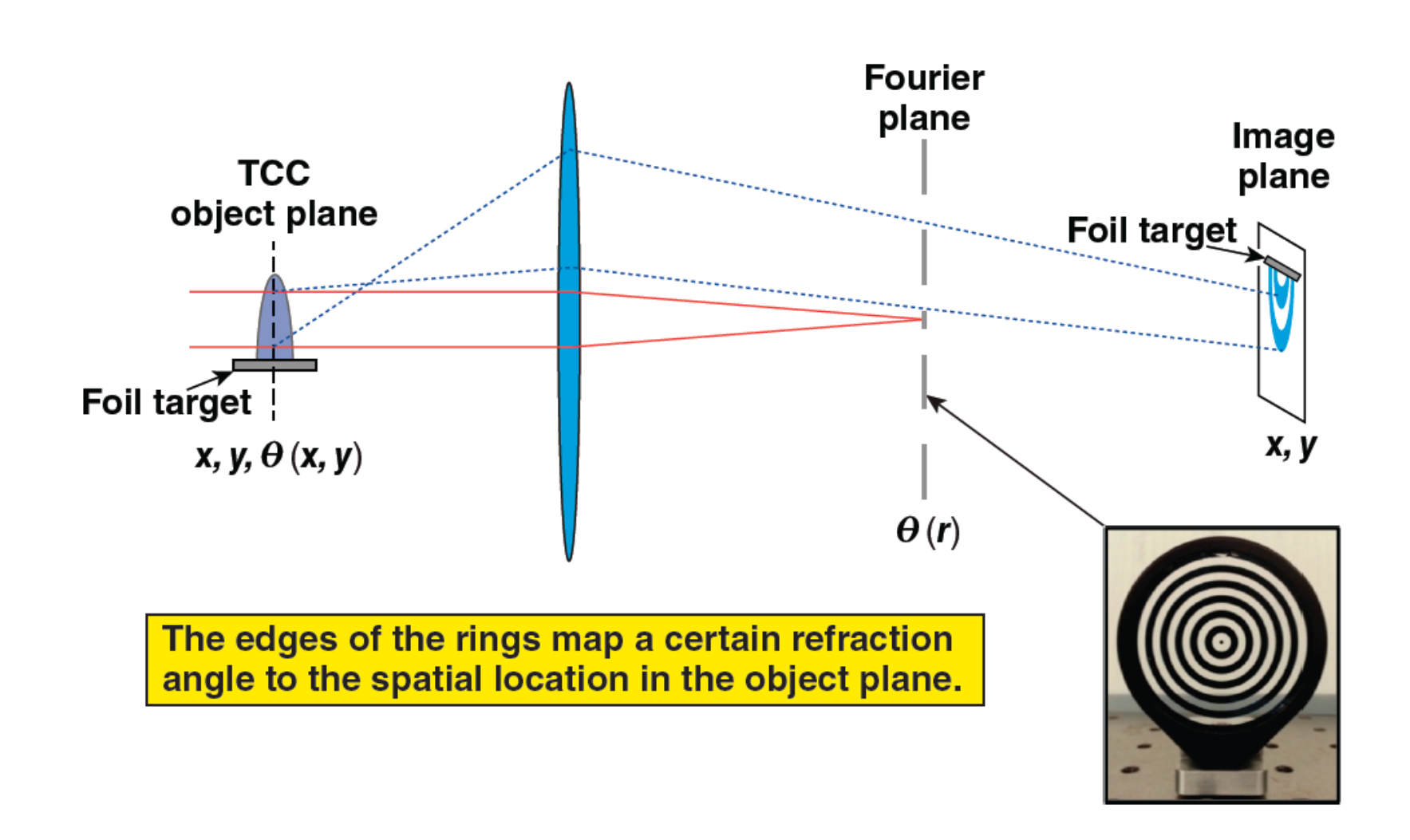






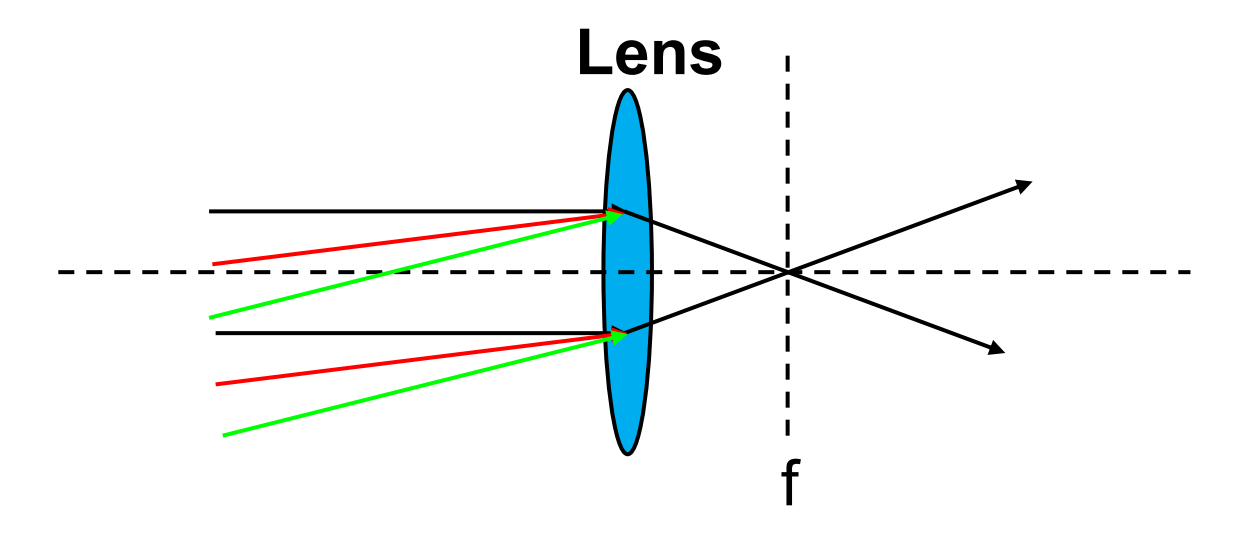
#### **Angular filter refractometry**

#### Angular filter refractometry (AFR) maps the refraction of the probe beam at TCC to contours in the image plane



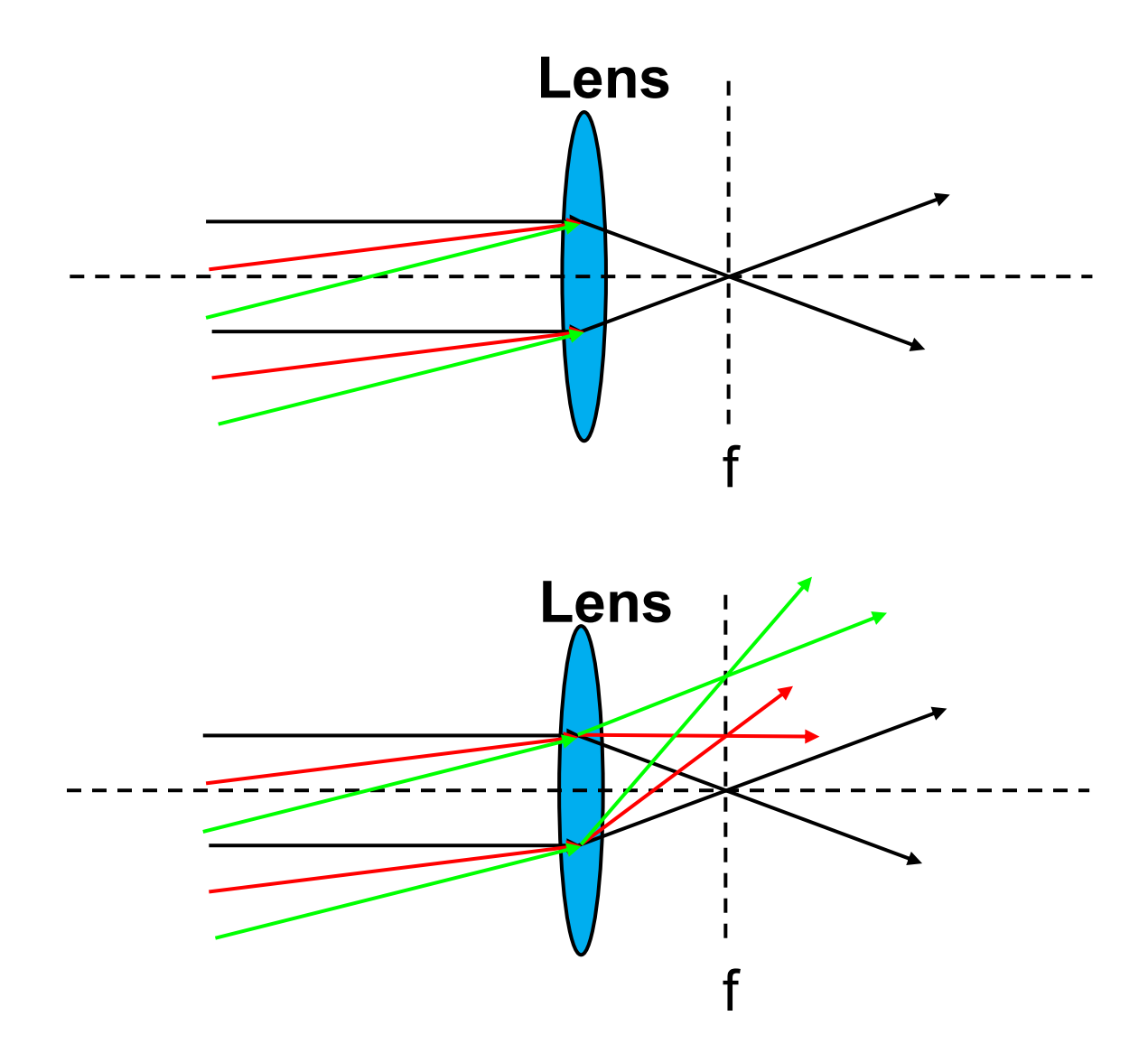
# Angular spectrum of plane waves can be used for diagnostic





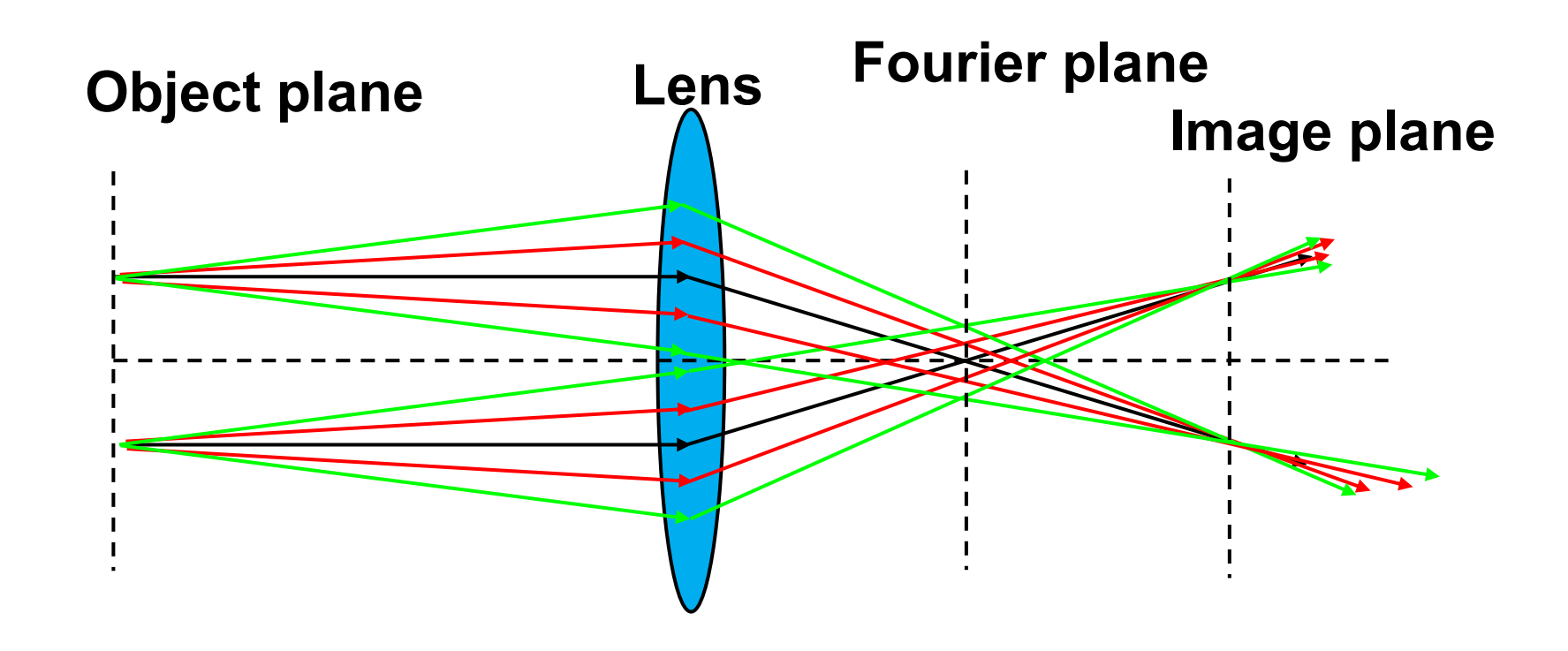
# Angular spectrum of plane waves can be used for diagnostic





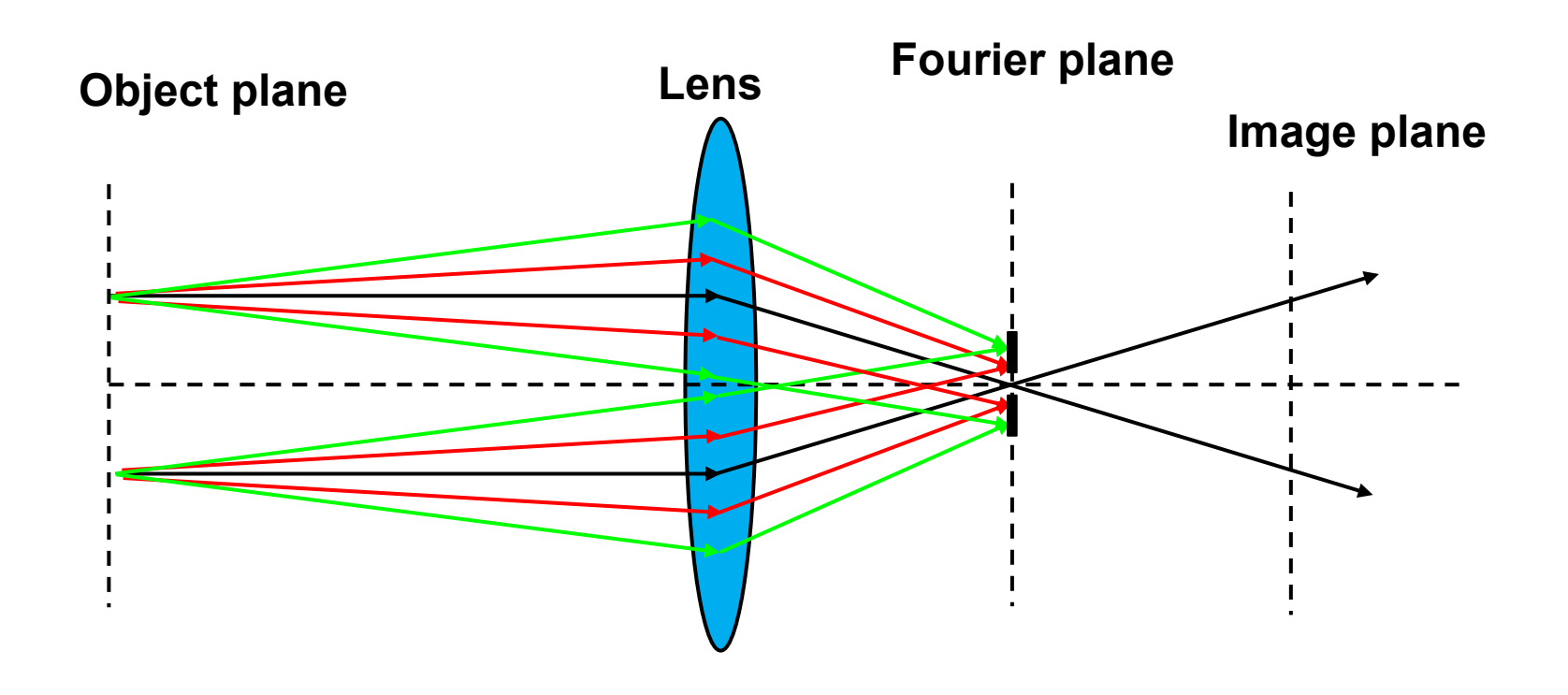
### Rays with different angles go through different focal points on the focal points





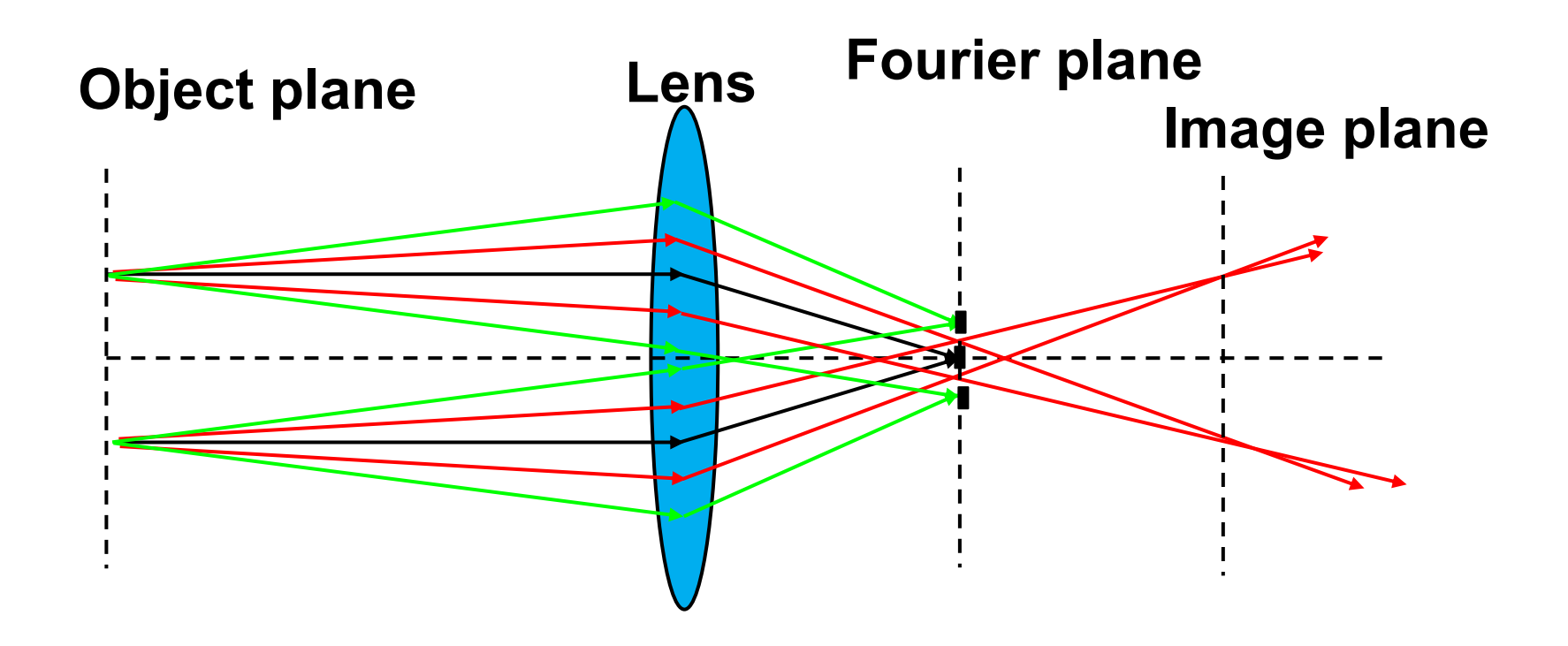
## Rays with different angles can be selected by blocking different focal points





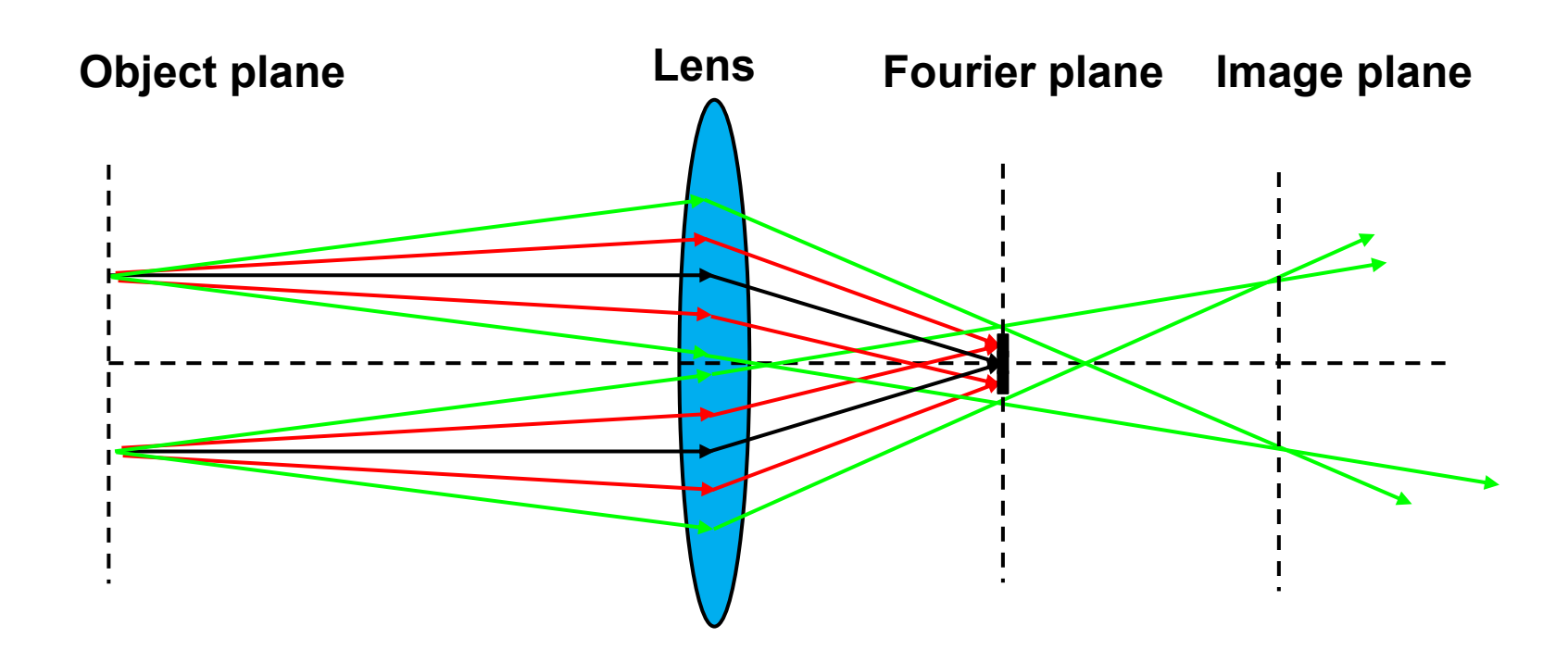
### Rays with different angles go through different focal points on the focal points



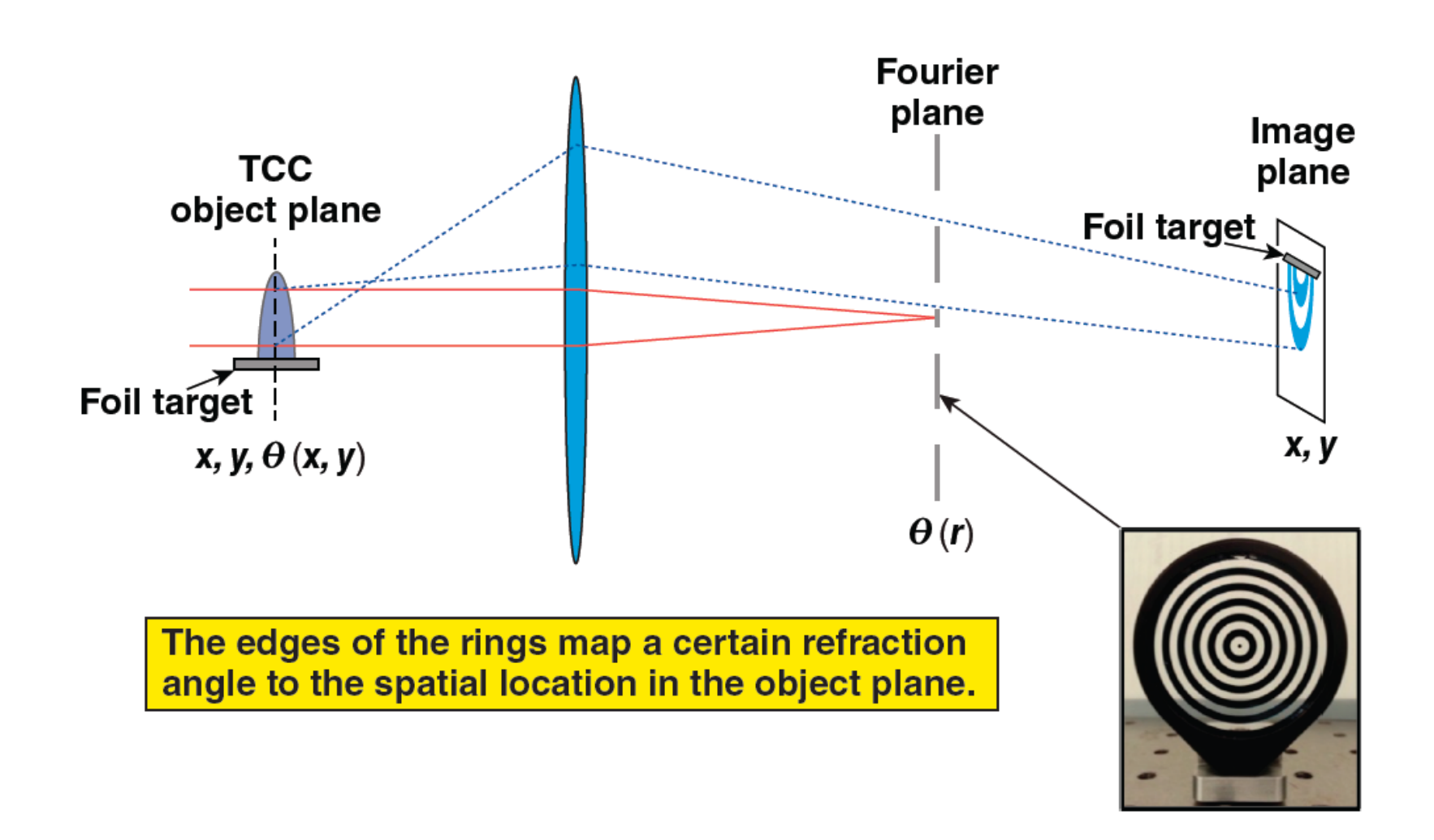


# Rays with different angles go through different focal points on the focal points

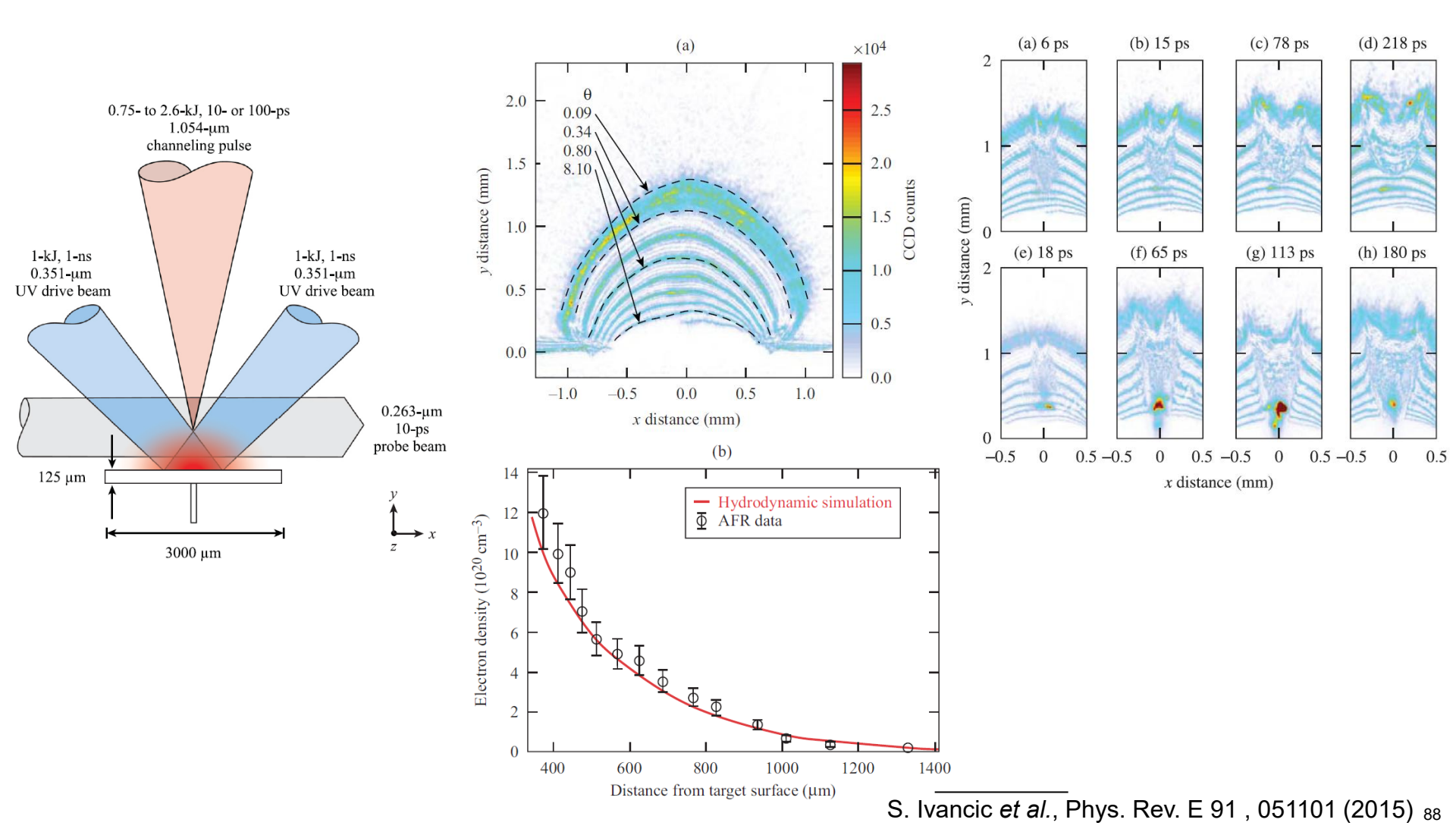




#### Angular filter refractometry (AFR) maps the refraction of the probe beam at TCC to contours in the image plane



# Channeling of multi-kilojoule high-intensity laser beams in an inhomogeneous plasma was observed using AFR



#### Electromagnetic wave can be used to measure the density or the magnetic field in the plasma



Nonmagnetized isotropic plasma (interferometer needed):

$$n^{2} = 1 - \frac{X(1-X)}{1-X - \frac{1}{2}Y^{2}\sin^{2}\theta \pm \left[\left(\frac{1}{2}Y^{2}\sin^{2}\theta\right)^{2} + (1-X)^{2}Y^{2}\cos^{2}\theta\right]^{1/2}}$$

$$= 1 - X = 1 - \frac{\omega_{\mathrm{p}}^{2}}{\omega^{2}} = 1 - \frac{n_{\mathrm{e}}}{n_{\mathrm{cr}}} \qquad \left(\mathbf{Y} \equiv \frac{\mathbf{\Omega}}{\boldsymbol{\omega}} \equiv \mathbf{0}\right)$$

$$\mathbf{Note:} \qquad \omega_{\mathrm{p}}^{2} = \frac{n_{\mathrm{e}}e^{2}}{\epsilon_{0}m_{\mathrm{e}}} \qquad n_{\mathrm{cr}} = \frac{\epsilon_{0}m_{\mathrm{e}}\omega^{2}}{e^{2}}$$

Magnetized isotropic plasma (Polarization detected needed):

Parallel to B<sub>0</sub> 
$$n^2 = 1 - \frac{\omega_{\rm p}^2}{\omega \left(\omega \pm \Omega\right)} \qquad \qquad \frac{E_{\rm x}}{E_{\rm y}} = \pm i \qquad \Omega \equiv \frac{eB_0}{m_{\rm e}}$$

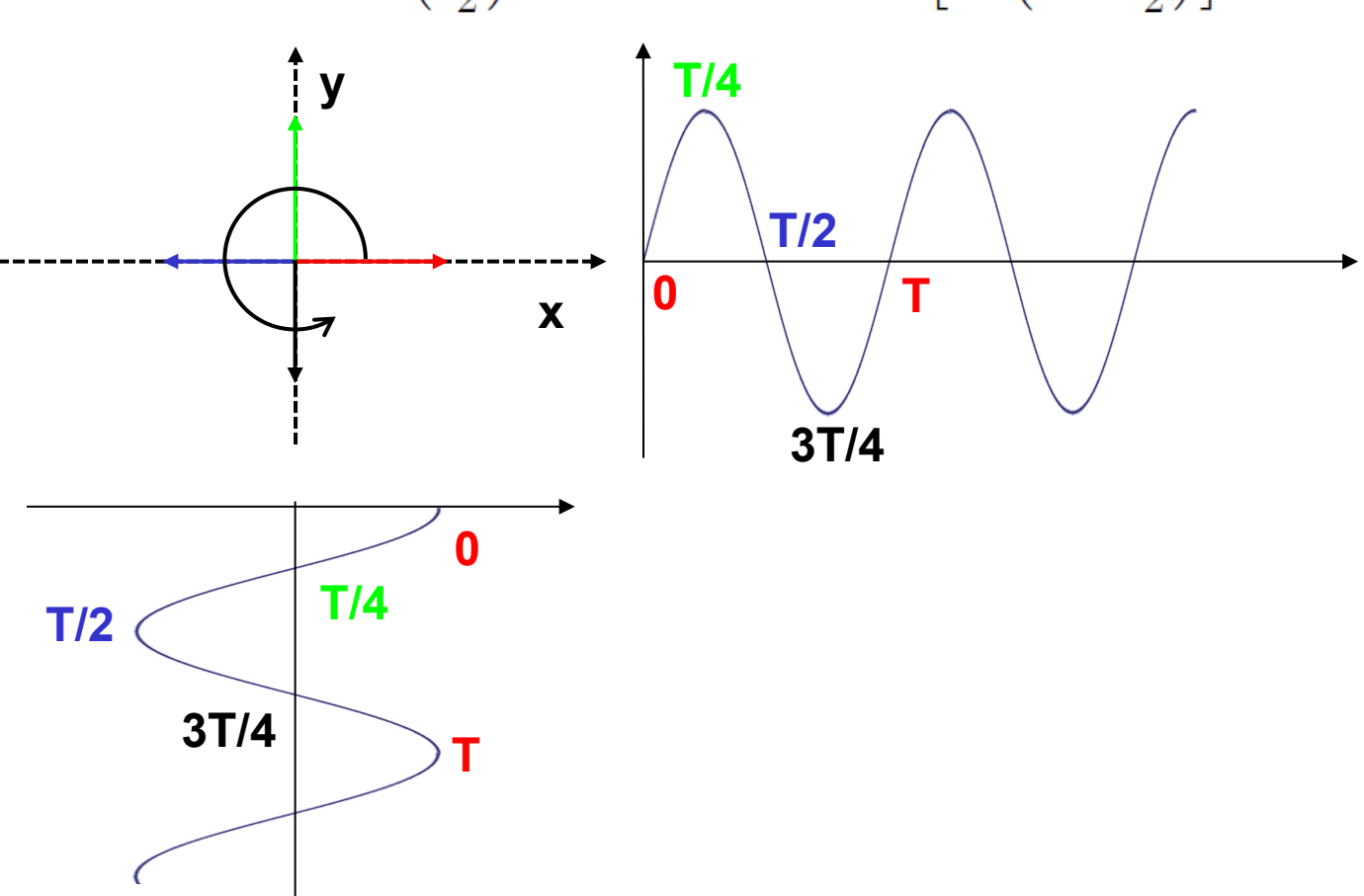
Faraday rotation: linear polarization rotation caused by the difference between the speed of LHC and RHC polarized wave.

#### **Circular polarization**



$$E_{\rm x} = E_0 \exp\left(-i\omega t\right)$$

$$E_{y} = iE_{x} = iE_{0} \exp\left(-i\omega t\right) = E_{0} \exp\left(i\frac{\pi}{2}\right) \exp\left(-i\omega t\right) = E_{0} \exp\left[-i\left(\omega t - \frac{\pi}{2}\right)\right]$$

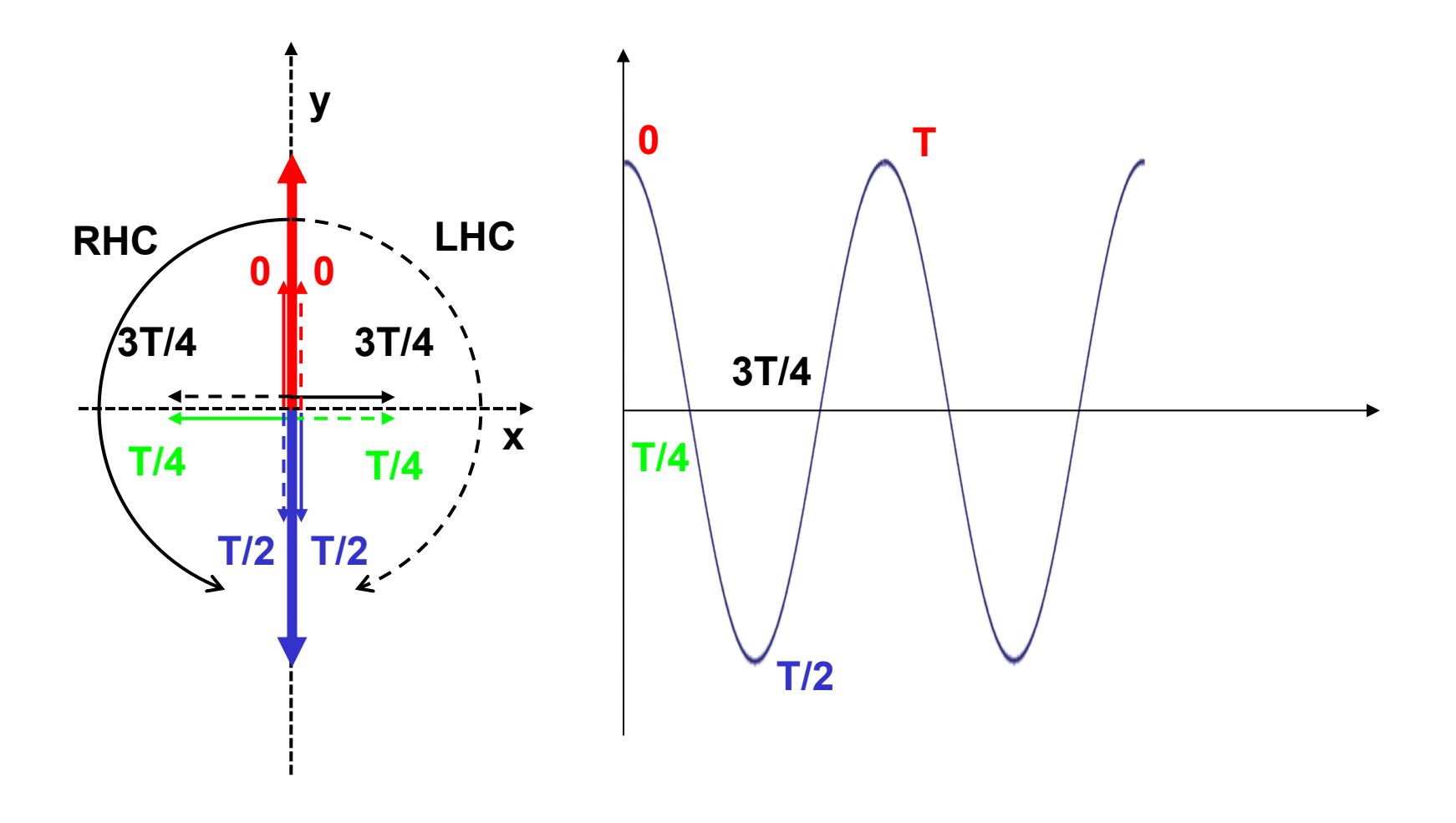


#### Linear polarization rotates as the wave propagates with different speed in LHC and RHC polarization



$$\begin{split} \vec{E} &= E_0 \hat{x} = \frac{E_0}{2} \left[ (\hat{x} + i\hat{y}) + (\hat{x} - i\hat{y}) \right] \qquad \vec{E} \left( z \right) = \vec{E} \exp \left( i\phi \right) \qquad \phi_{\mathrm{R}} \neq \phi_{\mathrm{L}} \\ \vec{E} \left( z \right) &= \frac{E_0}{2} \left[ (\hat{x} + i\hat{y}) e^{\mathrm{i}\Phi_R} + (\hat{x} - i\hat{y}) e^{\mathrm{i}\Phi_L} \right] \qquad \bar{\phi} \equiv \frac{\phi_{\mathrm{R}} + \phi_{\mathrm{L}}}{2} \qquad , \qquad \Delta \phi = \frac{\phi_{\mathrm{R}} - \phi_{\mathrm{L}}}{2} \\ &= \frac{E_0}{2} \left[ \hat{x} \left( e^{\mathrm{i}\Phi_R} + e^{\mathrm{i}\Phi_L} \right) + \hat{y} i \left( e^{\mathrm{i}\Phi_R} - e^{\mathrm{i}\Phi_L} \right) \right] \\ &= \frac{E_0}{2} \left[ \hat{x} \left( e^{i\left(\bar{\phi} + \frac{\Delta\Phi}{2}\right)} + e^{i\left(\bar{\phi} - \frac{\Delta\Phi}{2}\right)} \right) + \hat{y} i \left( e^{i\left(\bar{\phi} + \frac{\Delta\Phi}{2}\right)} - e^{i\left(\bar{\phi} - \frac{\Delta\Phi}{2}\right)} \right) \right] \\ &= E_0 e^{i\bar{\phi}} \left[ \hat{x} \left( e^{i\frac{\Delta\Phi}{2}} + e^{-i\frac{\Delta\Phi}{2}} \right) + \hat{y} i \left( e^{i\frac{\Delta\Phi}{2}} - e^{-i\frac{\Delta\Phi}{2}} \right) \right] \\ &= E_0 e^{i\bar{\phi}} \left[ \hat{x} \cos \left( \frac{\Delta\Phi}{2} \right) \cos + \hat{y} \sin \left( \frac{\Delta\Phi}{2} \right) \right] \end{split}$$

# A linear polarized wave can be decomposed into one left-handed circular polarized wave and a righ-handed circular polarized wave



#### The rotation angle of the polarization depends on the linear integral of magnetic field and electron density



$$\phi = \int k dl = \int n \frac{\omega}{c} dl$$
  $\qquad \qquad \alpha = \frac{\Delta \phi}{2} = \frac{\omega}{2c} \int (n_{\rm R} - n_{\rm L}) dl$ 

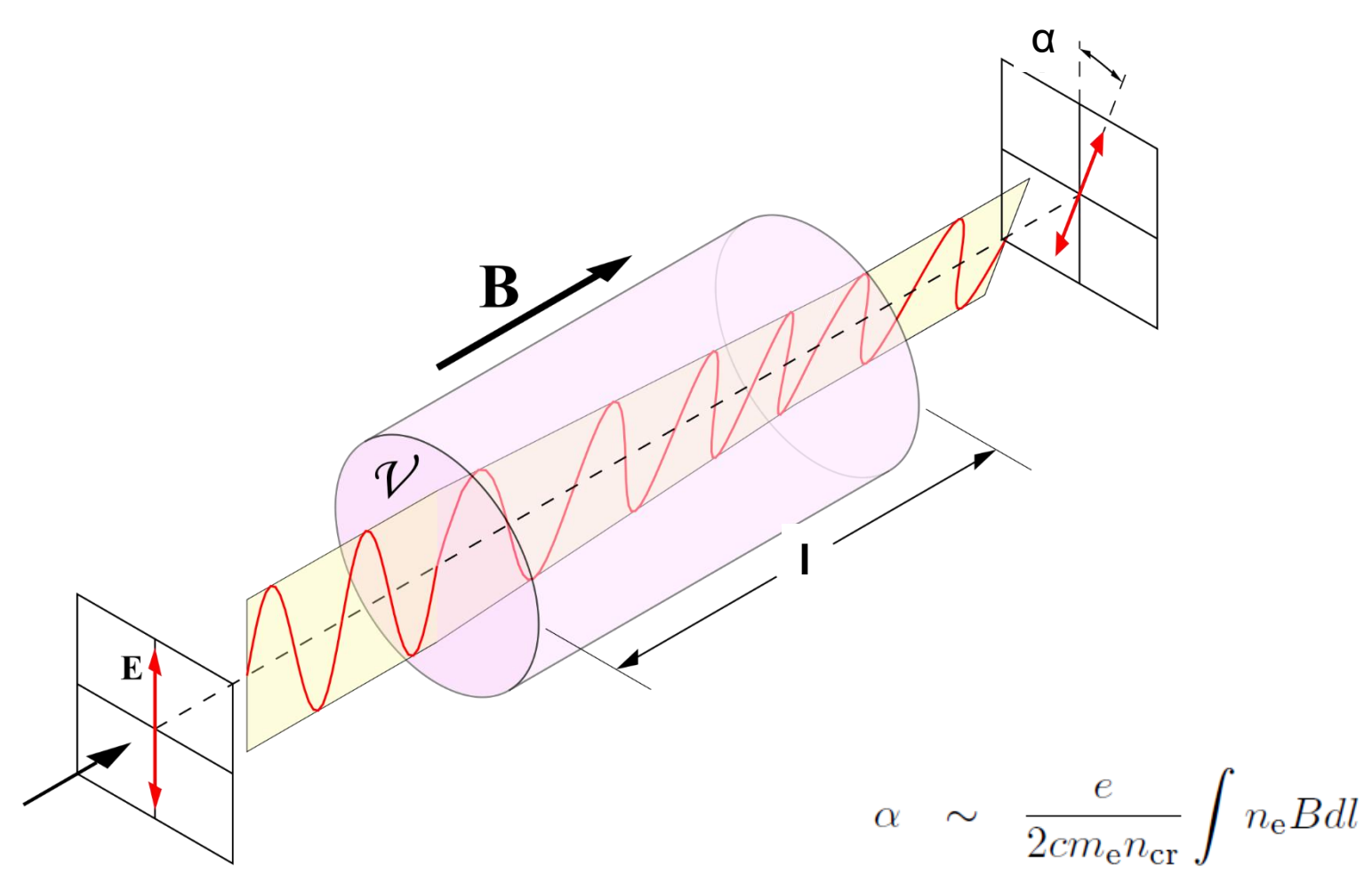
$$n_{\rm R} = \sqrt{1 - \frac{X}{1 + Y}} \sim 1 - \frac{1}{2} \frac{X}{1 + Y}$$
  $X, Y << 1$ 
 $n_{\rm L} \sim 1 - \frac{1}{2} \frac{X}{1 - Y}$   $\frac{X}{1 \pm Y} << 1$ 

$$n_{\rm R} - n_{\rm L} \sim \frac{X}{2} \left( \frac{1}{1 - Y} - \frac{1}{1 + Y} \right) = \frac{XY}{1 - Y^2} \sim XY$$

$$\alpha \sim \frac{\omega}{2c} \int XYdl = \frac{\omega}{2c} \int \frac{\omega_{\rm p}^2}{\omega^2} \frac{\Omega}{\omega} dl = \frac{1}{2c} \int \frac{n_{\rm e}}{n_{\rm cr}} \frac{eB}{m_{\rm e}} dl$$
$$= \frac{e}{2cm_{\rm e}n_{\rm cr}} \int n_{\rm e}Bdl$$

## The rotation angle of the polarization depends on the linear integral of magnetic field and electron density



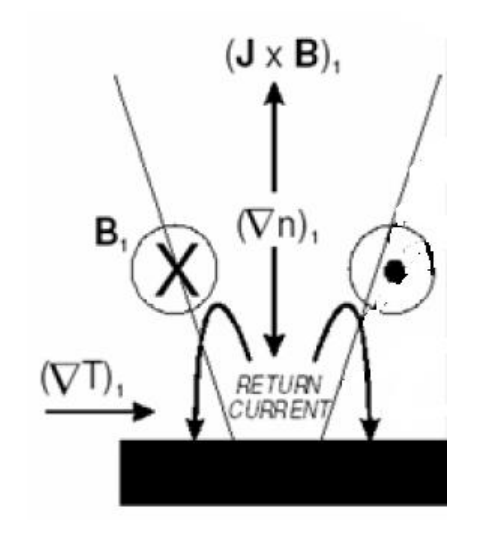


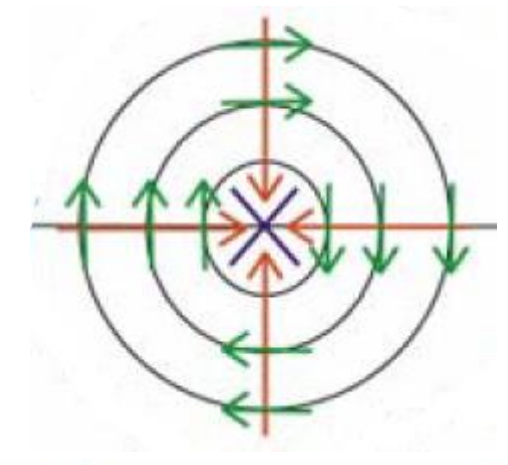
#### Magnetic field can be generated when the temperature and density gradients are not parallel to each other



$$\frac{\partial \vec{B}}{\partial t} = \nabla \times \left[ \underbrace{\vec{u} \times \vec{B}}_{\text{Convection term}} + \underbrace{\frac{1}{\sigma \mu_0} \nabla \times \vec{B}}_{\text{Diffusion term}} + \underbrace{\frac{\nabla p_e}{n_e e}}_{\text{self generated field}} - \underbrace{\frac{1}{\mu_0} \left( \frac{\nabla \times \vec{B}}{n_e e} \times \vec{B} \right)}_{\text{Hall term}} \right]$$

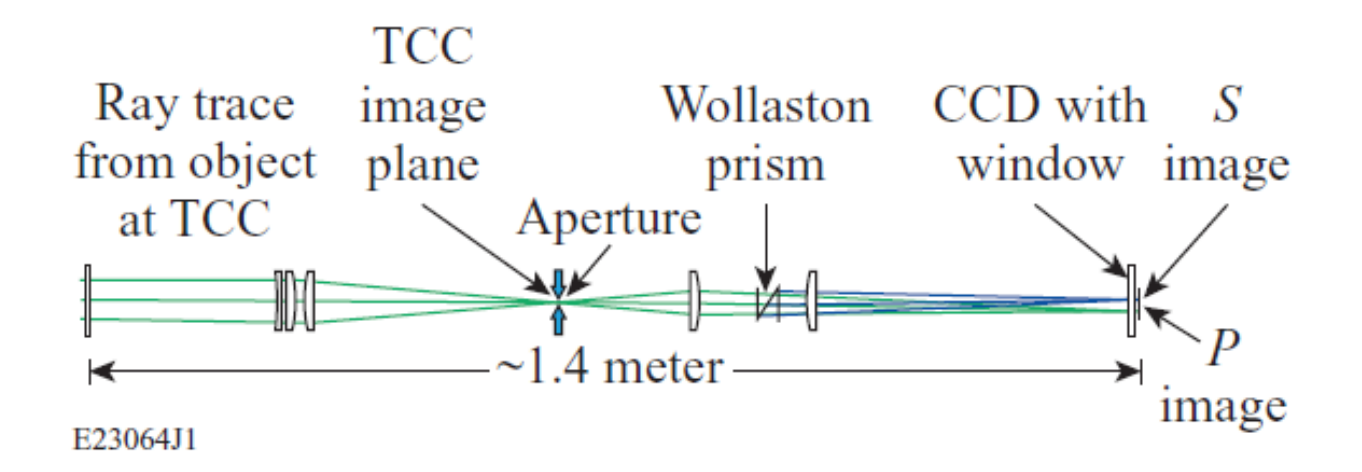
$$\nabla \times \frac{\nabla p_{\rm e}}{n_{\rm e}e} = -\frac{k_{\rm B}}{e} \frac{\nabla n_{\rm e} \times \nabla T_{\rm e}}{n_{\rm e}}$$

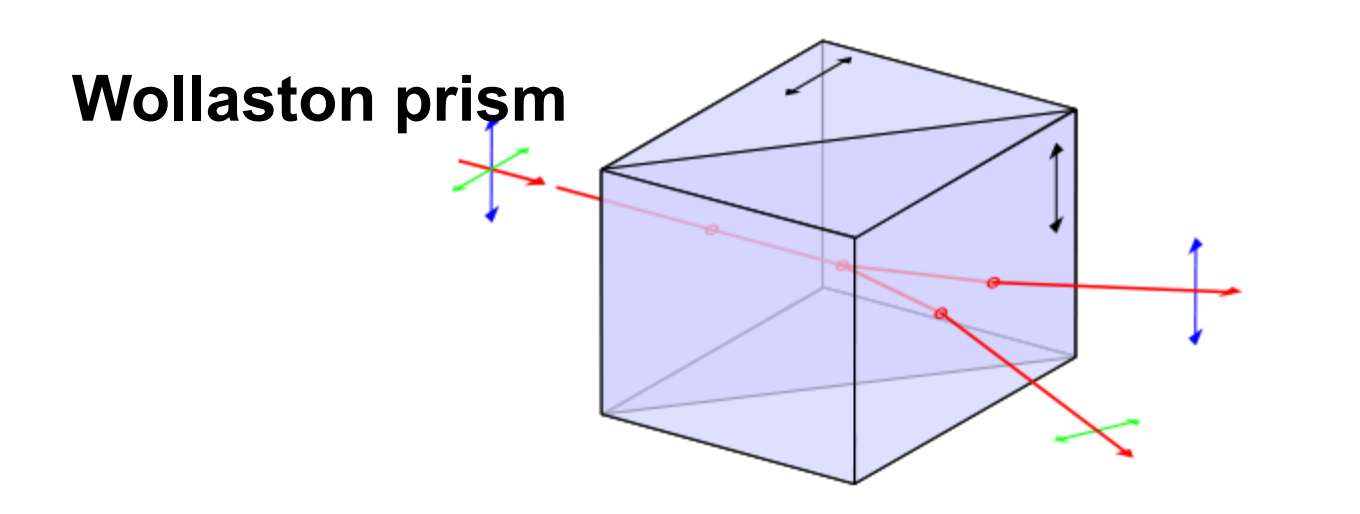




#### Polarimetry diagnostic can be used to measure the magnetic field

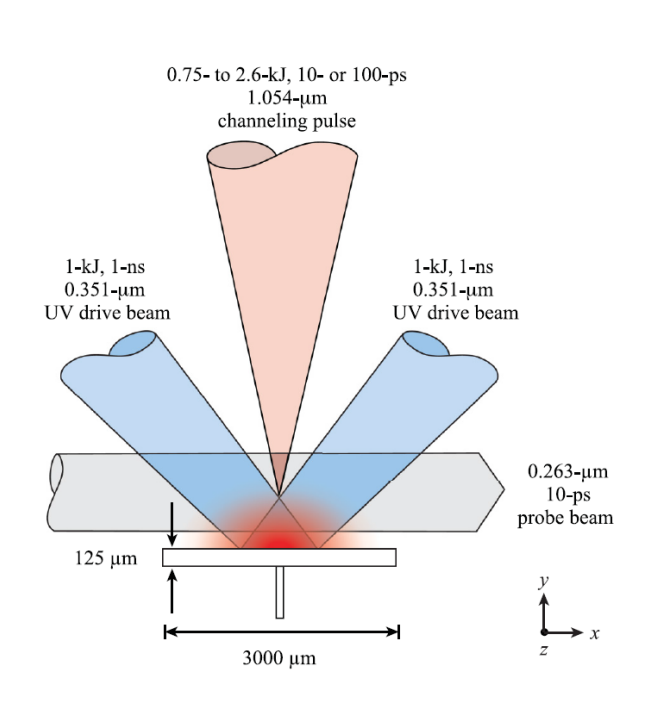


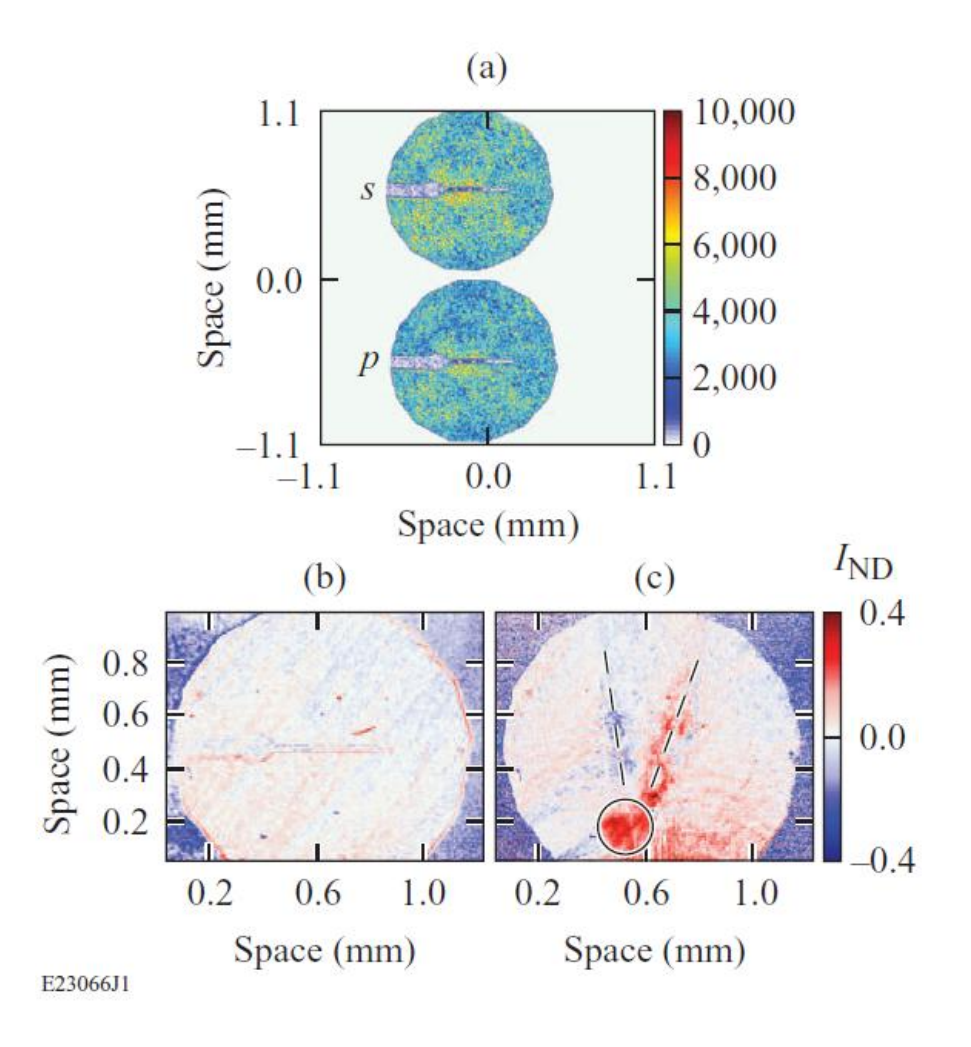




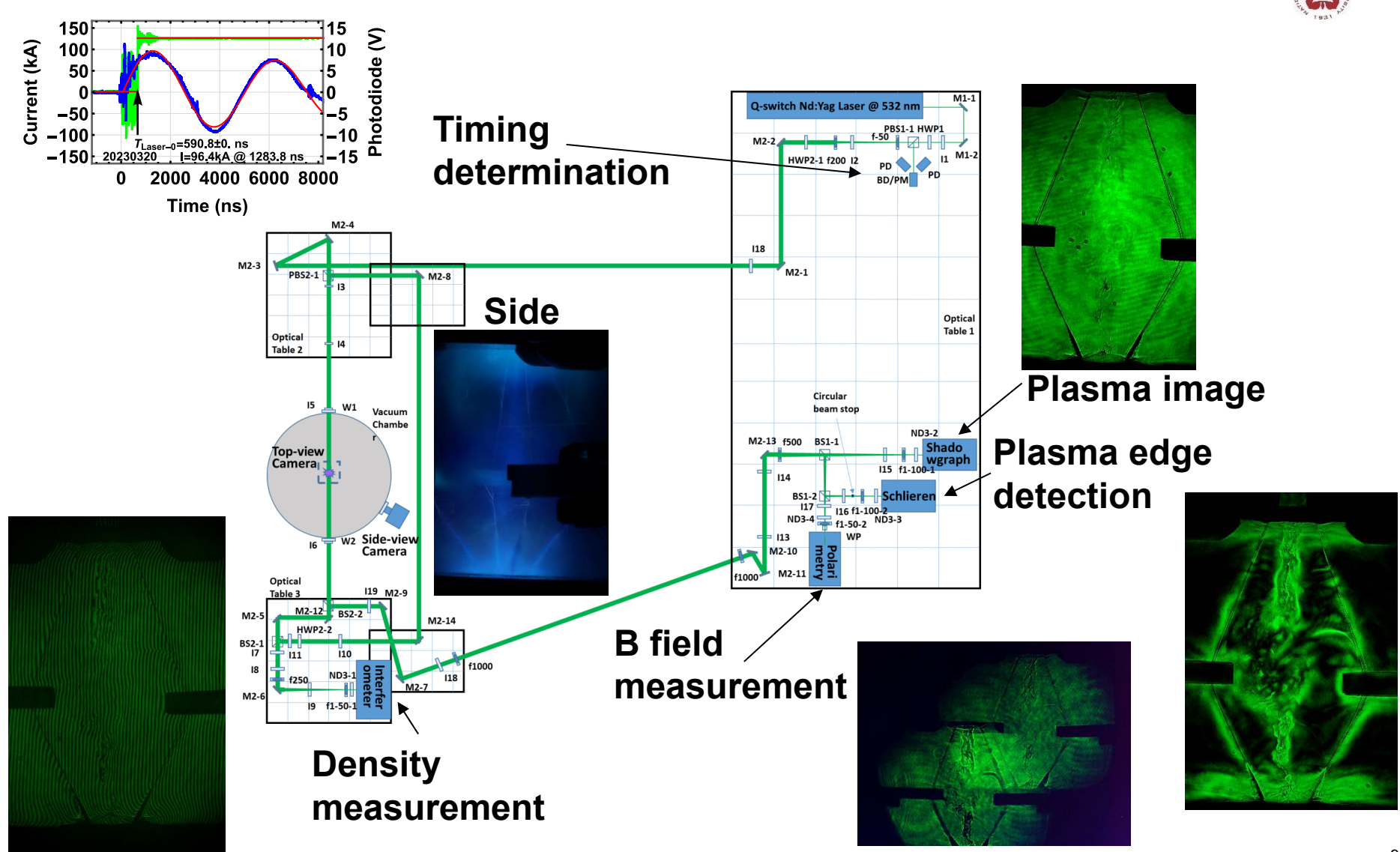
# Self-generated field was suggested when multi-kilojoule high-intensity laser beams illuminated on an inhomogeneous plasma





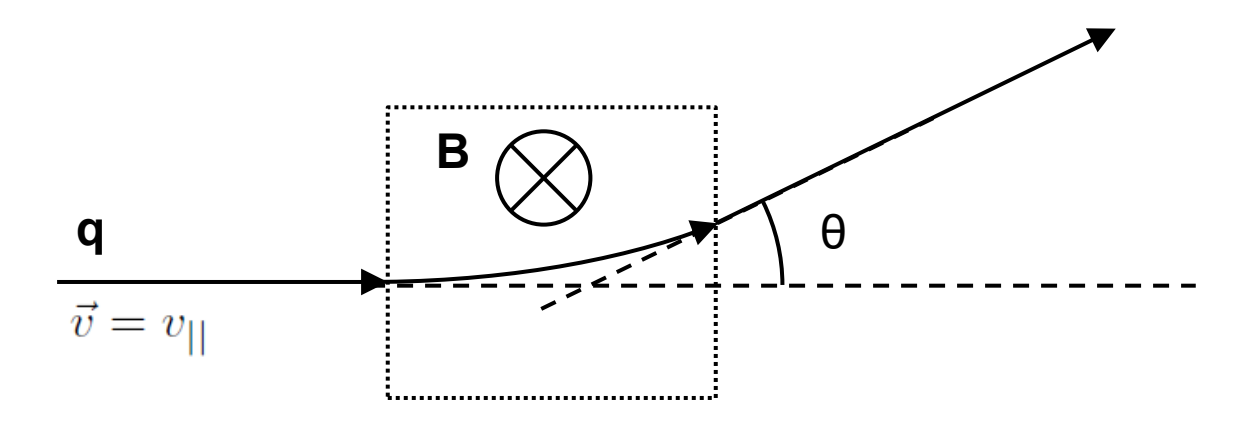


# Time-resolved imaging system with temporal resolution in the order of nanoseconds was implemented



### The magnetic field can be measured by measuring the deflected angle of charged particles





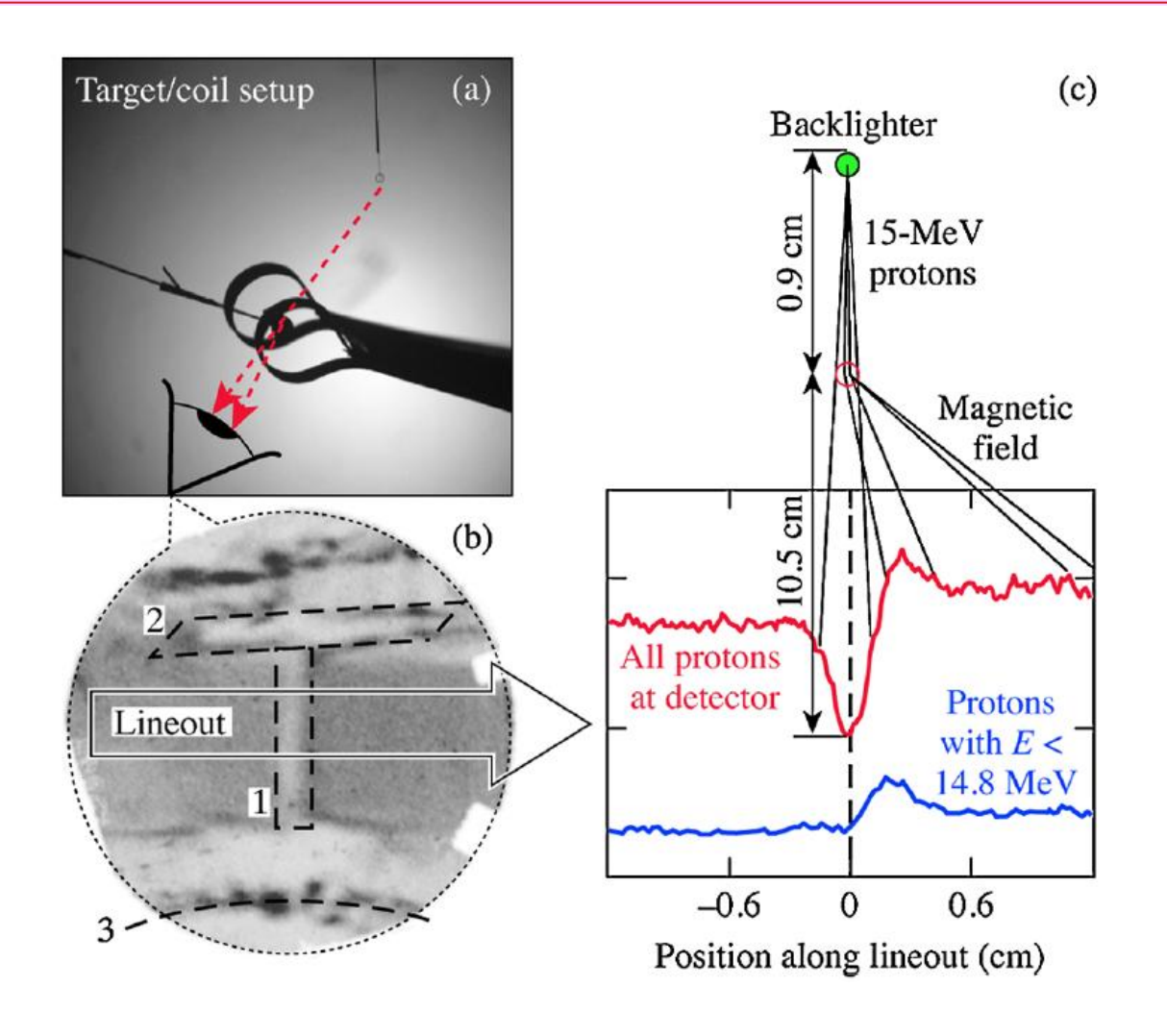
$$F_{\perp} = q\vec{v} \times \vec{B} = qv_{||}B = m\frac{dv_{\perp}}{dt}$$

$$v_{\perp} = \int \frac{qv_{||}B}{m}dt = \frac{qv_{||}}{m} \int Bdt \frac{dx}{dx} = \frac{qv_{||}}{m} \int \frac{B}{v_{||}}dx = \frac{q}{m} \int Bdx$$

$$\tan \theta = \frac{v_{\perp}}{v_{||}} = \frac{q}{mv_{||}} \int B dx = \frac{q}{\sqrt{2mE}} \int B dx \qquad \qquad \int B dx = \frac{\sqrt{2mE}}{q} \tan \theta$$

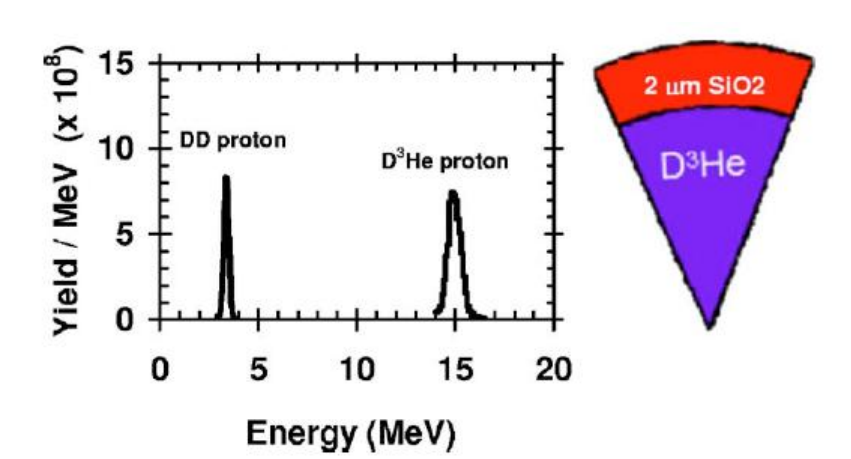
#### Magnetic field was measured using protons





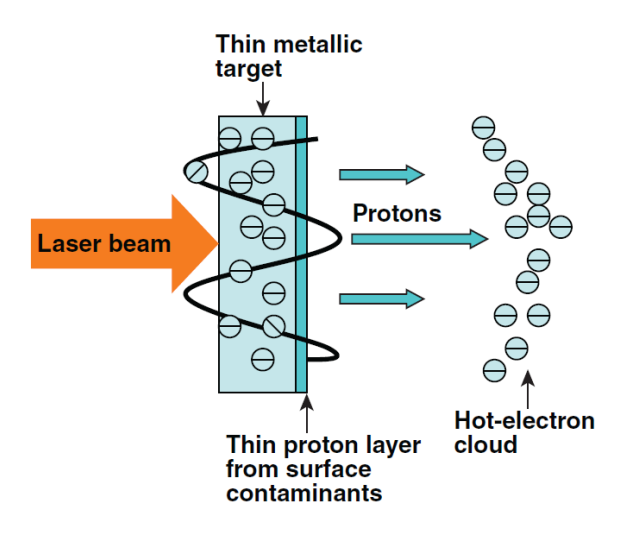
# Protons can be generated from fusion product or copper foil illuminated by short pulse laser

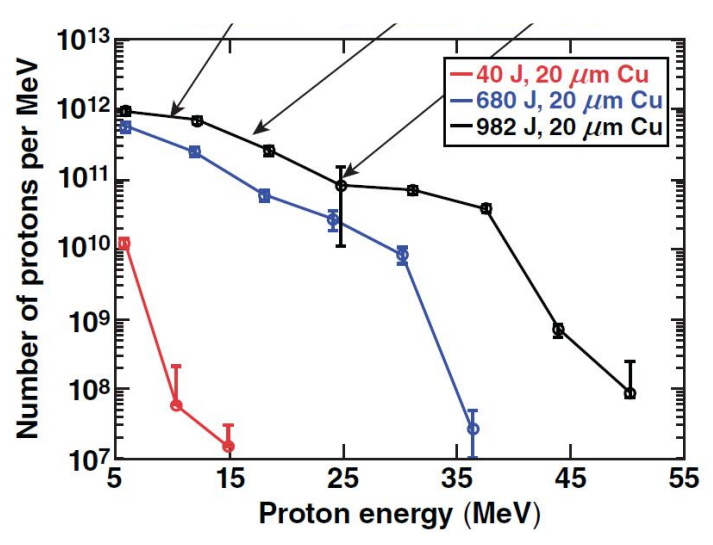




$$D + D \rightarrow T(1.01 \text{MeV}) + p(3.02 \text{MeV})$$

$$D + \mathrm{He^3} \rightarrow \mathrm{He^4}(3.6\mathrm{MeV}) + p(14.7\mathrm{MeV})$$





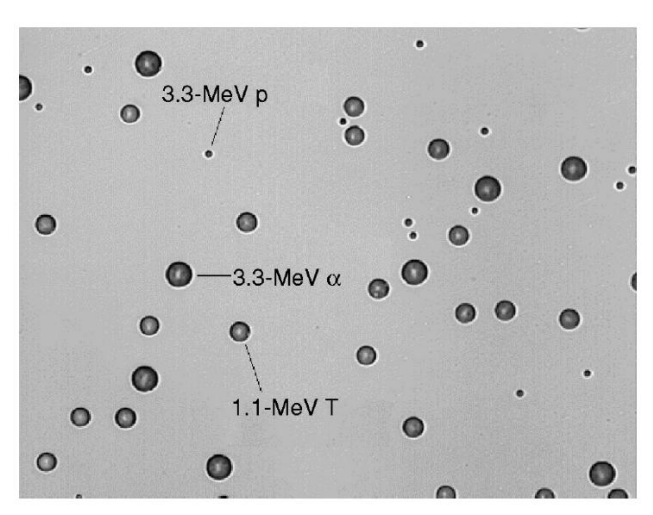
Target normal sheath acceleration (TNSA)

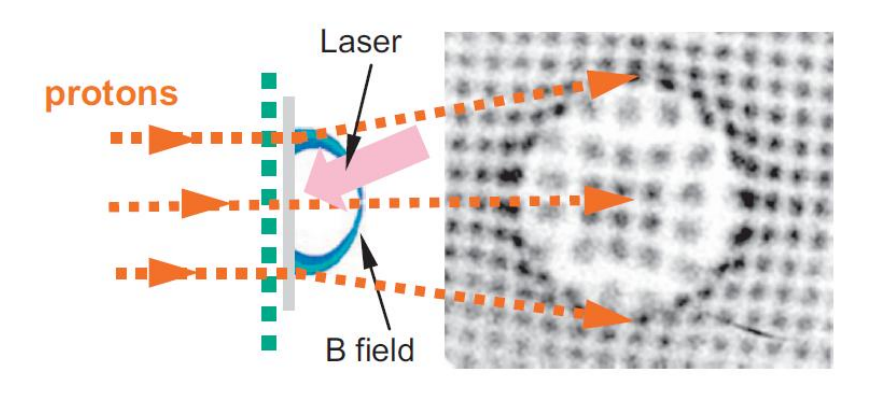
C. K. Li *et al.*, Rev. Sci. Instrum. **77**, 10E725 (2006) L. Gao, PhD Thesis

#### Protons can leave tracks on CR39 or film

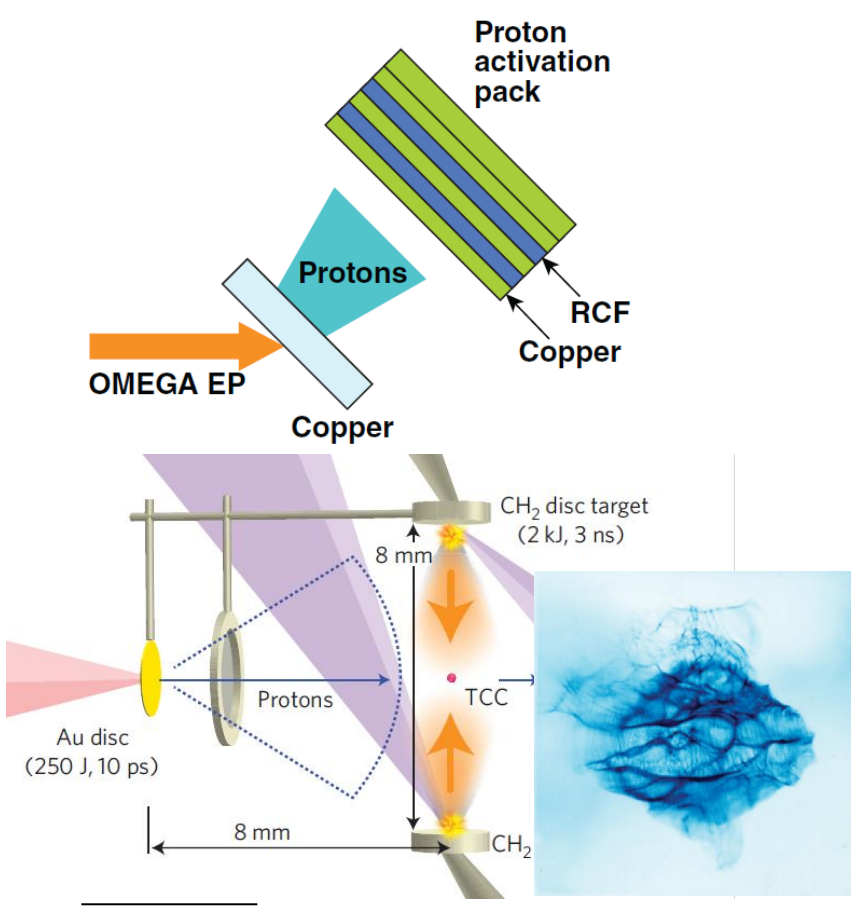


#### **CR 39**



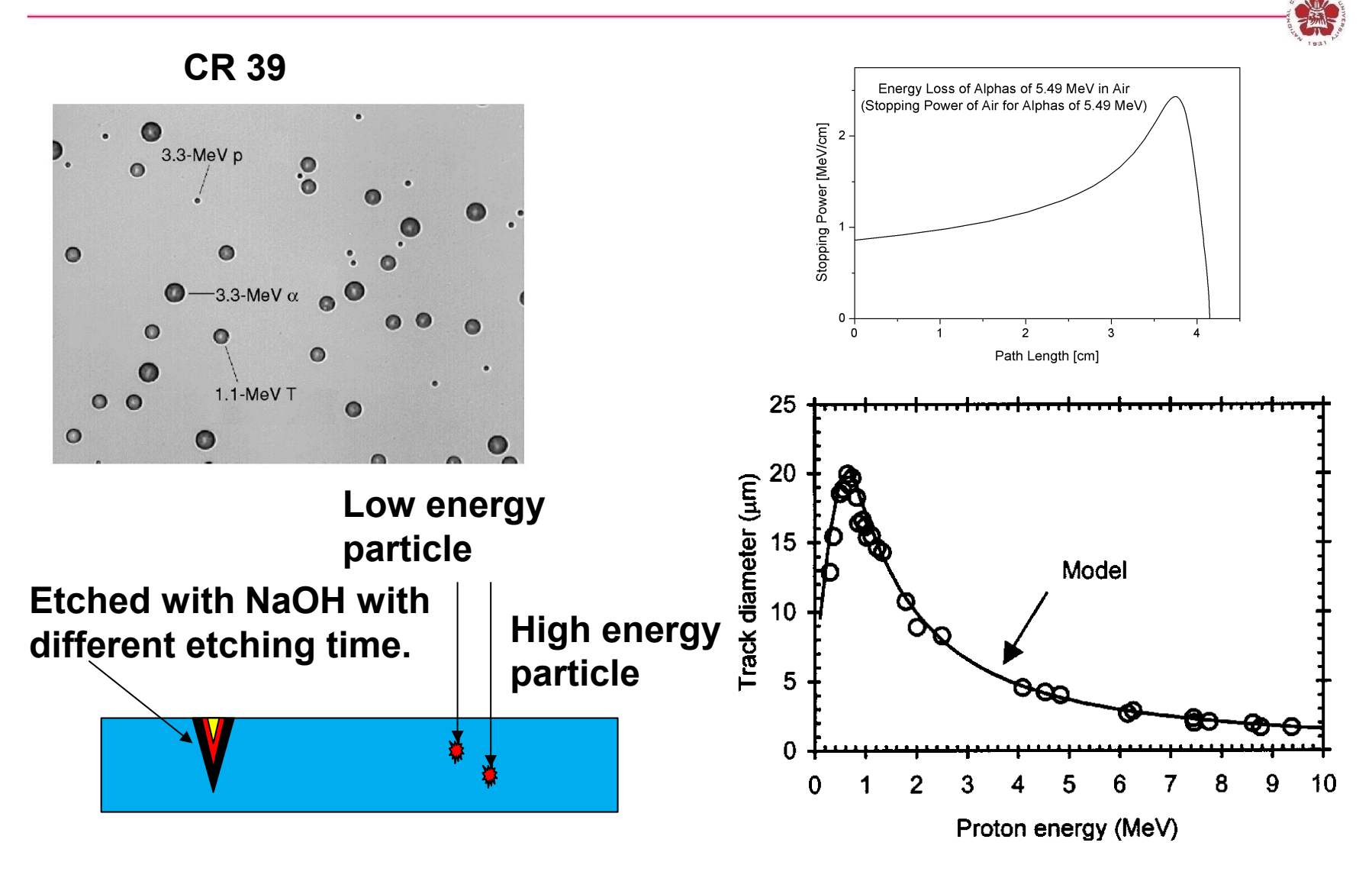


#### Radiochromic film pack

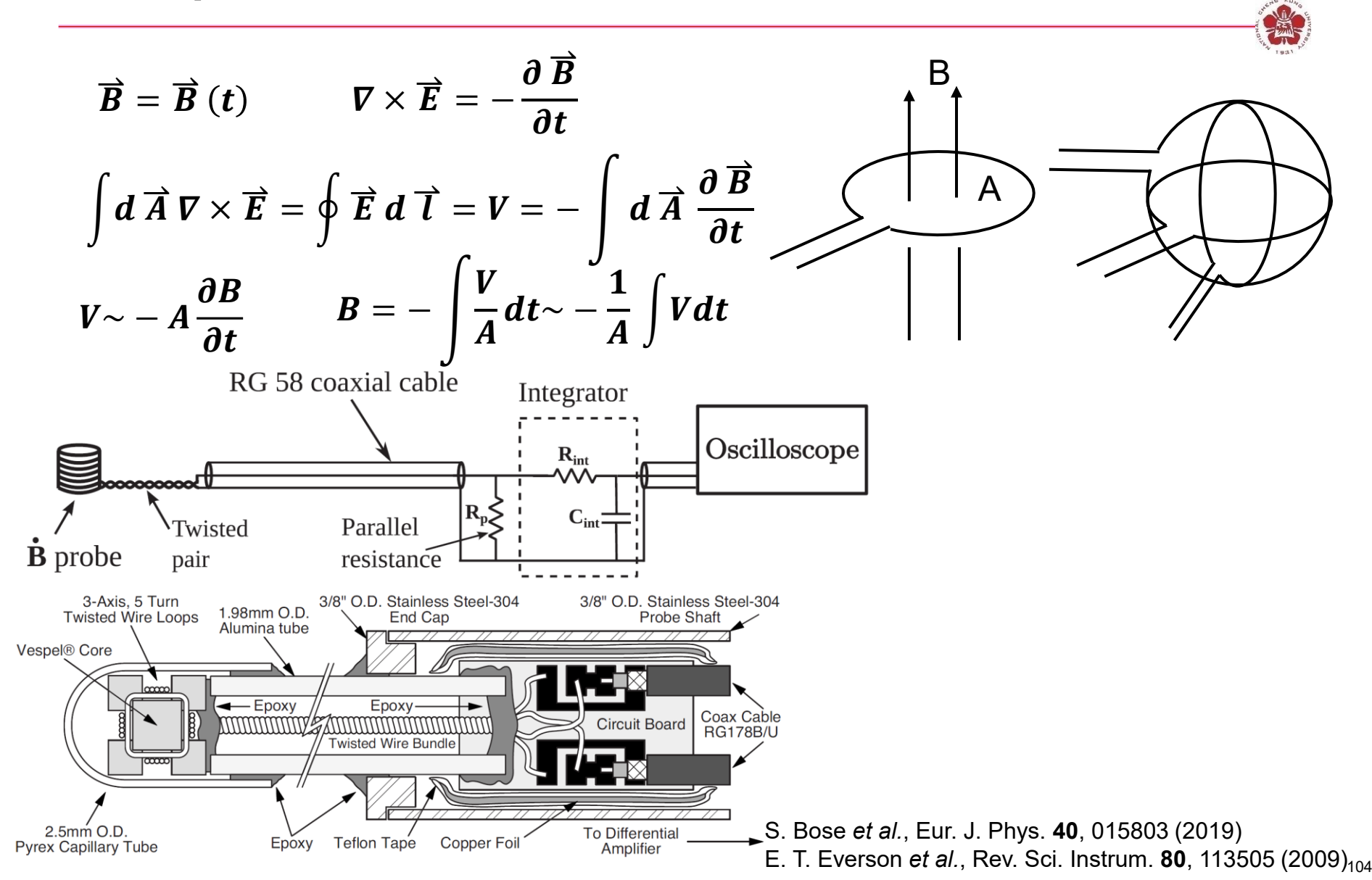


- F. H. Seguin et al., Rev. Sci. Instrum. 74, 975 (2003)
- C. K. Li et al., Phys. Plasmas 16,056304 (2009)
- L. Gao, PhD Thesis
- N. L. Kugland et al., Nature Phys. B, 809 (2012)

#### Track diameter on the CR39 is depended on the particle energy that incidents



# Time dependent magnetic field can be measured using B-dot probe

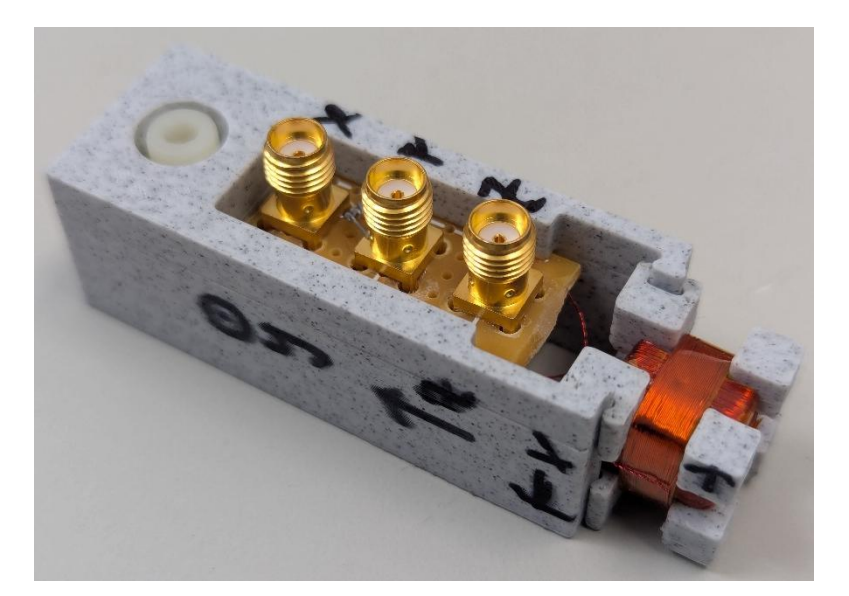


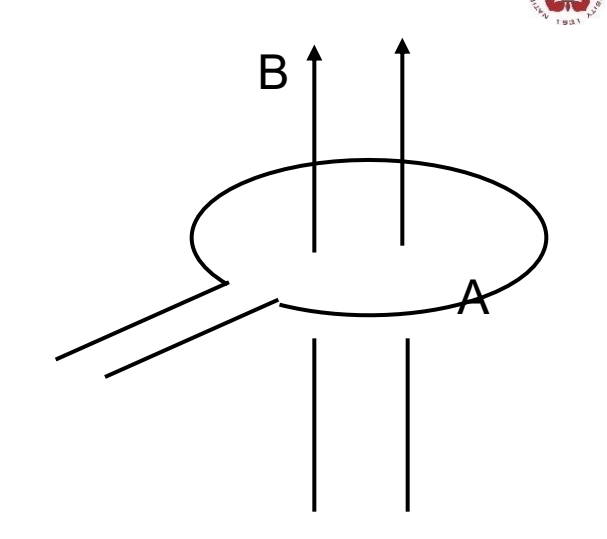
### Time dependent magnetic field can be measured using B-dot probe

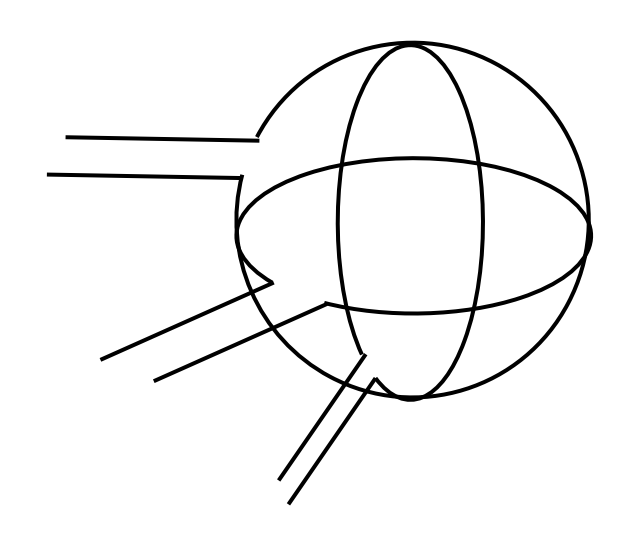
$$B = B(t)$$
  $\nabla \times \vec{E} = -\frac{\partial \vec{B}}{\partial t}$ 

$$\int d\vec{A} \nabla \times \vec{E} = \oint \vec{E} d\vec{l} = V = -\int d\vec{A} \frac{\partial}{\partial t} \vec{B}$$

$$V \sim -A \frac{\partial B}{\partial t}$$
  $B = -\int \frac{V}{A} dt \sim -\frac{1}{A} \int V dt$ 

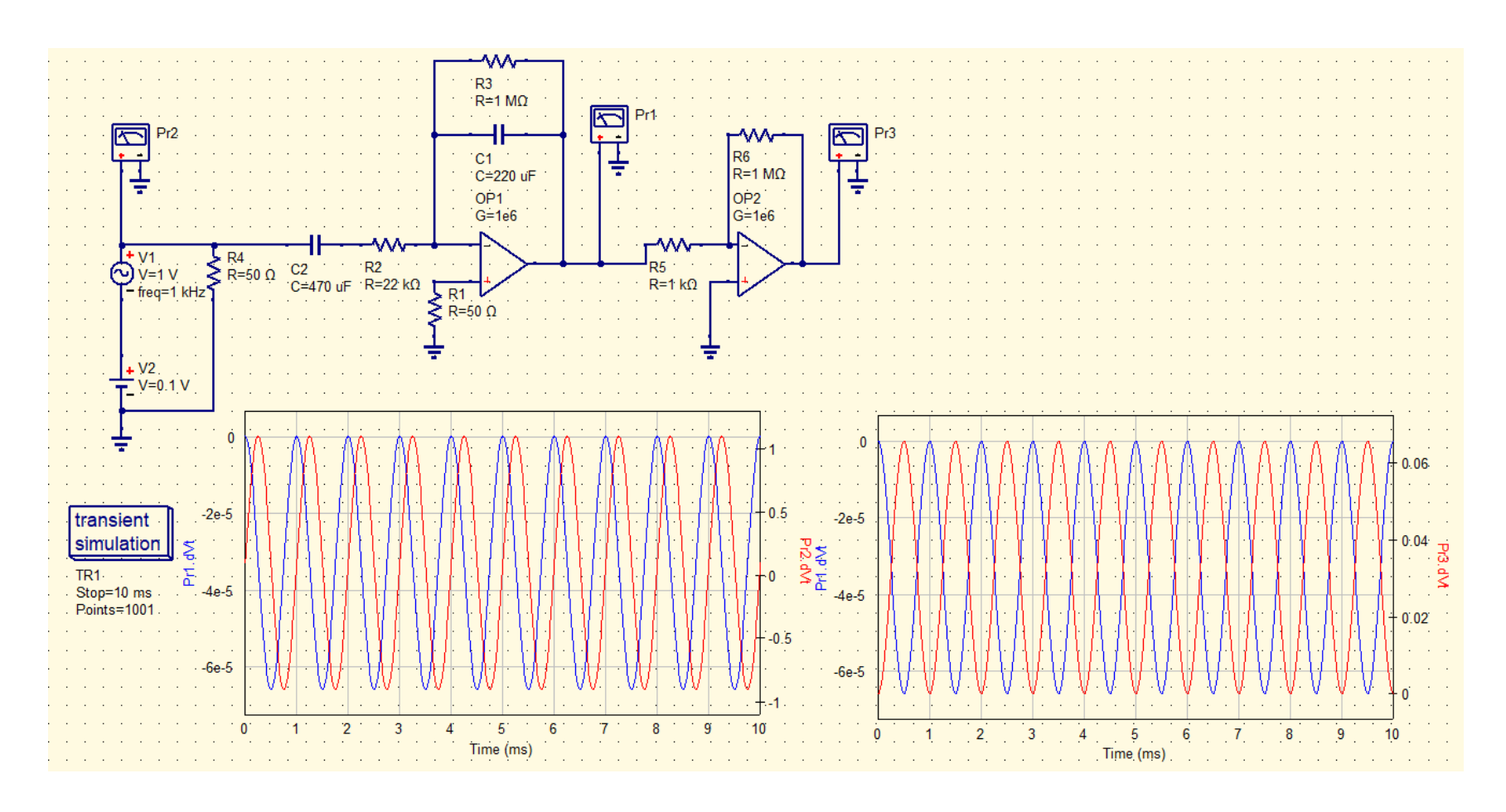






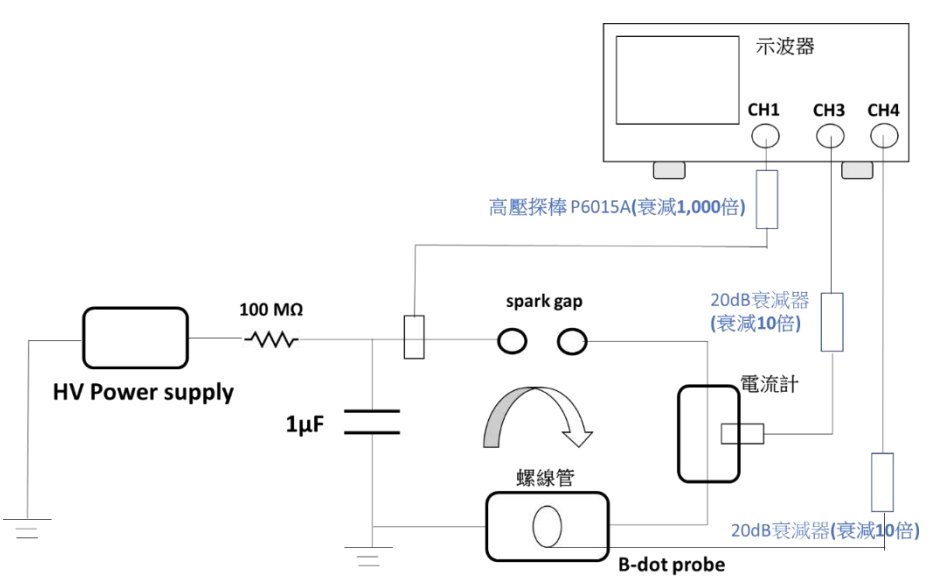
# The signal from the B-dot probe is integrated and amplified





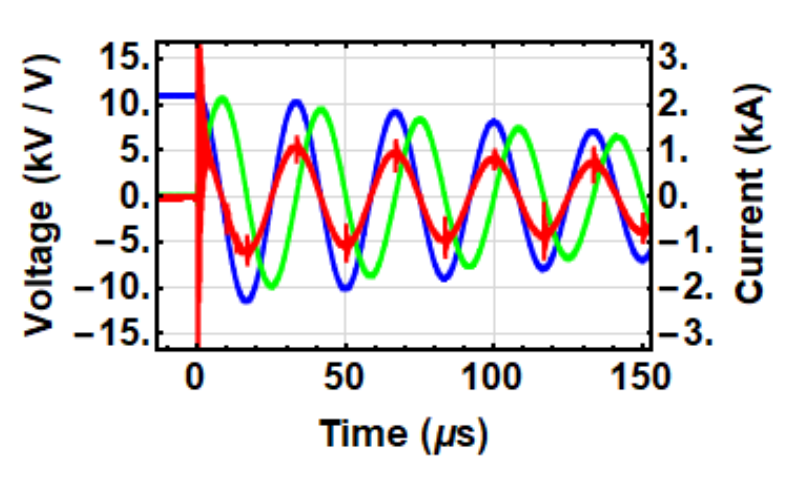
#### **B-dot probe experiments**



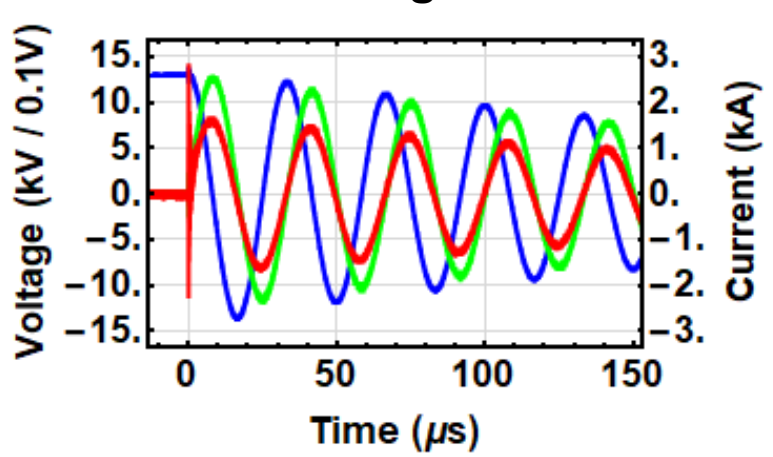




#### Without integrator



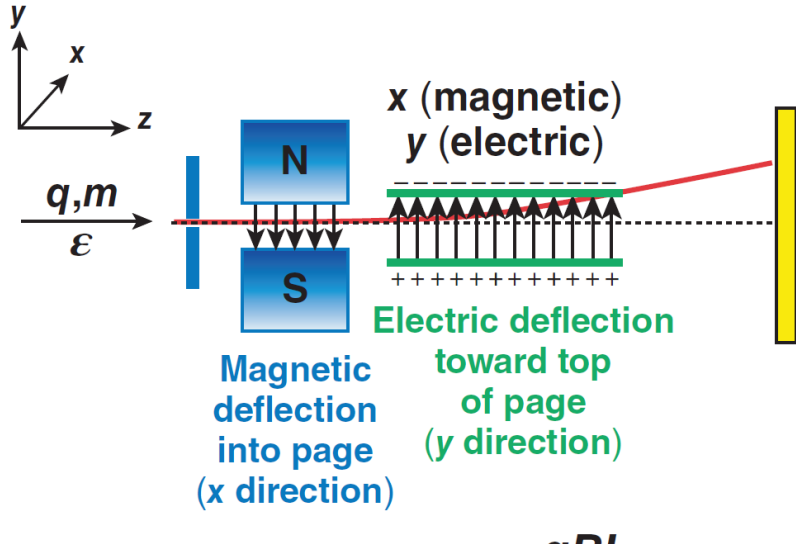
#### With integrator



Twisted pair

# A Thomson parabola uses parallel electric and magnetic fields to deflect particles onto parabolic curves that resolve q/m





$$\tan \Delta \theta_{\mathbf{X}} = \Delta \theta_{\mathbf{X}} = \frac{q\mathbf{BL}}{\mathbf{c}\sqrt{2}\,m\boldsymbol{\varepsilon}}$$

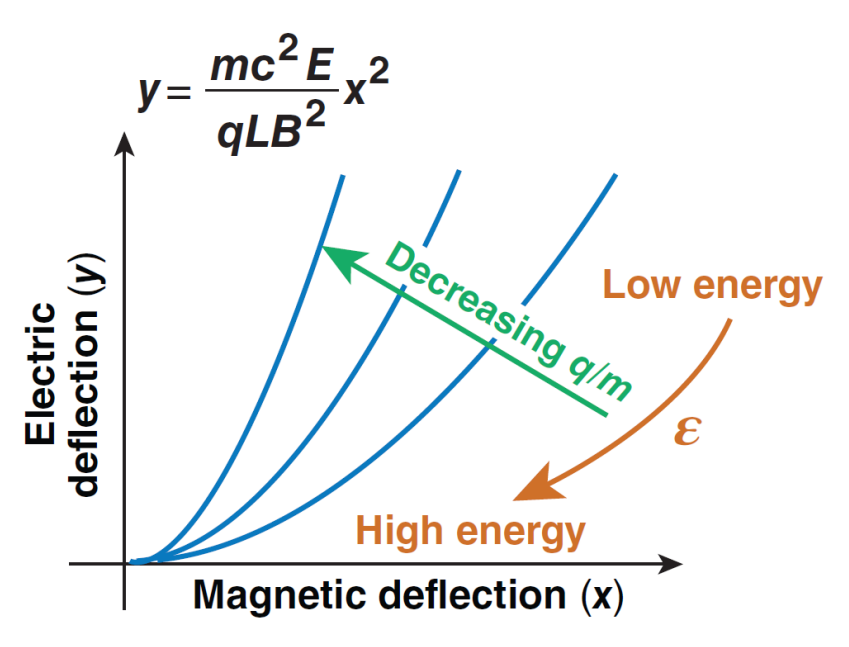
$$y \ \text{deflection}$$

$$F_{\perp} = q\mathbf{E}$$

$$\Delta m\mathbf{V}_{\mathbf{y}} = q\mathbf{E}\boldsymbol{\tau} = \frac{q\mathbf{EL}}{\mathbf{V}}$$

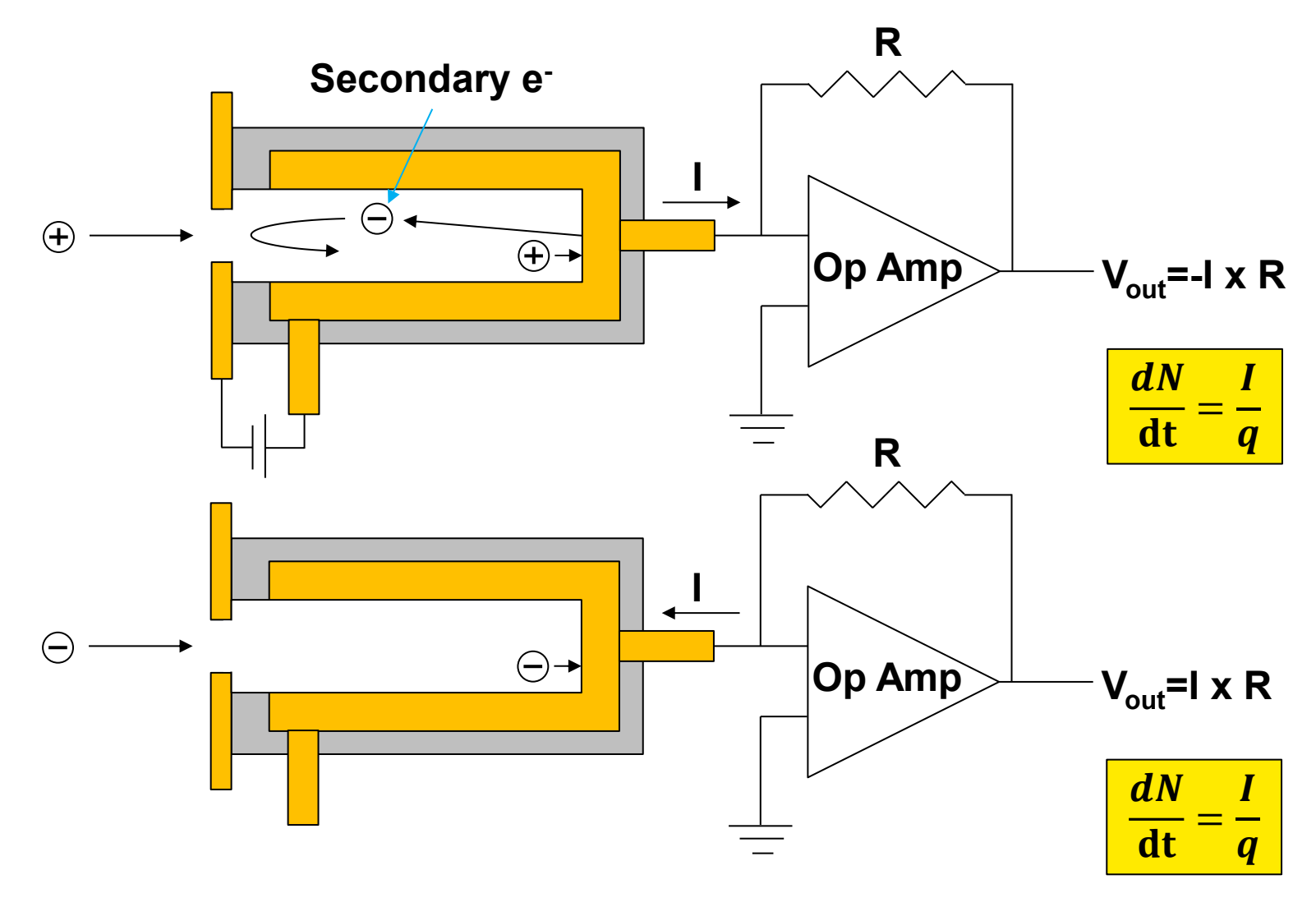
$$\tan \theta_{\mathbf{y}} \sim \theta_{\mathbf{y}} = \frac{\Delta m\mathbf{V}_{\mathbf{y}}}{m\mathbf{V}} = \frac{q\mathbf{EL}}{2\boldsymbol{\varepsilon}}$$

- Deflection caused by magnetic field ~q/p
- Deflection caused by electric field ~q/KE
- Ion traces form parabolic curves on detector plane

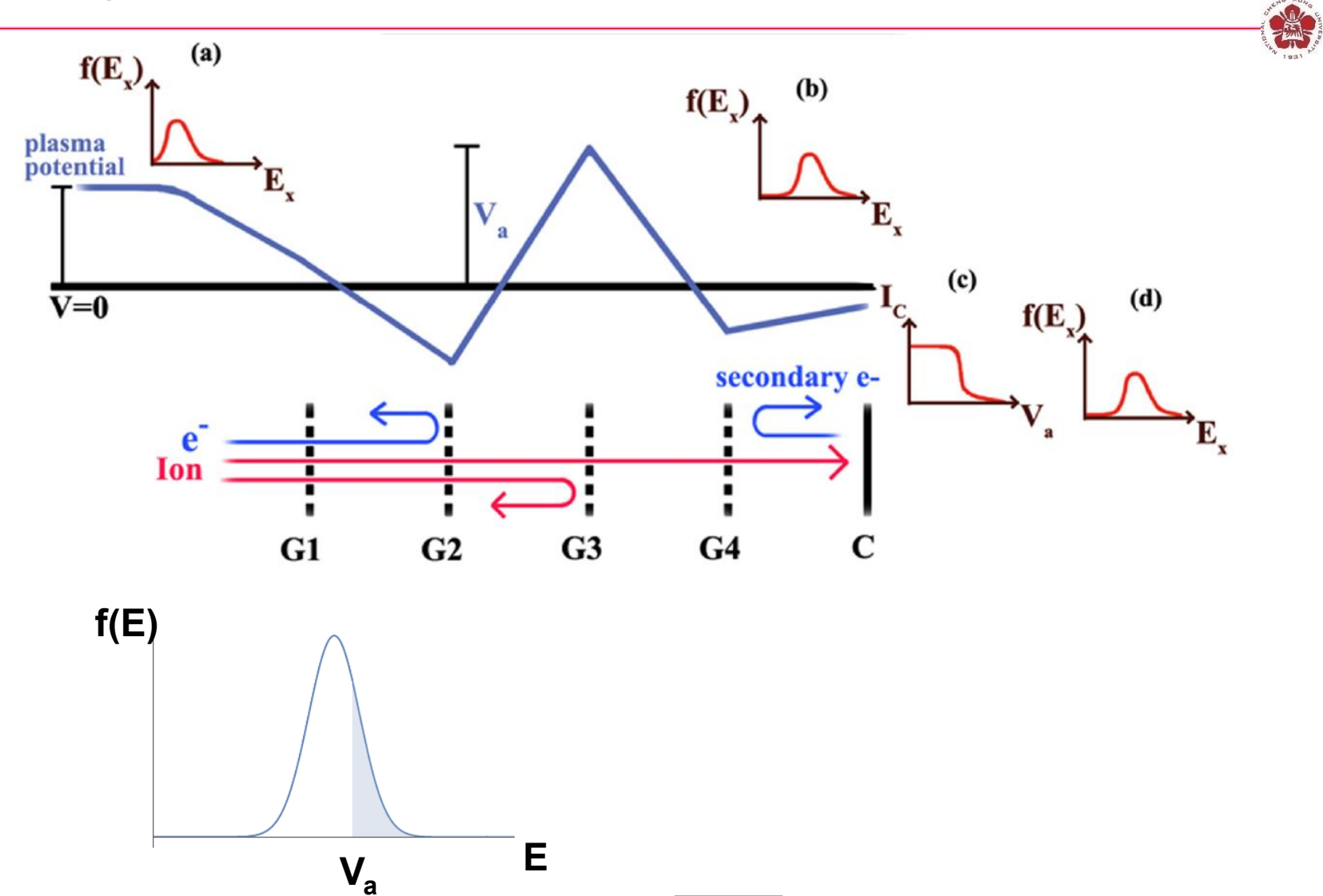


### A faraday cup measures the flux of charge particles





# Retarding potential analyzer measures the energy / velocity distribution function



### The photon energy spectrum provides valuable information

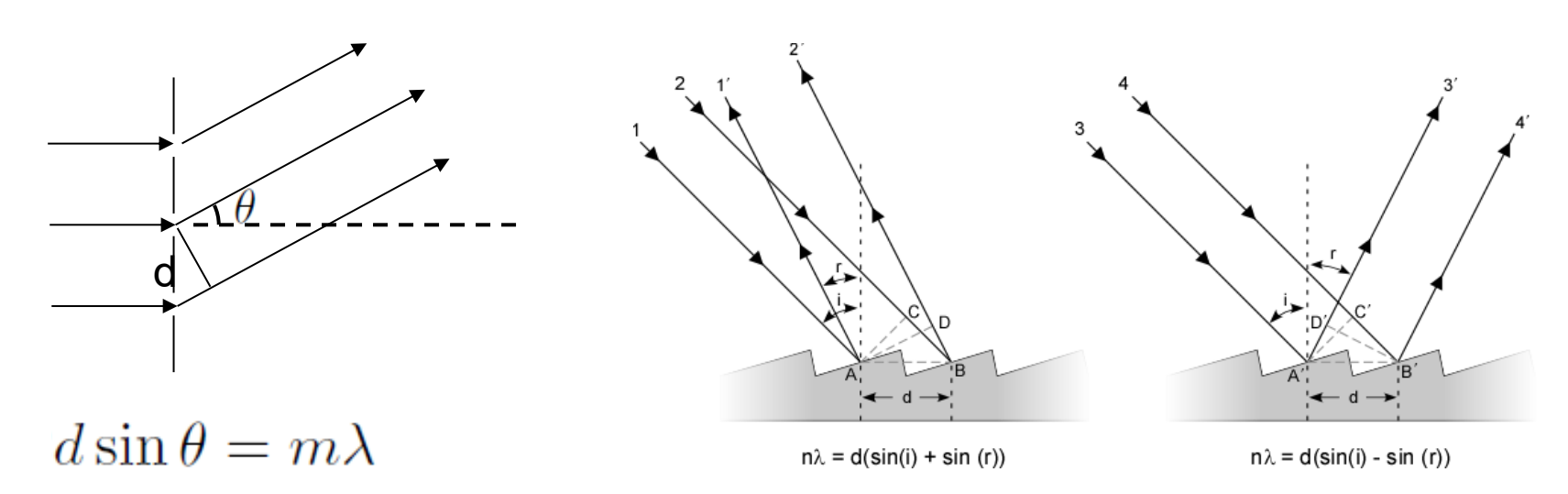


- Plasma conditions can be determined from the photon spectrum
  - visible light: absorption and laser-plasma interactions
  - x rays: electron temperature, density, plasma flow, material mixing
- There are three basic tools for determining the spectrum detected
  - filtering
  - grating spectrometer
  - Bragg spectrometer

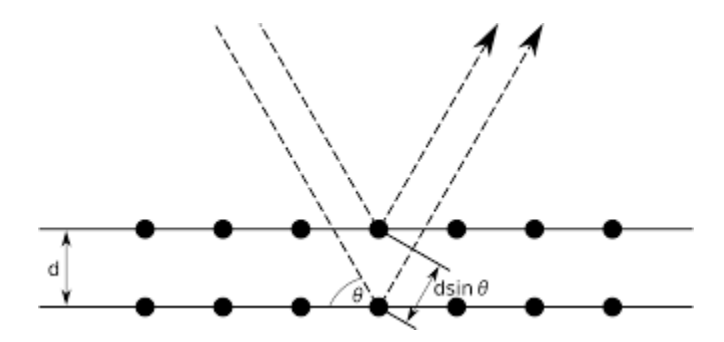
#### Spectrum can be obtained using grating



Grating is used to disperse the light



Bragg condition in the crystal is used for X-ray.

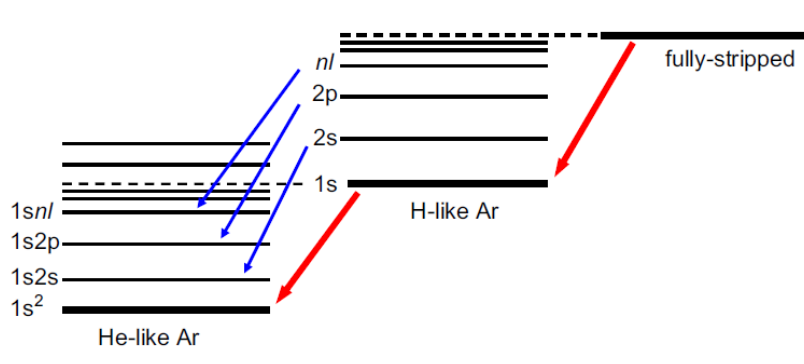


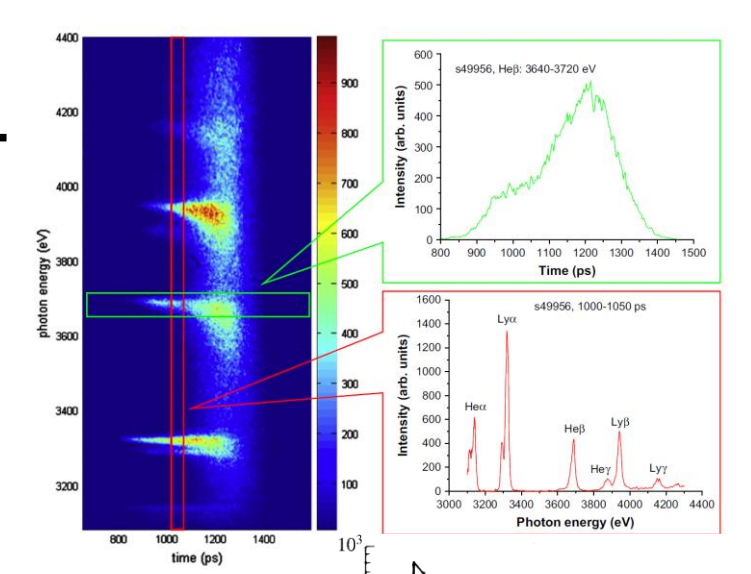
 $2d\sin\theta = m\lambda$ 

### Temperature and density can be obtained from the emission



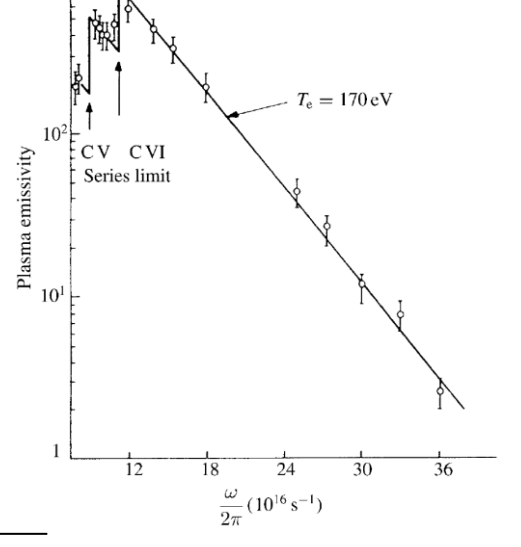
#### Line emission





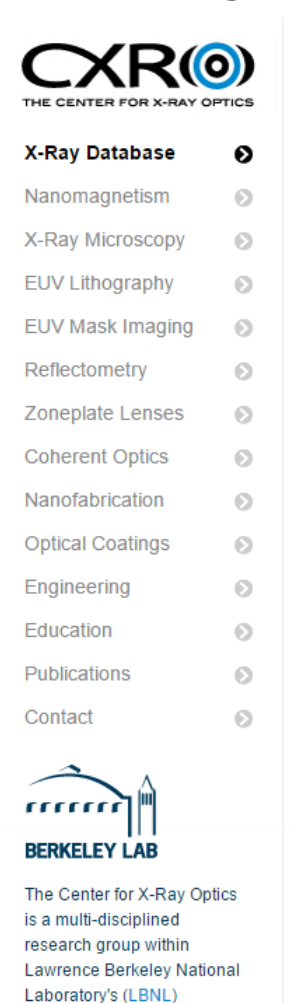
#### **Bremsstrahlung emission**

$$\eta_{\nu} = \frac{16\pi}{3\sqrt{6\pi}} \frac{e^6}{m_{\rm e}^2 c^3} \frac{Z_{\rm i}^2 n_{\rm e}}{\sqrt{k_{\rm B} T_{\rm e}/m_{\rm e}} A m_{\rm p}} \exp\left(-\frac{h\nu}{k_{\rm B} T_{\rm e}}\right)$$



# Information of x-ray transmission or reflectivity over a surface can be obtained from the Center for X-Ray Optics

http://henke.lbl.gov/optical\_constants/



#### X-Ray Interactions With Matter

#### Introduction

Access the atomic scattering factor files.

Look up x-ray properties of the elements.

The index of refraction for a compound material.

The x-ray attenuation length of a solid.

X-ray transmission

- Of a solid.
- Of a gas.

X-ray reflectivity

- · Of a thick mirror.
- Of a single layer.
- Of a bilayer.
- · Of a multilayer.

The diffraction efficiency of a transmission grating.

Related calculations:

Synchrotron bend magnet radiation.

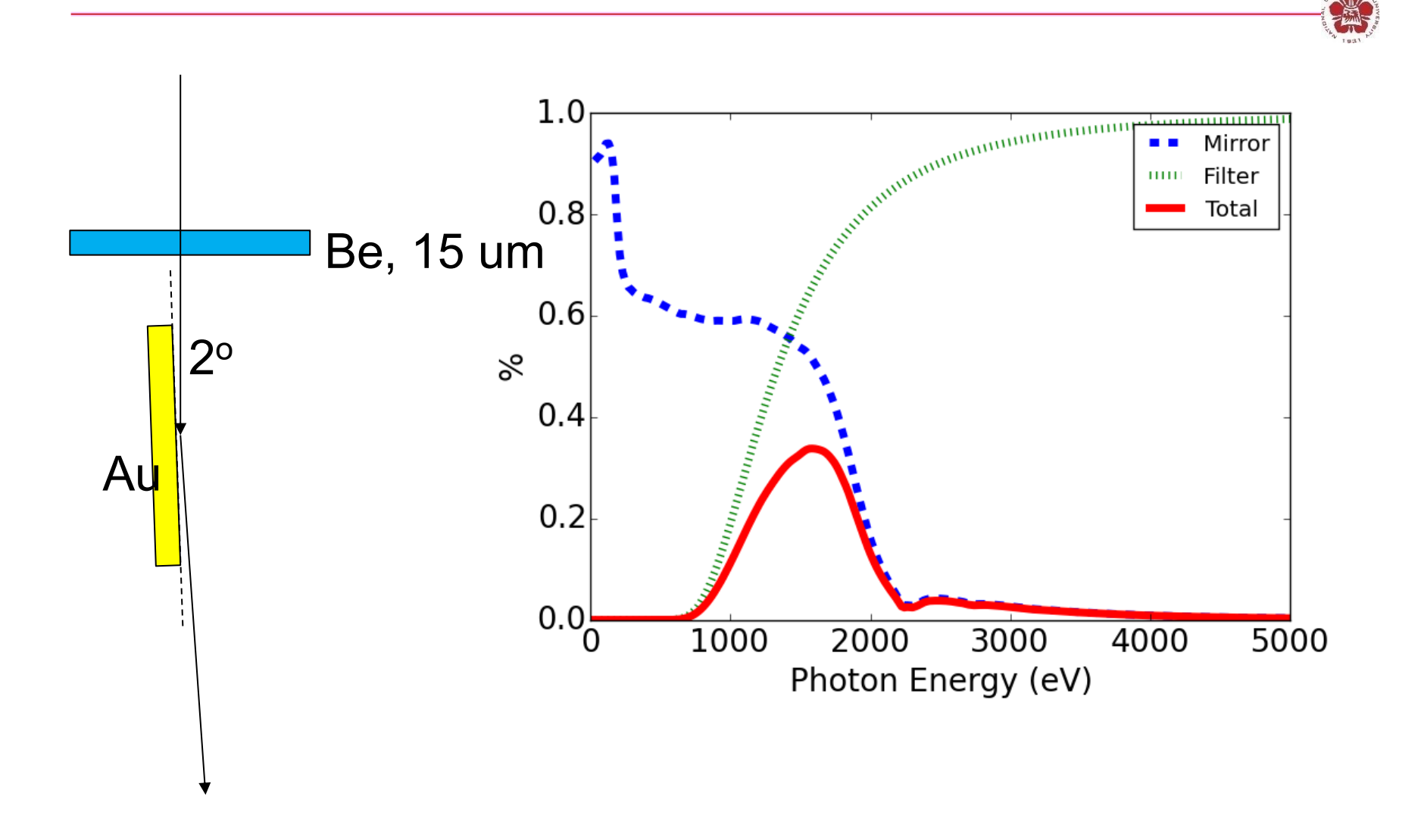
Other x-ray web resources.

X-ray Data Booklet

#### Reference

B.L. Henke, E.M. Gullikson, and J.C. Davis. *X-ray interactions: photoabsorption, scattering, transmission, and reflection at E=50-30000 eV, Z=1-92*, Atomic Data and Nuclear Data Tables Vol. **54** (no.2), 181-342 (July 1993).

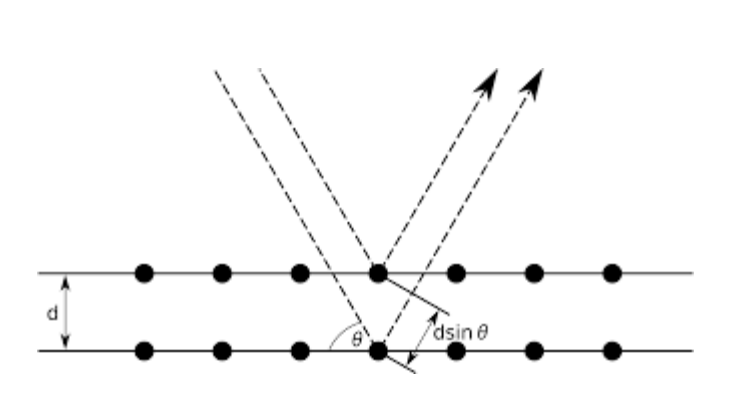
### A band pass filter is obtained by combing a filter and a mirror

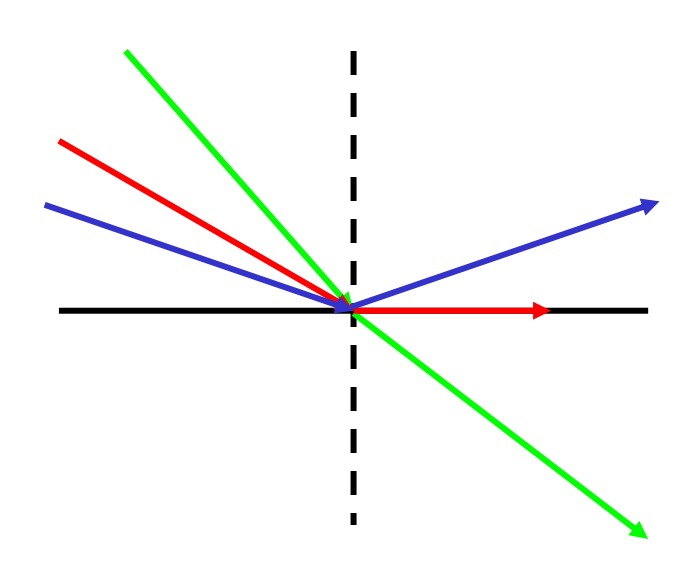


#### X rays can not be concentrated by lenses



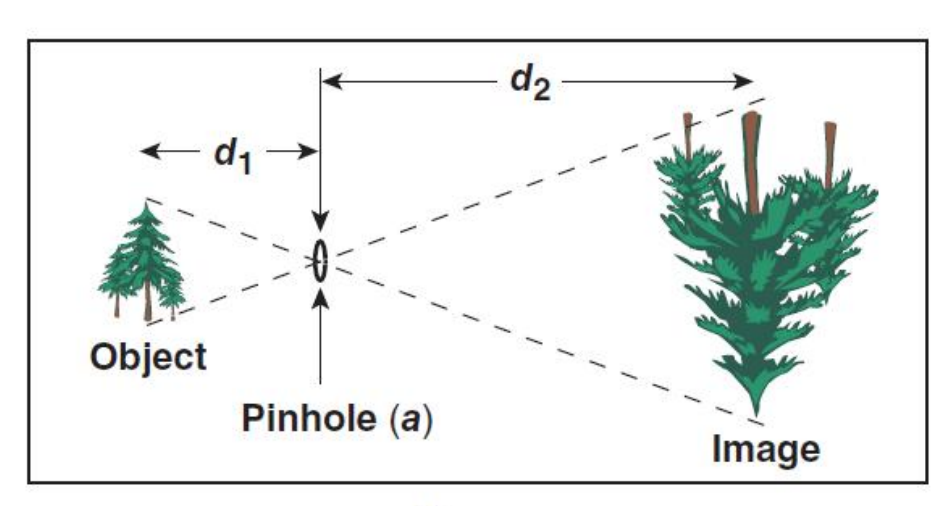
- X-ray refractive indices are less than unity,  $n \lesssim 1$
- For those with lower refractive indices, the absorption is also strong
- X-ray mirrors can be made through
  - Bragg reflection
  - External total reflection with a small grazing angle





#### The simplest imaging device is a pinhole camera





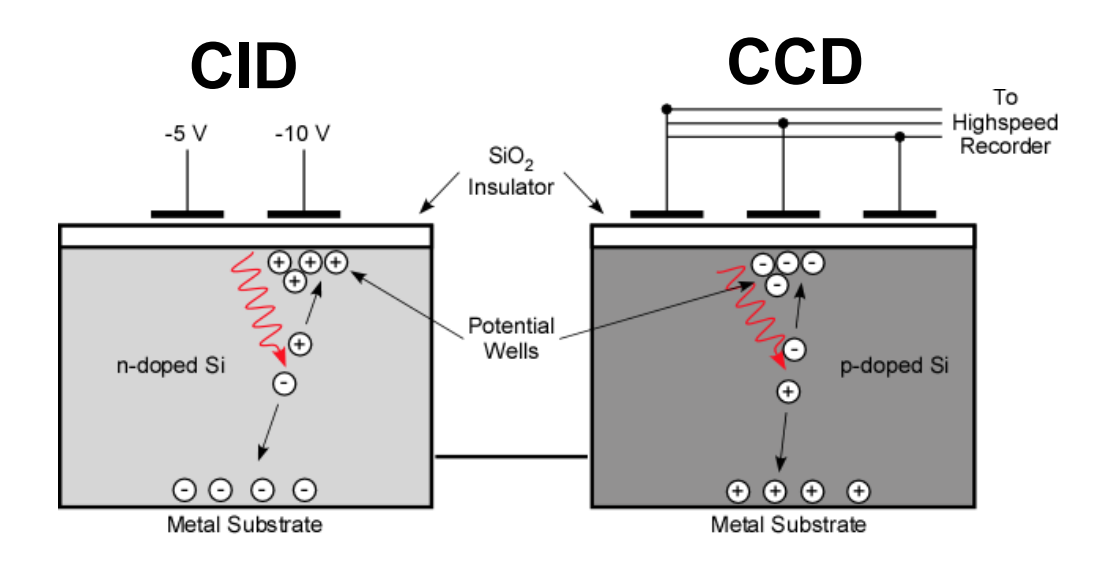
#### Kodak Brownie camera

- Magnification =  $\frac{d_2}{d_1}$
- Infinite depth of field (variable magnification)
- Pinhole diameter determines
  - resolution ~a
  - light collection:  $\Delta\Omega = \frac{\pi}{4} \frac{a^2}{d_1^2}$

Imaging optics (e.g., lenses) can be used for higher resolutions with larger solid angles.

# 2D images can be taken using charge injection device (CID) or charge coupled device (CCD)

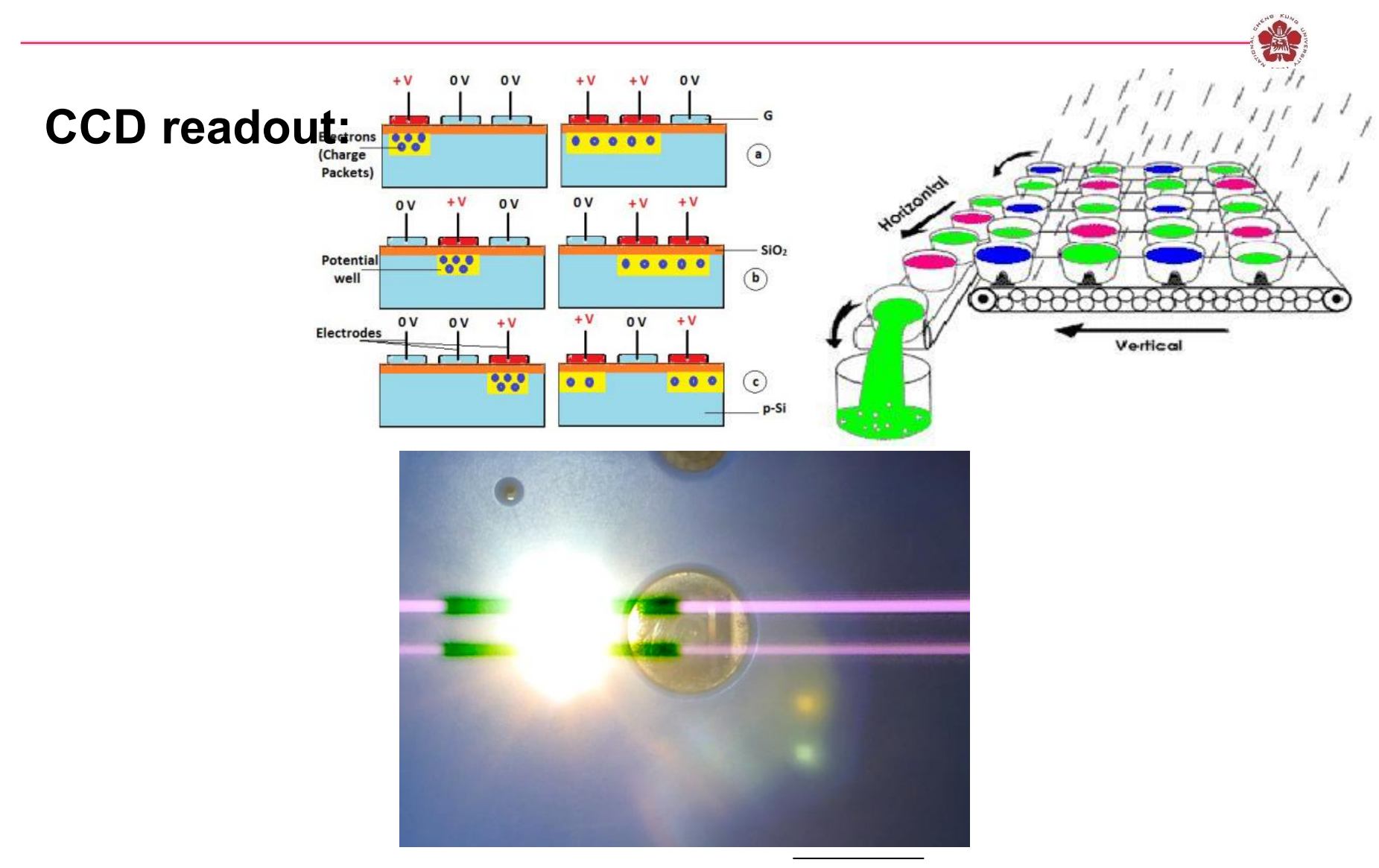




Color mask is used for color image

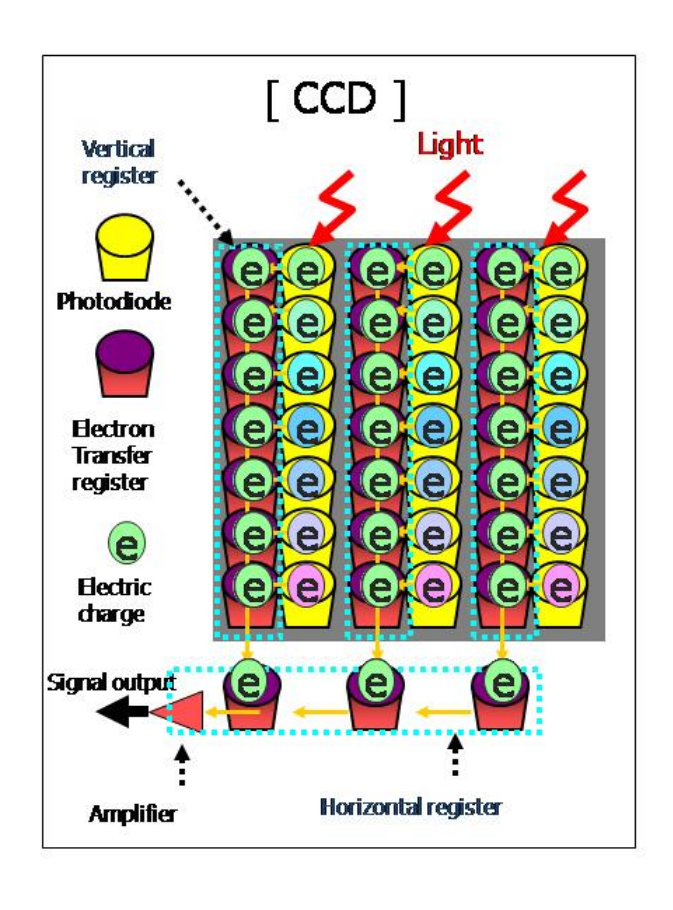


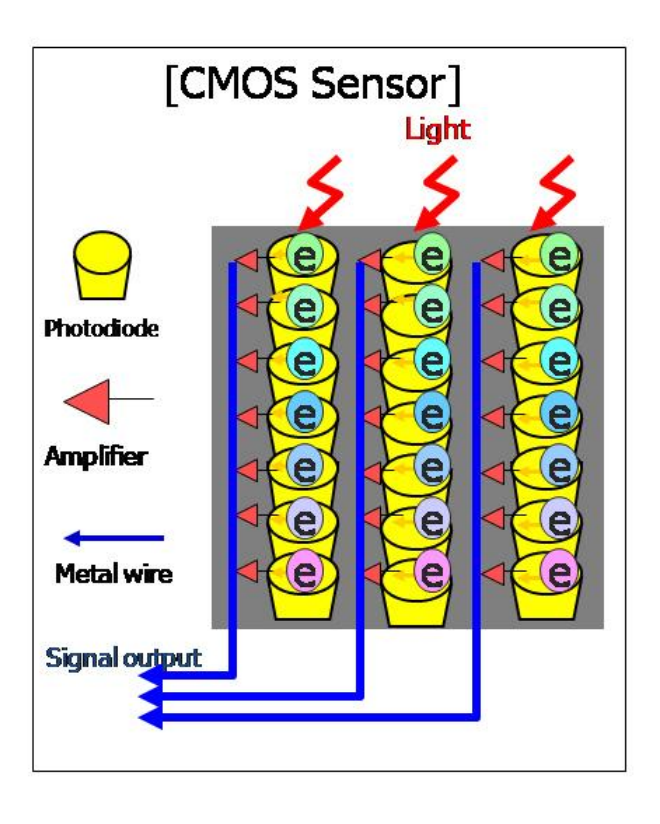
### Charges are transferred along the array for readout in CCD



### Signal is readout individually in CMOS sensor

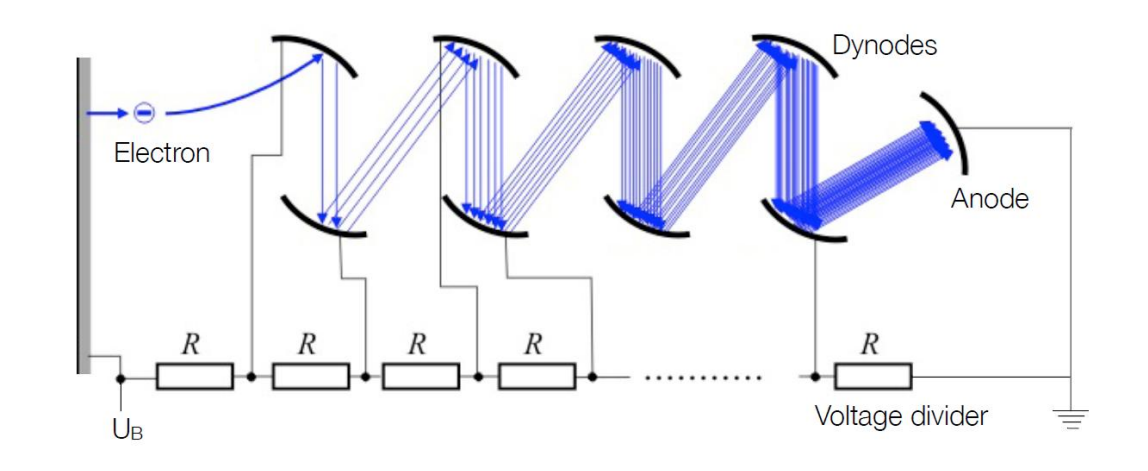


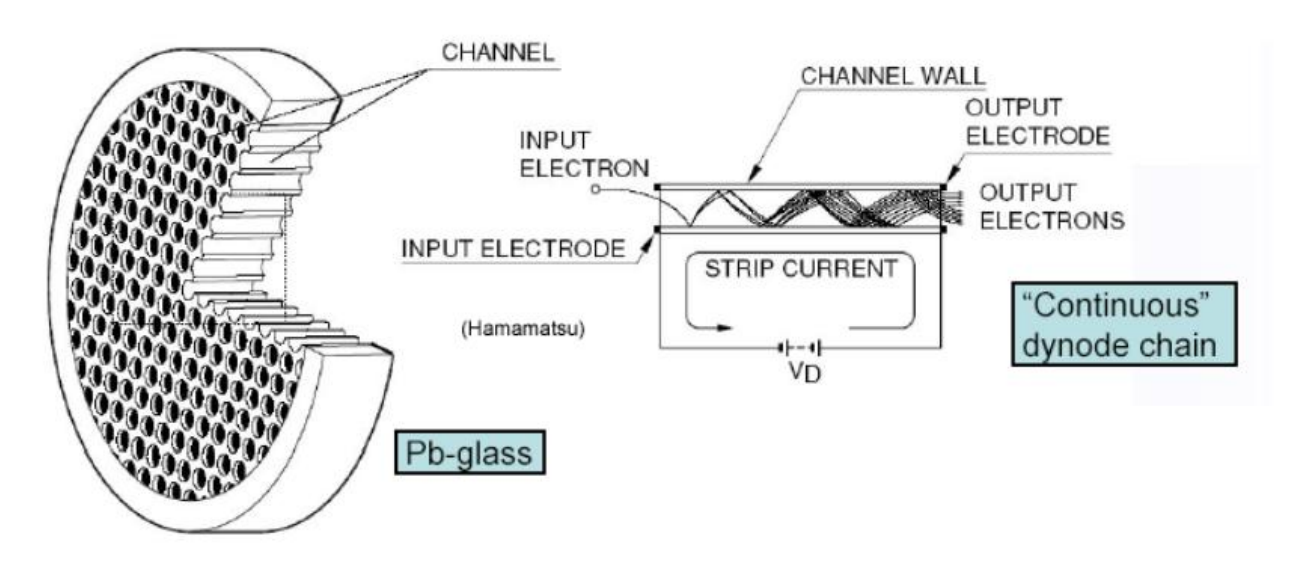




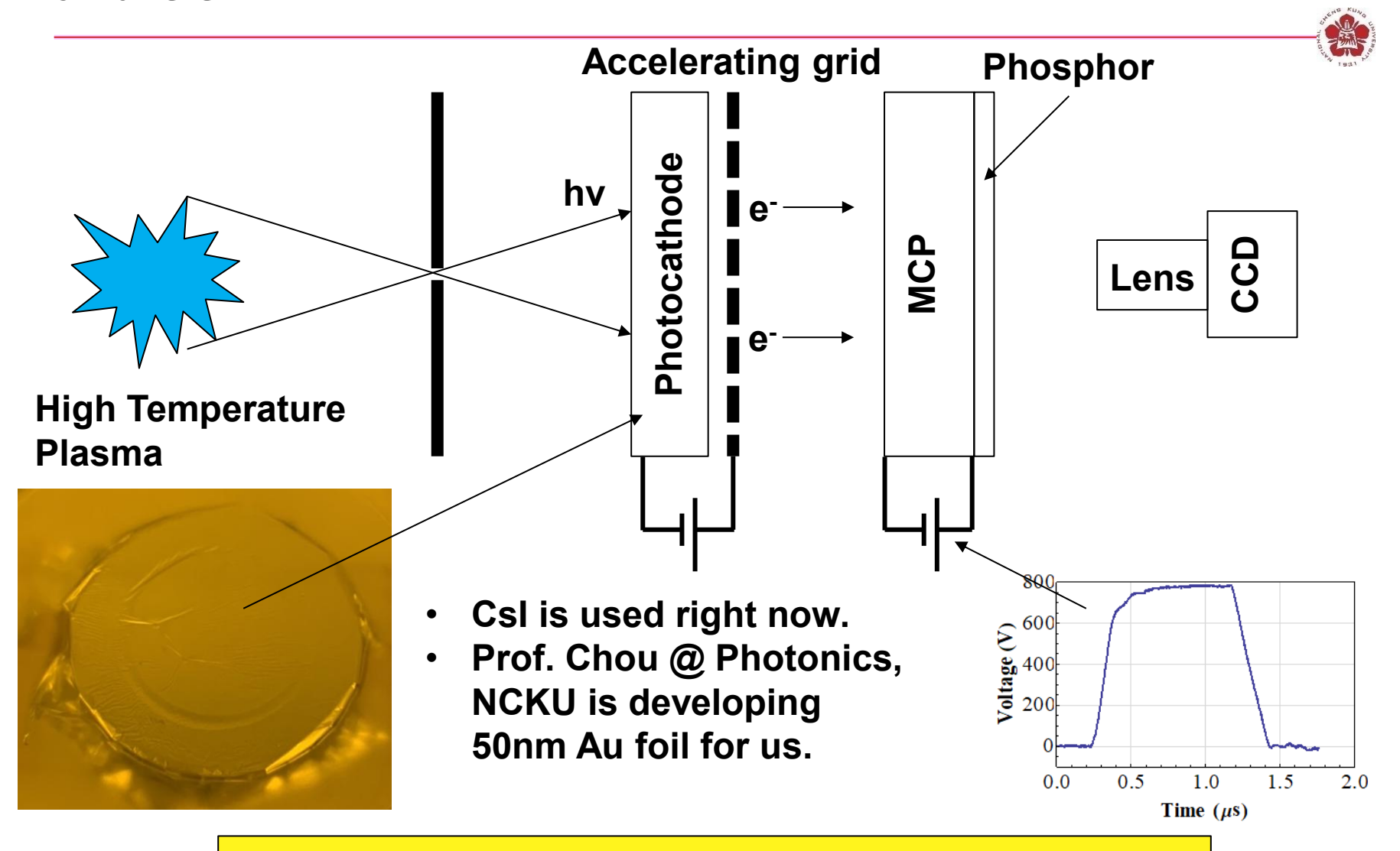
### The number of electrons can be increased through photomultipliers or microchannel plate (MCP)





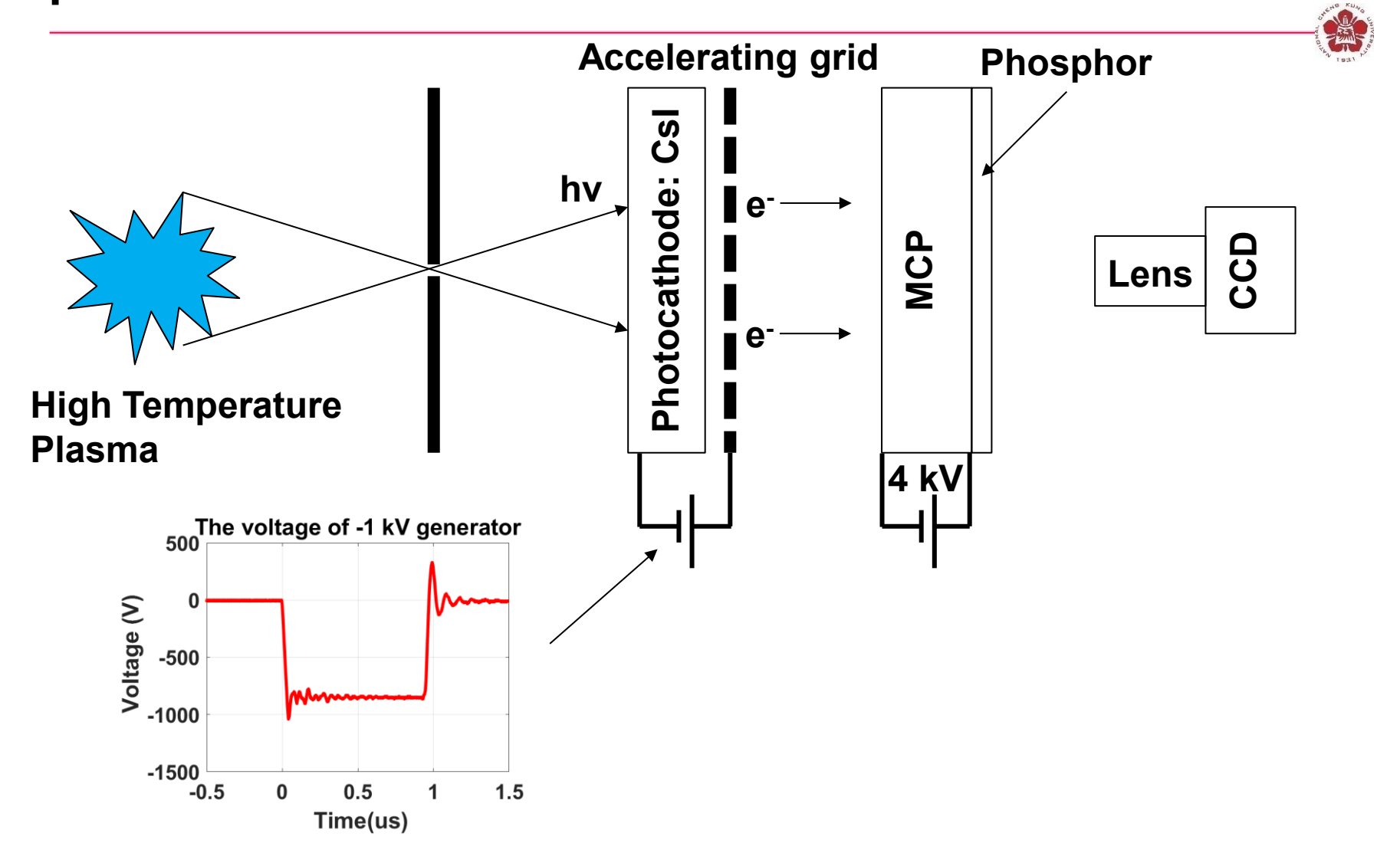


### X-rays are imaged using photocathode, MCP, phosphor, and CCD



Images can be gated using fast high voltage pulses.

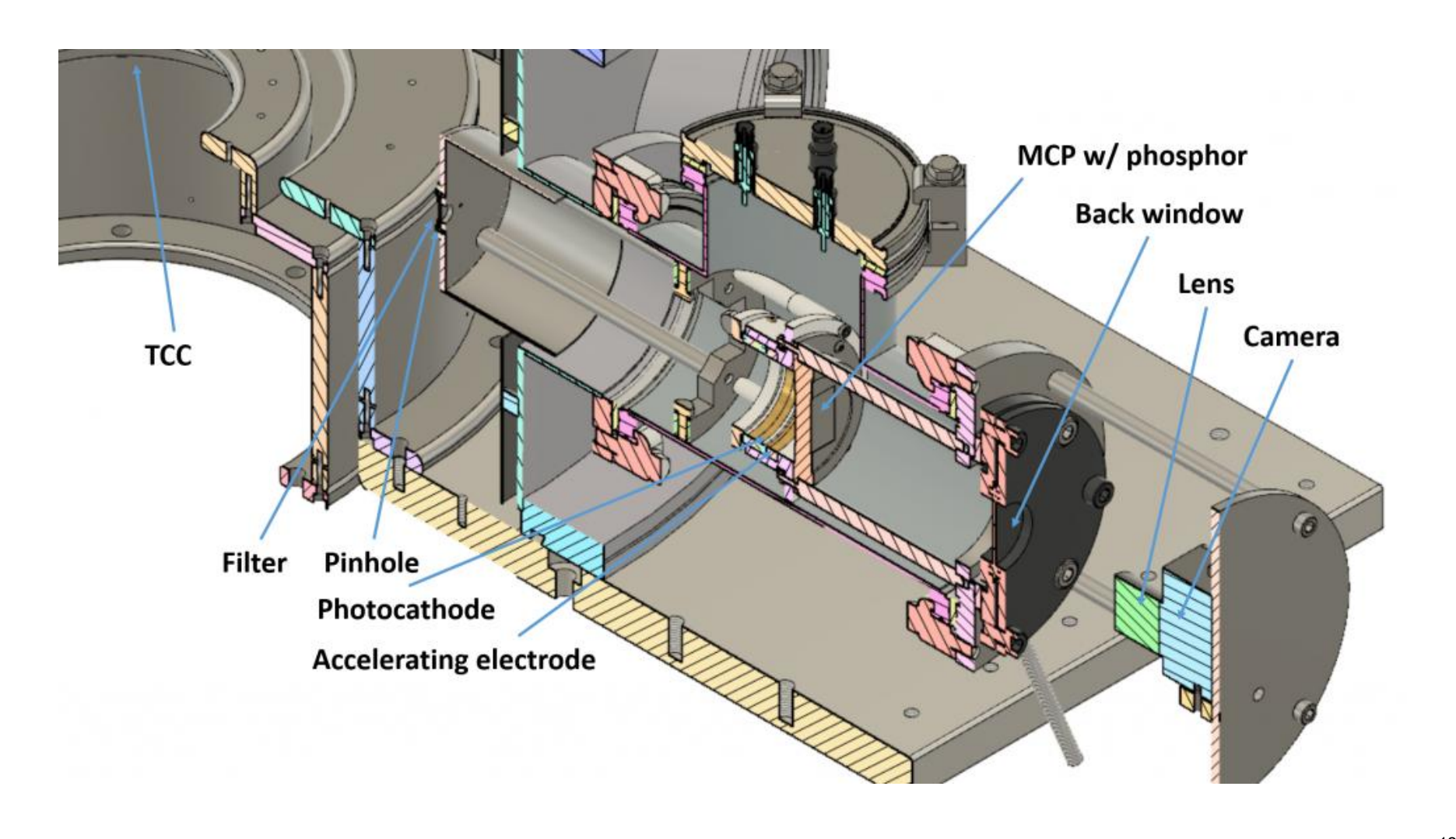
### A negative high-voltage pulse is used in our x-ray pinhole camera



The x-ray camera with a shutter opening time of ≤ 10 ns will be built.

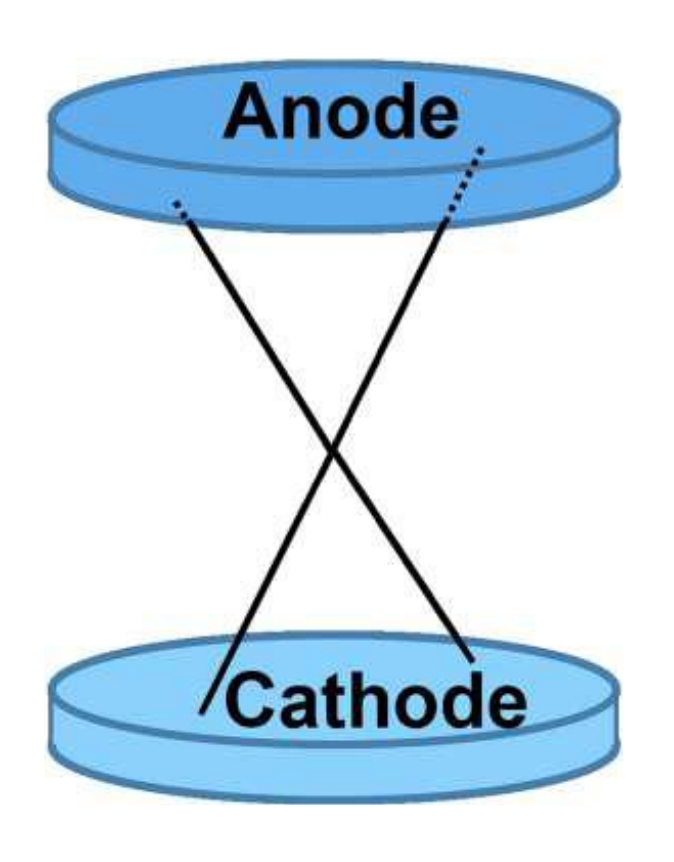
### A pinhole camera was designed and was built

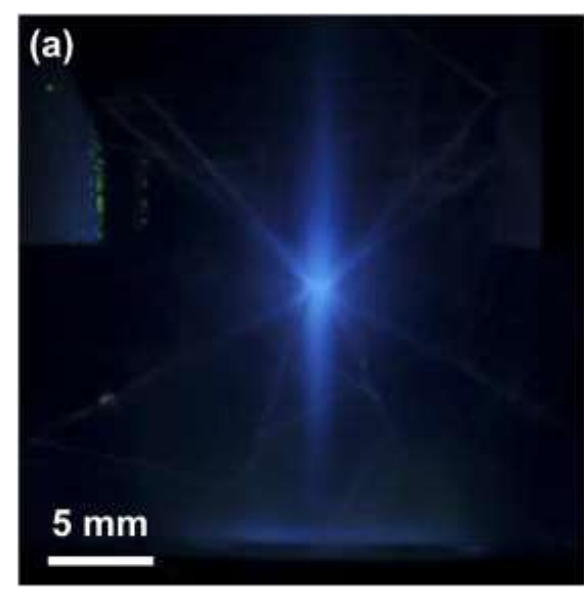


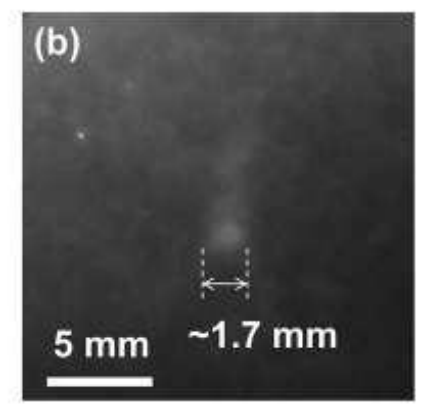


### Emission from an x pinch





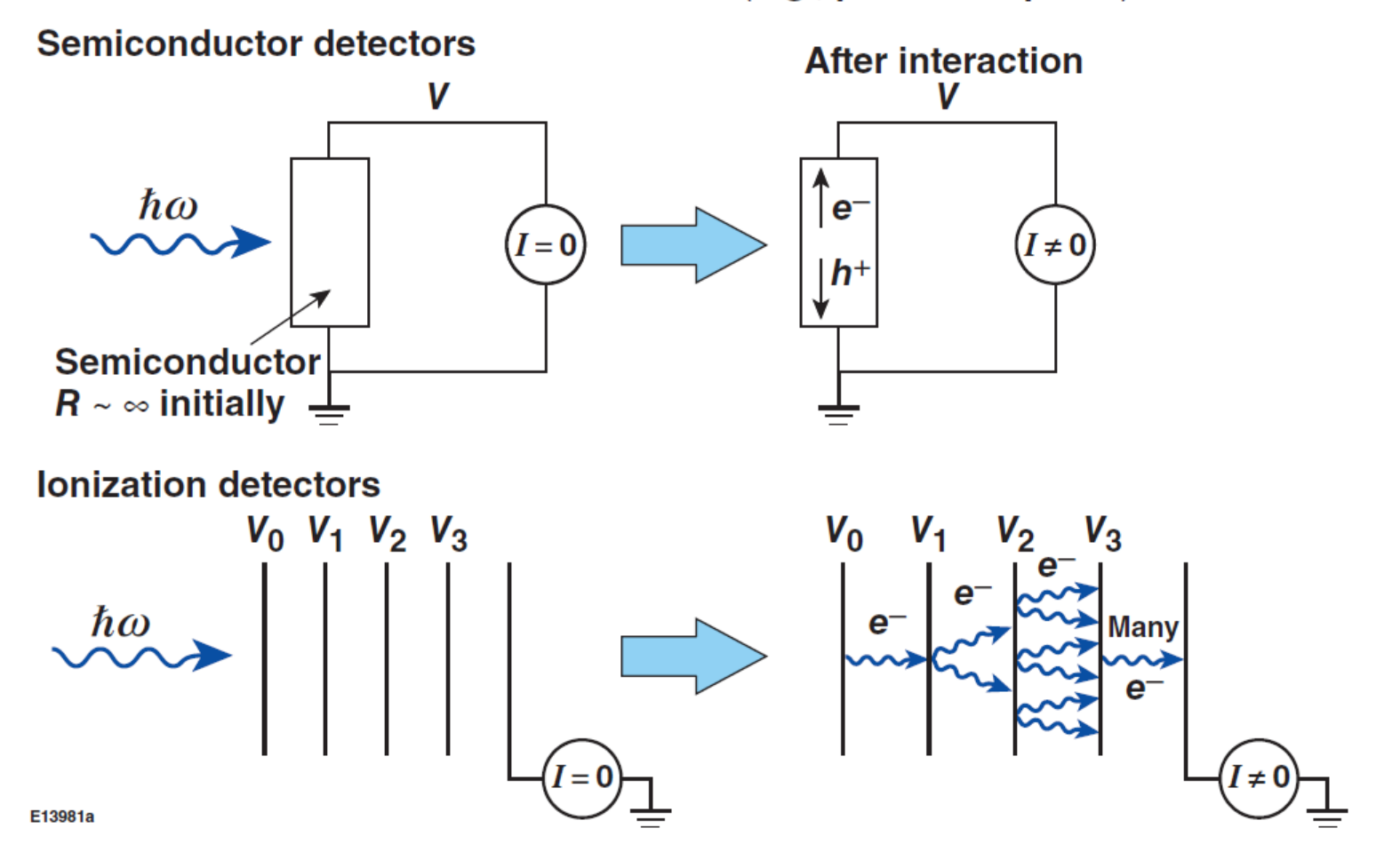




#### Electronic detectors provide rapid readout



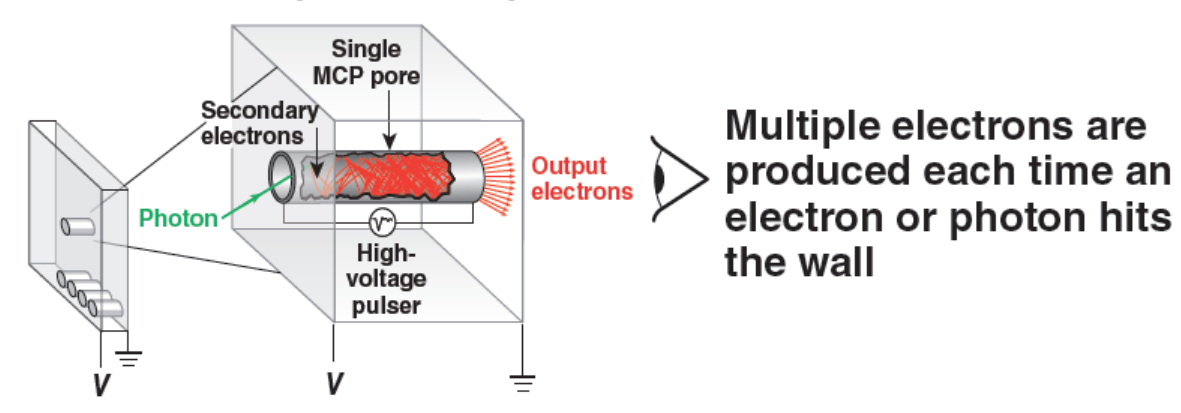
 Electronic detectors are typically semiconductors or ionization-based stacks (e.g., photomultipliers)



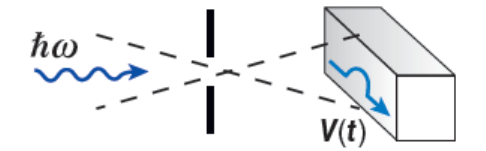
# A framing camera provides a series of time-gated 2-D images, similar to a movie camera



- The building block of a framing camera is a gated microchannel-plate (MCP) detector
- An MCP is a plate covered with small holes, each acts as a photomultiplier



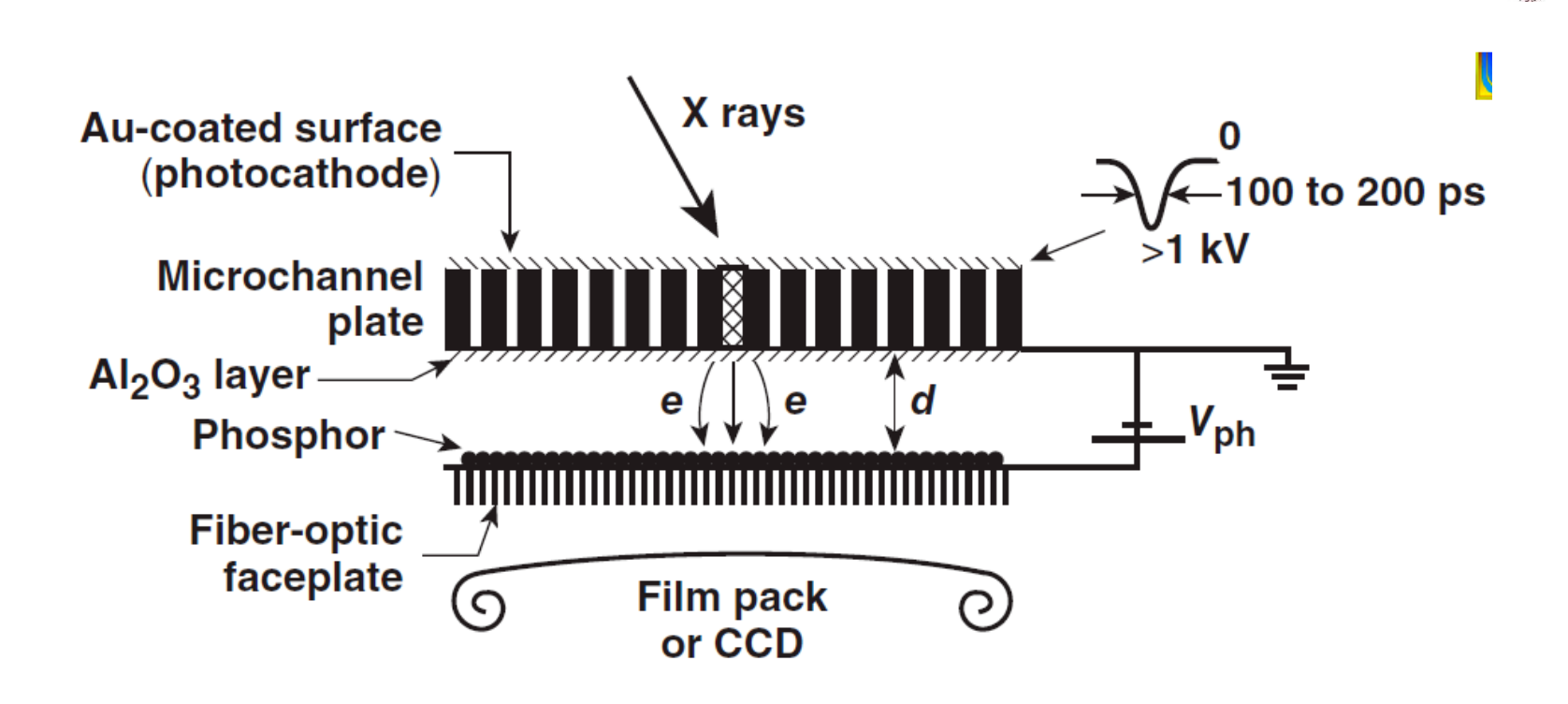
A voltage pulse is sent down the plate, gating the detector



The detector is only on when the voltage pulse is present

E13986b

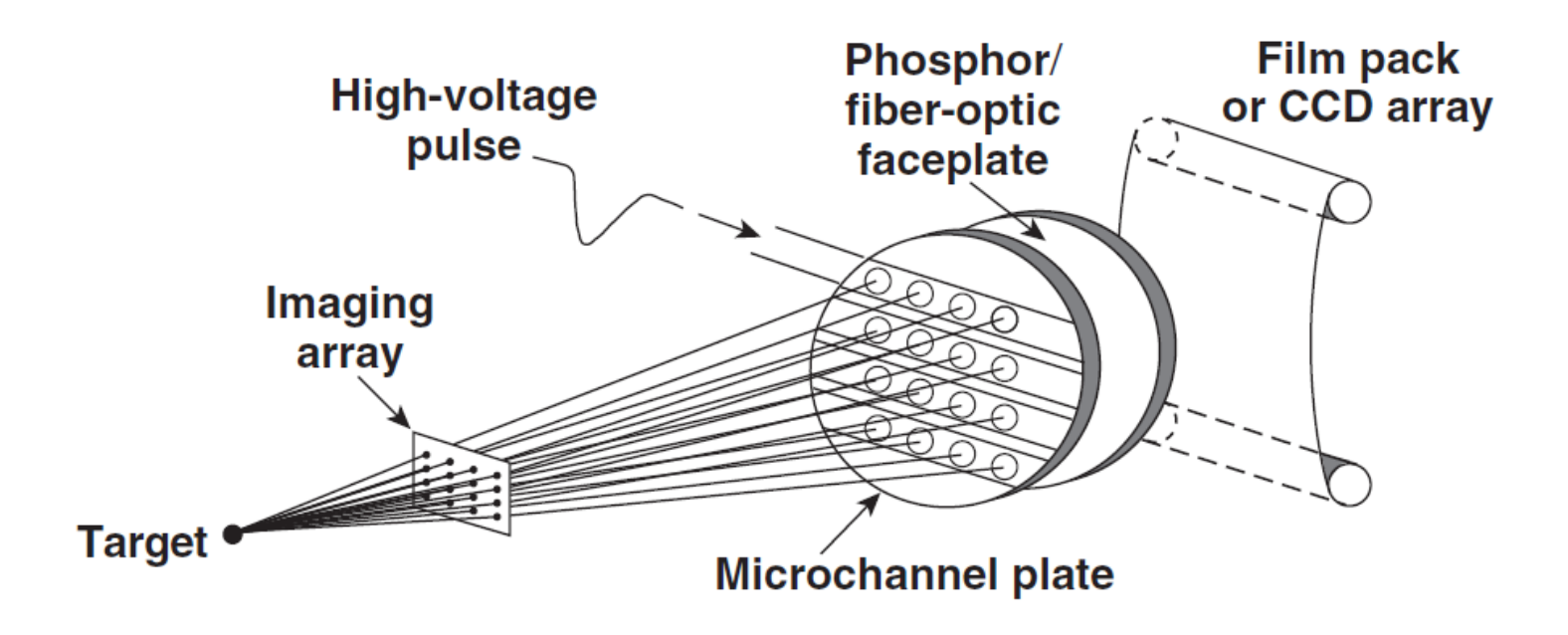
# A framing camera detector consists of a microchannel plate (MCP) in front of a phosphor screen



- Electrons are multiplied through MCP by voltage V<sub>c</sub>
- Images are recorded on film behind phosphor
- Insulating Al<sub>2</sub>O<sub>3</sub> layer allows for V<sub>ph</sub> to be increased, thereby improving the spatial resolution of phosphor

### Two-dimensional time-resolved images are recorded using x-ray framing cameras

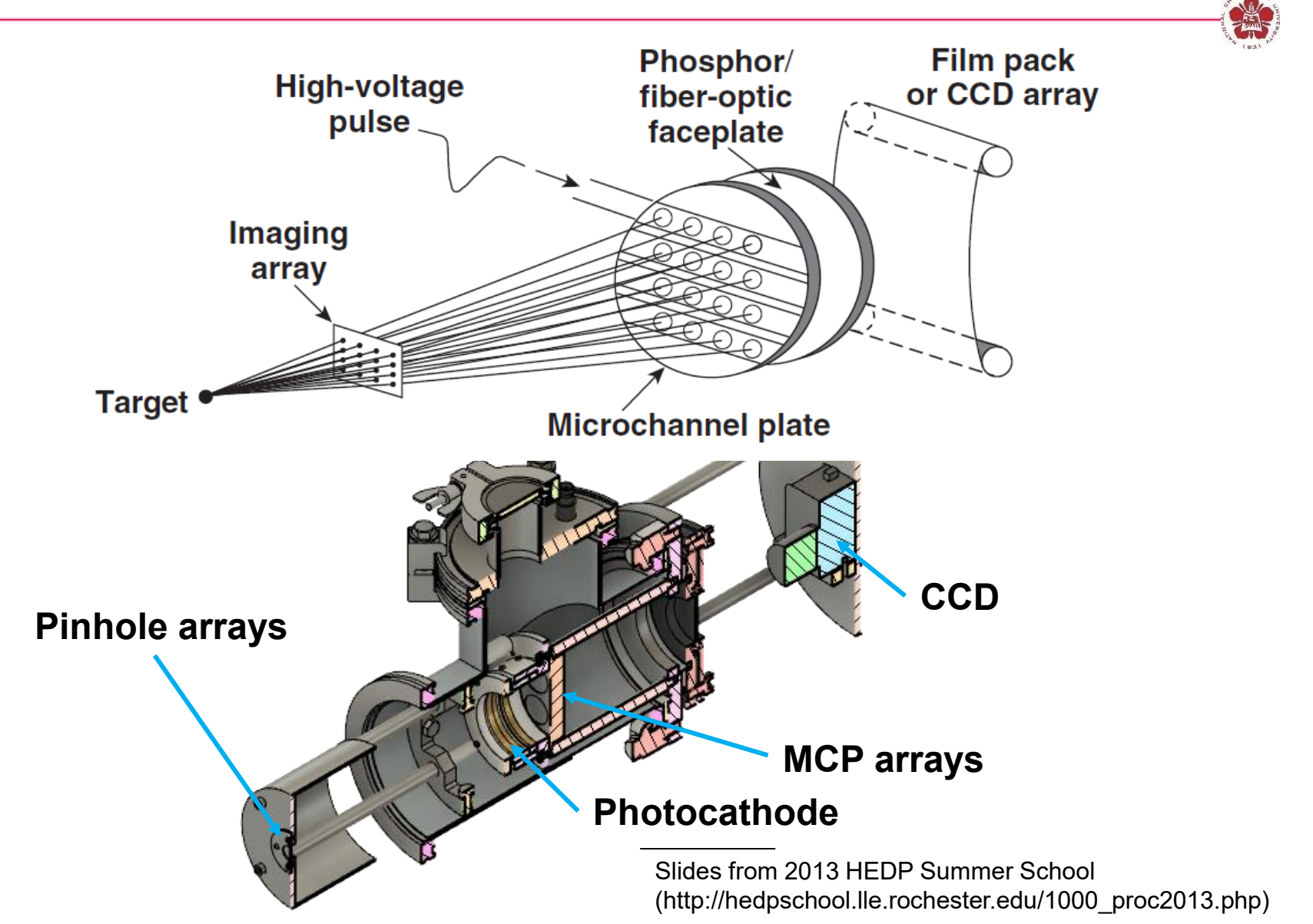




- Temporal resolution = 35 to 40 ps
- Imaging array: Pinholes: 10- to 12- $\mu$ m resolution, 1 to 4 keV
- Space-resolved x-ray spectra can be obtained by using Bragg crystals and imaging slits

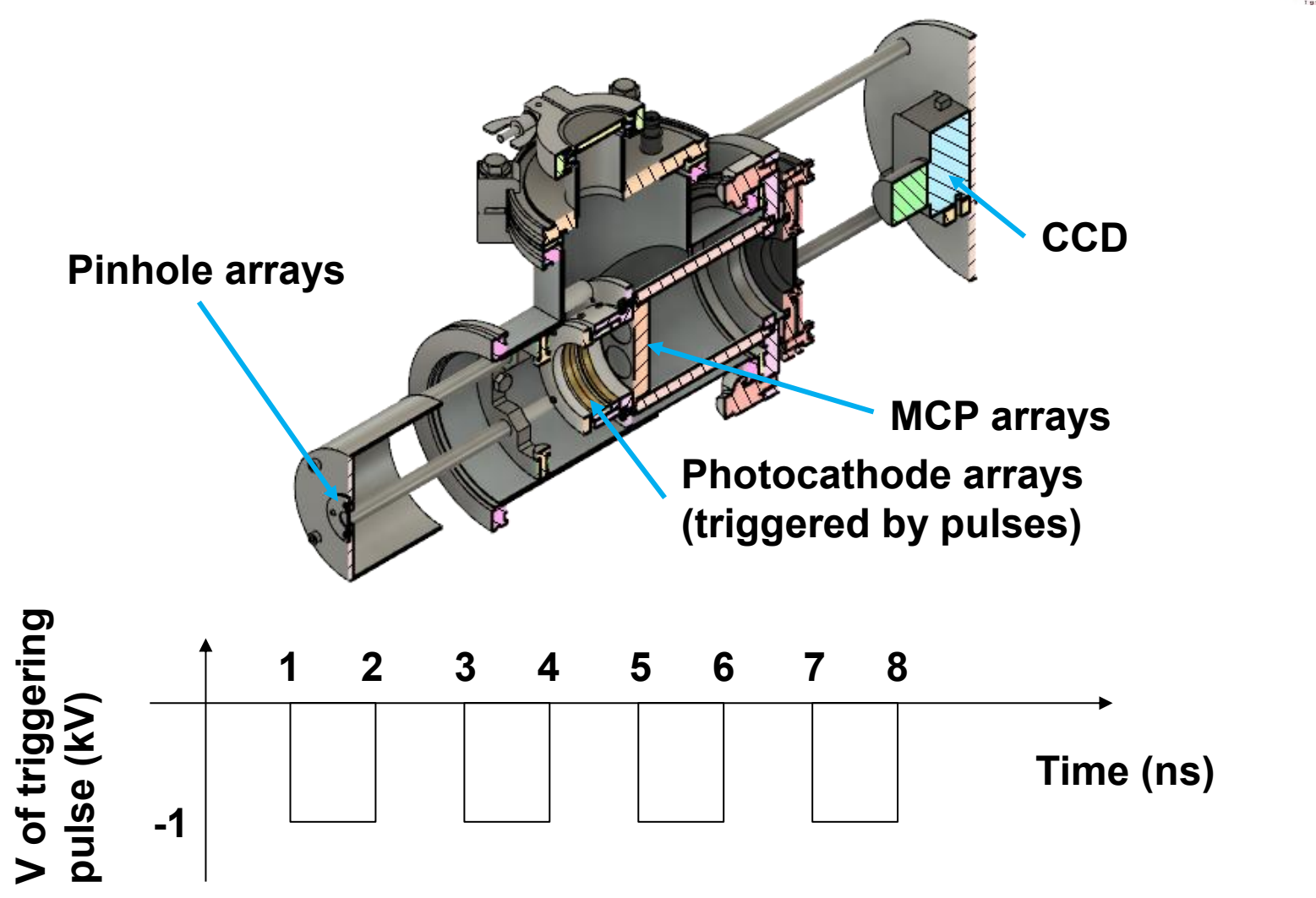
#### Framing camera

# X-ray framing cameras for recording two-dimensional time-resolved images will be built by the end of 2021



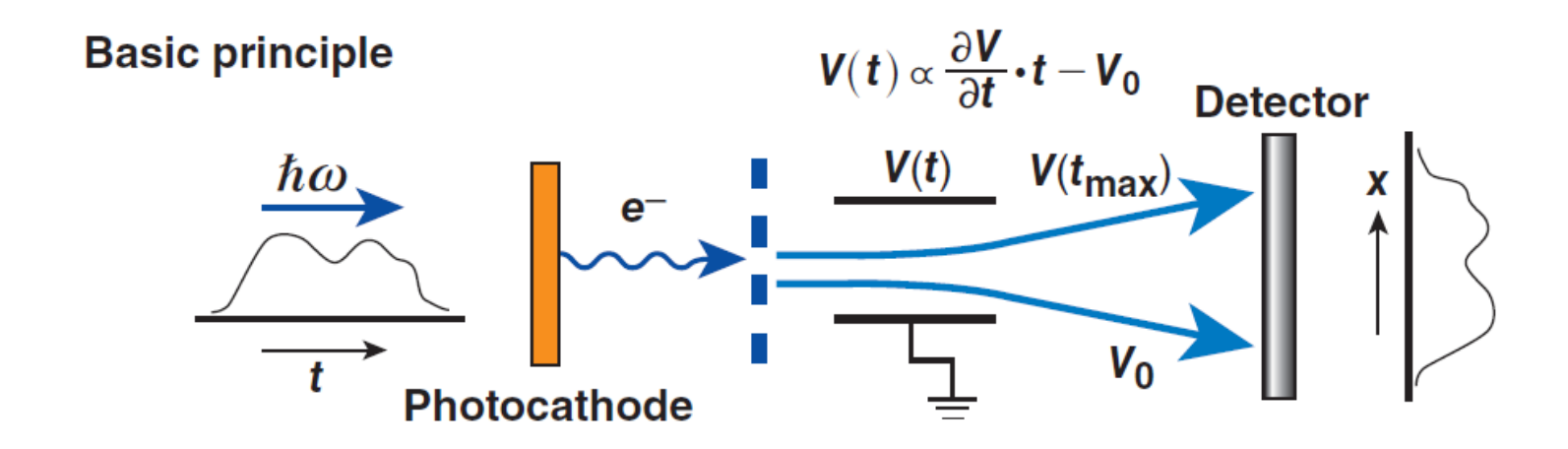
### Each pinhole camera will be triggered separately



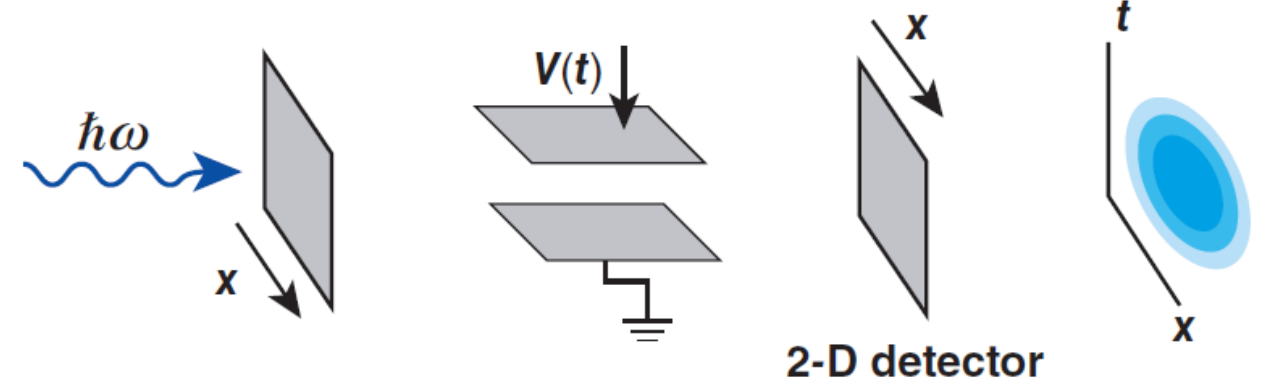


### A streak camera provides temporal resolution of 1-D data





#### A streak camera can provide 2-D information

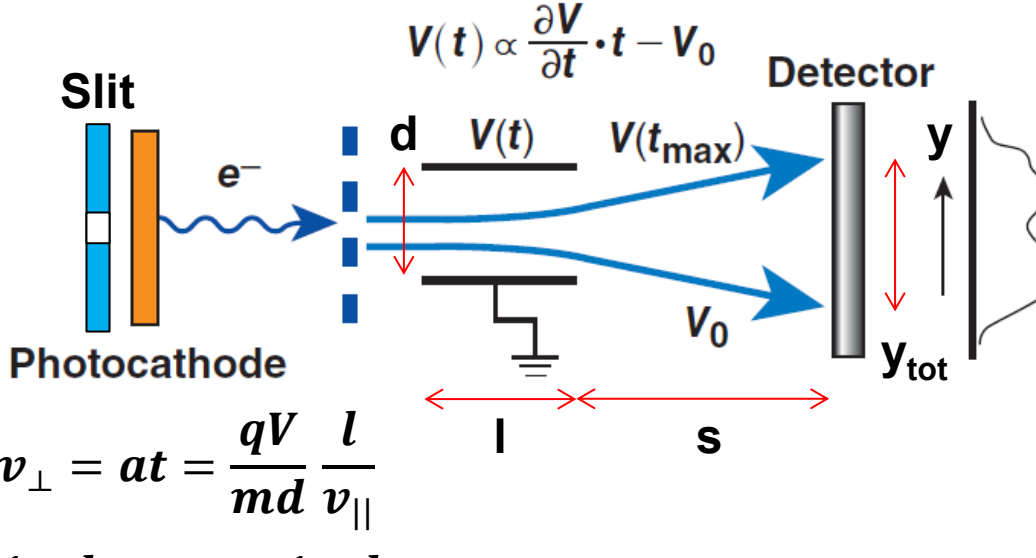


### A temporal resolution higher than 15 ps is expected



#### **Imaging system**

- Visible light: regular lens
- X rays: pinhole



$$a = \frac{F}{m} = \frac{qE}{m} = \frac{qV}{md}$$
  $v_{\perp} = at = \frac{qV}{md} \frac{l}{v_{||}}$ 

$$y = s \operatorname{Tan}\theta = s \frac{V_{\perp}}{V_{\parallel}} = \frac{1}{2E_{k}} \frac{l}{d} sqV = \frac{1}{2E_{k}} \frac{l}{d} sq(V_{0} + V't)$$

Let d=10 mm, l=20 mm, s=50 mm, E<sub>k</sub>=1 keV, V=-200 ~ 200 V

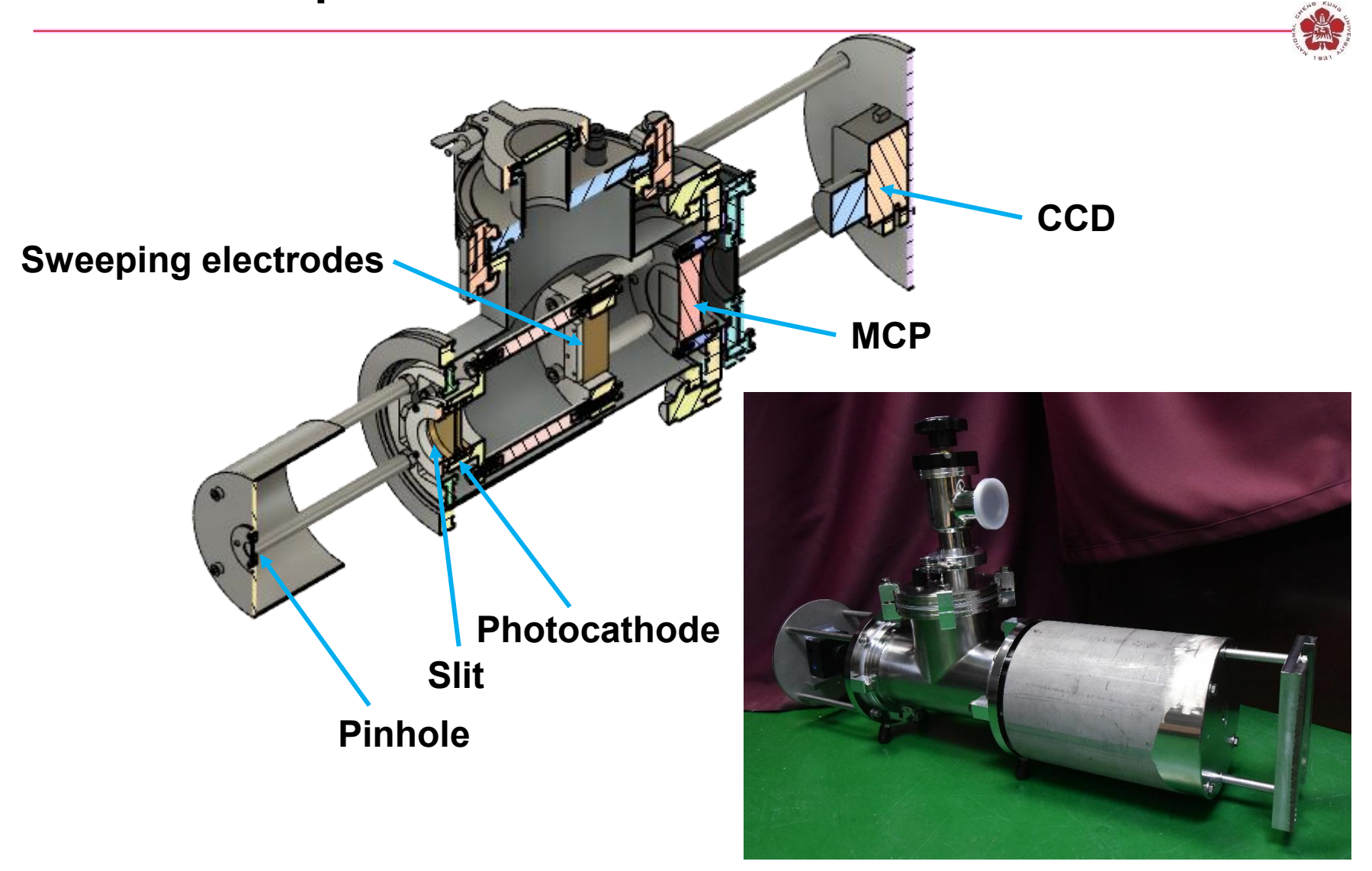
$$V' \equiv \frac{V_{\text{tot}}}{t_{\text{tot}}} = 0.06 \,\text{kV/ns}$$
  $y_{\text{tot}} = 15 \,\text{mm}$   $y_{\text{tot}} = 15 \,\text{mm}$ 

Temporal resolution:

$$\delta t = \delta y \frac{2E_k d}{lsqV'} = 15 \text{ ps for } \delta y = 45 \mu m$$

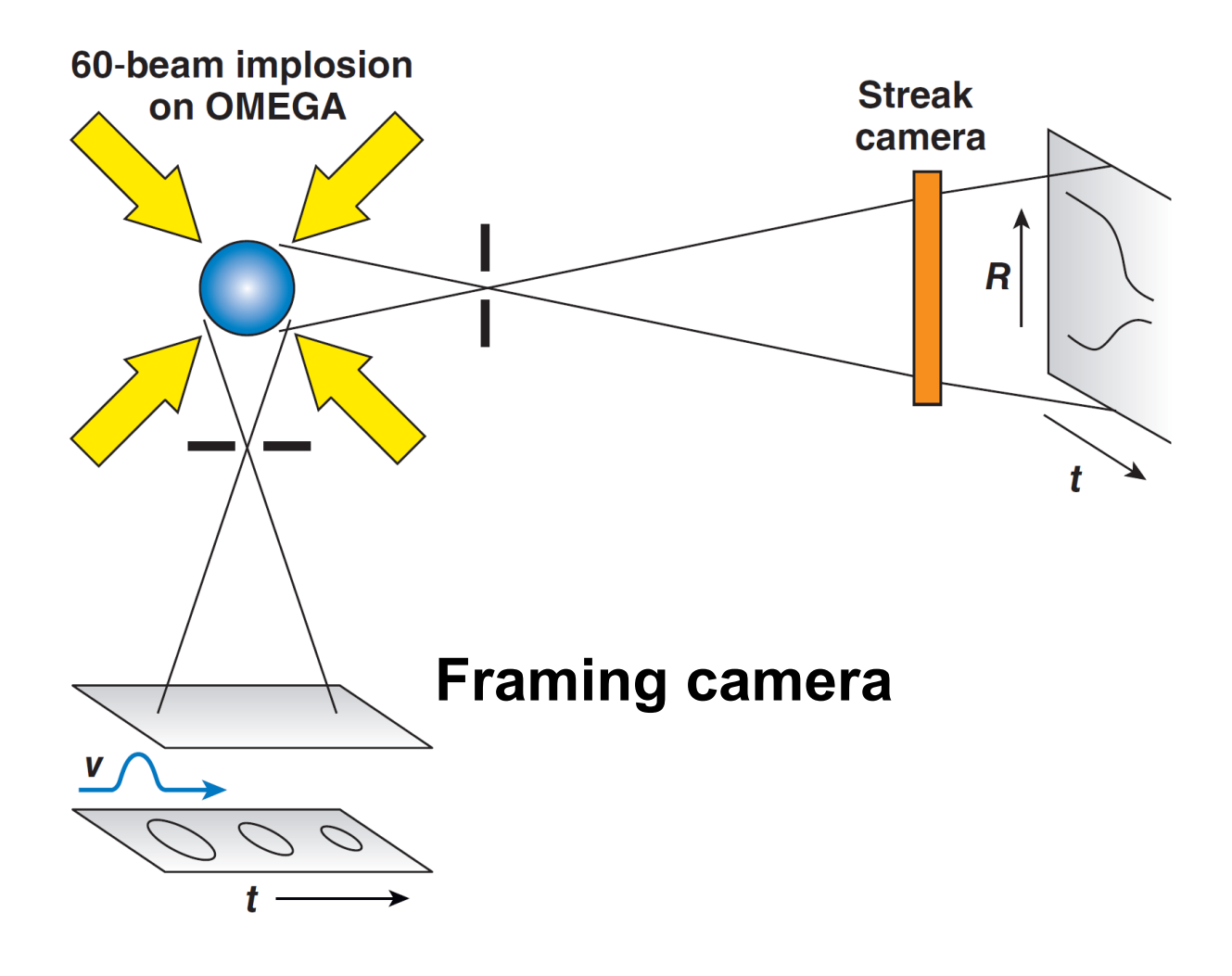
•  $\delta t$  will be adjusted by changing  $E_k$ .

# A streak camera with temporal resolution of 15 ps has been developed



### Shell trajectories can be measured using framing camera or streak camera



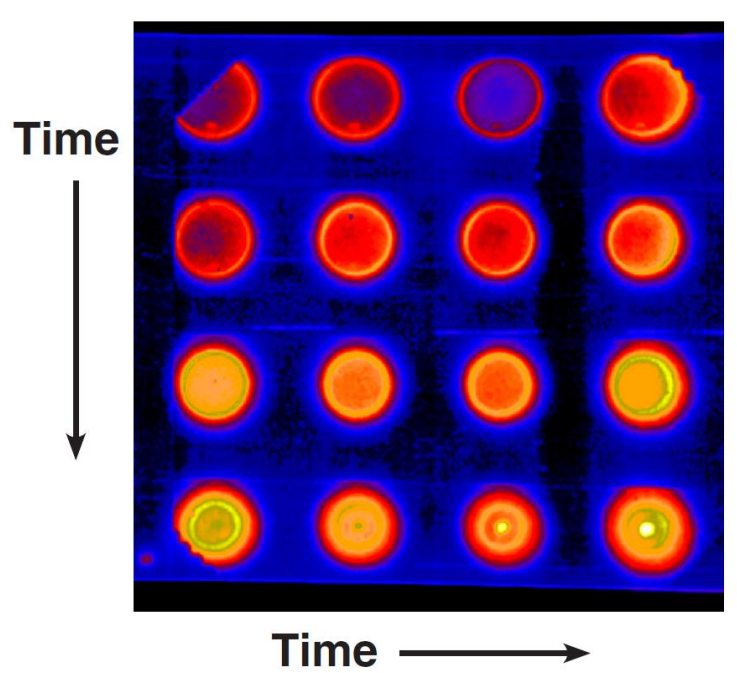


### Comparison of images from framing camera versus streak camera

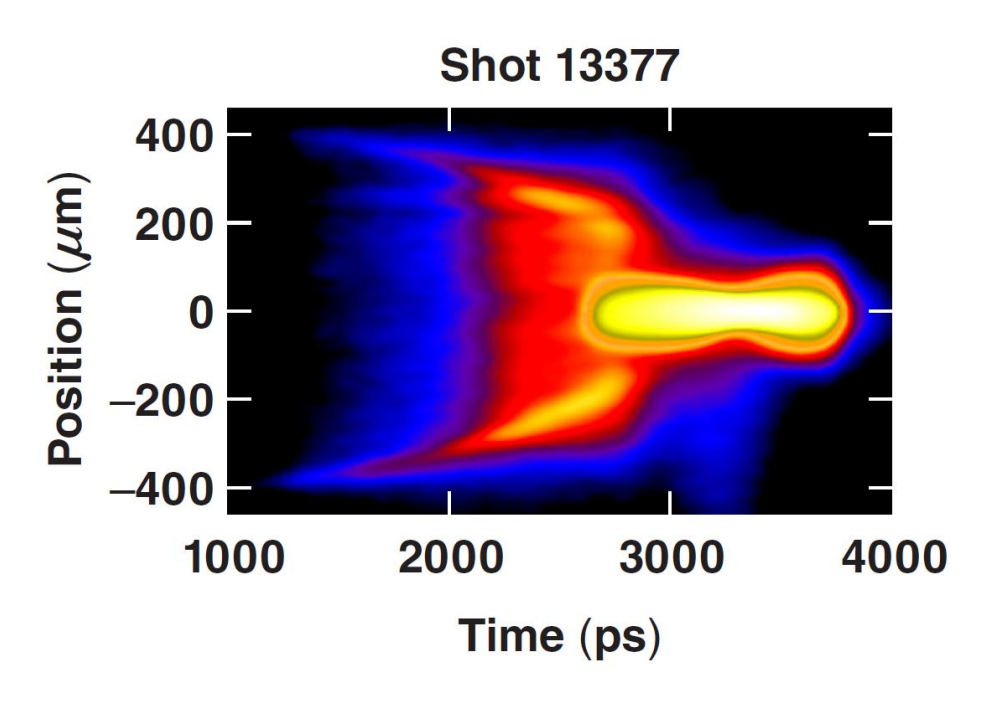




**Shot 13377** 

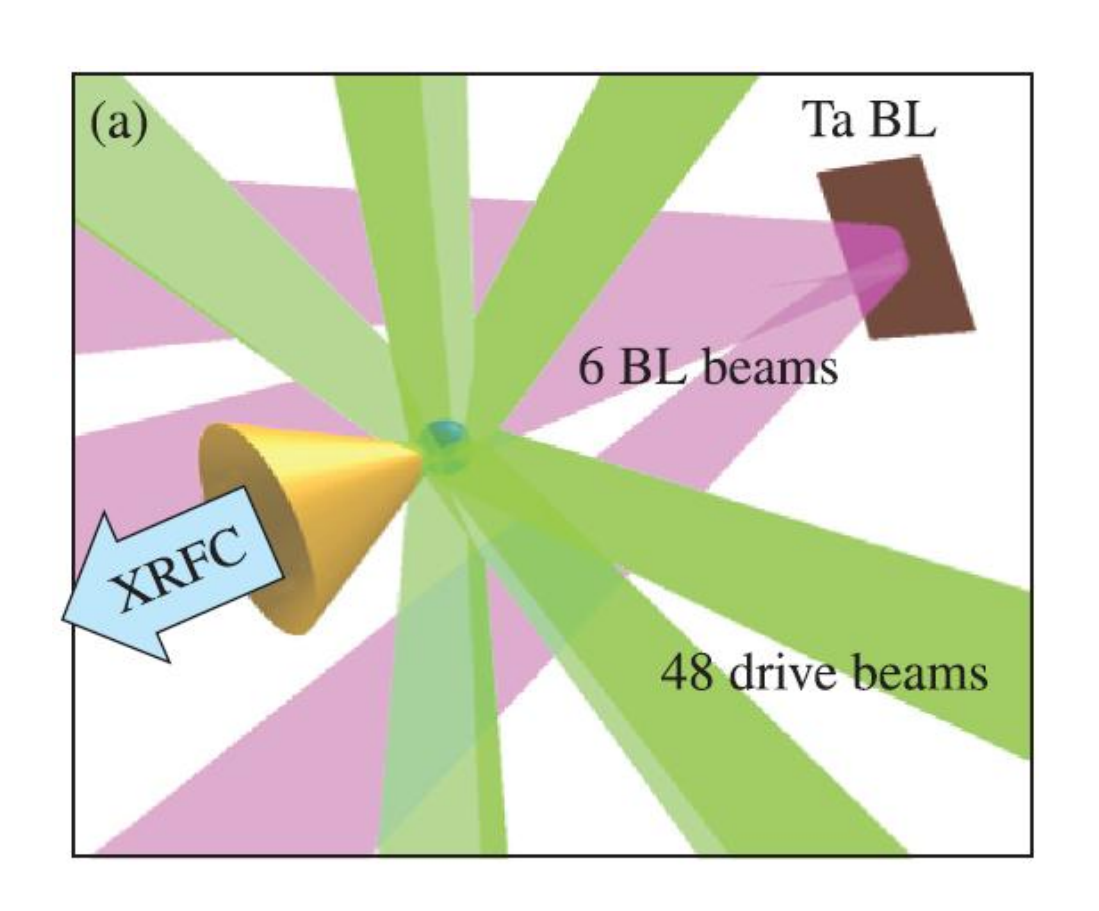


#### Streak-camera image



# The optical density can be measured using the absorption of a backlighter



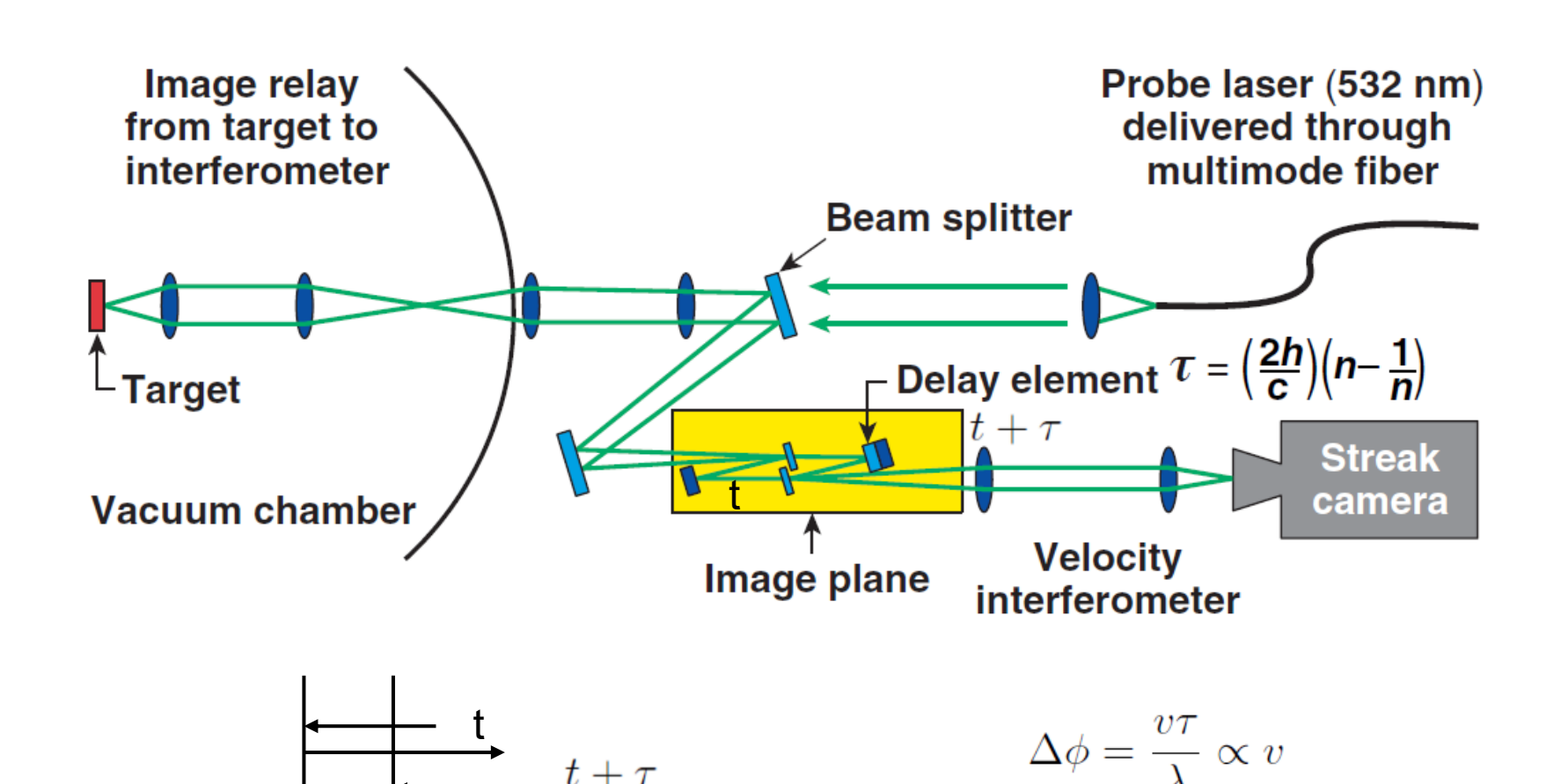


$$I = \int I(\varepsilon) \exp(-\mu(\varepsilon)\rho\delta) d\varepsilon$$

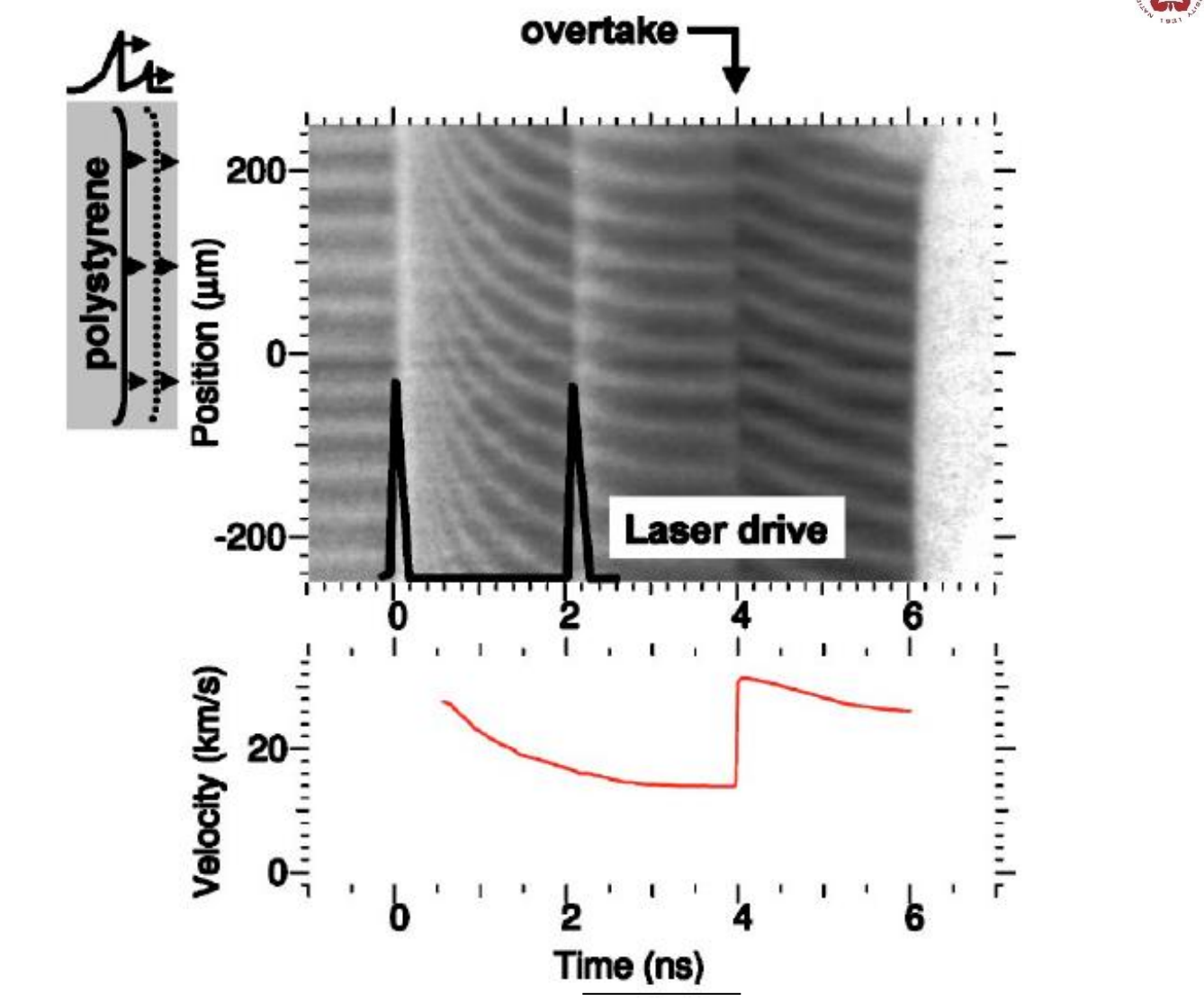
$$I = I_{\text{BL}} \exp(-\bar{\mu}\rho\delta)$$

$$\ln I = \ln I_{\text{BL}} - \mu\rho r$$

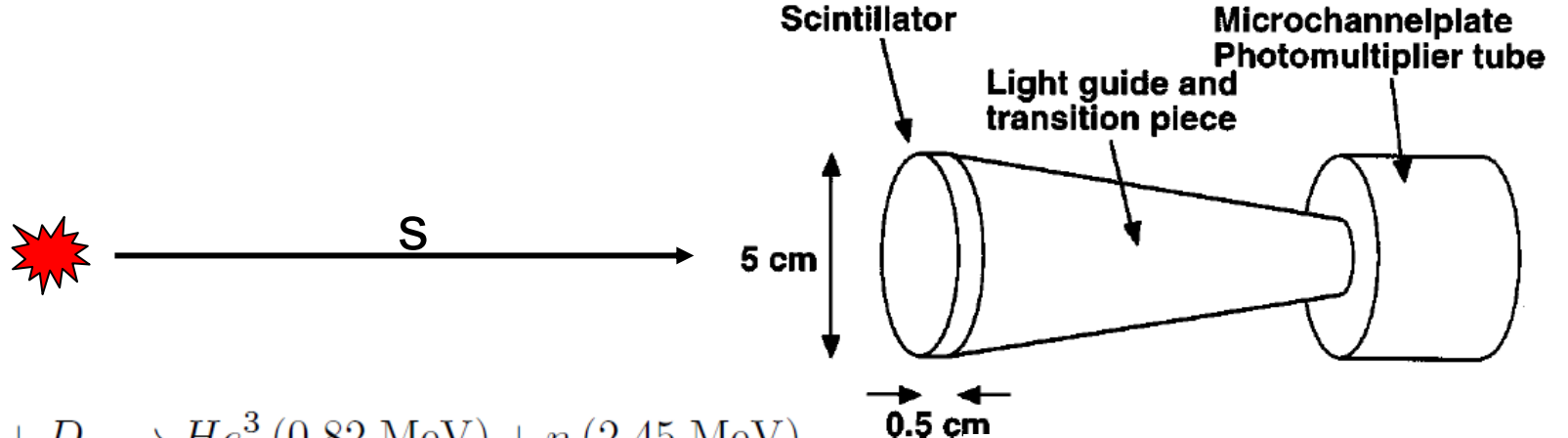
## Shock velocities are measured using time-resolved Velocity Interferometer System for Any Reflector (VISAR)



### Shock velocities are measured using time-resolved Velocity Interferometer System for Any Reflector (VISAR)



### Neutron average temperature is obtained using Neutron Time of Flight (NToF)

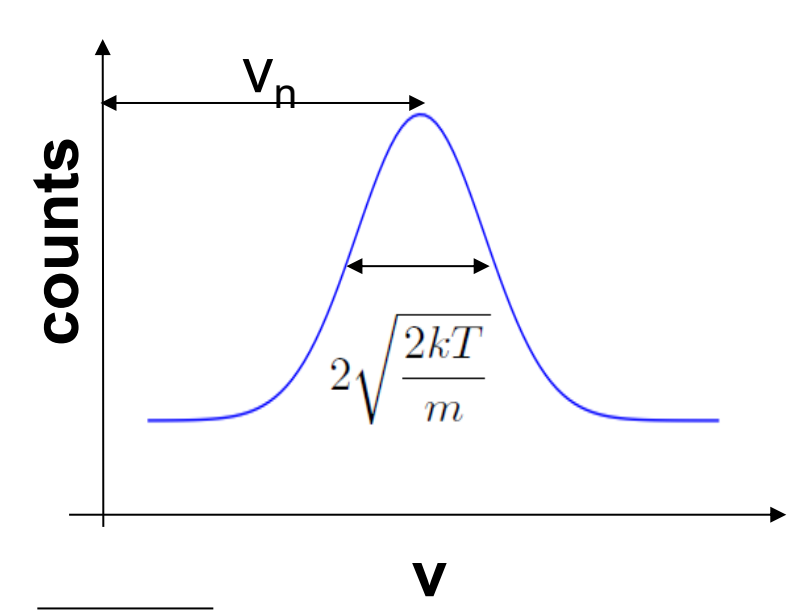


$$D + D \longrightarrow He^3 (0.82 \text{ MeV}) + n (2.45 \text{ MeV})$$

$$D + T \longrightarrow He^4 (3.5 \text{ MeV}) + n (14.1 \text{ MeV})$$

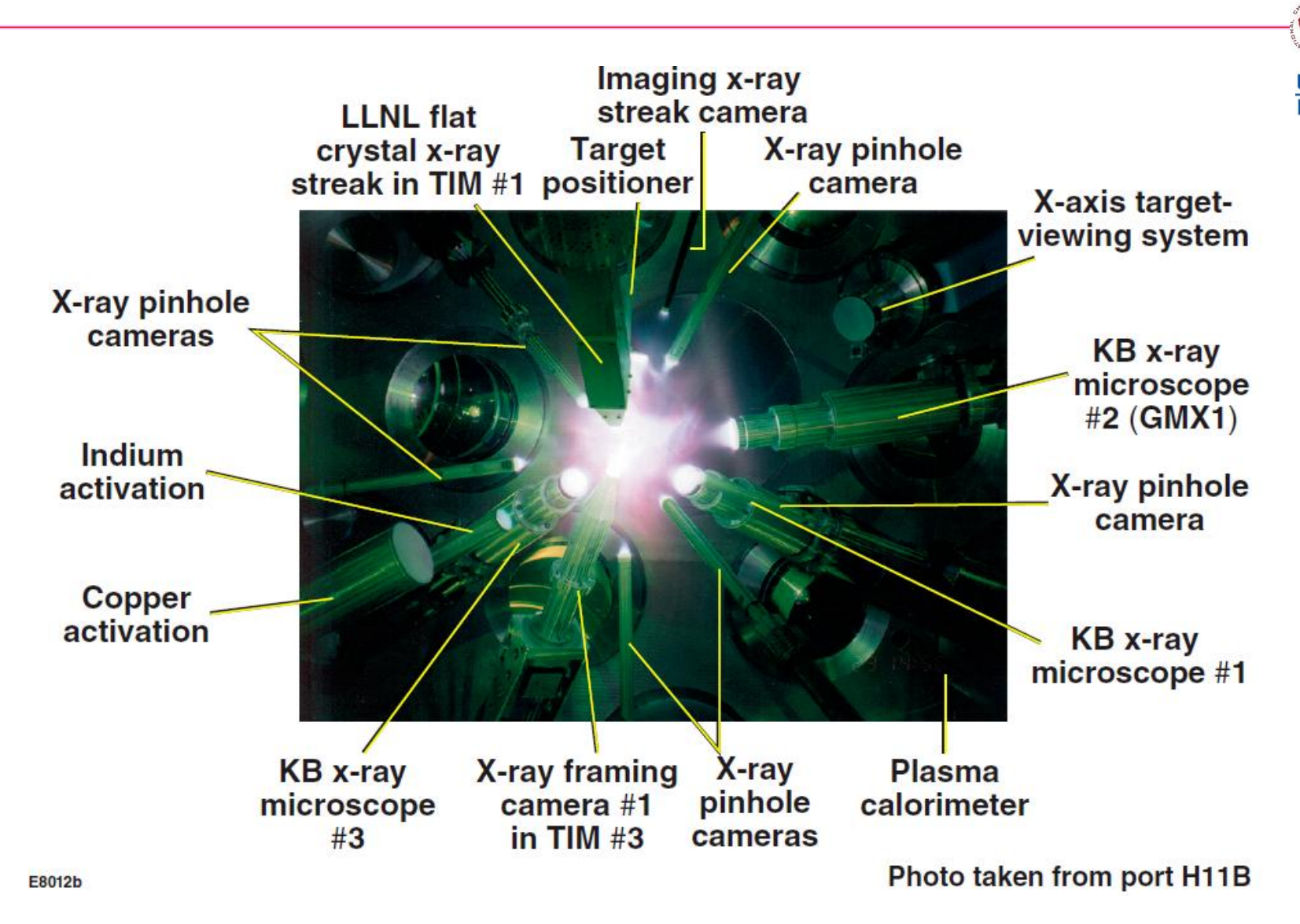
$$s = vt$$
  $v = \frac{s}{t}$ 

$$f(v) = \sqrt{\left(\frac{m}{2\pi kT}\right)} \exp\left(-\frac{mv^2}{2kT}\right)$$



T. J. Murphy et al., Rev. Sci. Instrum. 72, 773 (2001) 140

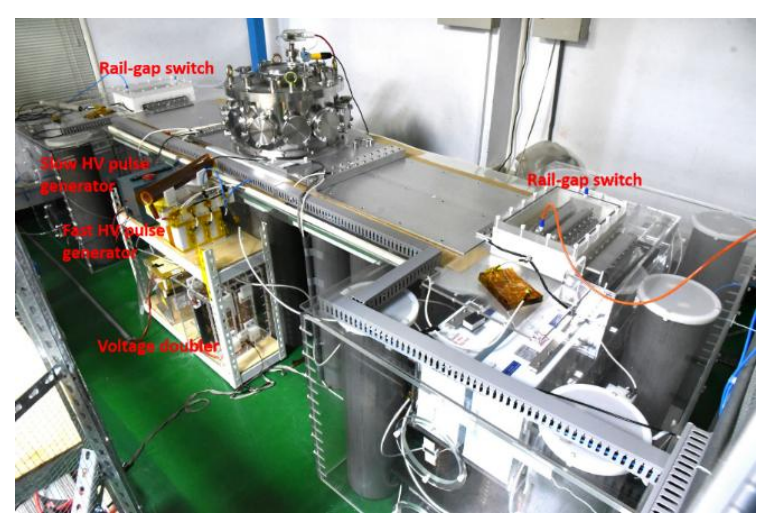
# The OMEGA Facility is carrying out ICF experiments using a full suite of target diagnostics



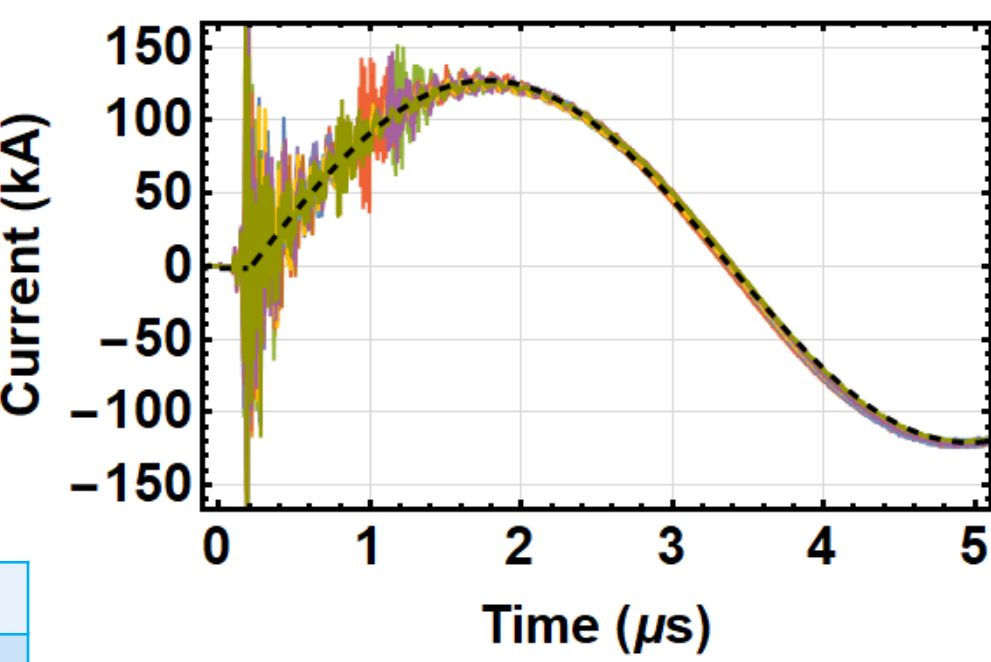
FSC

# A peak current of ~135 kA with a rise time of ~1.6 us is provided by the pulsed-power system



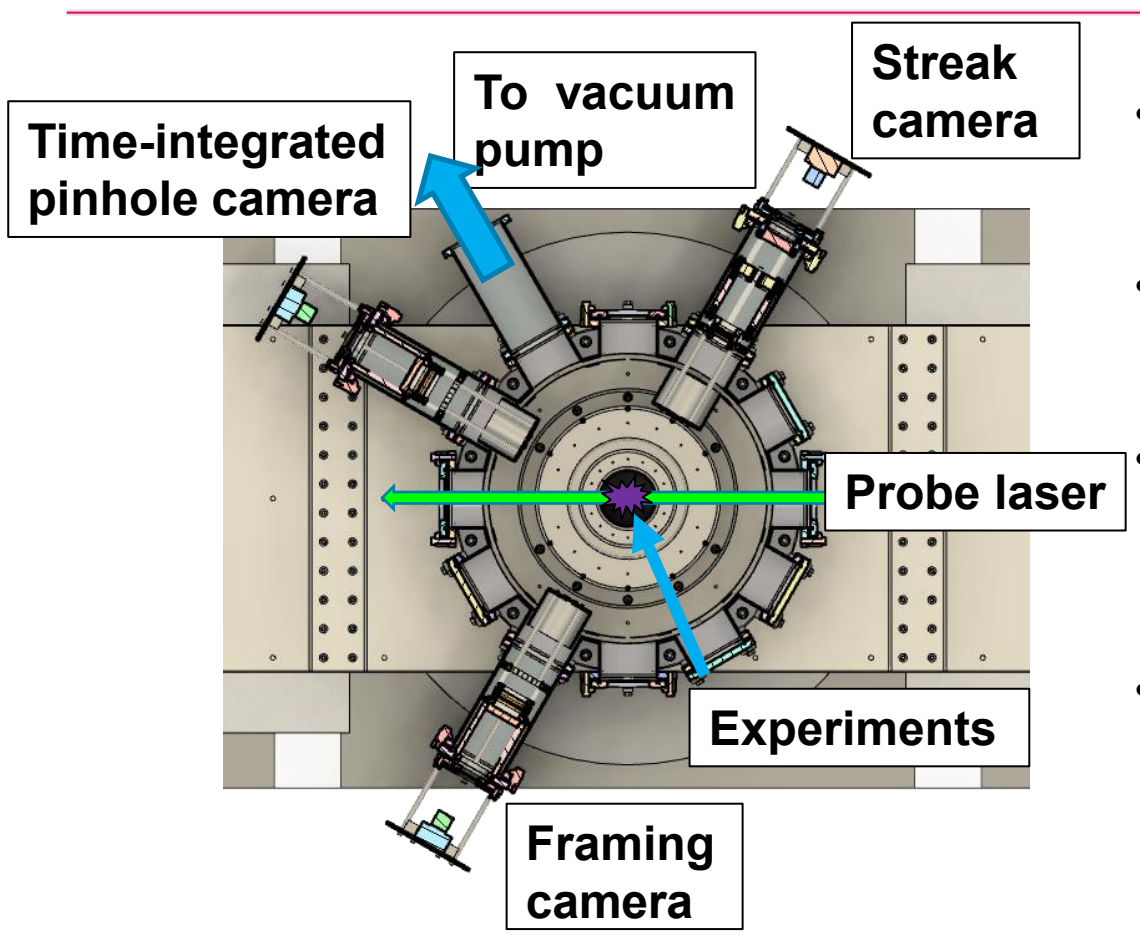


Capacitance (µF)	5
V <sub>charge</sub> (kV)	20
Energy (kJ)	1
Inductance (nH)	204 ± 4
Rise time (quarter period, ns)	1592 ± 3
I <sub>neak</sub> (kA)	135 ± 1



- EUV generation using discharged-produced plasma:
  - PP-PP-002 Chenghan Du
  - PP-PP-003 Jia-Kai Liu

# A suit of diagnostics in the range of (soft) x-ray are being built



- Csl are used as the photocathode for all xray imaging system.
- Au photocathode may be used in the future.

#### Pinhole camera:

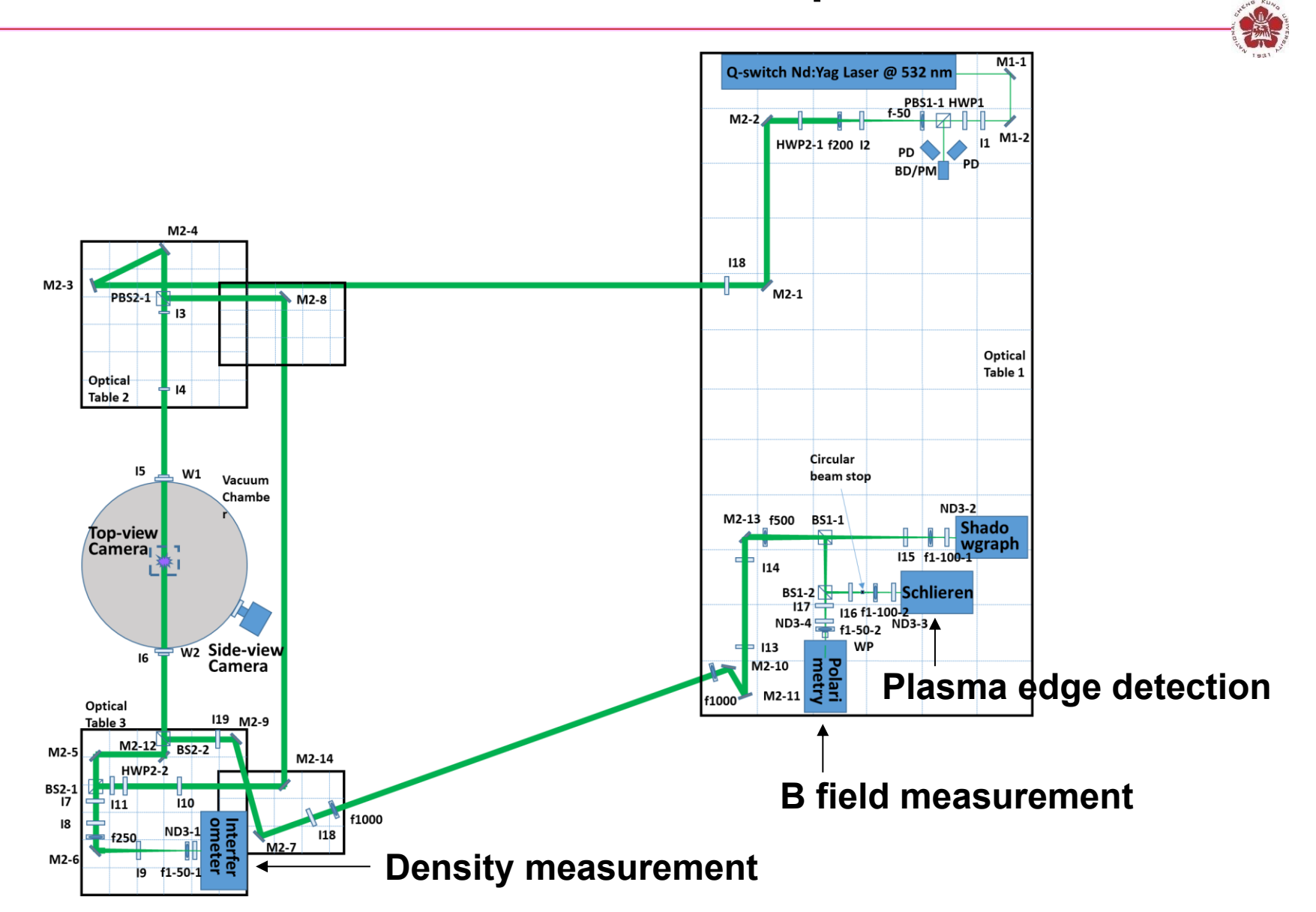
- Magnification: 1x

- Exposure time: 1 us

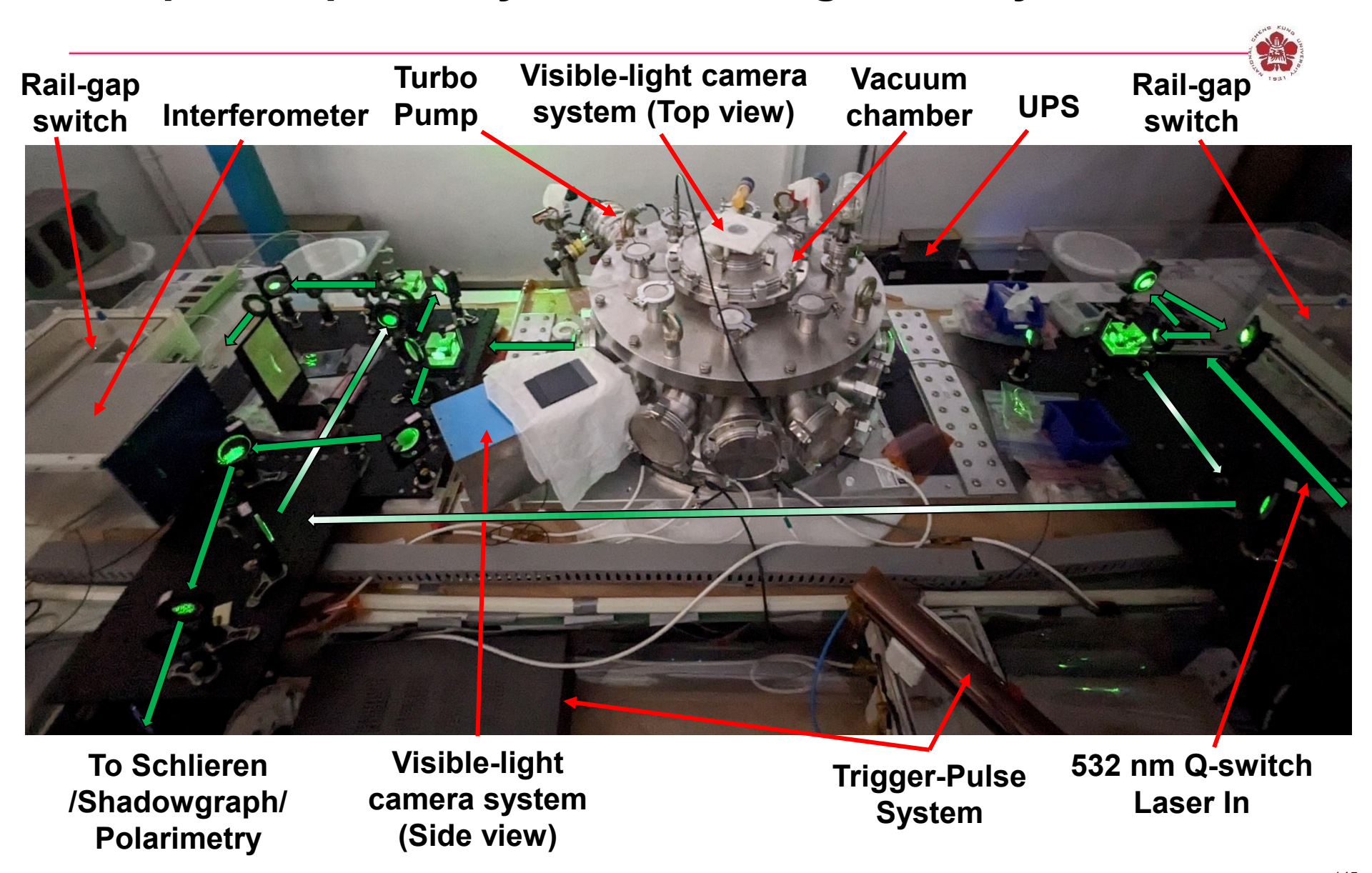
#### Streak camera:

- Magnification: 1x
- Temporal resolution: 15 ps
- Framing camera:
- Magnification: 0.3x
- Temporal resolution: ~ns using 4 individual MCPs
- Laser probing:
- For interferometer, schlieren, shadowgraphy, Thomson scattering.
- Temporal resolution: ~300 ps using stimulated brillouin scattering (SBS) pulse compression in water

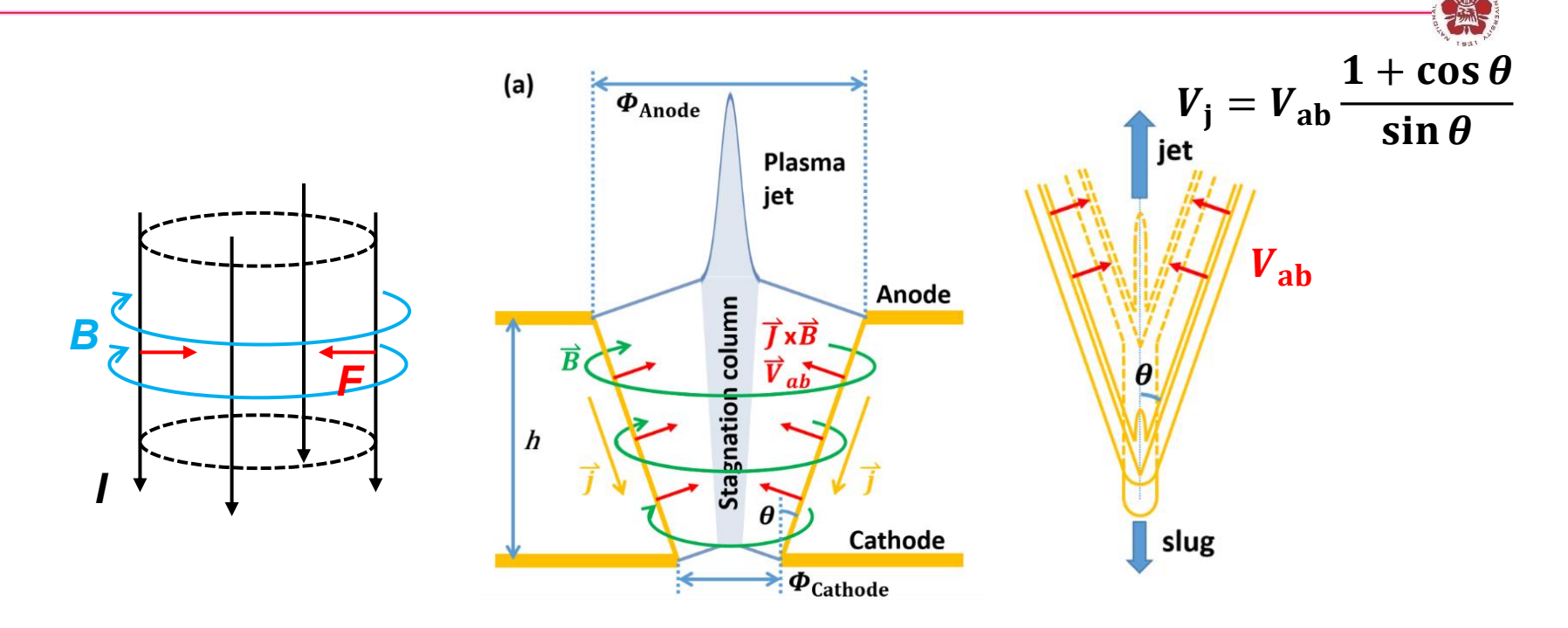
## Time-resolved imaging system with temporal resolution in the order of nanoseconds was implemented



### The pulsed-power system with diagnostic system



## A plasma jet can be generated by a conical-wire array due to the nonuniform z-pinch effect

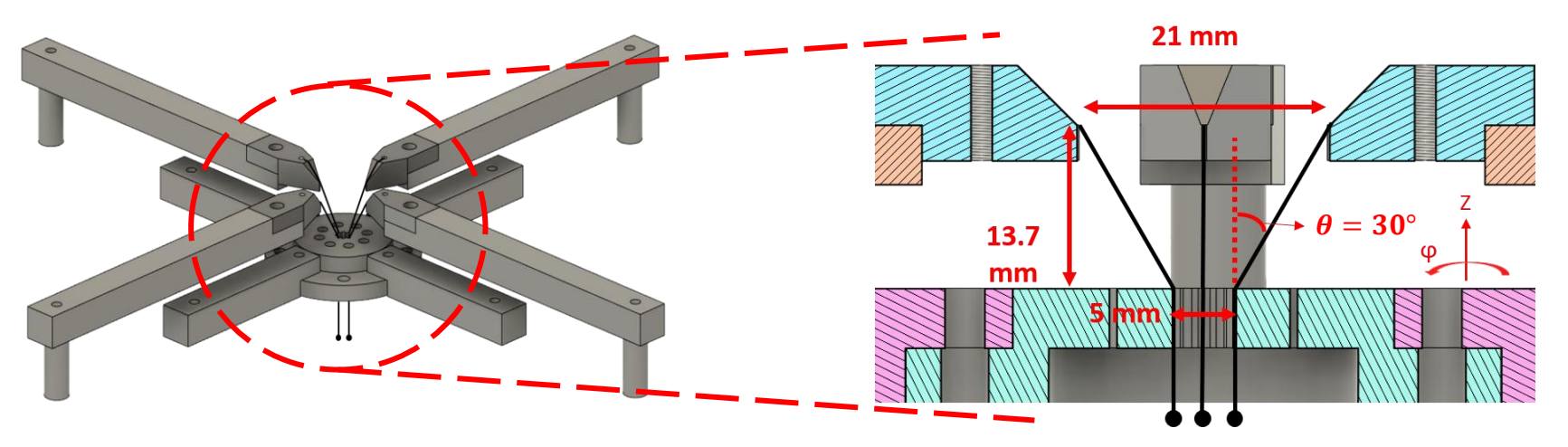


- 1. Wire ablation: corona plasma is generated by wire ablations.
- 2. Precursor : corona plasma is pushed by the  $\vec{J} \times \vec{B}$  force and accumulated on the axis forming a precursor.
- 3. Plasma jet is formed by the nonuniform z-pinch effect due to the radius difference between the top and the bottom of the array.

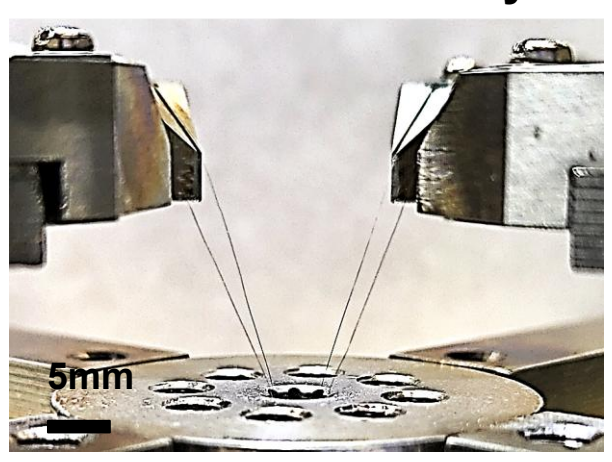
D. J. Ampleforda, et al., Phys. Plasmas 14, 102704 (2007)

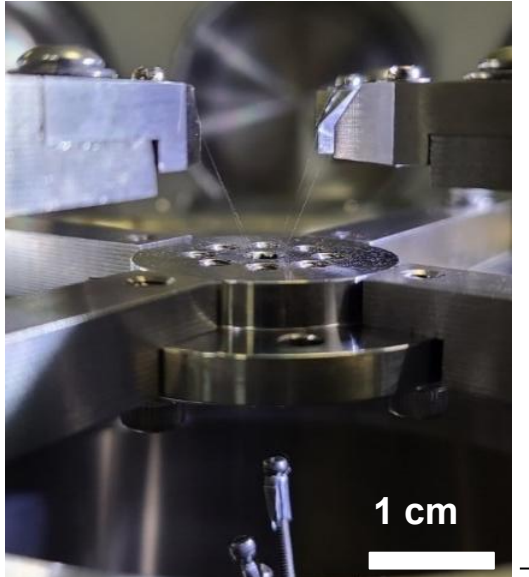
G. Birkhoff, et al., J. Applied Physics 19, 563 (1948)

## Our conical-wire array consists of 4 tungsten wires with an inclination angle of 30° with respect to the axis



#### Conical-wire array



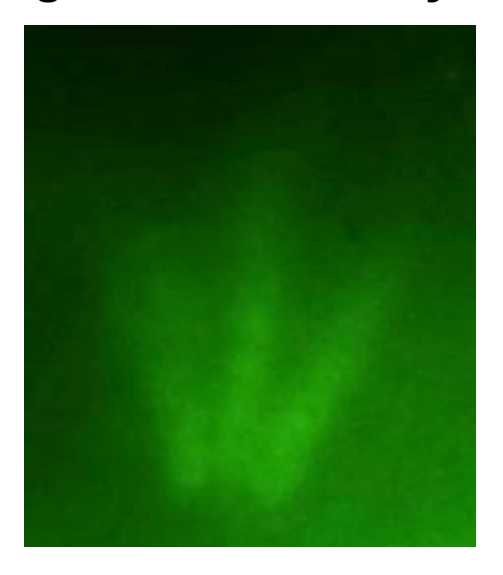


- Material : Tungsten.
- Number of wires: 4.
- Diameter : 20 µm.

## Self-emission of the plasma jet in the UV to soft x-ray regions was captured by the pinhole camera



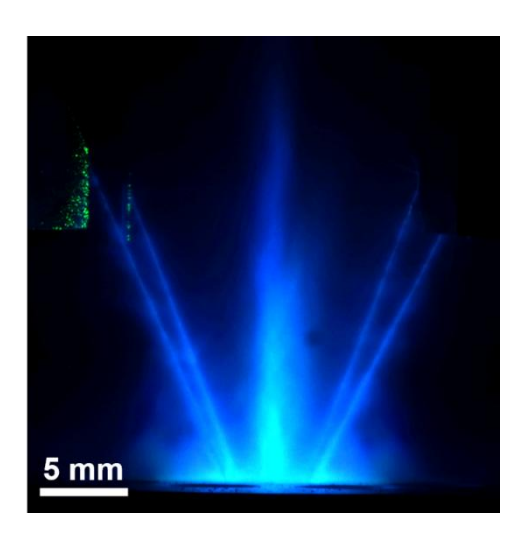
Image in UV/soft x ray



(Brightness is increased by 40 %.)

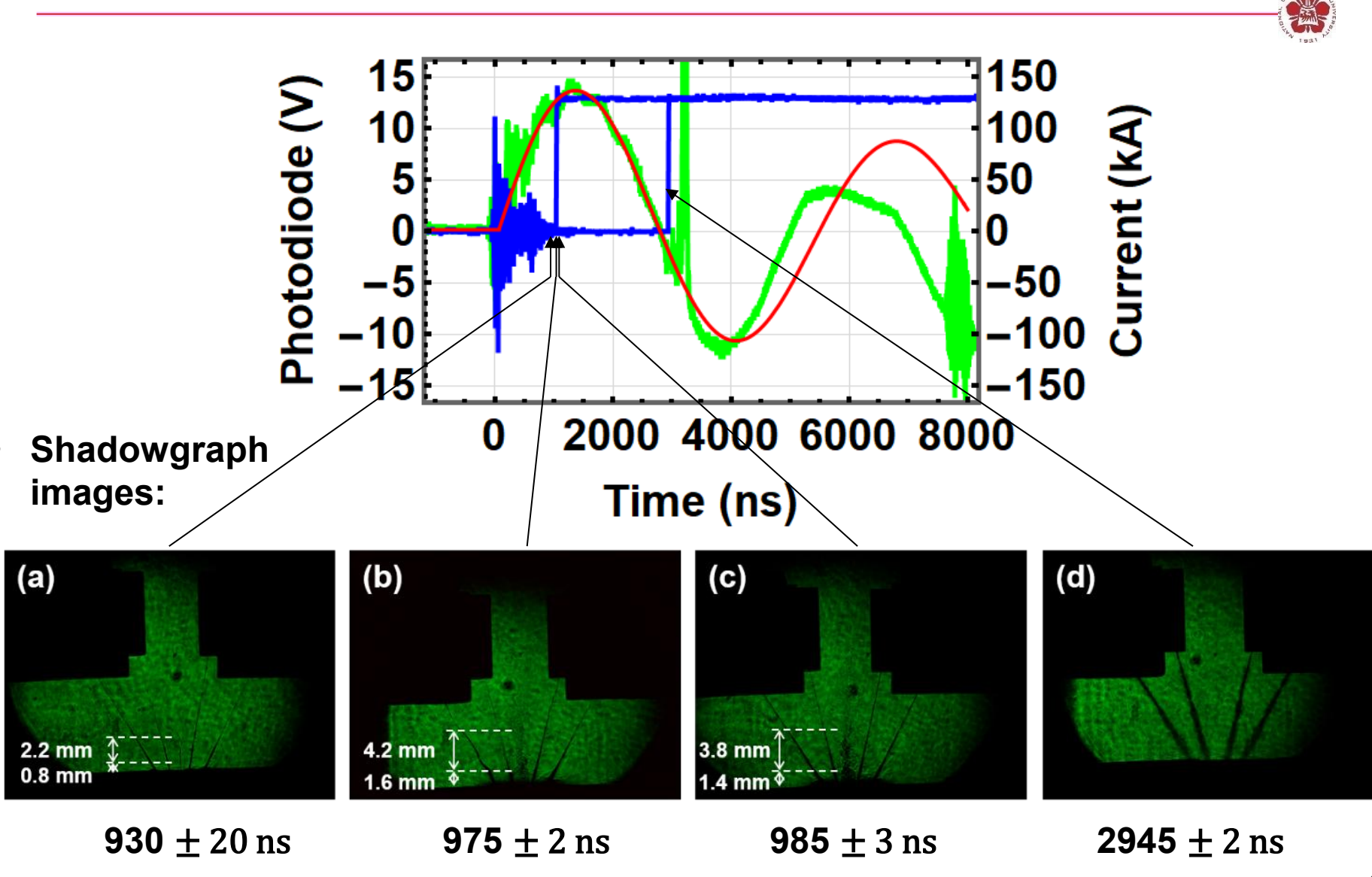
Pinhole diameter:
 0.5 mm, i.e., spatial resolution: 1 mm.

Image in visible light



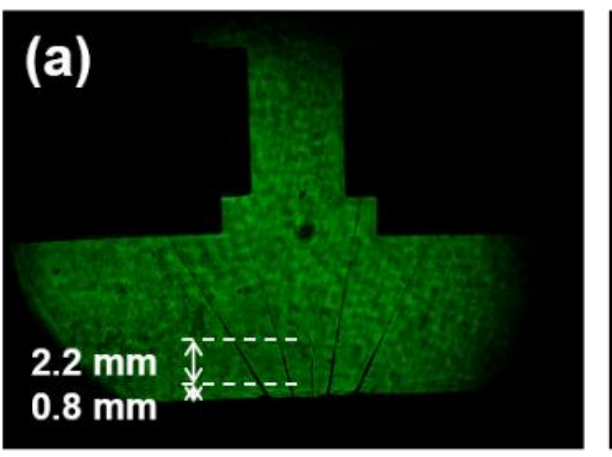
(Enhanced by scaling the intensity range linearly from 0 - 64 to 0 - 255.)

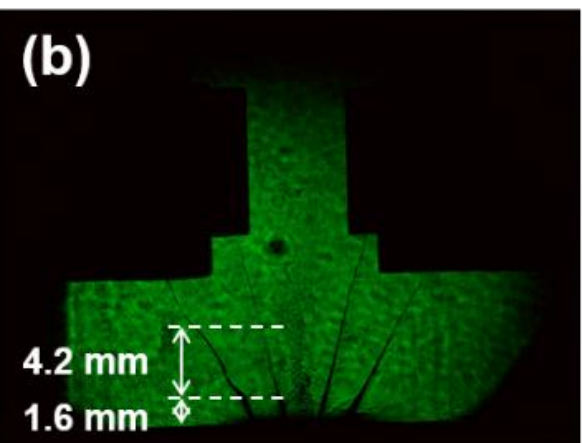
## Plasma jet propagation was observed using laser diagnostics

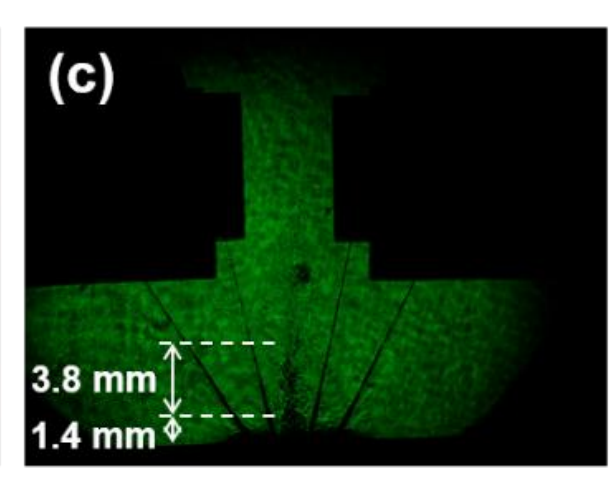


## Length of the plasma jet at different time was obtained by the Schlieren images at different times

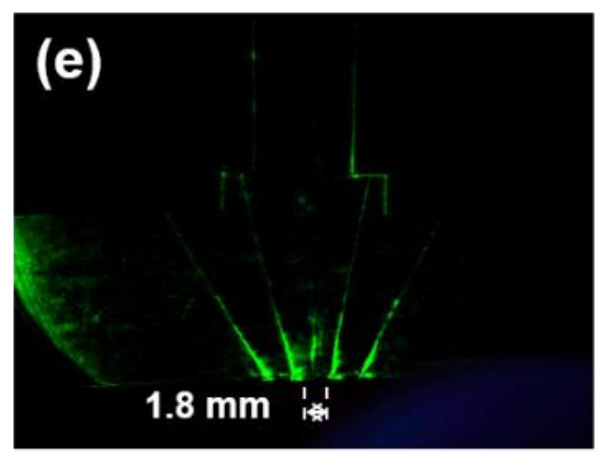
Shadowgraph images:

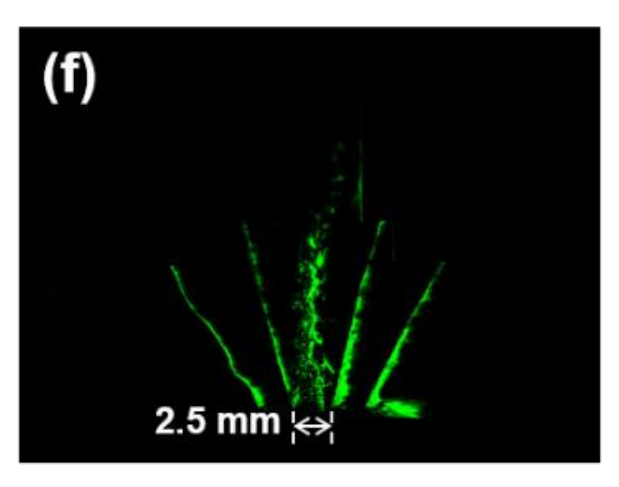


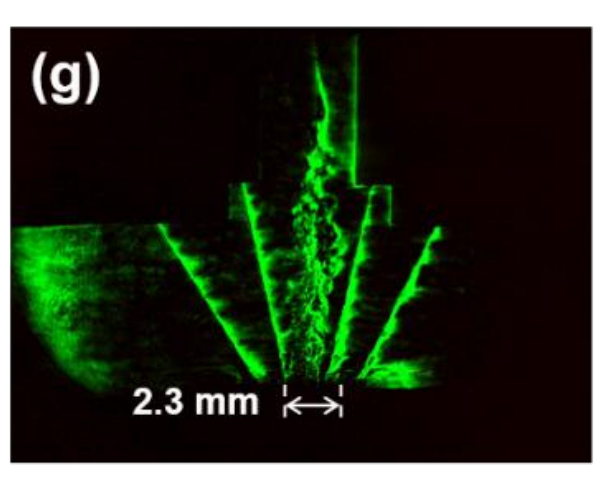




Schlieren images:







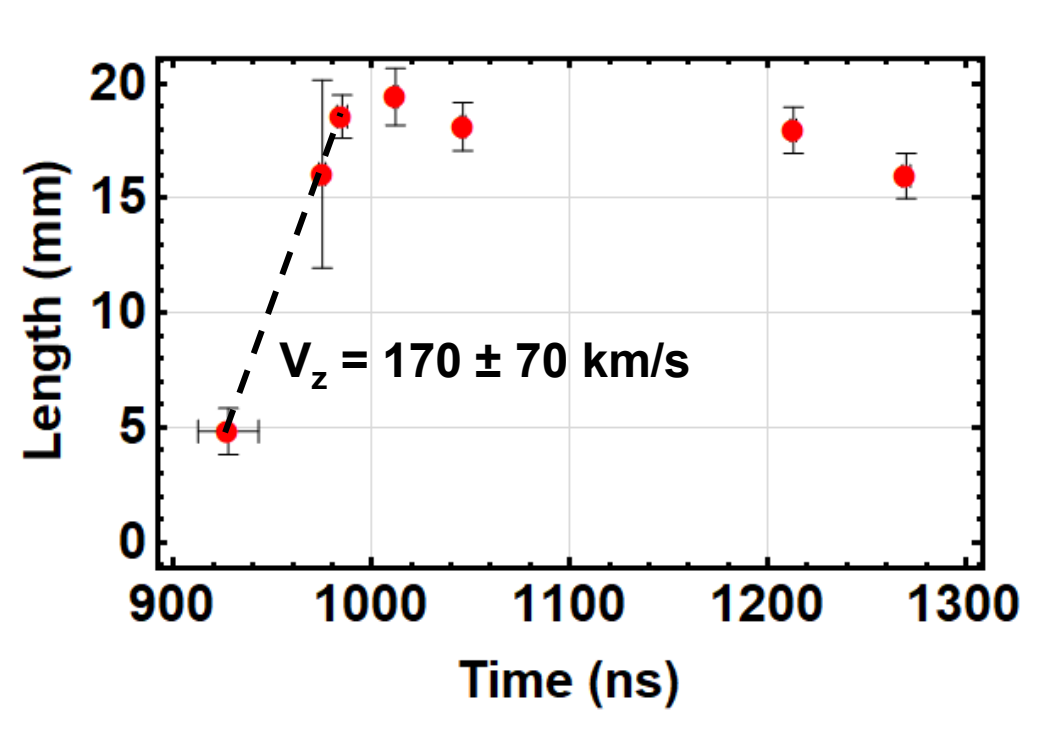
 $930 \pm 20 \, \text{ns}$ 

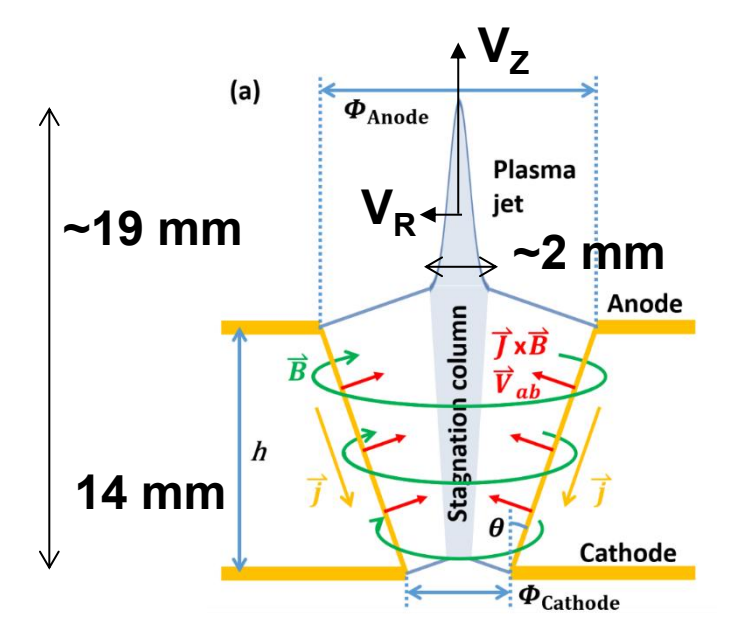
 $975 \pm 2 \text{ ns}$ 

 $985 \pm 3 \text{ ns}$ 

## The measured plasma jet speed is 170 ± 70 km/s with the corresponding Mach number greater than 5





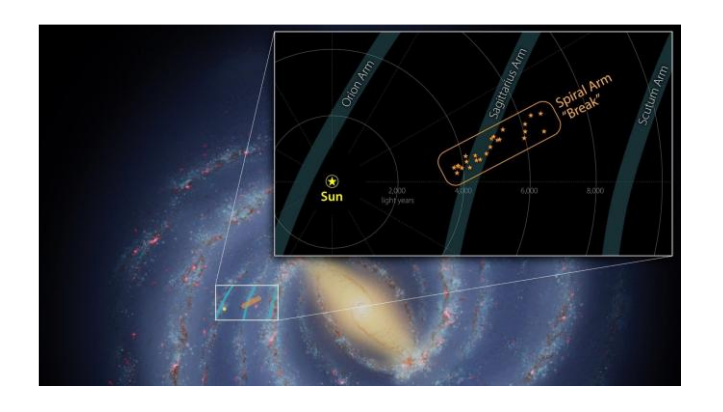


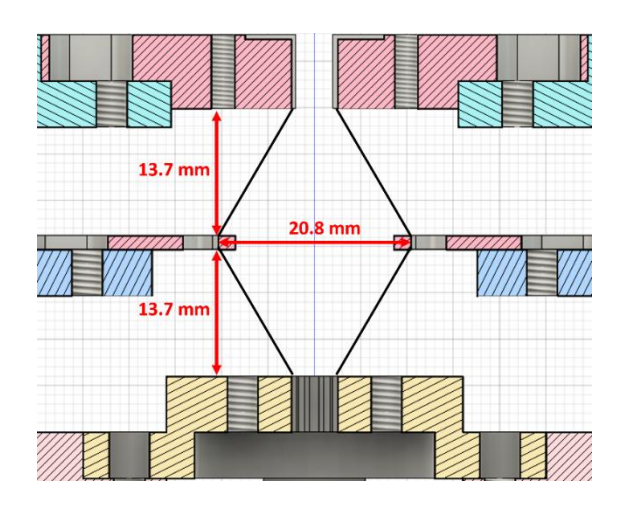
$$M = \frac{V_Z}{V_R} \ge \frac{Z}{r} \approx \frac{(19 - 14) \text{ mm}}{\frac{2 \text{ mm}}{2}} = 5$$

$$V_{ab} = V_{j} \frac{\sin \theta}{1 + \cos \theta} = 50 \pm 20 \text{ km/s}$$

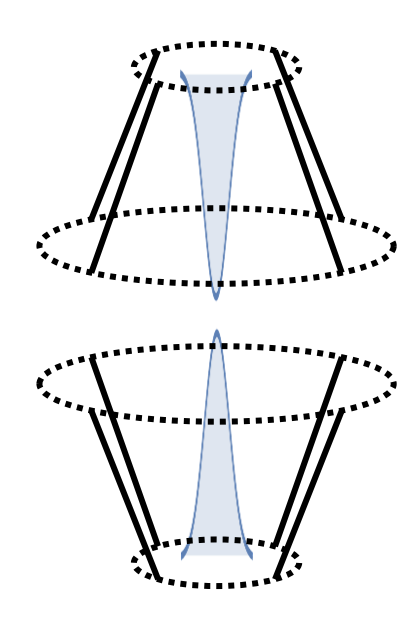
## Plasma disk can be formed when two head-on plasma jets collide with each other

 Astronomers Find a 'Break' in One of the Milky Way's Spiral Arms.



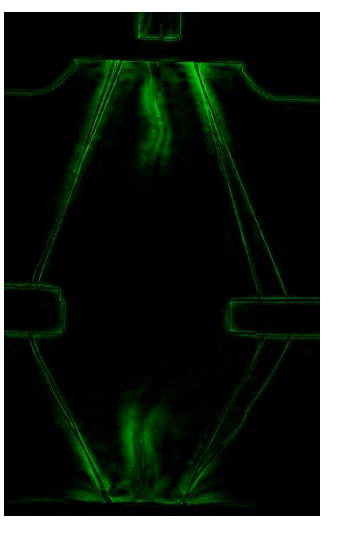


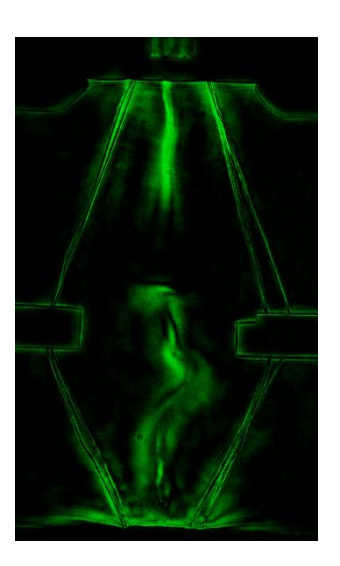




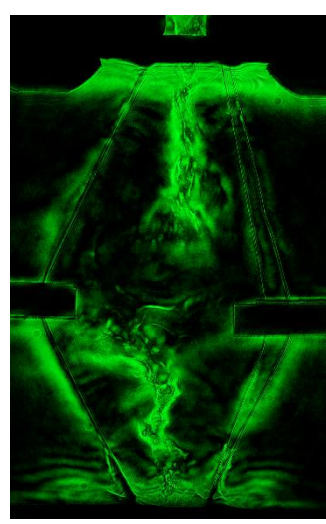
## Plasma disk can be formed when two head-on plasma jets collide with each other

Schlieren





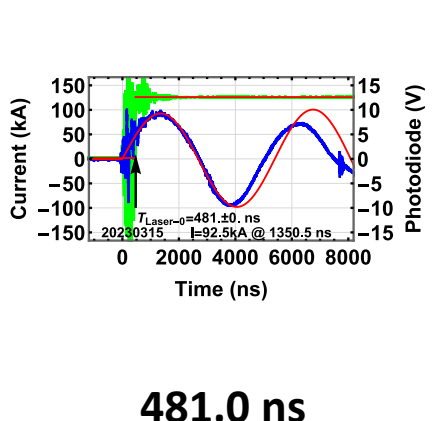






Interferometer











## Energetic charged particles losses most of its energy right before it stops



Momentum transfer:

$$\Delta p_{\perp} = \int F_{\perp} dt = \int F_{\perp} \frac{dt}{dx} dx = \int F_{\perp} \frac{dx}{v}$$

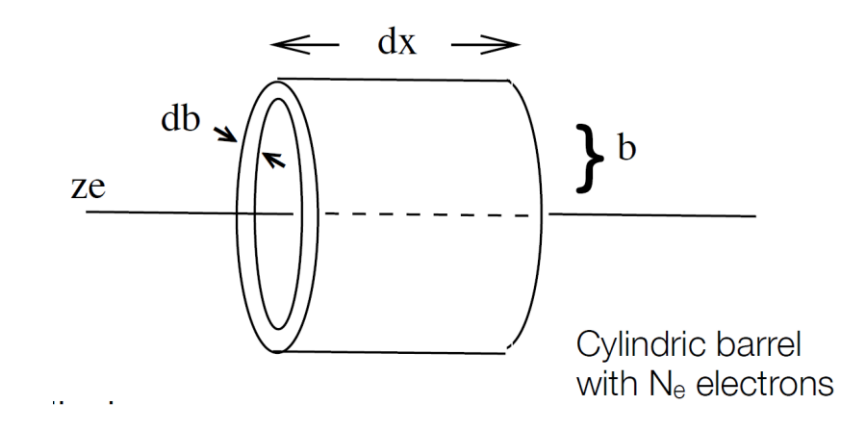
$$= \int_{-\infty}^{\infty} \frac{ze^2}{(x^2 + b^2)} \cdot \frac{b}{\sqrt{x^2 + b^2}} \cdot \frac{1}{v} \, dx = \frac{ze^2b}{v} \left[ \frac{x}{b^2 \sqrt{x^2 + b^2}} \right]_{-\infty}^{\infty} = \frac{2ze^2}{bv}$$

 $\Delta p_{\parallel}$ : averages to zero

$$\Delta E(b) = \frac{\Delta p^2}{2m_e}$$
 N<sub>e</sub> = n·(2πb)·dbdx

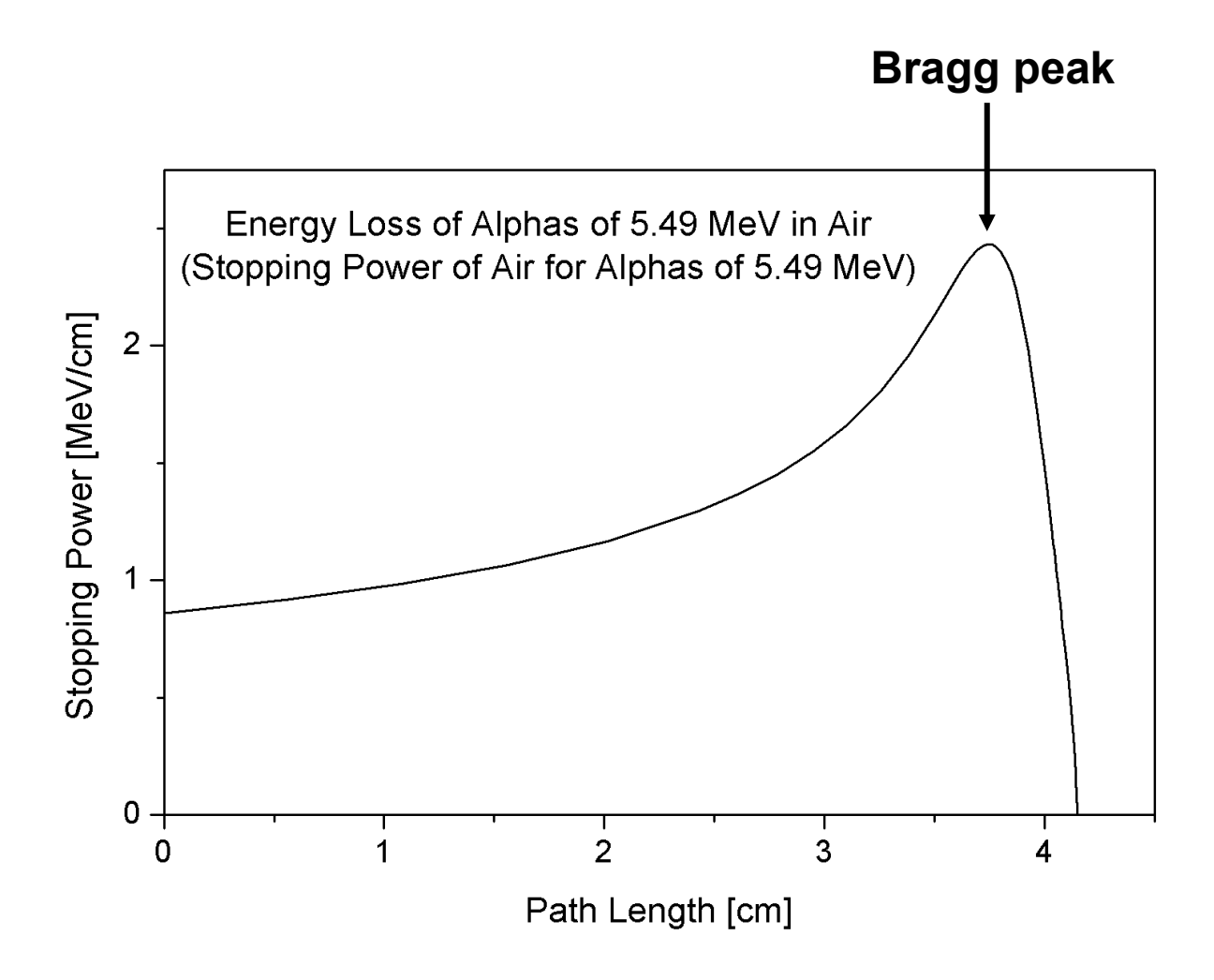
$$-dE(b) = \frac{\Delta p^2}{2m_e} \cdot 2\pi nb \, db \, dx$$

$$-\frac{dE}{dx} = \frac{4\pi \, n \, z^2 e^4}{m_{\rm e} v^2} \cdot \int_{b_{\rm min}}^{b_{\rm max}} \frac{db}{b} = \frac{4\pi \, n \, z^2 e^4}{m_{\rm e} v^2} \, \ln \frac{b_{\rm max}}{b_{\rm min}}$$



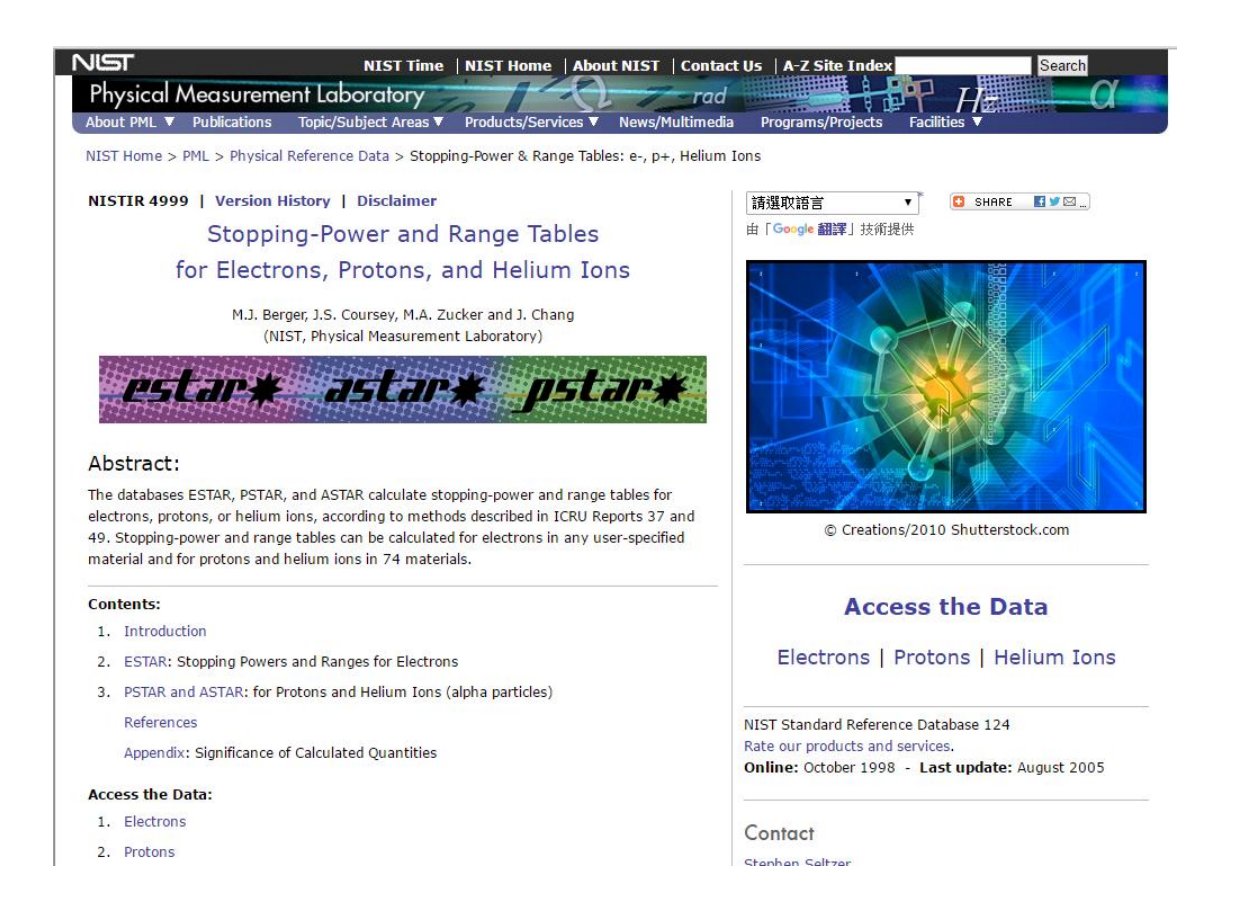
### A particle loses most of its energy right before it stops



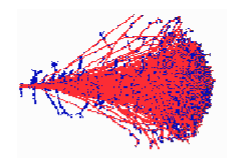


## There are two suggested website for getting the information of proton stopping power in different materials

#### http://www.nist.gov/pml/data/star/

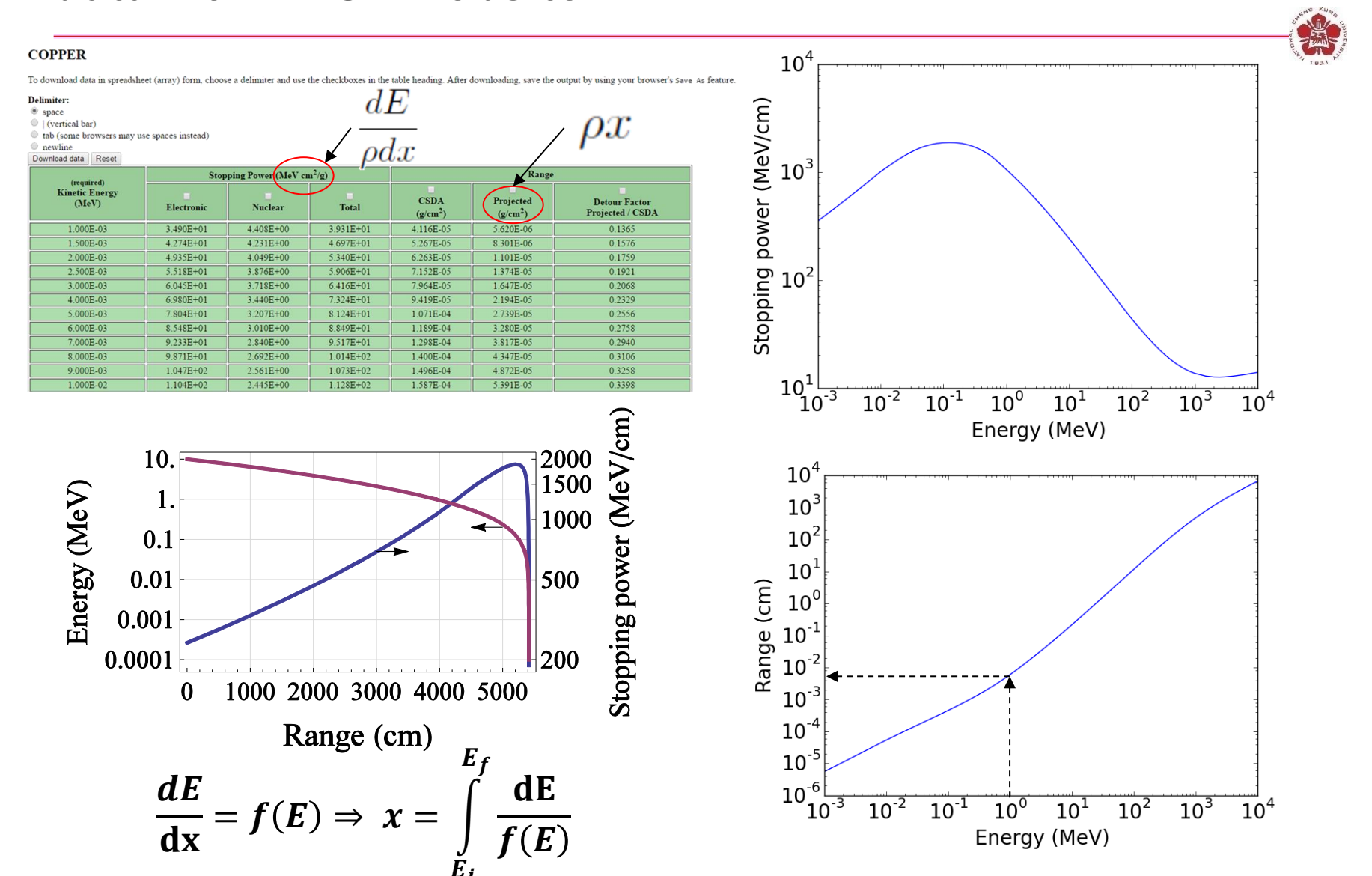


#### http://www.srim.org/



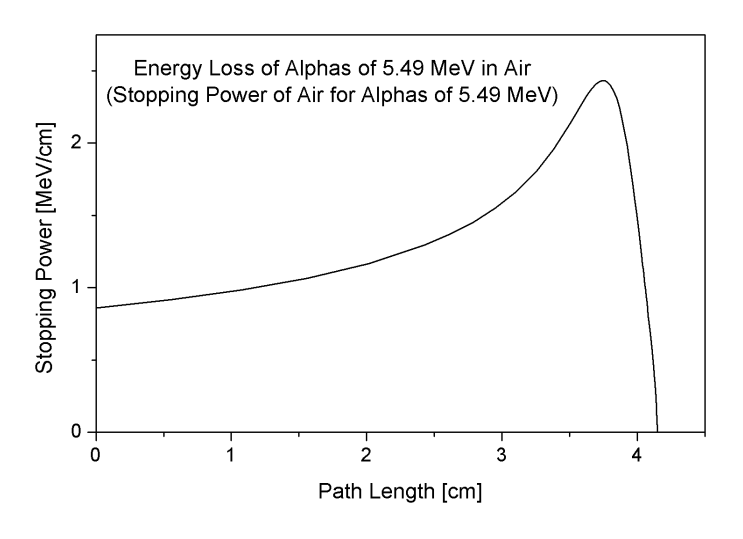
SRIM Textbook	
Software	Science
SRIM / TRIM Introduction	Historical Review
Download SRIM- 2013	Details of SRIM- 2013
SRIM Install Problems	Experimental Data Plots Stopping of Ions in Matter
SRIM Tutorials	Stopping in Compounds
Download TRIM Manual Part-1, Part-2	Scientific Citations of Experimental Data

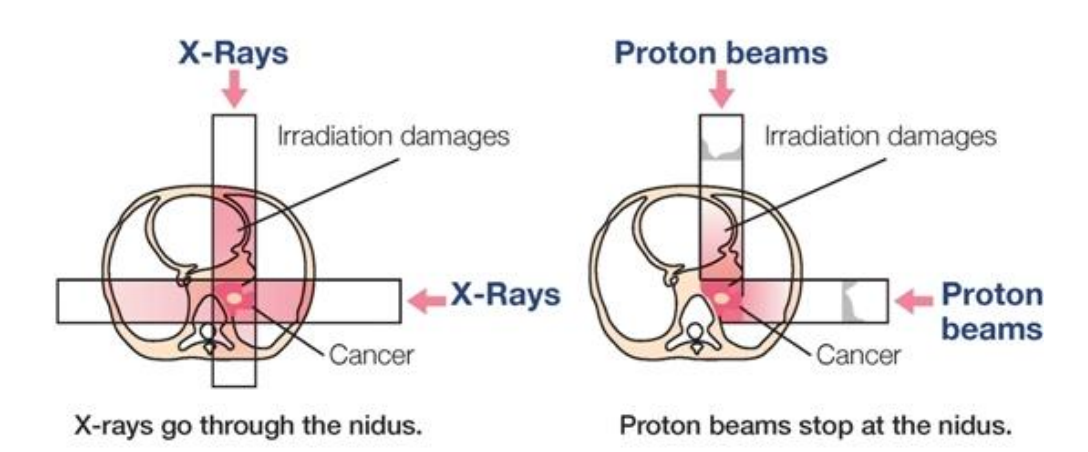
### The thickness of a filter can be decided from the range data from NIST website



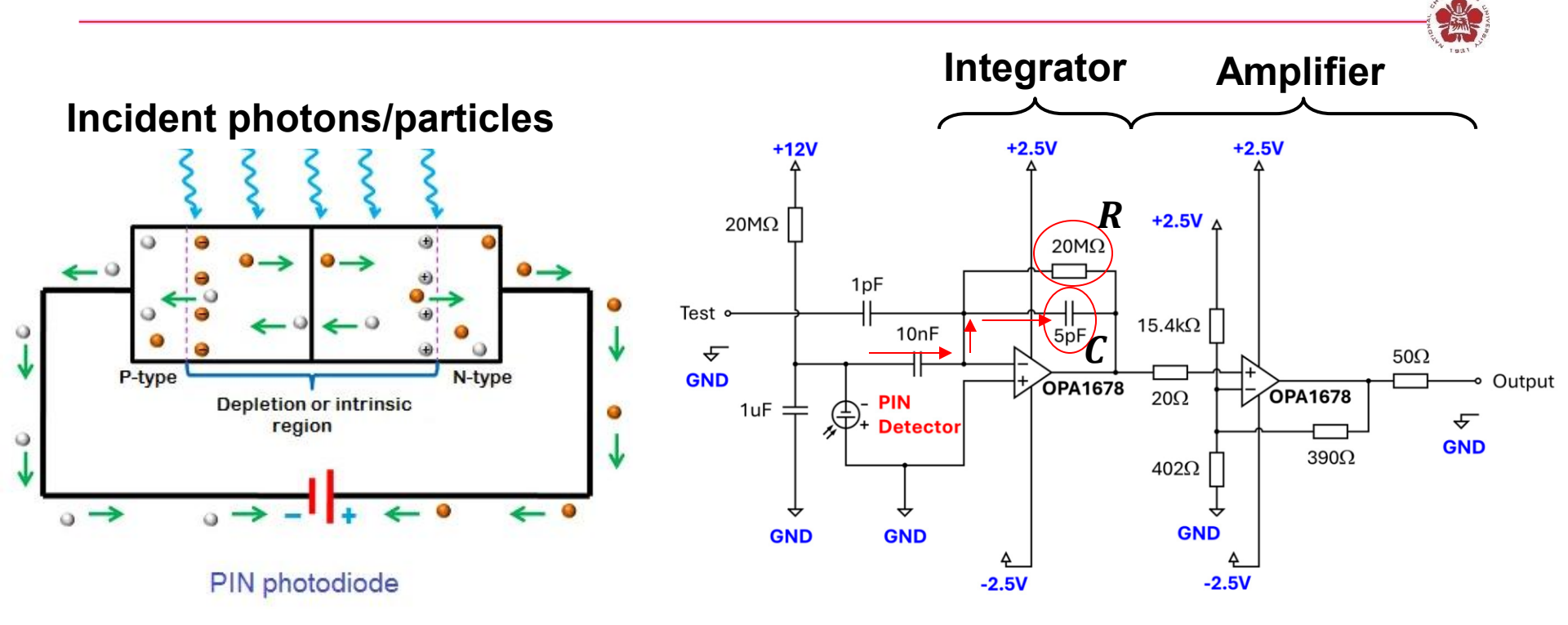
### Proton therapy takes the advantage of using Bragg peak



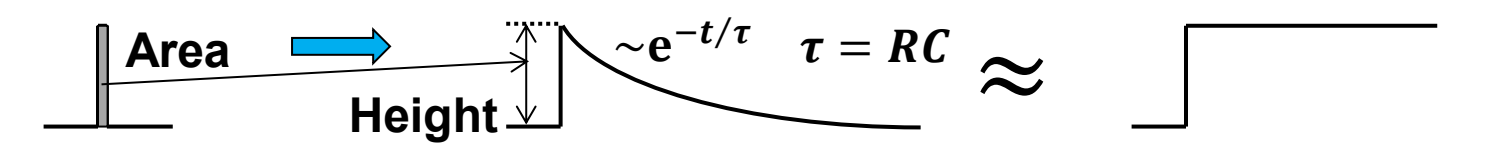




## A pulse signal is converted to a voltage signal using an integrator



- The 5-pF capacitor is charged by the current from the PIN detector.
- The 5-pF capacitor is discharged by the 20-MΩ resistor.



## Pulse Shaping is commonly used in nuclear and particle physics electronics



- Improve Signal-to-noise ratio S/N
   Restrict bandwidth to match measurement time.
  - => Increase pulse width.

Improve pulse-pair resolution

=> Decrease pulse width.

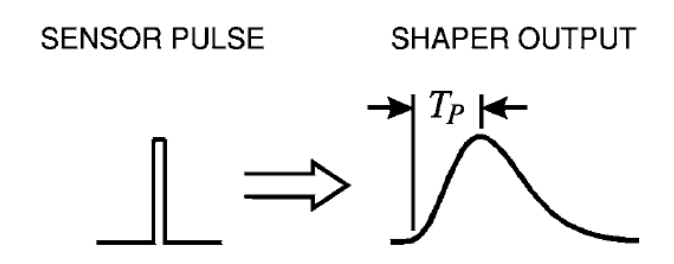


**FIGURE 13.** A pulse shaper transforms a short sensor pulse into a longer pulse with a rounded cusp and peaking time  $T_P$ .

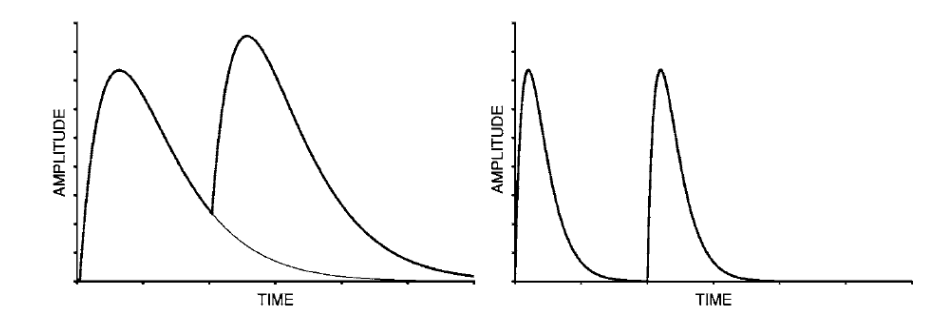
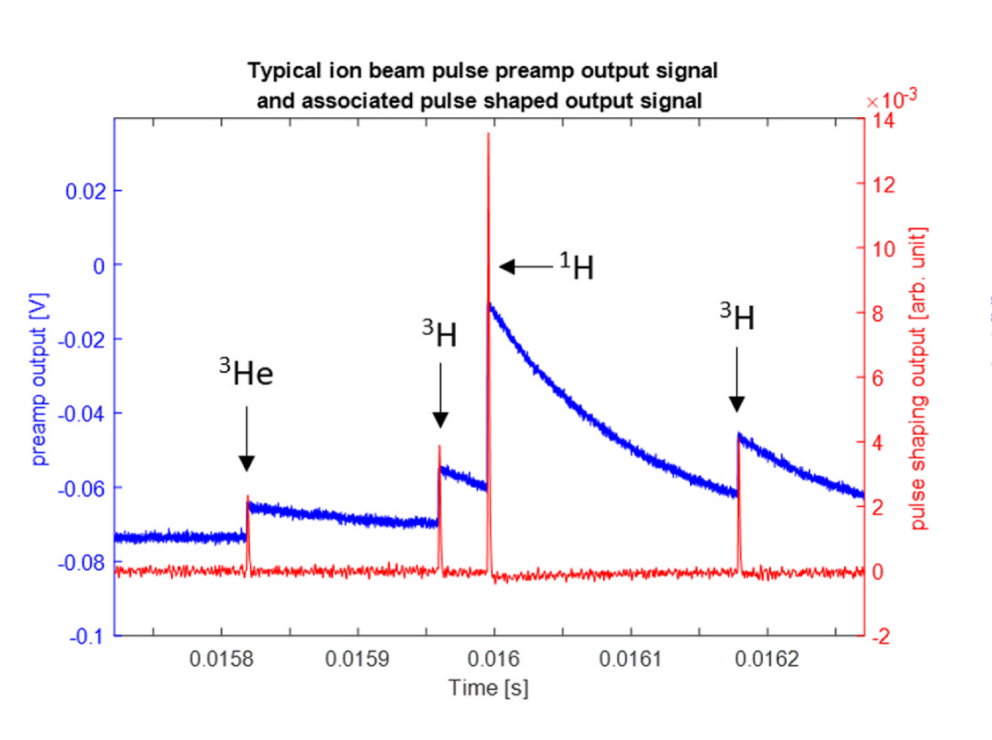
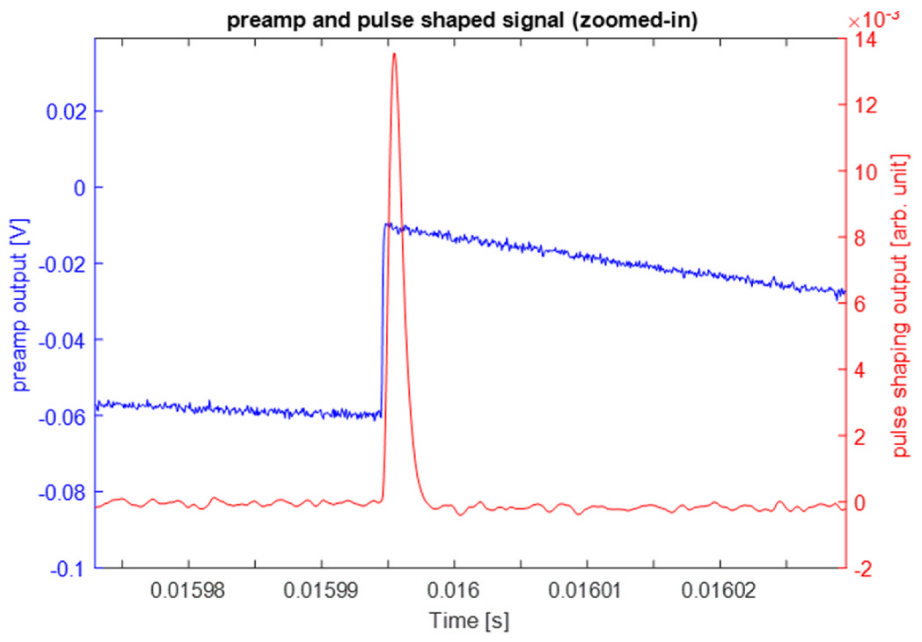


FIGURE 14. Amplitude pileup when two successive pulses overlap (left). Reducing the shaping time allows the first pulse to return to the baseline before the second arrives.

### **Expected data profile**

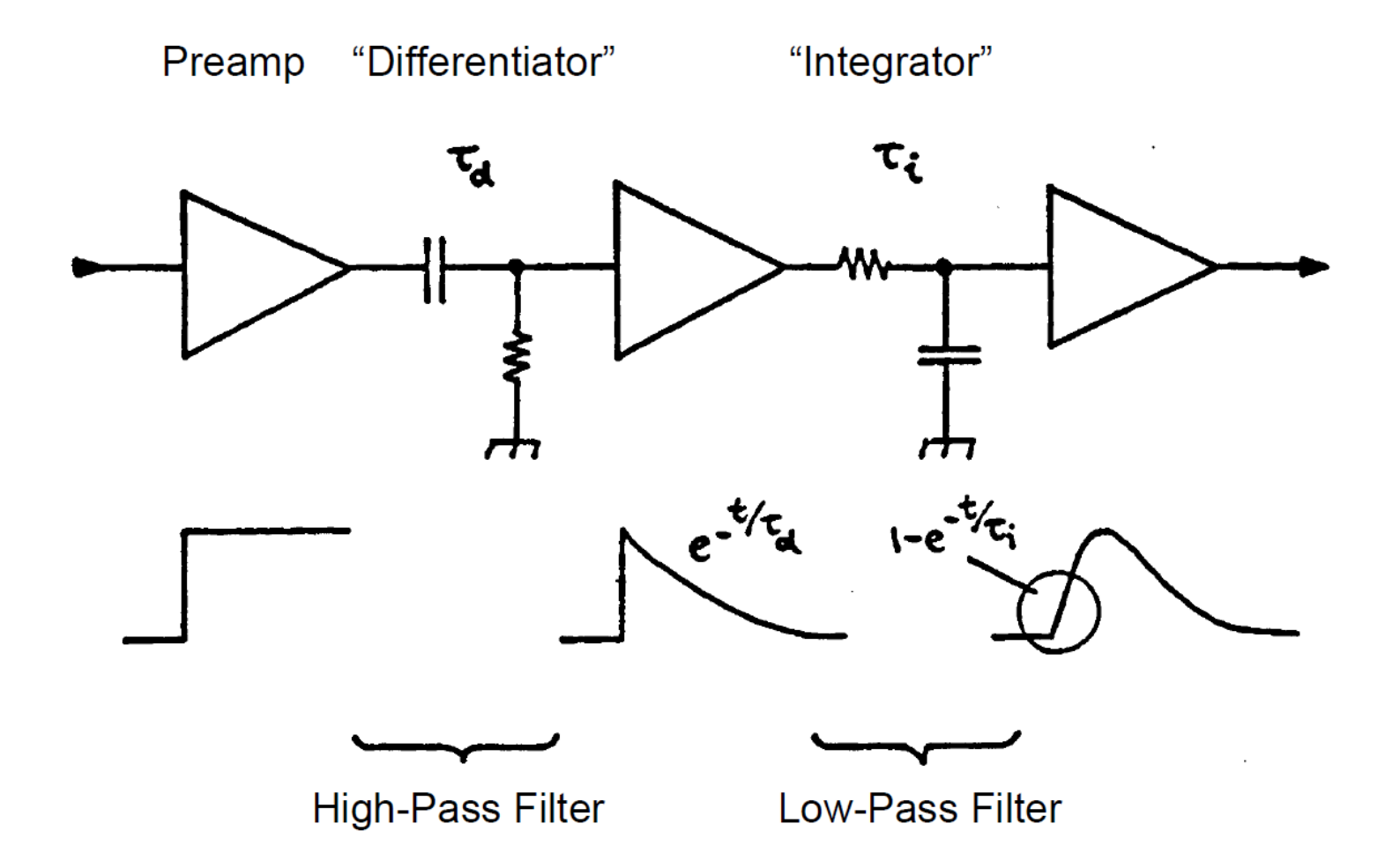






## CR-RC<sup>n</sup> pulse shaping combines a high-pass filter and n low-pass filter

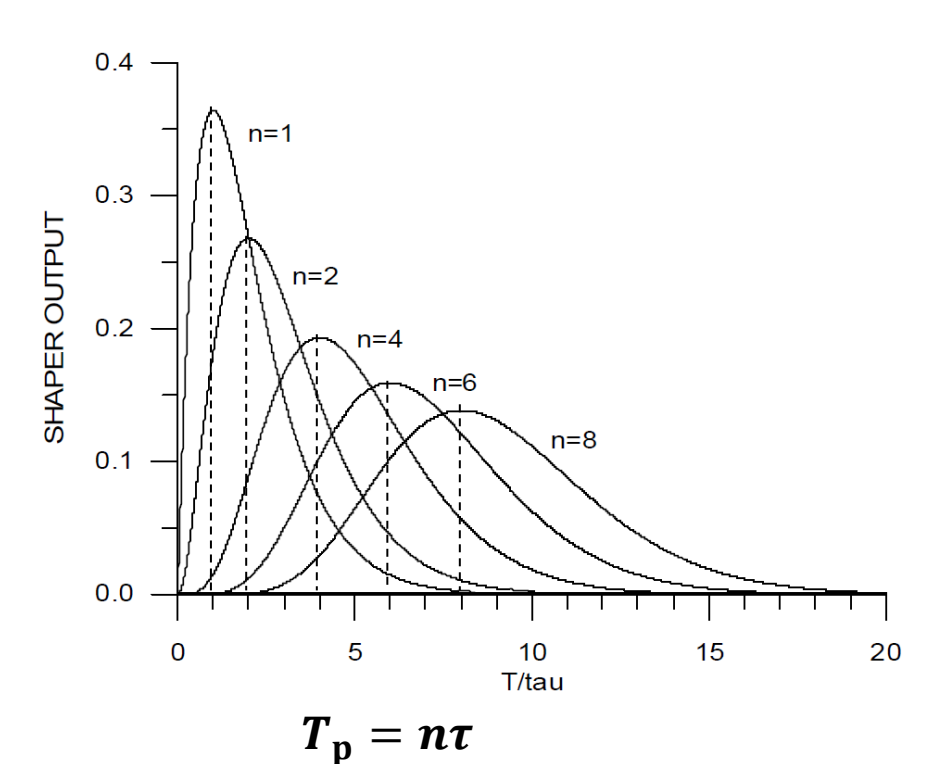




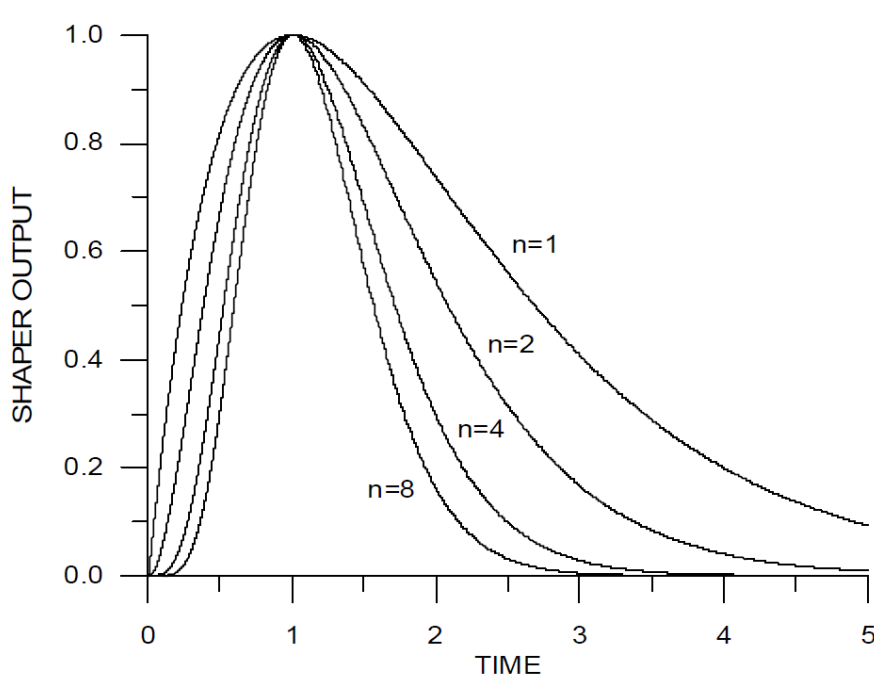
### Pulses become gaussian-like after multiple integrators



• Integrating with the same time constant  $\tau$ 



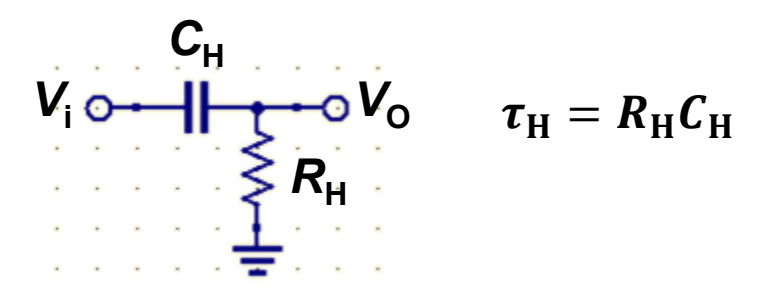
• Integrating with the reduced time constant  $\tau_{\rm n} = \frac{\tau_1}{\pi}$ 



### CR is the high pass filter while RC is the low pass filter



#### CR circuit:



$$V_{o} = V_{i} \frac{R_{H}}{\frac{1}{j\omega C_{H}} + R_{H}} = V_{i} \frac{1}{\frac{1}{j\omega R_{H}C_{H}} + 1}$$
$$= V_{i} \frac{1}{\frac{1}{j\omega \tau_{H}} + 1}$$

For  $\omega \tau_{\rm H} \gg 1$ , i. e.,

$$\frac{2\pi f}{f_{\rm H}} \gg 1 \text{ or } f \gg f_{\rm H} \text{ or } \tau_{\rm H} \gg t$$

 $V_0 \approx V_i$  • High-pass filter!

#### RC circuit:

$$V_{l} \circ V_{o} \circ V_{o} \qquad \tau_{L} = R_{L}C_{L}$$

$$V_{o} = V_{i} \frac{\frac{1}{j\omega C_{L}}}{\frac{1}{j\omega C_{L}} + R_{L}} = V_{i} \frac{\frac{1}{j\omega R_{L}C_{L}}}{\frac{1}{j\omega R_{L}C_{L}} + 1}$$

$$= V_{i} \frac{\frac{1}{j\omega \tau_{L}}}{\frac{1}{j\omega \tau_{L}} + 1}$$

For 
$$\omega \tau_{\rm L} \ll 1$$
, i. e.,

$$rac{2\pi f}{f_{
m L}} \ll 1 \ {
m or} \ f \ll f_{
m L} \ \ {
m or} \ \ t \ll au_{
m L}$$

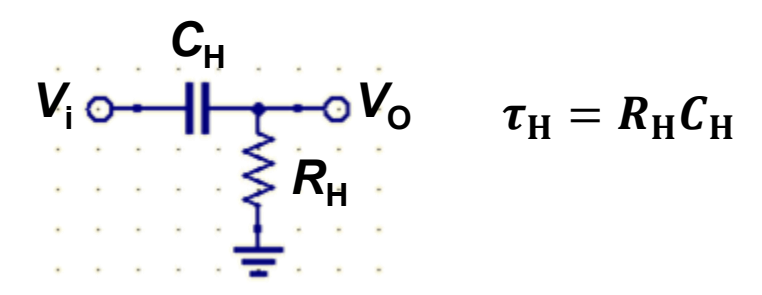
$$V_{\rm o} \approx V_{\rm i}$$

 $V_0 \approx V_i$  • Low-pass filter!

### CR is the high pass filter while RC is the low pass filter



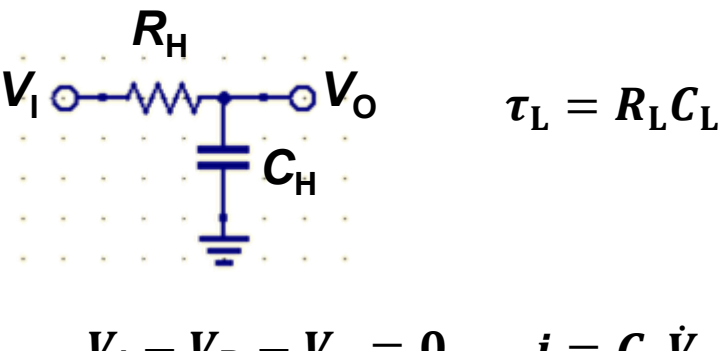
#### CR circuit:



$$V_{\rm i} - V_{\rm c} - V_{\rm o} = 0$$
  $V_{\rm o} = iR_{\rm H}$   $V_{\rm c} = \frac{1}{C_{\rm H}} \int idt = \frac{1}{C_{\rm H}} \int \frac{V_{\rm o}}{R_{\rm H}} dt$   $\dot{V}_{\rm i} = \frac{V_{\rm o}}{\tau_{\rm H}} + \dot{V}_{\rm o}$ 

$$V_o(t) = e^{-t/ au_{
m H}} \int_0^t \dot{V}_{
m i}(t') e^{t\prime/ au_{
m H}} dt'$$

#### RC circuit:



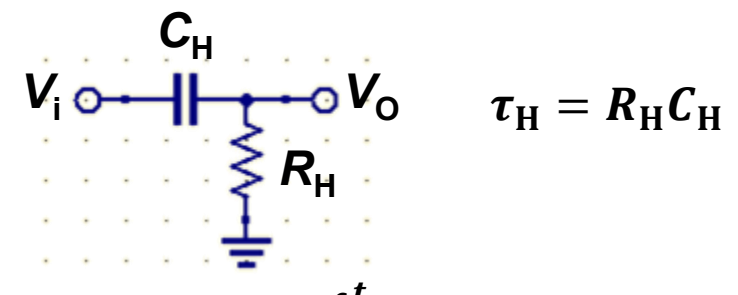
$$egin{aligned} V_{
m i} - V_{
m R} - V_{
m o} &= 0 & i = C_{
m L} \dot{V}_{
m o} \ V_{
m R} &= i R_{
m L} = R_{
m L} C_{
m L} \dot{V}_{
m o} \ V_{
m i} &= au_{
m L} \dot{V}_{
m o} + V_{
m o} \end{aligned}$$

$$V_{\mathrm{o}}(t) = e^{-t/ au_{\mathrm{L}}} rac{1}{ au_{\mathrm{L}}} \int_{0}^{t} V_{\mathrm{i}}(t') e^{t'/ au_{\mathrm{L}}} dt'$$

## A step function becomes an exponential decay after the high-pass filter

### The walk

#### CR circuit:

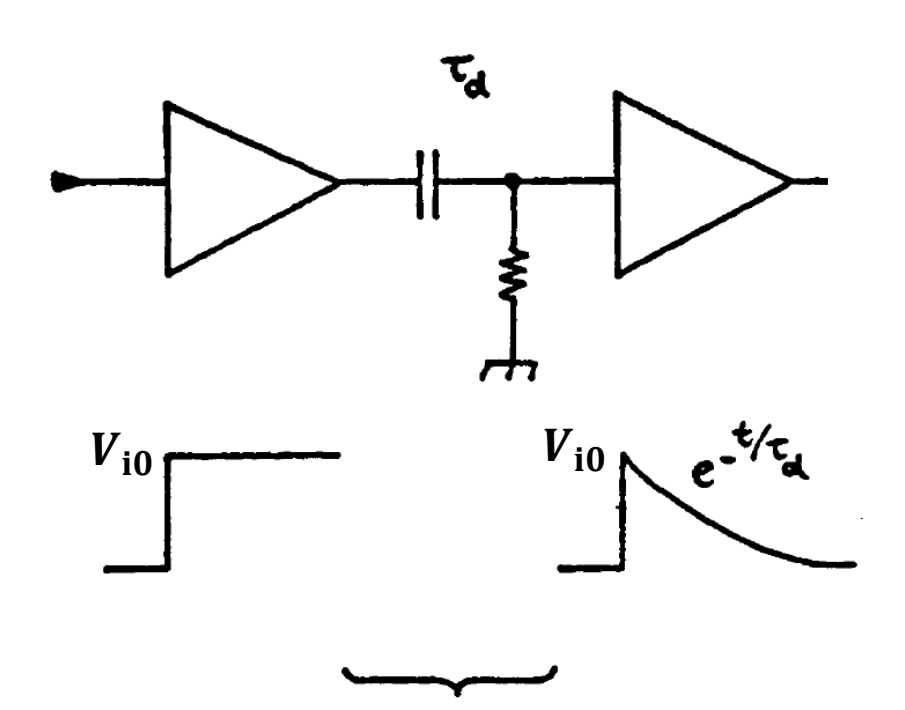


$$egin{aligned} V_{0}(t) &= e^{-t/ au_{\mathrm{H}}} \int_{0}^{t} \dot{V}_{\mathrm{i}}(t') e^{t\prime/ au_{\mathrm{H}}} dt' \ V_{\mathrm{i}}(t) &= egin{cases} 0 & t < 0 \ V_{\mathrm{i}0} & t \geq 0 \end{cases} \end{aligned}$$

$$\dot{V}_{i}(t) = V_{i0}\delta(t)$$

$$V_{0}(t) = e^{-t/\tau_{H}} \int_{0}^{t} V_{i0} \delta(t') e^{t'/\tau_{H}} dt'$$

$$= V_{i0} e^{-t/\tau_{H}} e^{t'/\tau_{H}} \Big|_{t'=0} = V_{i0} e^{-t/\tau_{H}}$$

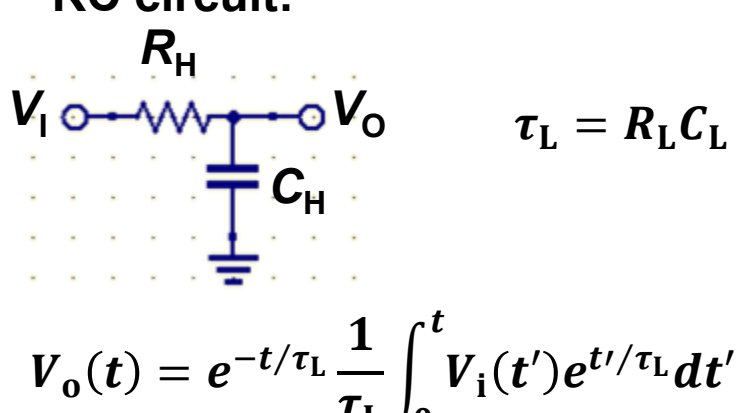


High-Pass Filter

### CR is the high pass filter while RC is the low pass filter



#### RC circuit:



$$V_{\rm i}(t) = V_{\rm i0}e^{-t/ au_{
m H}}$$

For 
$$t \ll \tau_L$$
  $e^{-t/\tau_L} \sim e^{t/\tau_L} \sim 1$ 

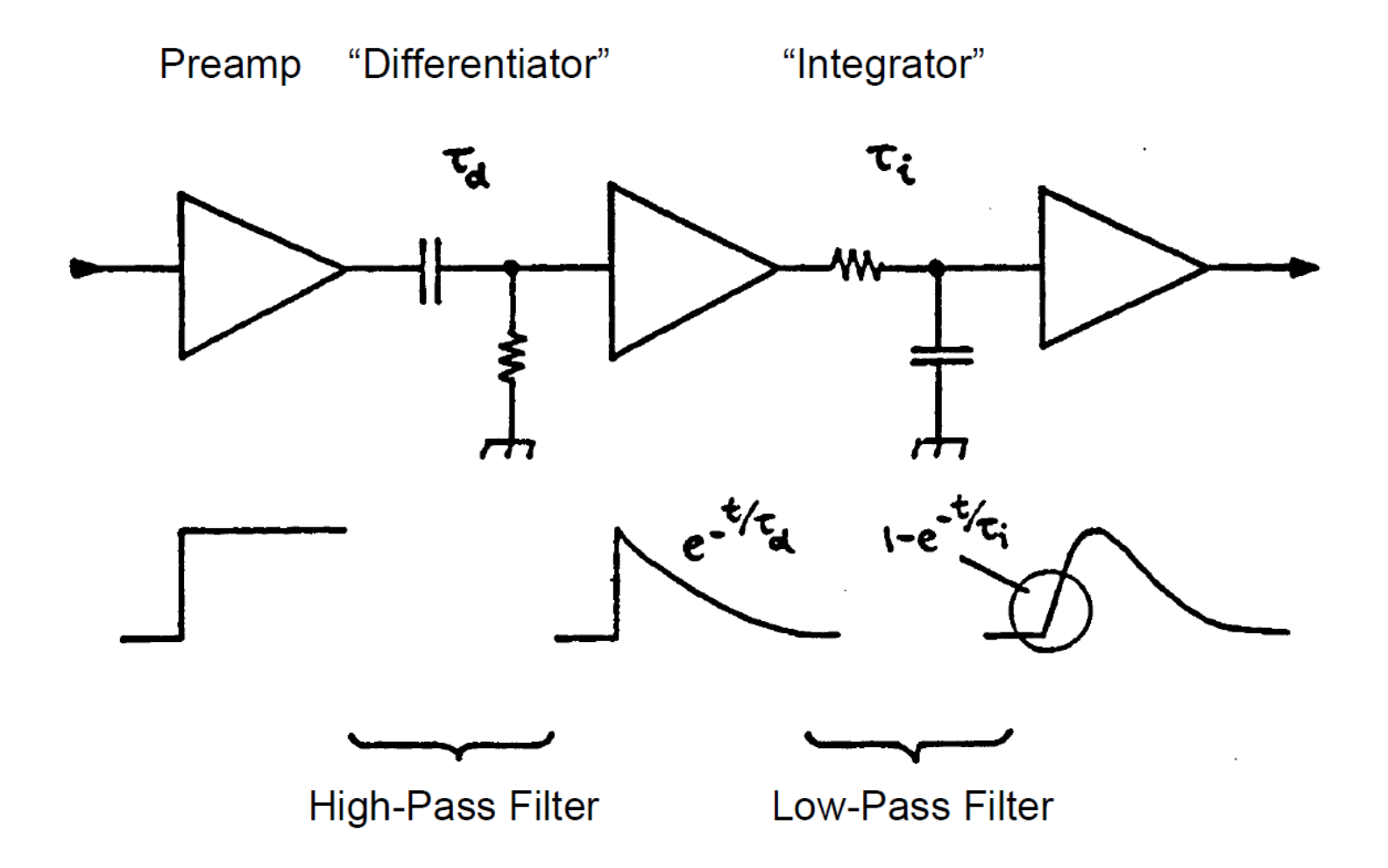
$$V_{0}(t) \sim \frac{1}{\tau_{L}} \int_{0}^{t} V_{i}(t') dt' = \frac{1}{\tau_{L}} \int_{0}^{t} V_{i0} e^{-t'/\tau_{H}} dt'$$
$$= \frac{\tau_{H}}{\tau_{I}} V_{i0} (1 - e^{-t/\tau_{H}})$$

$$egin{aligned} V_{0}(t) &= e^{-t/ au_{L}} rac{1}{ au_{L}} \int_{0}^{t} V_{i0} e^{-t'/ au_{H}} e^{t'/ au_{L}} dt' \ &= e^{-t/ au_{L}} rac{1}{ au_{L}} \int_{0}^{t} V_{i0} e^{t'/ au_{eff}} dt' \ &= e^{-t/ au_{L}} rac{ au_{eff}}{ au_{L}} V_{i0} ig( e^{t/ au_{H}} - 1 ig) \ &rac{1}{ au_{eff}} = rac{1}{ au_{L}} - rac{1}{ au_{H}} < rac{1}{ au_{L}} \end{aligned}$$



## CR-RC<sup>n</sup> pulse shaping combines a high-pass filter and n low-pass filter

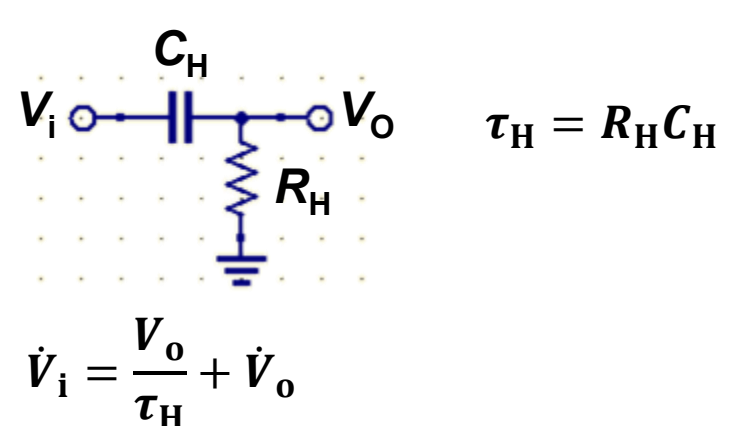




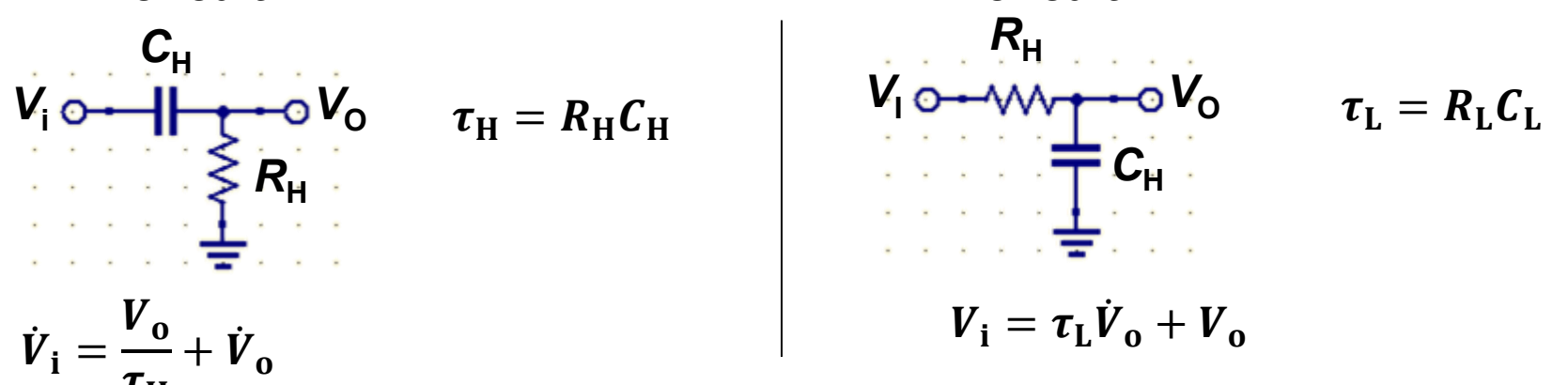
### Finite difference method is used to numerically applying the CR-RC pulse shaping



#### CR circuit:



#### RC circuit:



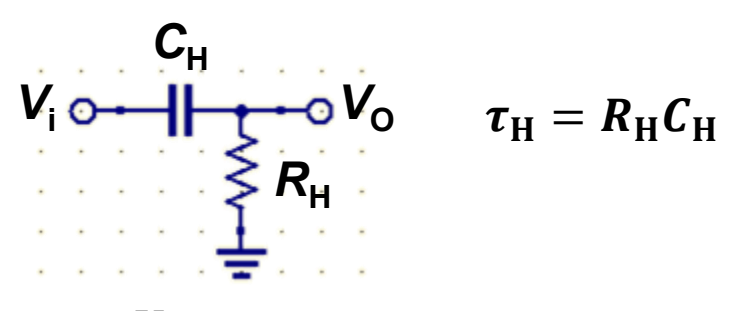
$$\begin{split} \frac{V_{i}(t_{j}) - V_{i}(t_{j-1})}{\Delta t} &\approx \frac{V_{o}(t_{j-1})}{\tau_{H}} + \frac{V_{o}(t_{j}) - V_{o}(t_{j-1})}{\Delta t} \\ &\approx \frac{V_{o}(t_{j})}{\tau_{H}} + \frac{V_{o}(t_{j}) - V_{o}(t_{j-1})}{\Delta t} \\ V_{o}(t_{j}) &= \alpha_{CR}V_{o}(t_{j-1}) + \alpha_{CR}[V_{i}(t_{j}) - V_{i}(t_{j-1})] \\ \alpha_{CR} &\equiv \frac{\frac{\tau_{H}}{\Delta t}}{\frac{\tau_{H}}{\Delta t} + 1} = \frac{\frac{R_{H}C_{H}}{\Delta t}}{\frac{R_{H}C_{H}}{\Delta t} + 1} \end{split}$$

$$egin{aligned} rac{dV}{dt} &= \lim_{\Delta t o 0} rac{V(t_{
m j}) - V(t_{
m j-1})}{\Delta t} \ &pprox rac{V(t_{
m j}) - V(t_{
m j-1})}{\Delta t} \ &rac{1}{\Delta t} \ & rac{1}{\Delta t} \ &rac$$

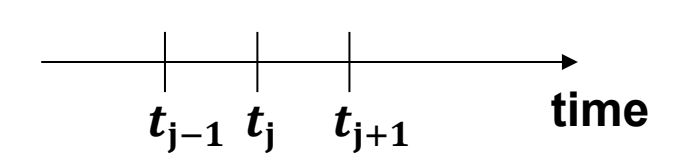
## Finite difference method is used to numerically applying the CR-RC pulse shaping



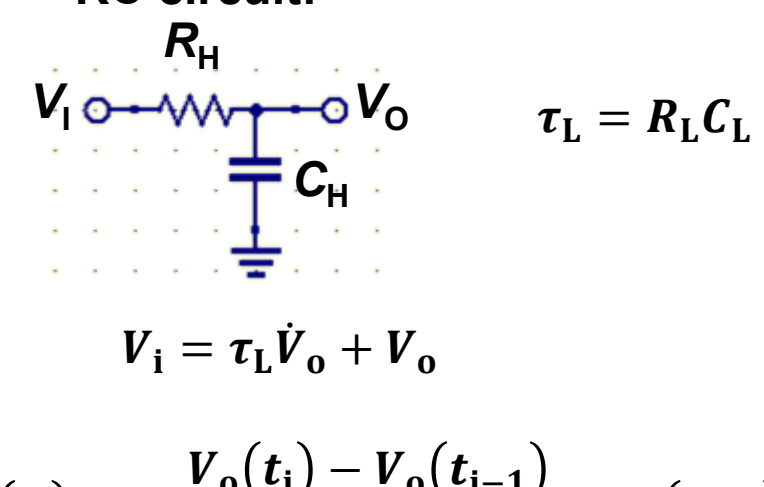
#### CR circuit:



$$\dot{V}_{i} = \frac{V_{o}}{\tau_{H}} + \dot{V}_{o}$$

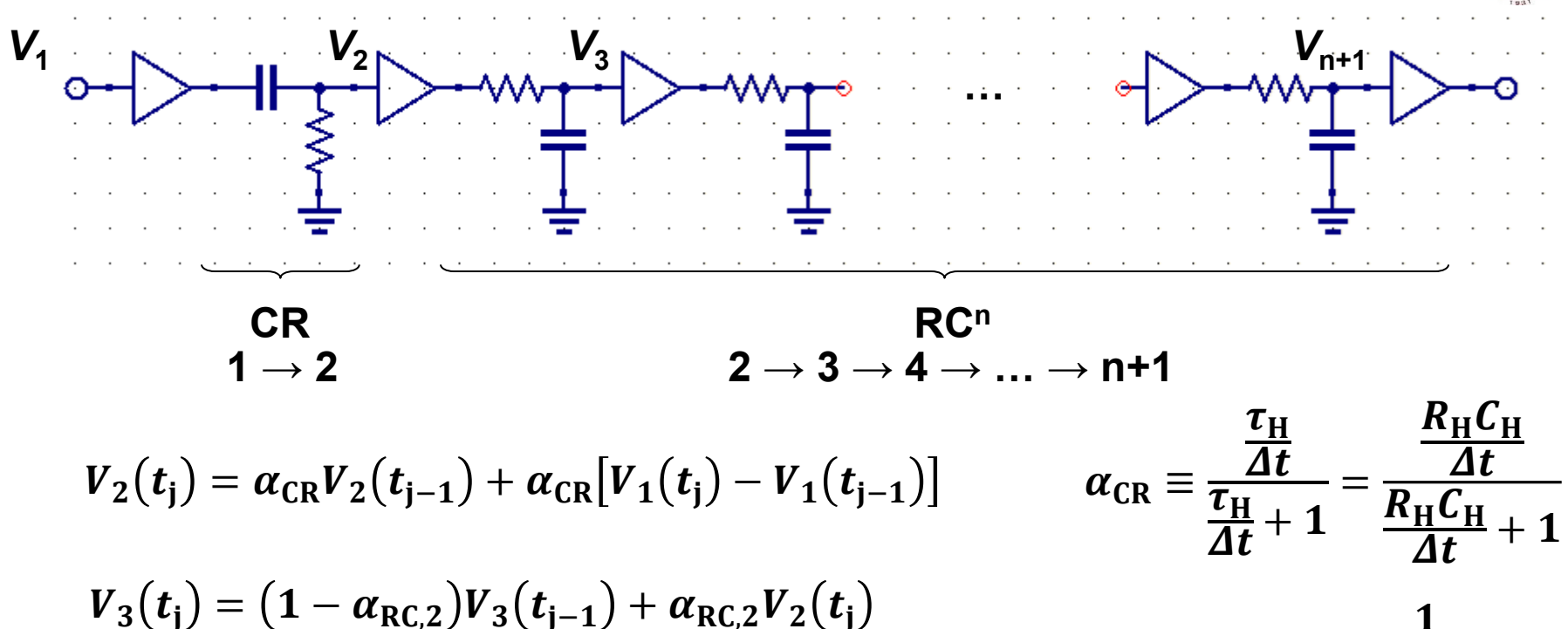


#### RC circuit:



$$\begin{split} V_{i}(t_{j}) &\approx \tau_{L} \frac{V_{o}(t_{j}) - V_{o}(t_{j-1})}{\Delta t} + V_{o}(t_{j-1}) \\ &\approx \tau_{L} \frac{V_{o}(t_{j}) - V_{o}(t_{j-1})}{\Delta t} + V_{o}(t_{j}) \\ V_{o}(t_{j}) &= (1 - \alpha_{RC})V_{o}(t_{j-1}) + \alpha_{RC}V_{i}(t_{j}) \\ \alpha_{RC} &\equiv \frac{1}{\frac{\tau_{L}}{\Delta t} + 1} = \frac{1}{\frac{R_{L}C_{L}}{\Delta t} + 1} \end{split}$$

## Iteration can be used to have more orders of CR-RC<sup>n</sup> pulse shaping



: 
$$V_{\rm m}(t_{\rm j}) = (1 - \alpha_{\rm RC,m-1})V_{\rm m}(t_{\rm j-1}) + \alpha_{\rm RC,m-1}V_{\rm m-1}(t_{\rm j})$$
 :

$$V_{n+1}(t_j) = (1 - \alpha_{RC,n})V_{n+1}(t_{j-1}) + \alpha_{RC,n}V_n(t_j)$$

$$rac{oldsymbol{\sigma_H}}{\Delta t} + 1$$
  $rac{oldsymbol{\kappa_H c_H}}{\Delta t} + 1$   $lpha_{
m RC,m} \equiv rac{1}{rac{ au_{
m L,m}}{\Delta t} + 1}$   $oldsymbol{ au_{
m L}} = R_{
m L} C_{
m L}$   $oldsymbol{ au_{
m L,m}} = rac{ au_{
m L}}{m-1}$   $m \geq 2$ 

### Let's try using excel first



$$\alpha_{\rm CR} \equiv 0.85$$

$$\alpha_{\rm RC.2} \equiv 0.15$$
  $\Delta t = 64 \text{ ns}$ 

$$lpha_{\mathrm{CR}} \equiv rac{rac{ au_{\mathrm{H}}}{\Delta t}}{rac{ au_{\mathrm{H}}}{\Delta t} + 1} = 0.85$$

$$lpha_{RC,m}\equiv rac{1}{rac{ au_{L,m}}{arDelta t}+1}=0.\,15$$

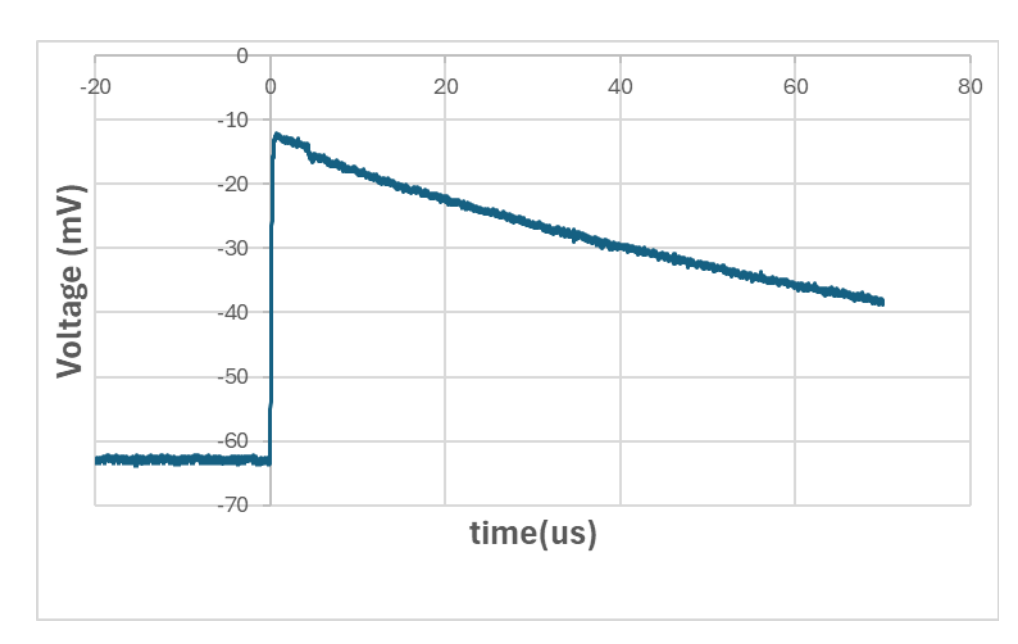
$$au_{ extsf{L}, ext{m}} = rac{ au_{ extsf{L}}}{m-1}$$

$$\tau_{\rm H} = 362.7 \ \rm ns$$

$$\tau_{\rm L.m} = 362.7/(m-1) \text{ ns}$$

$$\frac{\tau_{\rm L}}{\Lambda t} = \frac{0.85}{0.15}$$

$$\alpha_{\text{RC,m}} \equiv \frac{1}{\frac{0.85}{0.15} \frac{1}{m-1} + 1}$$



$$V_2(t_j) = \alpha_{CR}V_2(t_{j-1}) + \alpha_{CR}[V_1(t_j) - V_1(t_{j-1})]$$

$$\tau_{L,m} = 362.7/(m-1) \text{ ns} \quad V_3(t_j) = (1 - \alpha_{RC,2})V_3(t_{j-1}) + \alpha_{RC,2}V_2(t_j)$$

$$V_{\rm m}(t_{\rm j}) = (1 - \alpha_{\rm RC,m-1})V_{\rm m}(t_{\rm j-1}) + \alpha_{\rm RC,m-1}V_{\rm m-1}(t_{\rm j})$$

$$V_{n+1}(t_j) = (1 - \alpha_{RC,n})V_{n+1}(t_{j-1}) + \alpha_{RC,n}V_n(t_j)$$

### Let's try using excel first

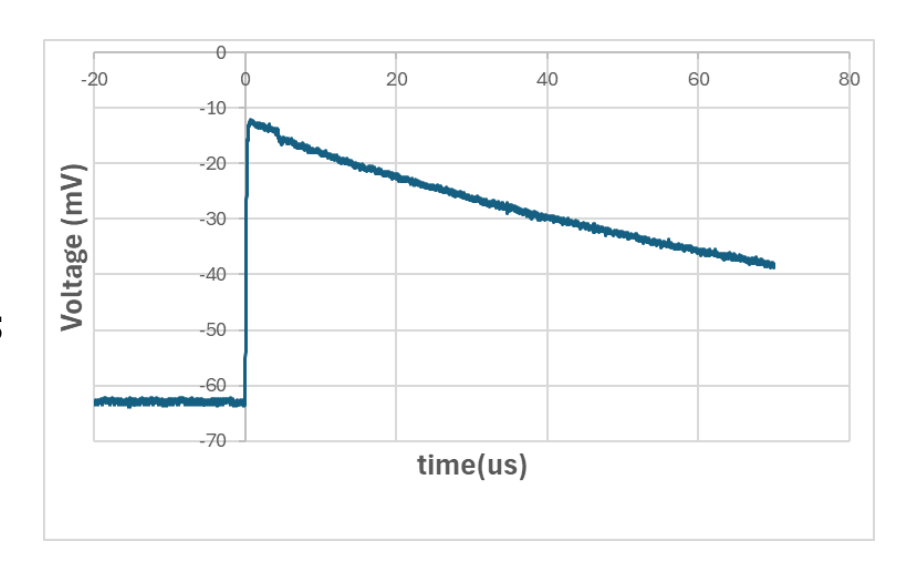


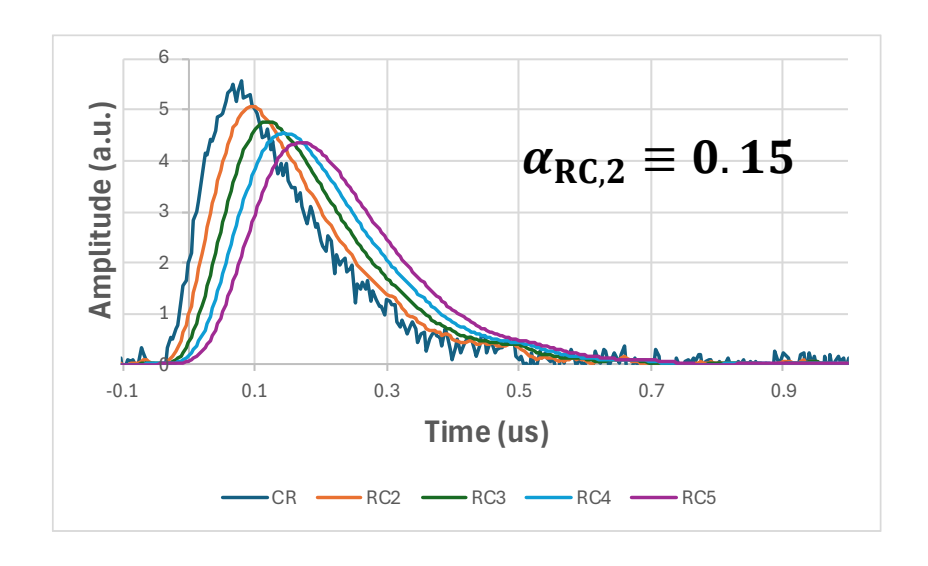
$$\Delta t = 64 \text{ ns}$$

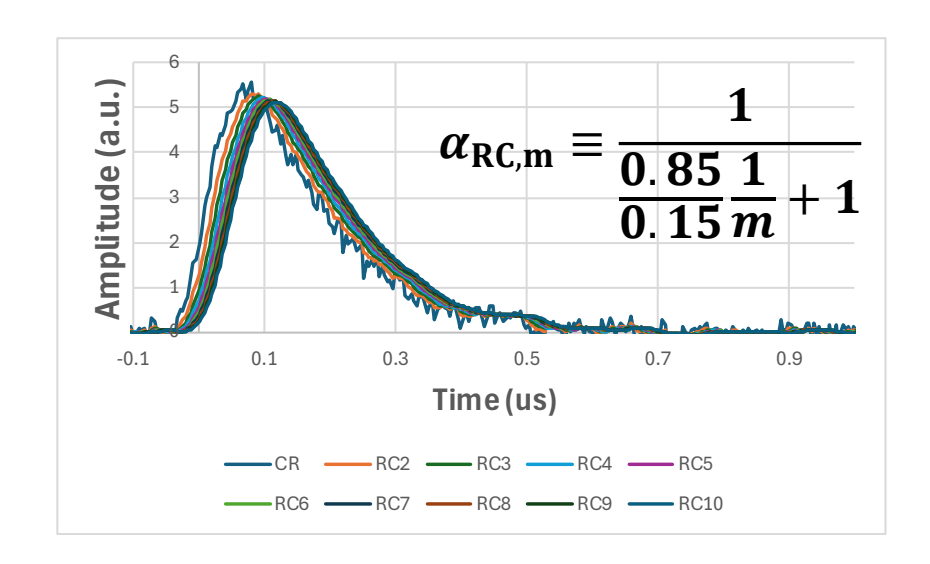
$$\alpha_{\rm CR} \equiv 0.85$$

$$\tau_{\rm H} = 362.7 \ \rm ns$$

$$\tau_{\rm L,m} = 362.7/(m-1)~{\rm ns}$$







## When the pulse is not sharp enough, no significant gaussian feature is observed

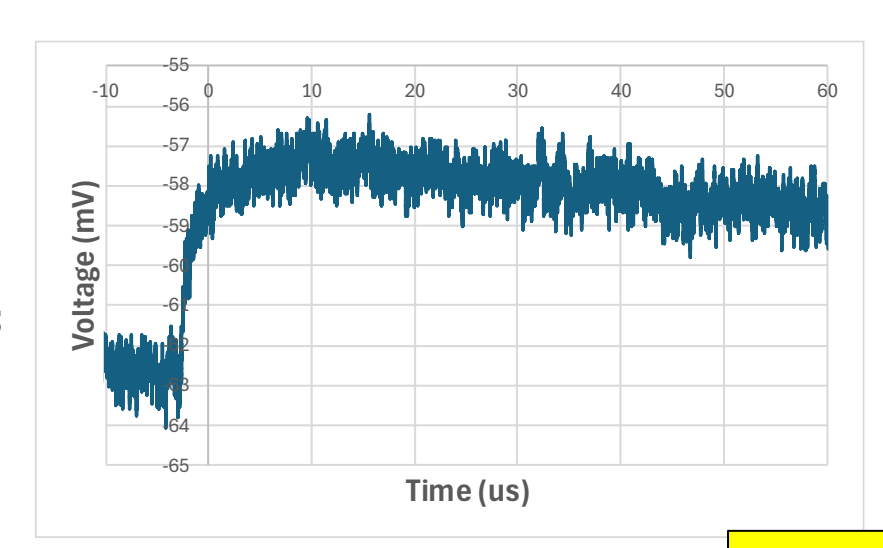


$$\Delta t = 64 \text{ ns}$$

$$\alpha_{\rm CR} \equiv 0.85$$

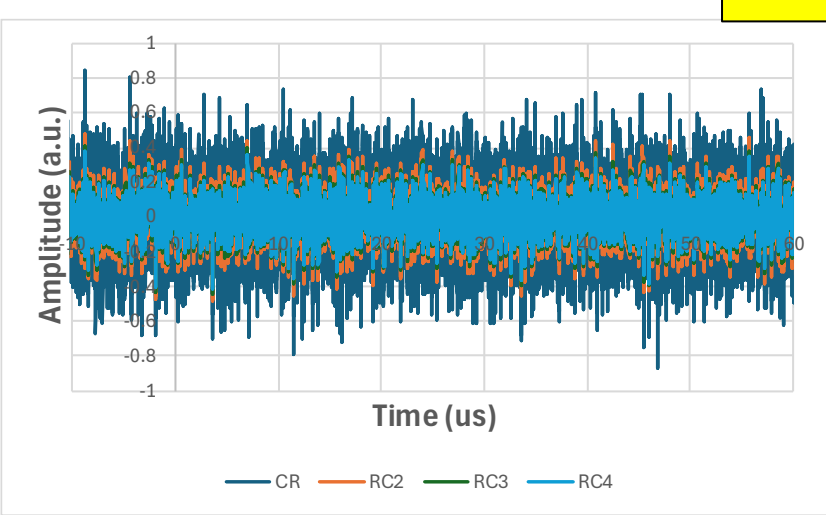
$$\tau_{\rm H} = 362.7 \ \rm ns$$

$$\tau_{\rm L,m} = 362.7/(m-1)~{\rm ns}$$



#### What's the source?

$$\alpha_{\text{RC,m}} \equiv \frac{1}{\frac{0.85}{0.15} \frac{1}{m-1} + 1}$$



# Saha equation gives the relative proportions of atoms of a certain species that are in two different states of ionization in thermal equilibrium



$$\frac{n_{r+1}n_e}{n_r} = \frac{G_{r+1}g_e}{G_r} \frac{(2\pi m_e KT)^{3/2}}{h^3} \exp\left(-\frac{\chi_r}{KT}\right)$$

- n<sub>r+1</sub>, n<sub>r</sub>: Density of atoms in ionization state r+1, r (m<sup>-3</sup>)
- n<sub>e</sub>: Density of electrons (m<sup>-3</sup>)
- G<sub>r+1</sub>, G<sub>r</sub>: Partition function of ionization state r+1, r
- g<sub>e</sub>=2: Statistical weight of the electron
- m<sub>e</sub>: Mass of the electron
- χ<sub>r</sub>: Ionization potential of ground level of state r to reach to the ground level of state r+1
- T: Temperature
- h: Planck's constant
- K: Boltzmann constant

### Some backgrounds of quantum mechanics



Planck blackbody function:

$$u(\nu, T) = \frac{8\pi h \nu^3}{c^3} \frac{1}{e^{h\nu/KT} - 1} (W/m^3 Hz)$$

- **Boltzmann formula:** 
  - g<sub>i</sub>, g<sub>j</sub>: statistical weight

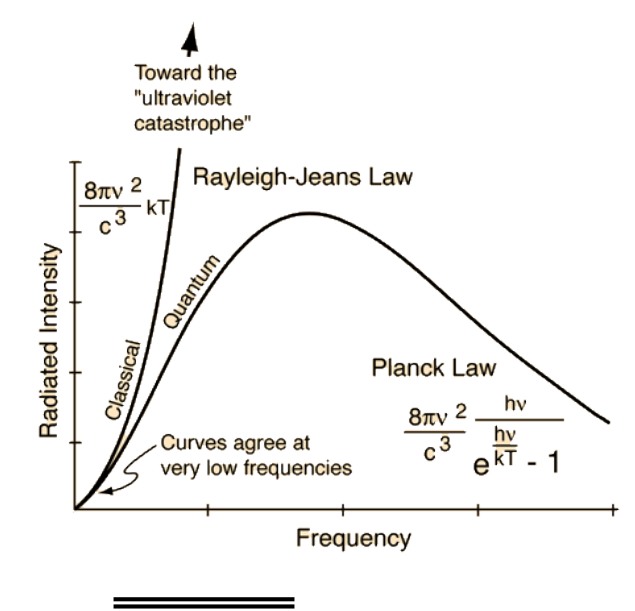
$$\frac{n_i}{n_j} = \frac{g_i e^{-\epsilon_i/\text{KT}}}{g_j e^{-\epsilon_j/\text{KT}}} = \frac{g_i}{g_j} e^{-h\nu_{ij}/\text{KT}} \qquad \frac{g_i}{g_j} = \frac{2J_i + 1}{2J_j + 1}$$

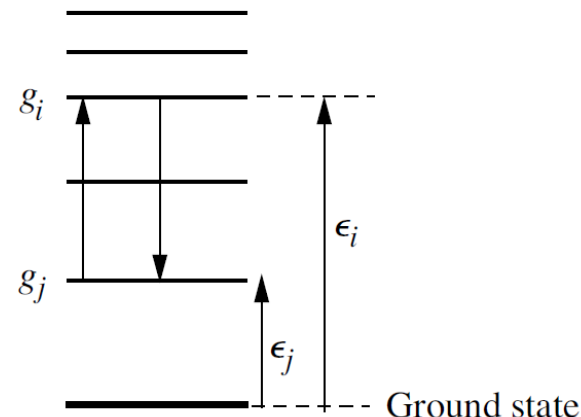
(J: angular momenta quantum number)

– Number in the i<sup>th</sup> state to the total atom:

$$\frac{n_i}{n} = \frac{n_i}{\Sigma n_i} \equiv \frac{g_i e^{-\epsilon_i/\text{KT}}}{G} \qquad G \equiv \Sigma g_j e^{-\epsilon_j/\text{KT}}$$

G: partition function of statistical weight for the atom, taking into account all its excited states.





#### Einstein coefficient



- Probability of electron energy transition:
  - Excitation ( $\uparrow$ ):  $P_{ji} = B_{ji}u(\nu, T)$
  - De-excitation ( $\downarrow$ ):  $P_{ij} = A_{ij} + B_{ij}u(\nu, T)$
- In thermal equilibrium:

$$n_{i}(A_{ij} + B_{ij}u) = n_{j}B_{ji}u$$

$$\frac{g_{i}}{g_{j}}e^{-x}(A_{ij} + B_{ij}u) = B_{ji}u$$

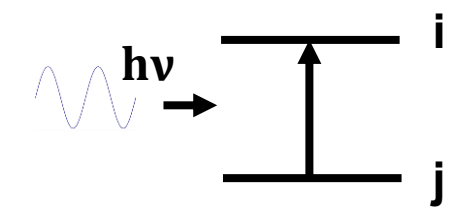
$$x \equiv \frac{h\nu}{KT}$$

$$u = a(e^{x} - 1)^{-1}$$

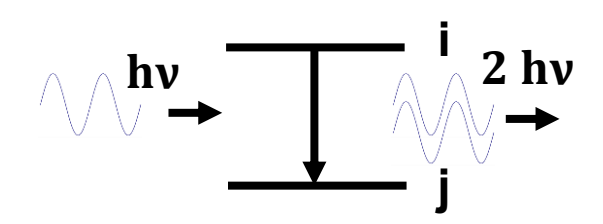
$$a \equiv \frac{8\pi h\nu^{3}}{c^{3}}$$

$$a\left(e^{x}B_{ji} - \frac{g_{i}}{g_{i}}B_{ij}\right) = (e^{x} - 1)\frac{g_{i}}{g_{i}}A_{ij}$$

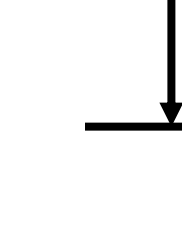
Photoexcitation:



Induced radiation:



Spontaneous radiation:



The Einstein coefficients are independent of T or v.

$$x \to 0, e^x \to 1$$
  $x \to \infty, e^x \to \infty$  
$$\frac{B_{ij}}{B_{ii}} = \frac{g_j}{g_i} \qquad aB_{ji} = \frac{g_i}{g_j} A_{ij} \quad \frac{A_{ij}}{B_{ij}} = \frac{8\pi h \nu^3}{c^3}$$

### Saha equation is derived using the transition between different ionization states

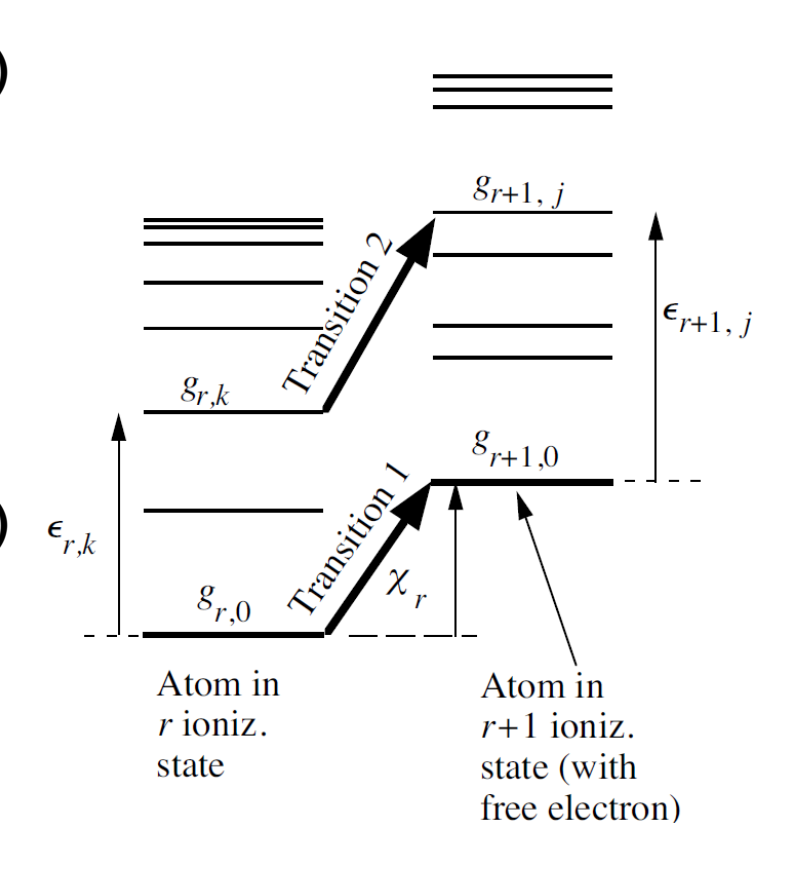


 Required photon energy for transition (1) from the ground state of r ionization state to the ground state of r+1 ionization state:

$$hv = \chi_r + \frac{p^2}{2m}$$
 Energy of the free electron

 Required photon energy for transition (2) from the energy level k of r ionization state to the energy level j of r+1 ionization state:

$$hv = \chi_r + \epsilon_{r+1,j} - \epsilon_{r,k} + \frac{p^2}{2m}$$



### Saha equation is derived using the transition between different ionization states



#### Photoionization:

$$R_{\mathrm{pi}} = n_{r,k} u(\nu) B_{r,k \to r+1,j}$$

Induced radiation:

$$R_{ir} = n_{r+1,j} n_{e,p}(p) u(\nu) B_{r+1,j \to r,k}$$

Spontaneous emission:

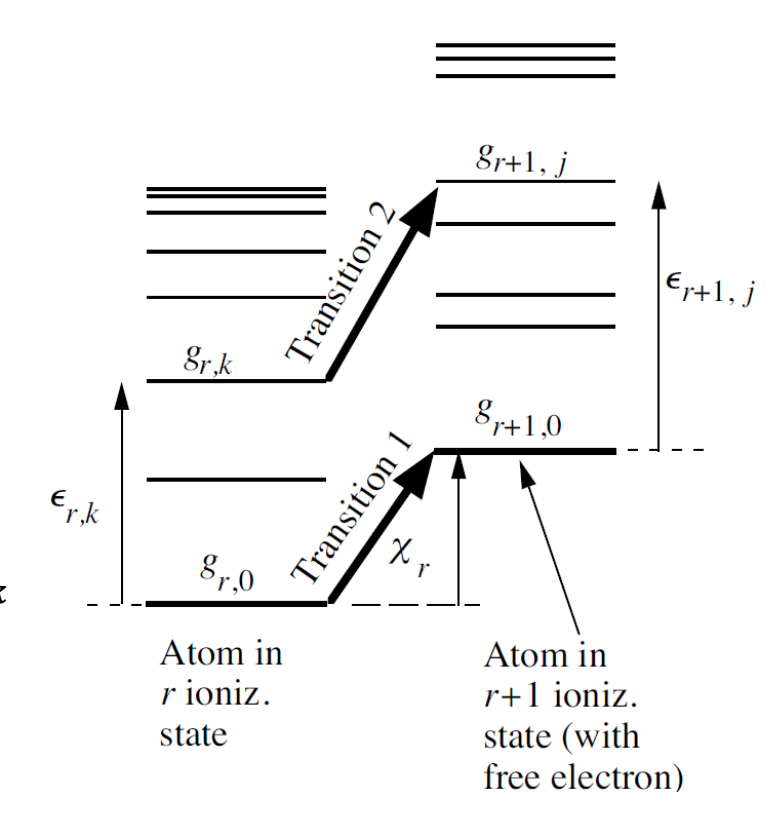
$$R_{\rm sr} = n_{r+1,j} n_{e,p}(p) A_{r+1,j\to r,k}$$

In thermal equilibrium:

$$n_{r+1,j}n_{e,p}A_{r+1,j\to r,k} + n_{r+1,j}n_{e,p}uB_{r+1,j\to r,k}$$
  
=  $n_{r,k}uB_{r,k\to r+1,j}$ 

Einstein coefficients:

$$\frac{B_{r,k\to r+1,j}}{B_{r+1,j\to r,k}} = \frac{g_{r+1,j}}{g_{r,k}} \frac{g_e 4\pi p^2}{h^3}$$



$$\frac{A_{r+1,j\to r,k}}{B_{r+1,j\to r,k}} = \frac{8\pi h \nu^3}{c^3}$$

### Saha equation - continued



$$n_{r+1,j}n_{e,p}A_{r+1,j\to r,k} + n_{r+1,j}n_{e,p}uB_{r+1,j\to r,k} = n_{r,k}uB_{r,k\to r+1,j}$$

$$n_{r+1,j}n_{e,p}rac{A_{r+1,j o r,k}}{B_{r+1,j o r,k}}+n_{r+1,j}n_{e,p}u=n_{r,k}urac{B_{r,k o r+1,j}}{B_{r+1,j o r,k}}$$

$$\frac{n_{r+1,j}n_{e,p}}{n_{r,k}} = \left(\frac{A_{r+1,j\to r,k}}{uB_{r+1,j\to r,k}} + 1\right)^{-1} \frac{B_{r,k\to r+1,j}}{B_{r+1,j\to r,k}}$$

$$n_{e,p}(p) = \frac{n_e 4\pi p^2}{(2\pi m KT)^{3/2}} \exp\left(-\frac{p^2}{2m KT}\right)$$

$$\frac{B_{r,k\to r+1,j}}{B_{r+1,j\to r,k}} = \frac{g_{r+1,j}}{g_{r,k}} \frac{g_e 4\pi p^2}{h^3}$$

$$\frac{A_{r+1,j\to r,k}}{B_{r+1,j\to r,k}} = \frac{8\pi h \nu^3}{c^3}$$

$$\frac{n_{r+1,j}n_e}{n_{r,k}} = \frac{(2\pi m KT)^{3/2}}{4\pi p^2} \exp\left(\frac{p^2}{2m KT}\right) \left[\frac{c^3}{8\pi h \nu^3} \left(e^{h\nu/KT} - 1\right) \frac{8\pi h \nu^3}{c^3} + 1\right]^{-1} \frac{g_{r+1,j}}{g_{r,k}} \frac{g_e 4\pi p^2}{h^3}$$

$$\frac{n_{r+1,j}n_e}{n_{r,k}} = \frac{(2\pi m KT)^{3/2}}{h^3} \frac{g_{r+1,j}g_e}{g_{r,k}} \exp\left[\frac{1}{KT} \left(\frac{p^2}{2m} - h\nu\right)\right]$$

### Saha equation - continued



$$\begin{split} &\frac{n_{r+1,j}n_e}{n_{r,k}} = \frac{(2\pi \text{mKT})^{3/2}}{h^3} \, \frac{g_{r+1,j}g_e}{g_{r,k}} \exp\left[\frac{1}{\text{KT}} \left(\frac{p^2}{2m} - \text{hv}\right)\right] \\ &\frac{n_{r+1,j}n_e}{n_{r,k}} = \frac{(2\pi \text{mKT})^{3/2}}{h^3} \, \frac{g_{r+1,j}g_e}{g_{r,k}} \exp\left[\frac{1}{\text{KT}} \left(\frac{p^2}{2m} - \chi_r - \epsilon_{r+1,j} + \epsilon_{r,k} - \frac{p^2}{2m}\right)\right] \\ &\frac{n_{r+1,j}n_e}{n_{r,k}} = \frac{(2\pi \text{mKT})^{3/2}}{h^3} \, \frac{g_{r+1,j}\exp\left(-\frac{\epsilon_{r+1,j}}{\text{KT}}\right)g_e}{g_{r,k}\exp\left(-\frac{\kappa_{r+1,j}}{\text{KT}}\right)} \exp\left(-\frac{\chi_r}{\text{KT}}\right) \\ &\frac{n_{r,k}}{n_r} = \frac{g_{r,k}e^{-\epsilon_{r,k}/\text{KT}}}{G_r} & G_r = \Sigma g_{r,k}e^{-\epsilon_{r,k}/\text{KT}} \\ &\frac{n_{r+1,j}}{n_{r+1}} = \frac{g_{r+1,j}e^{-\epsilon_{r+1,j}/\text{KT}}}{G_{r+1}} & G_{r+1} = \Sigma g_{r+1,j}e^{-\epsilon_{r+1,j}/\text{KT}} \end{split}$$

 $\frac{n_{r+1}n_e}{n} = \frac{G_{r+1}g_e}{G} \frac{(2\pi m_e KT)^{3/2}}{h^3} \exp\left(-\frac{\chi_r}{\kappa_T}\right)$ 

181

### Saha equation – example: hydrogen plasma of the sun



- Photosphere of the sun hydrogen atoms in an optically thick gas in thermal equilibrium at temperature T=6400 K.
  - Neutral hydrogen (r state / ground state)

$$G_r = \Sigma g_{r,k} = g_{r,0} + g_{r,1} \exp\left(-\frac{\epsilon_{r,1}}{KT}\right) + \dots = 2 + 8 \exp\left(-\frac{10.2 \text{ eV}}{0.56 \text{ eV}}\right) + \dots$$
  
= 2 + 9.8 × 10<sup>-8</sup> + \dots \approx 2

lonized state (r+1 state)

$$G_{r+1} = \Sigma g_{r+1,j} = g_{r+1,0} + g_{r+1,1} \exp\left(-\frac{\epsilon_{r+1,1}}{KT}\right) + \cdots \approx 1$$

– Other information:  $g_e=2$   $\chi_r=13.6 \,\mathrm{eV}$ ; KT  $=0.56 \,\mathrm{eV}$   $n_{r+1}=n_e$ 

$$\frac{n_{r+1}^2}{n_r} = 2.41 \times 10^{21} \frac{1 \times 2}{2} (6400)^{3/2} \exp\left(-\frac{13.6}{0.56}\right) = 3.5 \times 10^{16} m^{-3}$$

#### It is mostly neutral in the photosphere of the sun



Assuming 50 % ionization:

$$n_{r+1} = n_r = 3.5 \times 10^{16} m^{-3}$$
  $n = n_{r+1} + n_r = 7 \times 10^{16} m^{-3}$ 

- At lower densities n at the same temperature, there should be fewer collisions leading to recombination and thus the plasma to be more than 50 % ionization.
- In the photosphere of the sun:

$$ho \sim 3 imes 10^{-4} \, \mathrm{kg}/m^3 
ightarrow n = 2 imes 10^{23} m^{-3} \gg 7 imes 10^{16} m^{-3}$$
  $\Rightarrow$  Less than 50 % ionization

Use the total number density to estimate the ionization percentage:

$$n_{r+1} + n_r = 2 \times 10^{23}$$
  $\frac{n_{r+1}}{n_r} = 4 \times 10^{-4} @6400K$